Recycling Aspects of Natural Fiber Reinforced Polypropylene Composites

Doctoral Thesis
(Dissertation)

to be awarded the degree
Doctor of Engineering (Dr.–Ing.)

submitted by

Amna Ramzy

from Cairo, Egypt

Approved by the Faculty of Natural and Materials Science,
Clausthal University of Technology

Date of oral examination
16.01.2018

Chairperson of the Board of Examiners

Prof. Dr.-Ing. Heinz Palkowski

Chief Reviewer

Prof. Dr.-Ing. Gerhard Ziegmann

Reviewer

Prof. Gianluca Cicala

Acknowledgments

My warm gratitude is here to my husband Ahmed Elsabbagh, without his support and encouragement from the very beginning during my University studies in Egypt till now, I would never be able to accomplish and enjoy this academic level that I have reached.

Warm thanks and acknowledgment for my ‘’Doktorvater’’ i.e. Doctorate Supervisor Prof. Gerhard Ziegmann for his distinguished style in supervision and in building such a family atmosphere with all his PhD students, co-workers and colleagues, simply he made me feel home. I as well appreciatre deeply the long scientific discussion sessions which he extracted from his extremely busy schedule because of his ultimate dedication to supporting his co-workers in all fields that helped me a lot to crystallize my research point.

I wish to express as well my deep gratitude to Prof. Gianluca Cicala for the time he invested in reviewing my thesis and for his very interesting scientific comments and recommendations.

Dr. Leif Steuernagel who was extremely supporting – before he became extremely overloaded – particularly in my first years of working as a researcher in the team, when there was still a lot to learn. His friendly way in dealing with each problem made research contribution with him in the natural fibres field an interesting experience.

Thanks are also due to the head of the institute Prof. Dr. Dieters Meiners and all academic and technical colleagues as well as visitng students for their cooperation and support during my working period. Special thanks to Larissa Olivero, Arouna Fochive for their deep engagement in their summer research practice which as well helped me in this thesis. Thanks are also due to Omar Eldemellawy for his support in performing some tests.

My beloved parents and brother … my parents in law … my friends, thank you for your encouragement and payers and for the faith you had in me achieving this. Special gratitude to my parents for raising me up as a responsible and an open person, without these values I wouldn’t be what I am now.

Last but not least to my beloved kids Omar and Mariam … the light of my life … the sun and the air … the energy I live with … I dedicate this thesis to you for your love to nature and your high awareness of the envirnomental friendly practices, wishing you would be great scientists when you grow up.

Thanks are also due to all partners in the project “Material and Flow Models for Natural Fiber Reinforced Injection Molding Materials for Practical Use in the Automotive Industry’’ partly funded by the Federal Ministry of Food, Agriculture and Consumer Protection (BMELV) via the Agency for Renewable Resources (FNR), for their co-operation and testing materials supply.

Abstract

Natural fibers nowadays play a very important role in the composites industry due to their several attractive characteristics especially energy saving potential which addresses the most vital industrial problem. Hence, this increasing demand of natural fiber thermoplastic composites in the market requires a technique to be established for handling the waste products out of these composites. The limitation of literature regarding the effect of recycling these for composites is the motivation for this work.

This research focuses on recycling pre-consumer polypropylene compounds reinforced with sisal and hemp fibers up to five cycles. These two fibers are selected because they cover two main types of natural fibers: straight leaf fibers for sisal and branched bast fibers for hemp. Knowledge gained from these two types serves as a basis which could be implemented in future on other fibers from the same type.

Natural fibers – being natural products – unlike synthetic fibers, offer unusual scatter of values, which in turn leads to the difficulty of assessing the effect of several reprocessing cycles on the compound. To be able to set a good foundation for this research, a thorough investigation on sisal and hemp fibers in both dry and compounded (with polypropylene) states is performed in the first section of this research followed by recycling of sisal and hemp compounds. A thorough investigation for determining the evolution of fiber shape and morphology is conducted on extracted fibers at selected cycles using dynamic image analysis in addition to FESEM and digital microscopy. Followed by rheological, flowability and thermal tests, the effect of number of cycles on the resulting properties could be analyzed based on the understanding of fibers morphology. Finally, mechanical tests are performed to assess the change in the compounds' properties after recycling regarding the gained knowledge from the previous analysis.

Understanding the difference in nature and consequently the difference in behavior between sisal and hemp fibers in the polypropylene melt gives an insight into comprehending the rheological and mechanical behavior of the compounds under study. Sisal with its straight and stiff fibers is less likely to agglomerate and build fiber clusters and is homogeneously distributed in the PP matrix. On the contrary, hemp fibers which are thin, branched and flexible tend to tangle up and build agglomerations of fiber clusters which hinder the homogenous distribution of the fibers in the matrix PP. This behavior affects the development of the viscosity along recycling cycles where sisal compound proves higher viscosity than hemp compound in the first cycles. Afterwards, due to recycling, hemp agglomerations disentangle and hemp fibers are shortened and distributed homogenously in the PP matrix causing increase in the overall compound viscosity. Flowability values show a three-stage behavior where compounds start at relatively low values (long sisal fibers / agglomerated hemp fibers). After the first and second cycles, a step in the flowability values could be observed for both hemp and sisal compounds due to shortening of sisal and hemp fibers which cause the de-agglomeration of fiber clusters.

Starting the third cycle after fibers have reached the shortest length and could no longer be affected by the screw action of the injection molding machine, flowability values reach a relatively stable plateau.

Evolution of fiber shape as a function of recycling cycles proves to influence the mechanical properties in a remarkable course where mechanical properties improve for certain number of cycles before they start to degrade. This certain number of cycles depends on the measured property (E-modulus, strength, impact strength and elongation)

Recycling of sisal and hemp compounds proves no critical degradation of thermal properties where hemp compound shows less sensitivity to recycling than sisal compound. On the other hand, melting points increased after recycling 3 cycles before they started to decrease again.

In addition to influencing rheological, thermal and mechanical properties, this research shows that fiber shape also influences the degree of crystallinity of the compounds where compounds at late cycles prove higher degree of crystallinity than original compounds. This also reflects on thermomechanical properties where an improvement of the storage modulus is detected as a result to the restriction of segmental motion of the molecular chains. This statement is confirmed by the higher measured glass transition temperature of the recycled samples. Modulus of retention ratio is calculated where sisal compound proves a higher efficiency in reinforcing the composite after structural transitions.

Based on the previous comprehension of the effect of recycling on the characteristics of sisal and hemp compounds enlightened by the special effect of fiber shape, an analytical model is developed to describe the flowability in terms of cycle number for hemp and sisal compounds. The model describes the three assumed stages using two power equations where conditions are set for applying the equations according to the fiber type. Similarly, non-linear functions of symmetrical sigmoidal type (4 PL) are assumed to correlate between fiber aspect ratio and selected mechanical properties such as E-modulus and tensile strength.

Keywords: Recycling, Natural fiber, Polypropylene, Structure, Mechanical properties.

Kurzfassung

Naturfasern spielen aufgrund ihrer zahlreichen attraktiven Eigenschaften, insbesondere des Energieeinsparpotentials, heutzutage eine sehr wichtige Rolle in der Verbundwerkstoffindustrie. Die zunehmende Nachfrage nach Naturfaser-Thermoplast-Verbundwerkstoffen auf dem Markt erfordert eine Technik für die Wiederverwertung der Abfallprodukte aus diesen Verbundwerkstoffen. Der Mangel an genügend Literatur über die Wirkung des Recyclings dieser Verbundwerkstoffe ist die Motivation für diese Arbeit. Diese Forschungsarbeit konzentriert sich auf das Recycling von „Pre Consumer"-Polypropylen-Verbunden, die mit Sisal- und Hanffasern verstärkt sind. Diese beiden Fasern wurden ausgewählt, weil sie exemplarisch zwei Haupttypen von Naturfasern abdecken: Sisal weist gerade Blattfasern auf und Hanf verzweigte Bastfasern. Die aus diesen beiden Typen zu gewinnenden Kenntnisse sollen in Zukunft auf andere Fasern des gleichen Typs angewandt werden können. Für diese Arbeit wurden die Sisal- und Hanfverbunde in fünf Recycling-Vorgängen verarbeitet. Naturfasern stellen im Gegensatz zu synthetischen Fasern keine stabile Qualität dar. Das führt zu der Schwierigkeit, die Wirkung mehrerer Aufbereitungszyklen auf die Verbundmaterial-Eigenschaften zu beurteilen. Um eine gute Grundlage für diese Forschung zu schaffen, wird im ersten Teil dieser Forschung eine gründliche Untersuchung über Sisal- und Hanffasern im ursprünglichen Zustand als auch im Verbund mit Polypropylen durchgeführt. Die Verbundwerkstoffe werden durch mechanische, rheologische, fließfähigkeits- und thermische Prüfungen geprüft. Eine umfassende Untersuchung der Evolution von Faserform und Morphologie wird an extrahierten Fasern in ausgewählten Zyklen mittels dynamischer Bildanalyse, FESEM und Digitalmikroskopie durchgeführt. Das Verständnis des Unterschiedes in Natur und Verhalten zwischen Sisal- und Hanffasern in der Polypropylenschmelze bildet die Grundlage für das Verständnis der unterschiedlichen rheologischen und mechanischen Verhaltensweisen der zu untersuchenden Verbunde. Sisal mit seinen geraden und steifen Fasern zeigt eine geringere Wahrscheinlichkeit, Agglomerate und Fasercluster zu bilden und ist homogener in der PP-Matrix verteilt. Hanffasern sind im Gegensatz dazu dünn, verzweigt und flexibel und weisen einer höheren Wahrscheinlichkeit auf, Agglomerate und Fasercluster zu bilden, die die homogene Verteilung der Fasern in der PP-Matrix behindern. Dieses Verhalten beeinflusst die Entwicklung der Viskosität entlang von Recycling-Zyklen. Das Hanf-Compound zeigt in den ersten Zyklen eine geringere Viskosität als das Sisal-Compound. Danach lösen sich Hanf-Agglomerate auf, da sich die Hanffasern durch die Scherbeanspruchung im Recycling-Prozess verkürzen und sich homogener in der PP-Matrix verteilen. Dies führt zu einer Erhöhung der Gesamtviskosität der Hanf-Compound-Schmelze.

Es stellt sich heraus, dass die Fließwerte ein dreistufiges Verhaltensmuster aufweisen. In der ersten Stufe, die den ersten und zweiten Zyklus umfasst, kann ein Sprung in den Fließfähigkeitswerten sowohl für Hanf- als auch für Sisal-Compounds beobachtet werden. Das liegt an der Faserverkürzung im Recycling-Prozess. Die zweite Stufe beginnt mit dem dritten Zyklus. Die Fasern beider Compounds

verkürzen sich weiter und verteilen sich noch homogener in der PP-Matrix. Dadurch verbessert sich das Fließverhalten stetig. Nachdem die Fasern die kürzeste Länge erreicht haben und nicht mehr durch die Schneckenwirkung der Spritzgussmaschine beeinflusst werden, erreichen die Fließfähigkeitswerte ein relativ stabiles Plateau (dritte Stufe).

Die Evolution der Faserform und -länge in den Recyclingzyklen beeinflusst die mechanischen Eigenschaften (E-Modul, Festigkeit, Schlagzähigkeit und Dehnung): für eine gewisse Anzahl von Zyklen nehmen die jeweiligen Werte zu, bevor sie wieder abnehmen. Neben der Beeinflussung der rheologischen, thermischen und mechanischen Eigenschaften zeigt diese Untersuchung, dass die Faserform auch den Kristallinitätsgrad der Verbindungen beeinflusst: Compounds in späten Zyklen weisen einen höheren Kristallinitätsgrad auf als die ursprünglichen Compounds. Dies wird auch durch die thermomechanischen Eigenschaften bestätigt. Durch die Beschränkung der Segmentbewegung der Molekülketten verbessert sich das Speichermodul. Dies wird durch den höher gemessenen Glasübergang der recycelten Proben bestätigt. Die Sisalfasern weisen nach dem Strukturübergang eine höhere Effizienz bei der Verstärkung des Verbundstoffs auf.

Basierend auf dem bisherigen Verständnis der Wirkung des Recyclings auf die Eigenschaften von Sisal- und Hanf-Compounds wurde ein analytisches Modell entwickelt, um die Fließfähigkeit in Bezug auf die Zykluszahl für Hanf- und Sisalverbindungen zu beschreiben. Das Modell beschreibt die drei angenommenen Stufen unter Verwendung von zwei Leistungsgleichungen. Die Bedingungen für die Anwendung der Gleichungen werden nach dem Fasertyp ausgewählt. Für die ausgewählten mechanischen Eigenschaften (E-Modul und Zugfestigkeit) wird in ähnlicher Weise angenommen, dass nichtlineare Funktionen des symmetrischen sigmoideum Typs (4 PL) zwischen dem Faser-Seitenverhältnis und den ausgewählten mechanischen Eigenschaften korrelieren.

Die Forschungsarbeit zeigt das Recyclings-Potenzial von Sisal- und Hanf-Compounds und entwickelt ein Modell, mit dem die Veränderungen der Compounds-Eigenschaften beschrieben werden können.

Summary

This dissertation consists of seven chapters. The first chapter explains the motivation of this work with a short introduction about the recycling topic. It includes definition, classification and important European regulations related to recycling. The research in natural fiber thermoplastic composites is relatively new. This new category of materials will encounter in the near future the problem of recycling and waste management. The motivation of this work in then justified. Scope of work is limited to the pre-consumer products to focus on the effect of multi-processing cycles.

Second chapter discusses the state of the art. This includes a brief presentation of some statistical facts about recycling industry in the world and Europe in specific. The recycling methods are then discussed. Mechanical, chemical, biological and at last incineration technologies are presented as different recycling approaches which target different levels of recycled materials namely pre-consumer and post-consumer products (pure and contaminated products). A more complex recycling is the recycling of fiber reinforced composites where more than one material is involved. Fibers are either stable synthetic ones like glass fibers or less thermal resistant like natural fibers. Finally, a literature survey is carried out to study the effect of recycling on the thermoplastic matrix, the fibers, the thermal characteristics and mechanical properties of the recycled composites.

Third chapter describes the research strategy of this work and the applied methodical approach to study the effect of recycling on the rheological, thermal properties and morphology of the NFTC (PP Thermoplastic, natural fibers of hemp and sisal) and relate them to the evolution in the mechanical properties. Afterwards all performed characterization tests, namely mechanical, rheological, flowability, fiber extraction and measurement, microscopy and dynamic image analysis, thermal gravimetric analysis, differential scanning calorimetry and dynamic mechanical analysis are explained.

A full understanding of the compounds and the reinforcing fibers is developed in chapter four where the results of the systematic characterization tests are discussed in terms of rheological, thermal and mechanical properties of the virgin compounds in addition to fibers' morphology.

The influence of recycling on the behavior of sisal and hemp compounds is discussed in the fifth chapter based on the knowledge foundation developed in chapter four. Resulting compounds' rheological, mechanical and thermal properties are discussed based on the change in the fibers morphology after recycling. Further processing of the measured data is performed to calculate the activation energy required to transform from glassy to rubbery state. Also, the modulus of retention and its modification are calculated to assess the reinforcing efficiency of the fibers introduced into polypropylene.

In the sixth chapter, the mathematical modeling and simulation are presented based on the gained knowledge from the previous chapters. An analytical model is

developed to describe the flowability in terms of fiber dimensions and cycle number. For modeling mechanical properties such as tensile strength and E-modulus, fiber aspect ratio is considered.

Seventh and last chapter deduces the potential of recycling natural fibers through summarizing the main conclusions of this work. Effect of recycling on the morphological, rheological, flowability and thermal properties of the composites and their relation to the development of mechanical properties during recycling are correlated together to explain the special attractiveness of recycling natural fibers. Finally, a brief description of the future work is discussed based on the findings from this thesis and from the literature survey.

List of Symbols

(h_{ls})	fiber length efficiency term	
l_c	the critical fiber length	[mm]
v_f	fiber volume fraction	
W0	weight of dry fiber	[mg]
Wi	weight of fibers at measuring time	[mg]
Tg	glass transition temperature	[°C]
T_c	crystallisation temperature	[°C]
Tm	melt temperature	[°C]
Tc	crystalliztion temperature	[°C]
Tbp	boiling temperature	[°C]
ΔHc	crystallisation enthalpy	[J/g]
ΔHm	melting enthalpy	[J/g]
x	crystallinity index	[°C]
E	Youngs modulus	[Mpa]
‘s’	strength	[Mpa]
e	elongation	[%]
h	viscosity	[Pa.s]
s_f	fiber strength	[MPa]
d	fiber diameter	[mm]
t	interfacial shear strength	Mpa
c	composite	
m	matrix	
f	fiber	
o	orientation	
Tan d	Damping factor	
E'	Storage modulus	Gpa
E"	Loss modulus	Gpa
f	frequency	Hz
Eact	Activation energy	
R	Gas constant	j/mol.K
E'g	Storage modulus in glassy region	
E'r	Storage modulus in rubbery region	
Vs	separation speed	
Dr	difference between densities	
h	fluid kinematic viscosity	

R	radius of particles in fluid	
Cd	drag coefficient	
h_l	head loss due to friction	
D	mould pipe diameter	
F	Spiral length	
μ	Coefficient of friction	
P	Pressure	Bar
ρ	Density	kg/m3
g	gravitational constant	m/s^2
Vf	Flow velocity	
Vs	separation Velocity	
E'	Storage Modulus	
E''	Loss modulus	

List of Abbreviations

PP	Polypropelyne
PE	Polyethylene
PLA	Poly Lactic acid
PCL	Polycaprolactone
PBS	polybutylebe succinate
PU	Polyurethane
PES	Polyethersulfone
PHB	polyhydroxybutyrate
AcC	Acetyl cellulose
PET	Polyethylenetetraphthalate
PC	Polycarbonate
PBT	Polybutylene terephthalate
FRP	Fiber reinforced plastics
NFTC	Natural fibers thermoplastic composites
TGA	thermal gravimetric analysis
DSC	differential scanning calorimetry
DMA	dynamic mechanical analysis
AR	aspect ratio
GHG	greenhouse gases
MMR	Monitoring Mechanism Regulation
3R	Reduce, Reuse and Recycle
NFC	natural fibers composites
WPC	wood plastic composite
Mw	Molecular weight
MWD	molecular weightr distribution
Mn	number average molecular weight
MA-g-PP	Maleic anhydride grafted polypropylene
PP-H	polypropylene compound with 30% hemp
PP-S	polypropylene compound with 30% sisal
FTIR	fourier transformation infrared sprectroscopy
MRR	Modulus of Retention Ratio
MMRR	Modulus of Retention Ratio
MFR	Melt Flow Rate

Table of contents

1 Introduction and Motivation

1.1 Introduction

1.1.1 Potential of natural fibers as reinforcing fibers

Plastics and polymer composite industry have gained a critical reputation regarding the environmental issues for being responsible of environmental problems such as the climate change, energy resources scarcity and the increasing hazardous contaminated landfills which are saturated with degradation remnants or even toxic gases. As an effective and practical approach to reduce the negative impact of polymer compounds, the introduction of natural fibers as reinforcements in engineering and industrial products is considered the most reasonable and economical environmental friendly option. Natural fibers are well known for their technical applications over centuries in various forms from complicated structures like ships and boats and war instruments from catapults to simple constructions like arcs and finally simple applications like flags and sails [Men92].

For modern industrial applications, natural fibers are considered very important candidate for their attractive characteristics such as economical price, low density, and lower abrasion in addition to their very high energy saving potential [Cic10]. Natural fibers require 300 times less energy to be produced than synthetic fibers. On the other hand, the inconsistency of their mechanical properties due to the variations in the length and diameter of the fibers makes it very difficult to predict the resulting mechanical properties of the compounds. This is considered the main technical drawback of the natural fibers.

Despite of this, natural fibers are widely implemented in several industrial sectors such as automotive and construction. Generally, the most applicable types of natural fibers for industrial purposes in the market are the bast (e.g., flax, hemp, kenaf…etc.) and leaf (e.g., sisal, abaca…etc.) fibers. However, the incomplete characterization of the rheological behavior of such composites hinders their marketing and further applications. [Ram14a]

1.1.2 Challenges facing the Recycling of NFTC

Despite the questions raised about the feasibility of implementation of NFTC in modern applications, their market keeps growing exponentially. This is attributed to their high recycling potential which abides with the governmental, regional and world legislations. The recycling of materials used in industrial applications / products is a very vital topic at the time being. The urgency of many current environmental problems such as increased emission of CO_2, the Ozone depletion and the continuous demolishing of rainforests, led to the growing attention towards recycling.

The term “Recycling” implies the conversion of waste materials into new products with reproducible properties to avoid loss of useful material, reduce the energy consumption, lower the greenhouse gas emissions and decrease the air, water and land pollution. Although the global objective is to 100% recycle the plastics’ wastes,

the fact is that the wastes are not all recyclable. The post treatment of the plastic wastes is divided into recycling, energy recovery and land filling. Figure 1-1 describes the waste post treatment shares in the European countries [Pla15a].

The materials subjected to recycling are classified either to internal (pre-consumer) or external (post-consumer) sources of scraps. Internal scrap means internal rejected materials in the production sites due to any deviations. However, the composition of the material is under control. Whereas the external scrap materials are either controlled material of end-of-life products like computer cases or collections of materials from various sources with un-controlled composition.

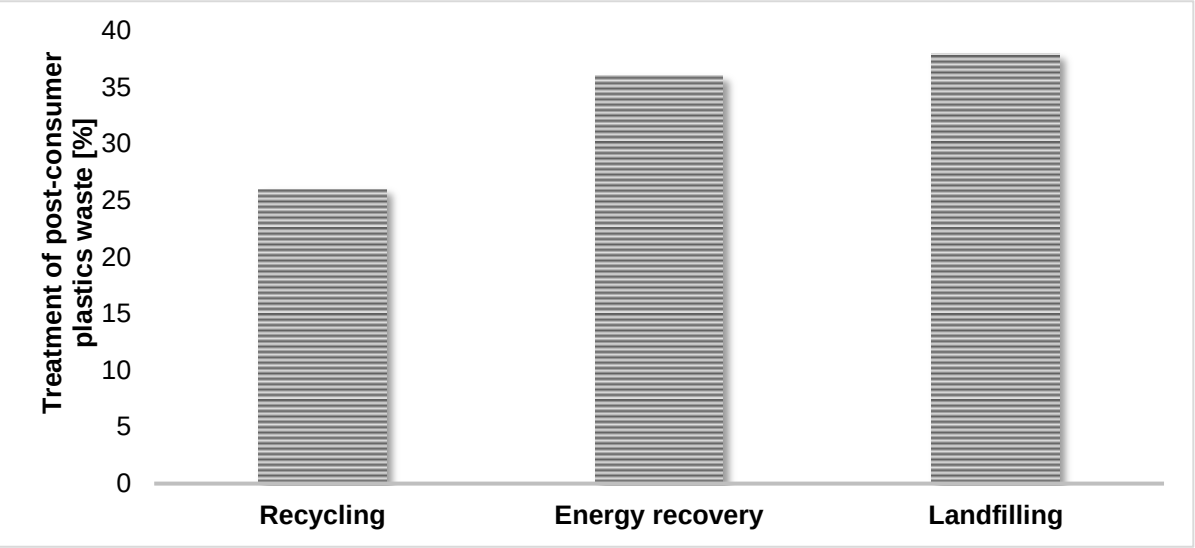

Figure 1-1: Treatment of post-consumer plastics waste in the EU27+Norway and Switzerland

Recycling is a key component of modern waste reduction and is the third component of the 3R "Reduce, Reuse and Recycle" waste hierarchy in order to get the maximum practical benefits from the material starting by the decrease in the consumption amount. Otherwise, when the material is not anymore recyclable, it is either incinerated for energy recovery or safe disposed according to the European directive 2008/98/EC [The08]. The 3R is the basis of the actual waste management system explained in [Wor14] and simplified in Figure 1-2. The Waste disposal raised another problem which is the limitation of landfills, usually needed for non-recyclable items like hybrid materials for example [Men92]. Therefore, the legislations [The13] concerning the monitoring and reporting greenhouse gases (GHG), provide a new Monitoring Mechanism Regulation to make the whole disposal and incineration process more expensive. This new regulation aims to stabilize atmospheric concentrations of GHG and consequently prevent dangerous climate changes.

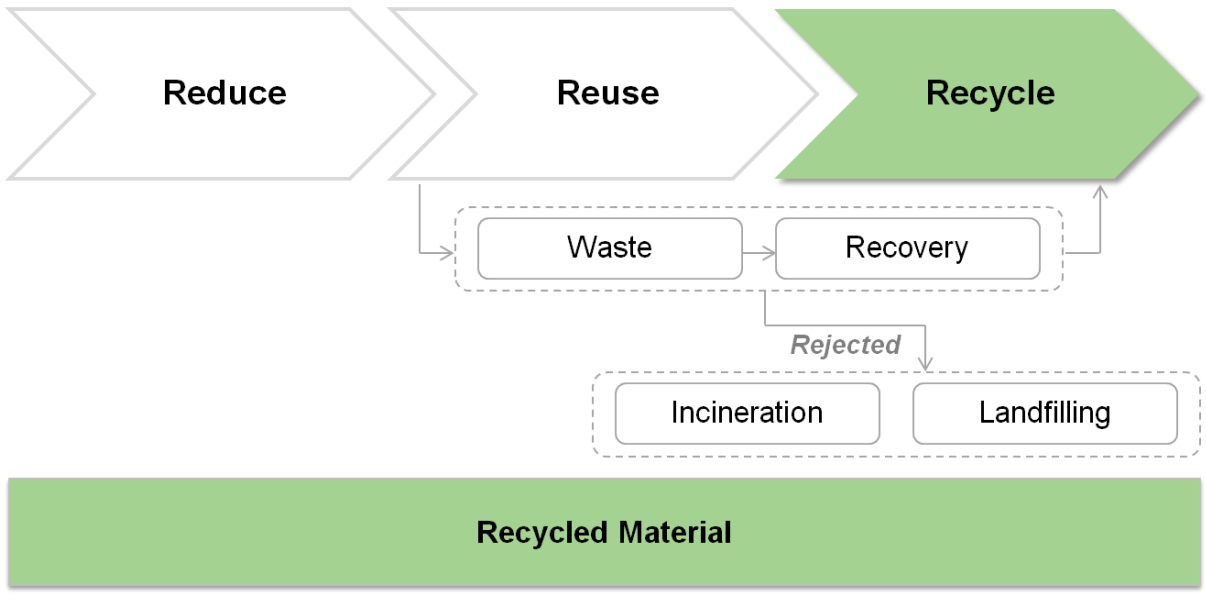

Figure 1-2: Waste management chain according to [Wor14]

1.2 Motivation

In the modern industry and especially automotive industry in Europe, natural fibers are playing an increasingly important role in the production of passengers' cars. As reported in [Dam13], in 2011 each European car contained at least 1.9 kg of natural fibers whereas in Germany due to the high environmentally awareness the natural fibers content reached up to 3.5 kg per car. Nowadays, for example the Mercedes-Benz A and B classes contain an average of 33 kg of natural and wood fibers composites in 26 different parts of the car. This shows the tremendously increasing implementation of natural fibers as quality environmental friendly engineering fibers. This huge amount of NFTC is expected to come back as end-of-life products in the near future.

Despite of that, recycling of natural fibers composites hasn't attracted much attention from researchers till the current time. Meanwhile, many investigations are carried out on recycling other synthetic fibers specially carbon fibers due to its high manufacturing costs and its industrial importance. The main concerns regarding the recycled materials are generally the drop in the mechanical properties and the unpredicted physical characteristics. These drawbacks of recycling are attributed to the different recycling methods as well as the inconsistency in the properties of the recycled materials.

Since the research in the field of NFTC is relatively new, to simplify the problem and to avoid the effect of the material variation spectrum, this work focuses only on internal injection molded materials. Thermoplastic commodity plastic namely polypropylene (PP) is the thermoplastic of interest. This is attributed to the fact that PP represents the main injection-molded thermoplastic of the 15000 tons production of NFTC in Europe [Dam13].

The aim of this research is to explore the effect of recycling natural fibers thermoplastic composites (NFTC) on the evolution of fibers morphology which in turn affects the viscosity and flowability to develop an understanding to the resulting mechanical and physical properties after recycling. The considered factors in this research work are: number of the reprocessing cycles, fiber type, fiber form and shape.

1.3 Methodical approach

As previously discussed, the 3R policy approach is the modern market trend to face the increasing environmental problems, this work focuses on one aspect of this approach namely the recycling of natural fibers which is not thoroughly investigated till now. Figure 1-3 illustrates the classification of this research in the 3R policy.

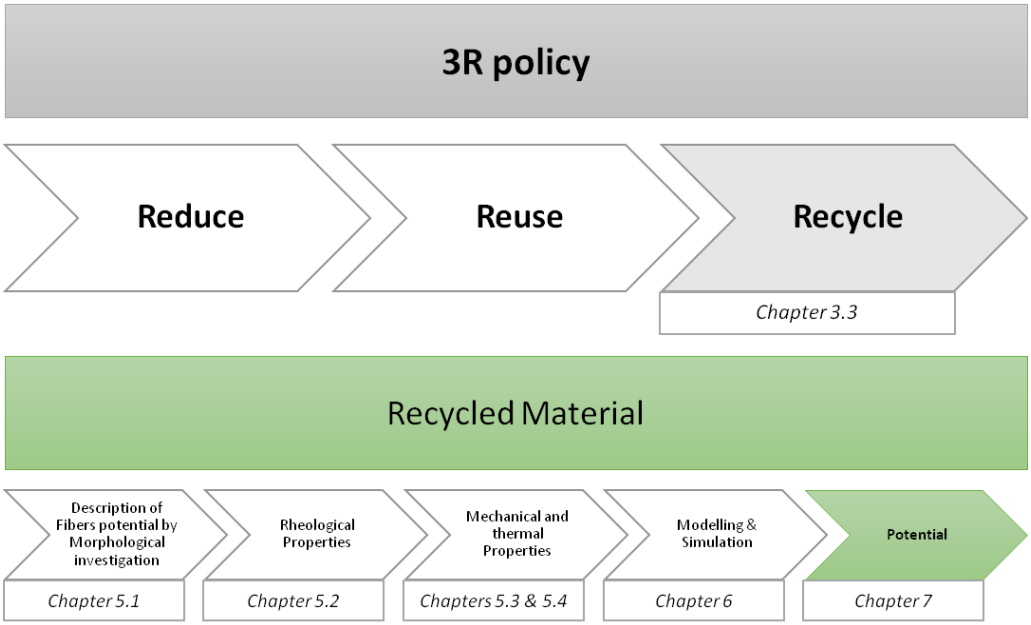

Figure 1-3: Classification of the presented work in the 3R chain policy

Compounds in this research are investigated for:

- Morphological properties
- Rheological Properties
- Mechanical properties
- Thermal Properties

A thorough analysis is carried out to determine the potential of the compounds for recycling.

Findings from this research are presented in a methodical way so that it would be possible to be transferred to other recycling cases and provide the required fundamentals and thus the best utilization of the research work could be achieved.

2 State of the art

2.1 Recycling of polymers

The term “Recycling” denotes to the process of waste minimization in which the produced or consumed materials are re-oriented from the waste stream track to the original track or to a different use. Recycling of polymers depends on different factors [Hop09] namely the type of the polymer (thermoplastic, thermosetting, fiber, adhesive, coatings), the application type (electrical, vehicle, construction), the quantity of the polymers to be recycled, the degree of its contamination and the available technologies for recycling.

The global production of plastics in the world and Europe is shown in Figure 2-1. The production of plastics is more than 300 million tons and the European share is almost 20% with 58 million tons. The topic of recycling is more developed in the European countries. However, the recycling activities are not alike among all European countries; Germany and Scandinavian countries show more interest in plastics’ sorting more than other countries.

The amount of plastics reported to undergo recycling processes is less than 45%. Recycling in Europe lies in the 25.1-million-ton level according to 2011 statistics with an increasing trend of 2.4 % per year in average. As seen in Figure 2-2, 10.3 million tons are completely disposed while the others can be recovered [Pla12]. The land filling disposed plastics are decreasing because of the efforts done in increasing the recovered share. The recovered plastics are the sum of the recycling and the energy recovery.

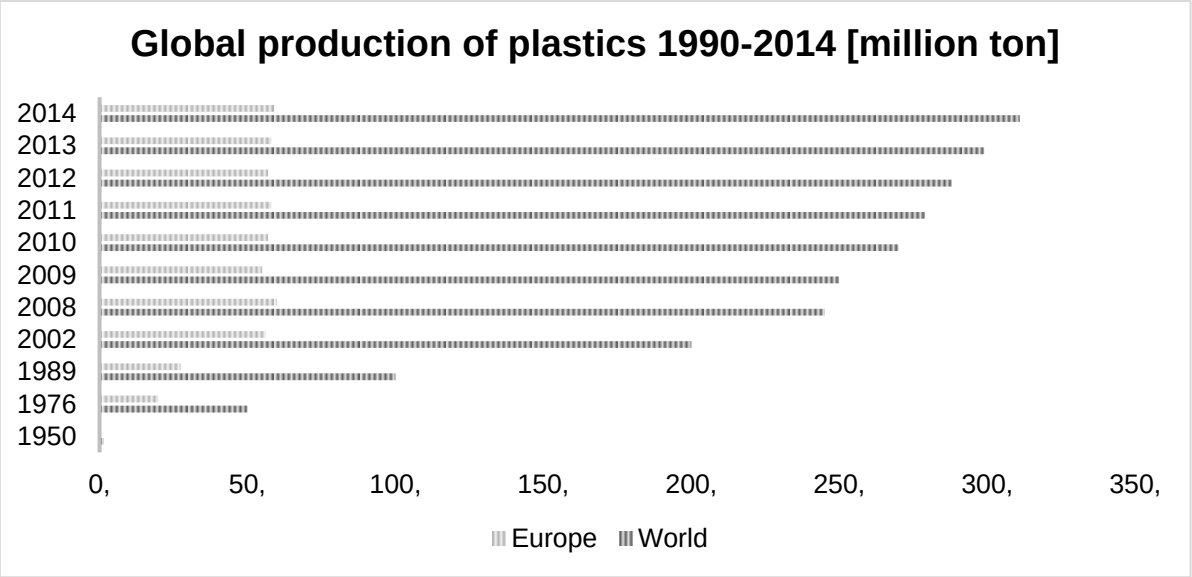

Figure 2-1: Global and Europe production of plastics till 2014 [Pla15b]

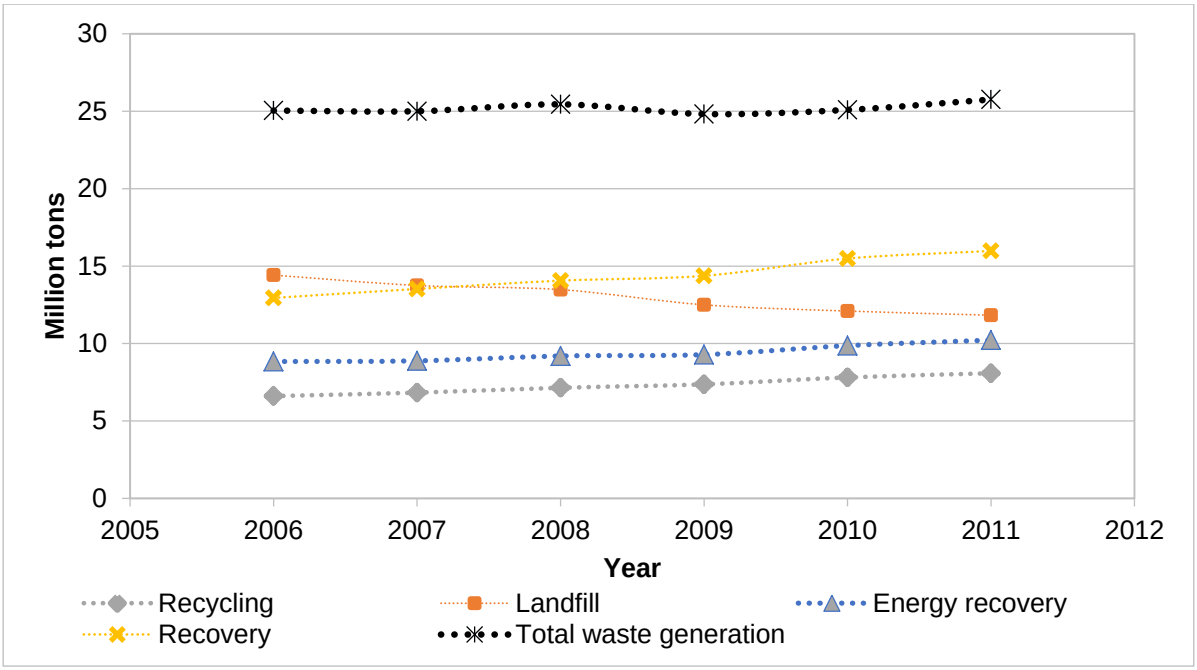

Figure 2-2: Total plastics waste recycling and recovery 2006 – 2011 [Pla12]

According to the data mentioned in the reviews of [Pla10] and [Ign14], the collected material for recycling consists of almost 70% packaging products. They are mainly thermoplastics (> 90%), which in turn constitute of 55% polyolefins such as polypropylene (PP) and polyethylene (PE).

2.2 Recycling methods

The selection of the recycling method depends on:

Matrix type of the composite: whether it is thermoset or thermoplastic. Remolding of thermoset-matrix is not possible. Therefore, if not recovered by solvolysis or pyrolysis, they are usually mechanically recycled by grinding and milling to produce cheap fillers.

- *Purity of the polymer matrix in the composite:* whether it is reinforced with fillers or not, or whether the recycling pool is a mixture of different types of polymers.

The following section describes briefly the up-to-date of current techniques for recycling:

2.2.1 Mechanical recycling

It is meant by mechanical recycling to grind the material using one of the mechanical processes like milling, crushing or shredding. Mechanical recycling of thermoplastic polymers results in outputs which undergo subsequent hot molding or shear processing like injection molding or extrusion. Mechanical techniques are entirely classified according to the expected level of polymer contamination or the product life stage (before or after consumption).

- ***Primary mechanical recycling*** is limited to the uncontaminated thermoplastic products which are produced by the manufacturer himself. The reuse of these products does not require preparatory steps like separation or purification [Al-10a], [Bai11]. Thermal stability is essential for the recycled polymers candidates for primary mechanical recycling. Therefore, PVC, PET and polyolefins like PP and PE are the most popular thermoplastics for this recycling method.
- ***Secondary mechanical recycling*** is expanded to cover the consumed products (out of the manufacturer premises) such as packages, plastic bags and detergent containers. Here the secondary recycling requires an additional purification step. After the mechanical step, solvents like toluene and petroleum ether [Had12] are implemented to dissolve the polymer and re-precipitate it again. This prerequisite process of purification can lead to chain scissions, lower molecular weight and hence a reduction in mechanical properties. However, this is not the main reason of polymer degradation. The efficiency of the purifying process defines the level of contamination in the main polymer by another one (i.e. PET in PVC). Thus results in reduced mechanical properties, change in odor and color of the recycled material [Hop09]. Some additives are proposed to maintain the chain length and target special properties in the final recycled product. For example, to enhance the long-term stability Recyclostab 451 is usually applied for stabilizing battery cases. Light stabilizers such as Recyclossorb 550 in addition to processing and long-term stabilizers, are used for PE pellets, and HDPE applications such as bottle crates and profiles. Commercial light stabilizers like Recycloblend 660 [Kar03] which contain antioxidants are used for polyolefin recycling, to keep constant melt flow rate to maintain a stable flow behavior.

2.2.2 Chemical recycling

Chemical recycling, known also as feedstock or tertiary recycling, involves elevated temperature process to break the structure bonds in the polymer to be recycled [Bre12]. Chemical recycling has different forms such as hydrolysis, pyrolysis, hydrocracking and gasification [Ign14].

Hydrolysis is the breaking of large molecules to smaller ones in the presence of water. An example for this process in recycling is the hydrolysis depolymerization of condensation polymers like PLA, PET and PU [Agu99]. Thus, the resulting monomers can be reused in the synthesis of new polymers. Pyrolysis is carried out in an oxygen-lean environment to break large molecules into smaller ones by the heat effect. Pyrolysis is suitable in dealing with heterogeneous waste or residuals of automotive parts (after being shredded) [Bre12] or the used car tires which are converted into carbon black. Pyrolysis process transforms plastics into gases, a mixed liquid of hydrocarbons and a solid char.

The high molecular weight products, due to the absence of hydrogen and oxygen, are refined to produce high added value petrochemical feedstock as listed in Table 2-1.

Table 2-1. Recycling products out of pyrolysis [Sch01] [Pan10]

Polymer	Low-temperature products	High-temperature products
PE	waxes, paraffin, oils, α-olefins	Gases, light oils
PP	Vaseline, olefins	Gases, light oils
PVC	HCl, benzene	Toluene
PS	Styrene	Styrene
PMMA	Methyl methacrylate (MMA)	Tetrafluoroethylene (TFE)
PTFE	Monomers	TFE
PET	Benzoic acid, vinyl terephthalate	TFE
PA-6	Caprolactam	Aramid (aromatic polyamides)

Hydrocracking is the conversion of high boiling chemicals in crude oil to low boiling point such as gasoline or jet fuel, using a high partial pressure of hydrogen [Bre12]. Gasification process is the exposure of carbon containing material such as coal and biomass to a controlled amount of air or oxygen, so that the molecules are broken to carbon monoxide, hydrogen and other gases [Al-15].

2.2.3 Biological recycling (Degradation)

The term recycling here is used in because large molecules are also down broken to smaller ones and hence the waste materials can be returned back to the production cycle [Sco02]. Bacteria [Cho11], microorganisms and fungi [Sch06] can assist in polymer degradation by the aid of air and water [Mül13]. Biosynthesized polymers like cellulose, chitin and PLA (poly Lactic acid) can be biodegraded under a combination of different processing parameters (pressure, presence of certain microorganisms, PH value) to compost [Dav05].

It is worthy here to note that bioplastics are not all biodegradable as shown in Figure 2-3 [Tok09]. Plastics like PCL (polycaprolactone) and PBS (polybutylebe succinate) can be made out of petrochemical products but they are biodegradable. On the other side, nylon, acetyl cellulose and PE are considered non-biodegradable although they are made out of biomasses. However, acetyl cellulose can be converted into a degradable material depending on the acetylation grade. Similarly, PE with its wide-spread applications can be degraded initially using abiotic factors (temperature and UV light) by the oxidation of polyethylene chains. Then, the size of polyethylene molecules decreases to an acceptable range for the enzymatic action (typically from 10 to 50 microns) [Res14].

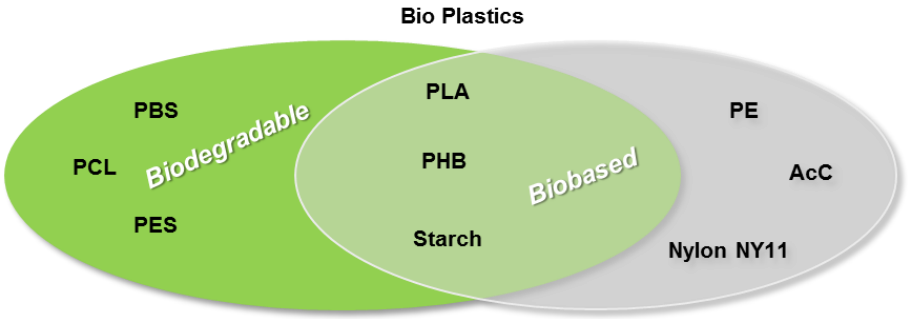

Figure 2-3: Bio-plastics comprised of biodegradable plastics and bio-based plastics

2.2.4 Incineration

This is the last way to get an added value from the disposable plastics before landfilling. That's why it is called quaternary recycling as shown in Figure 2-4. Actually, this is the first approach and still the most popular for plastics conversion even in many developed countries. Incineration is suitable for processing of mixed and heavily contaminated wastes, which cannot be processed by any of the previously stated recycling methods [Al-10]. The energy gained by incineration is considered a dense fuel source. This takes the form of heat and electricity in civil buildings and even in industrial plants like cement furnaces, chemicals' incineration facilities, and melting furnaces for metallic scrap [Ign14]. Incineration method is also characterized with the reduction of the waste volume up to 1% of its original size. It is highly needed to deal with the most hazardous wastes like the toxic, contagious and medical wastes.

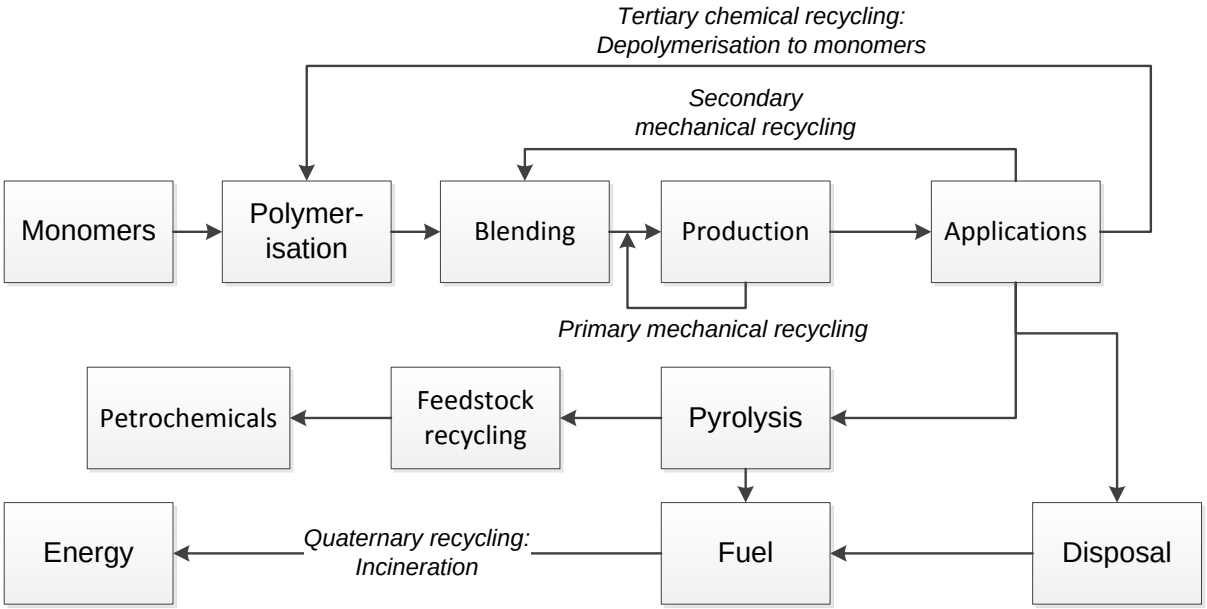

Figure 2-4: Schematic showing the alternatives for recycling methods quoted from [Ign14], [Al-10]

2.3 Recycling of fiber reinforced thermoplastics

Polymer composites filled with particles or reinforced with fibers represent a challenge in the recycling process. The target is not only to retrieve the material for

reuse in the same application but also to extract the fillers or the fibers if the polymer is not used anymore.

Figure 2-5 shows the recycling processes for fiber reinforced polymers (FRP). Mechanical method, as mentioned before, helps in obtaining fillers (in case of thermoset composites) or granulates ready for further thermal shear processes like extrusion and injection molding (in case of thermoplastic composites). It is a common practice to add virgin raw material to the recycling process [Mor12]. It is worth to note here that mechanical recycling has only an effect on the long fiber's length. This means that for short fibers composites, no difference is to be expected.

Chemical recycling using sovolysis method is classified to low temperature or super critical temperature [Mor12] at temperatures higher than 400°C [Oli15]. Sovolysis method is developed mainly to extract the expensive carbon fibers from the epoxy matrix of the carbon fiber composites, which have a lot of limitations to be landfilled. The process is very expensive and environmentally polluting as it depends on dissolving the entire matrix like PET, PC, nylon and PU using environmentally unfriendly chemicals. Solvolysis is a depolymerisation process like alcoholysis, hydrolysis, acidolysis and amniolysis that produce oligomers or monomers by breaking the C-X bonds. Where X represents the heteroatom such as O, N, P, S and halogens [Aza03].

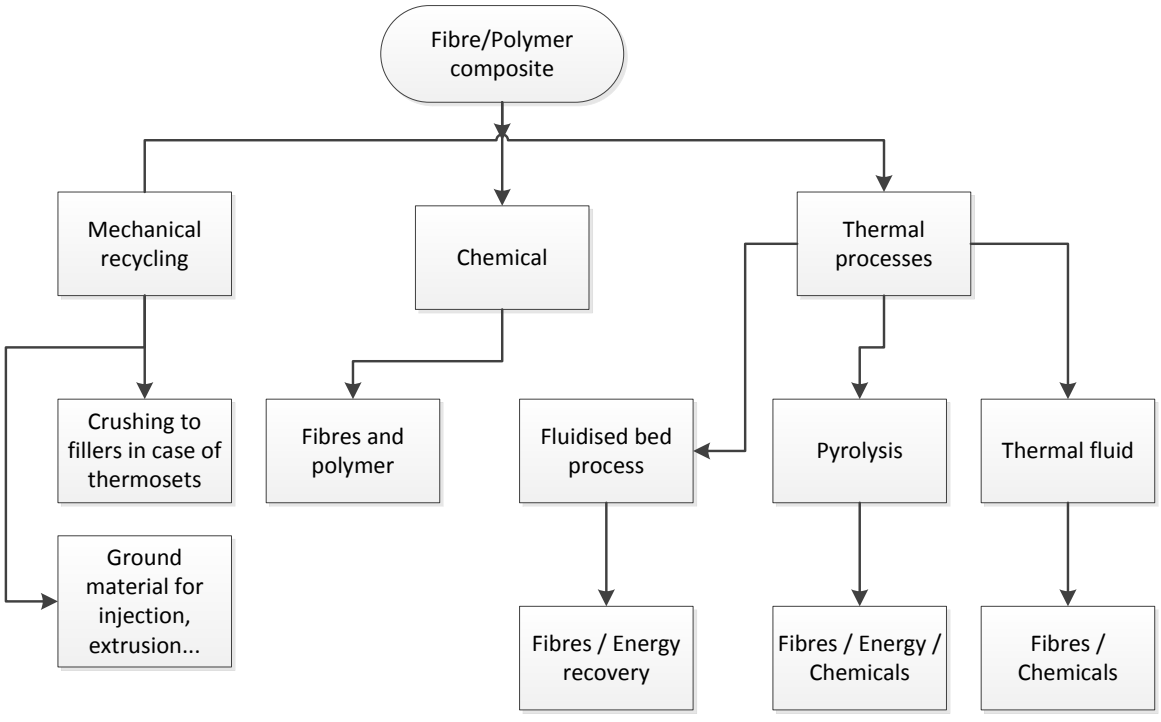

Figure 2-5: Schematic showing the recycling methods of FRP adapted from [Oth09] [Pic06]

Thermal processes like fluidized bed process or pyrolysis depend on burning the matrix to regain the fibers. Figure 2-6 shows the concept of the fluidized bed process where the carbon fibers can be separated from the burning matrix [Pic06].

Thermoplastic matrix is considered an easy recyclable matrix and hence besides chemical and thermal recycling, re-melting and remolding is the most popular recycling option which produces granules or pellets for injection purposes. This method is mostly recommended since it preserves the fiber from extensive thermal or chemical damages especially when reinforced with natural fibers.

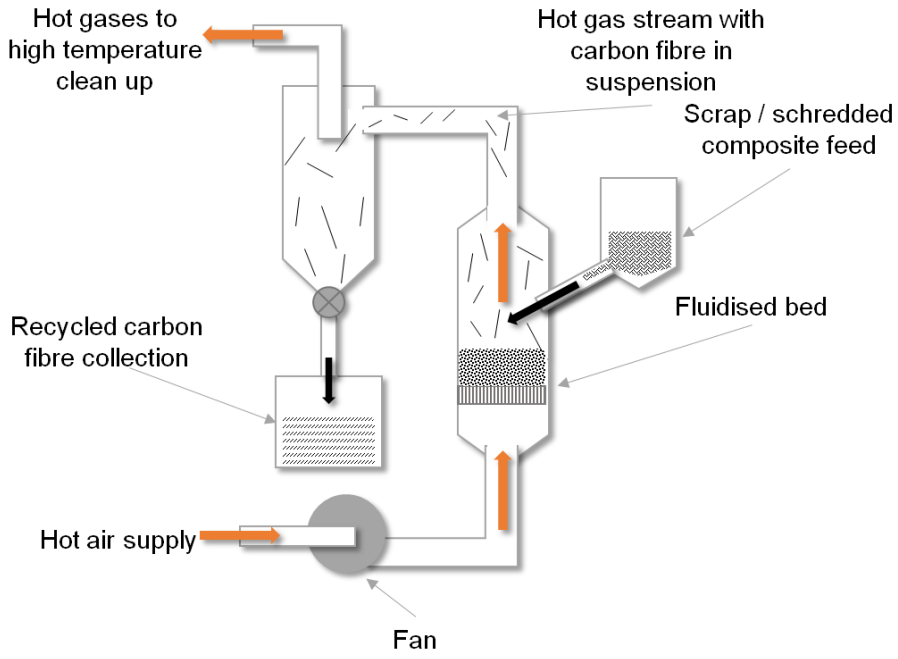

Figure 2-6: Schematic showing the principle of the fluidized bed process [Pic06]

Despite the wide establishment of synthetic fibers recycling procedures, recycling of natural fiber thermoplastic composites does not receive the expected attention due to the following reasons:

- The low size of production with respect to synthetic fiber thermoplastic composites. Bio composites (natural fiber and wood polymer composites) represent 352000 tons which is about 15% of the whole production of FRP (reinforced with synthetic fibers like carbon and glass fibers as well as the NFC and WPC) according to [Car14]
- Natural fibers do not represent a problem for the environment. Actually, they are selected because of their safe degradation, low price and reduced burden of needed energy for production (low carbon footprint).

However, it is expected that the market of NFC will remarkably increase to 6.5 billion USD in 2021 [Mar16]. Therefore, the need to establish a reliable method of recycling this type of engineering NFC becomes now a vital topic.

This thesis focuses on the NFTC. Taking into consideration the scarcity in the research of NFTC recycling, according to [Bal11], [Al-15], [Bou07], [Bou09], [Bou08], there are some questions that are arising with the increasing production of NFTC like:

- Reuse of thermoplastic composites reinforced with synthetic fibers is applicable especially in the primary and secondary mechanical recycling. In the secondary mechanical recycling, some sort of thermal degradation can take place in the host matrix by decreasing the molecular weight. But the synthetic fibers are not expected to be thermally affected. On the other side, natural fibers are expected to decompose under thermal effect.
- Similarly, the length of the synthetic fiber is affected by the recycling processes as reported in [Col15]. This is believed to depend on the original fiber size and fiber content. The shortening of synthetic fibers takes place through fibers' fragmentation but in case of natural fibers, it is believed to take place in other forms like fiber splicing besides to the fragmentation as shown in Figure 2-7. Also fiber size can be reduced due to the thermal degradation or volatilization of some fiber constituents.

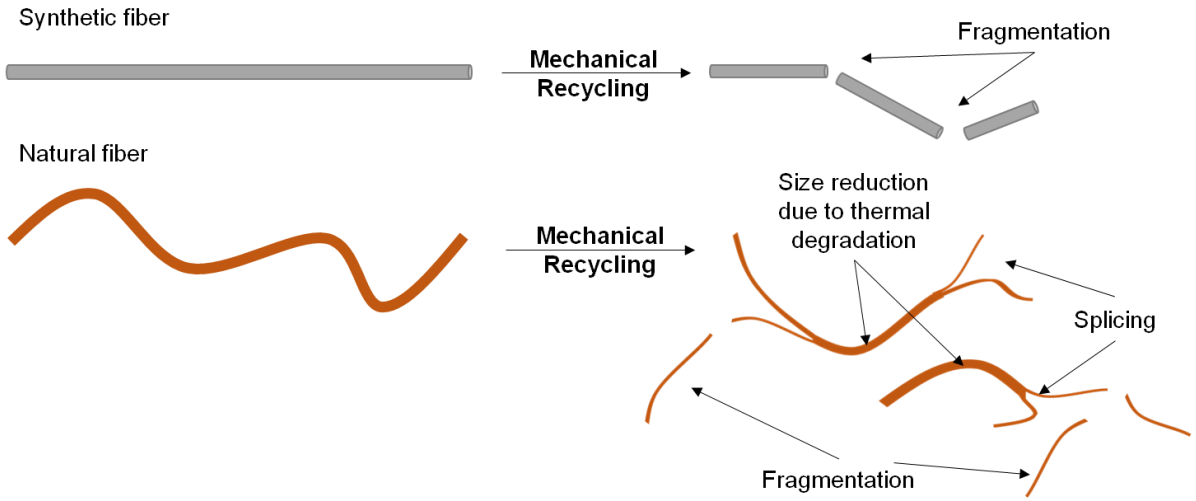

Figure 2-7: Schematic showing the fiber fragmentation experienced by synthetic fiber and fragmentation/ splicing/ thermal degradation by natural fiber

2.4 Effect of recycling on composite constituents and properties

This part considers the effect of the recycling process and the corresponding changes taking place in the composite constituents (thermoplastic matrix and fibers) regarding the mechanical, rheological, thermal properties as well as geometrical features.

2.4.1 Impact on thermoplastic matrix

The effect of recycling on the thermoplastic matrix is not a simple linear relation of degrading properties with increasing processing steps. The main influence of recycling according to [Aur01] is the reduction of the melt viscosity due to the decrease in the molecular weight. Molecular weight reduction or in other words shorter polymer chains of recycled PP lead to several significant changes in the compounds' crystallization rates, crystallinity as well as melting temperature in comparison to the original non-recycled PP.

As reported by [Cic17] also mechanical properties such as Elastic modulus and yield strength are affected by recycling, where an improvement in both flexural modulus and strength with the increase of number of recycling steps is observed for PP/Hemp compounds with 20-wt. % up to 3 cycles. On the contrary, the impact strength is negatively affected by recycling.

Similarly, according to [Inc99], the viscosity of homo-polymer PP decreases as a result of the reduction of the weight average molecular weight (M_w) and the narrowing of the molecular weight distribution (MWD), described by the quotient of M_w to the number average molecular weight (M_n). However, the mechanical behavior behaves differently [Inc99]. E-modulus here doesn't increase with the recycling number as in [Cic17] and [Aur01] but decreases after one cycle and remains almost stable. The yield stress shows the same behavior. Elongation at break exhibits a close trend to [Aur01], as it decreases with the increase of recycling number. The change in M_w, M_n and the mechanical properties with respect to the recycling up to the seventh cycle is listed in Table 2-2. Similar reaction to [Inc99] in yield stress and elongation is reported in [Kur15] with Poly(butylene terephthalate)/polycarbonate (PBT/PC) binary blends exposed to consecutive five recycling cycles. Viscosity reduction with more recycling is proved by the measurement of melt flow index (MFI) where higher MFI is an evidence of low viscosity.

Table 2-2. Development of Mw and the corresponding mechanical properties at different recycling number [Inc99]

Recycling #	**η (Pa.s)**	**Mw**	**Mn**	**Mw/Mn**	**E [MPa]**	**σ_y [MPa]**	**ε_b [%]**
0 (virgin PP)	7371	537000	61000	8.8	523	11.3	373
1	7102	--	--	--	610	10.6	350
2	6716	--	--	--	600	10.5	370
3	5947	420000	60400	7	610	10.1	351
5	4607	--	--	--	611	11.2	325
7	4437	366500	58000	6.3	615	9.4	309

Regarding the effect of recycling on thermoplastic matrix in case of using natural fibers; Le Duigo [Le 08], in a pioneer work, studied the recycling of bio composites namely flax/ poly (L-lactide) at 20 and 30 wt.% flax loading. The molecular weight is measured and found to decrease remarkably from 220000 to almost 85000 g/mole after 6 cycles of reprocessing. With the implementation of fibers, the molecular weight decreases more to 25000 g/mole in case of 30 % flax fiber as shown in Figure 2-8. This extreme reduction is attributed mainly to the hydraulic degradation of PLLA especially with the presence of water in flax fibers and the application of high temperature conditions. However, other types of degradation are also expected to occur such as de-polymerization, radical and non-radical reactions, cis-elimination, trans-esterification besides to the mechanical degradation due to the shearing processes.

A same phenomenon was observed by Kozderka et al. [Koz17] for the PP matrix. A decrease in M_w from 166000 to 69000 g/mol after 6 cycles in the PP matrix was reported. This deterioration of the molecular weight is known as ''Cavitation'' where chain scissions occur in parallel to increasing embrittlement of the amorphous matrix as a result of the thermal and mechanical stresses induced by recycling.

This high degradation in the molecular weight after recycling leads to a corresponding reduction in viscosity. The polymer reinforced with fibers show higher viscosity than non-reinforced ones. But it is worthy to note that the viscosity stabilization level shows a local minimum at the fifth cycle. This is explained in terms of the increasingly generated fibers (due to successive shortening or splitting / splicing) which hinder the mobility of PLLA chains [Le 08].

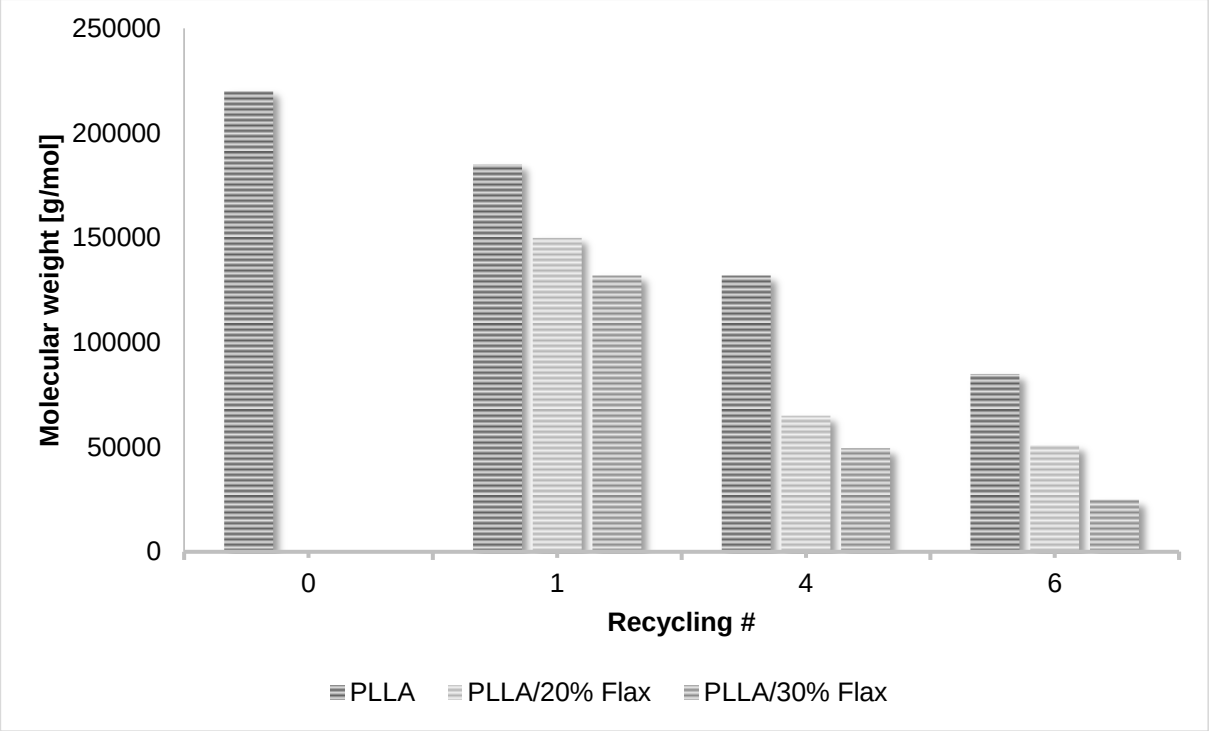

Figure 2-8: Effect of recycling number on the molecular weight of PLLA in flax/ poly (L-lactide) composites [Le 08]

In another work by Bourmaud et al. [Bou07], the effect of recycling PP-Hemp and PP-Sisal compounds (70% loading) showed a remarkable decrease in the melt viscosity of both compounds by 73% and 65% respectively. The decrease in the viscosity was denoted to two factors; the first is the scissions in the polymer chains as a result of the shearing stresses applied during the mechanical recycling processes. The second factor was the fibers' shortening which is discussed in the following section.

2.4.2 Impact on fibers

As mentioned in 2.3, recycling processes for the thermoplastic compounds are usually performed for the synthetic fiber reinforced thermoplastic compounds. These recycled composites can suffer from the decrease in the mechanical properties after recycling due to the damage and shortening of the fibers which consequently affect the load carrier body in the composite system. Chrysostomou et al [Chr96] reported

that polycarbonate with 20% glass fibers are subjected to five cycles. Cycle number Zero corresponds to the virgin granulates. Out of 500 extracted fibers by combustion at 650°C, the length of the glass fibers is measured microscopically. The mean and the median values show the reduction in the measured value in a negative exponential trend, as seen in Figure 2-9. The recycled fibers show that only the fragmentation mode is taking place. The evidence of the fragmentation is that the mean fiber diameter is the same and the fiber length is decreasing.

In case of natural fibers, the fiber is broken according to different modes as explained and described in Figure 2-7 namely fragmentation and splicing besides to the thermal degradation expressed in fiber thinning. Few literature studies try to describe the influence of recycling on the fiber length and the corresponding aspect ratio such as [Le 08]. As shown in Figure 2-10, the fiber length decreases remarkably in a negative exponential trend. But the remarkable behavior is the reduction of average fiber diameter as shown in Figure 2-11. However, the reduction of the fiber diameter is less than that of the length so the aspect ratio, in Figure 2-12, maintains a similar trend to the development of the fiber length.

The effect of recycling on the fiber length and accordingly the fiber aspect ratio should be correlated with the development of the composite thermal and mechanical properties. However, to achieve better analysis, the following points should be discussed:

- In order to avoid fiber extraction in case of natural fiber, fiber measurement is still limited to time-consuming microscopic work,
- The composite properties are not well analyzed in terms of the fiber shape and the properties of the single fiber,

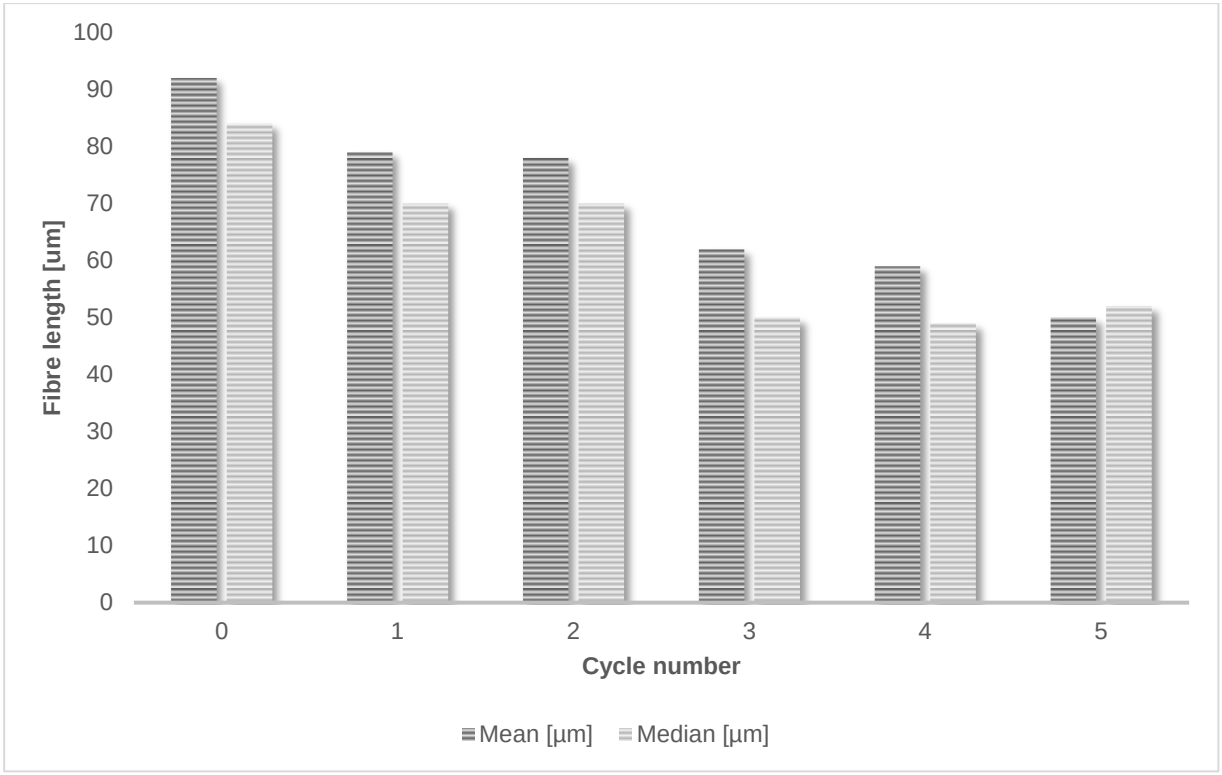

Figure 2-9: Effect of recycling number on the mean and the median fiber length [Chr96]

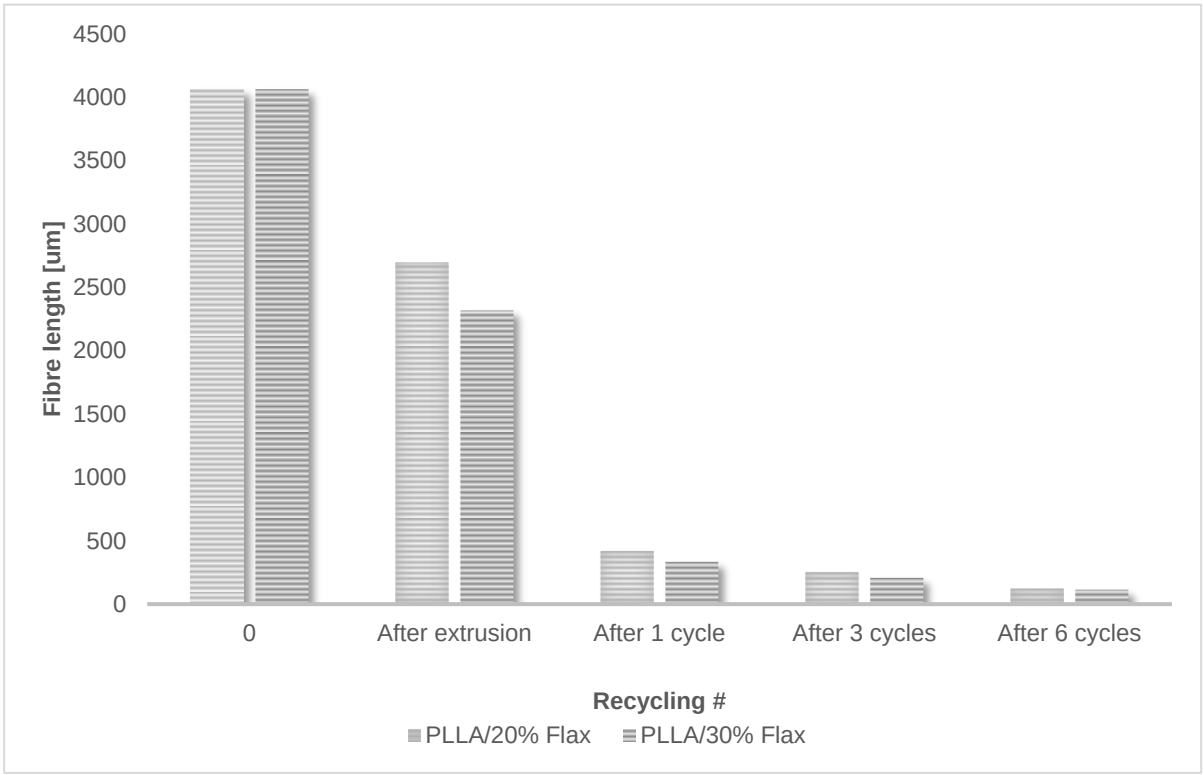

Figure 2-10: Effect of recycling number on the fiber length of flax fiber [Le 08]

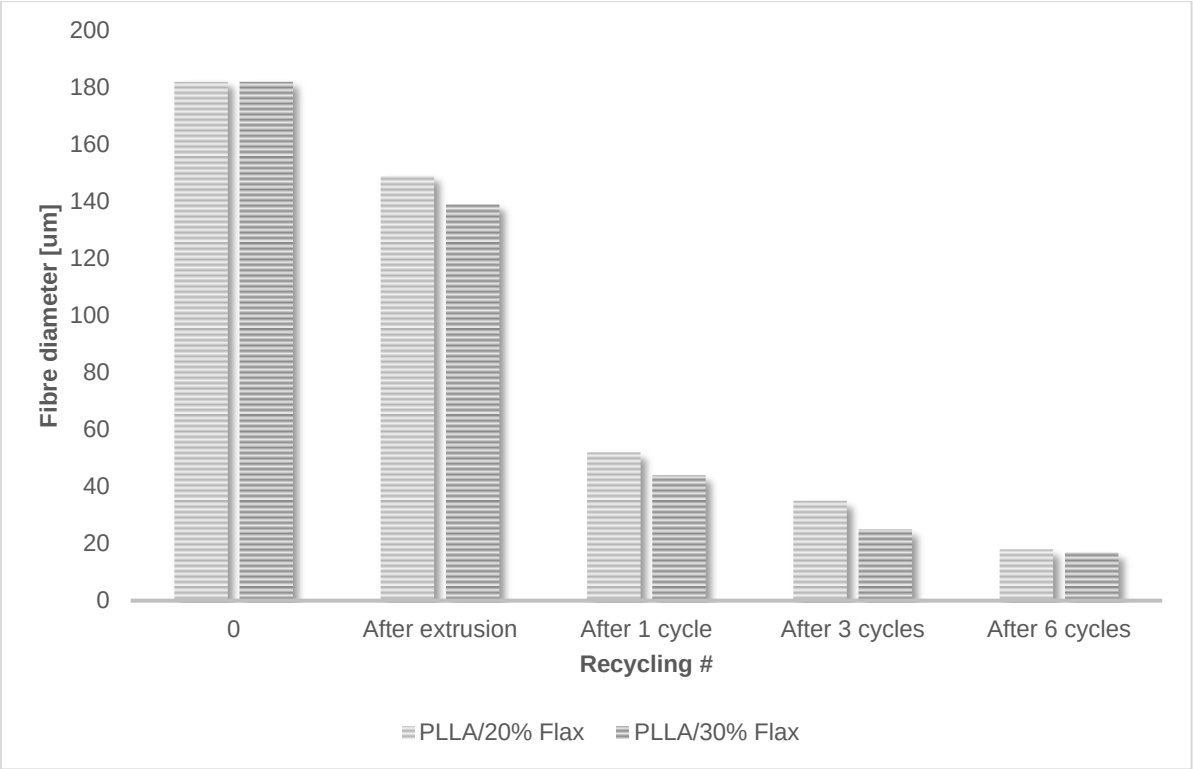

Figure 2-11: Effect of recycling number on the fiber diameter of flax fiber [Le 08]

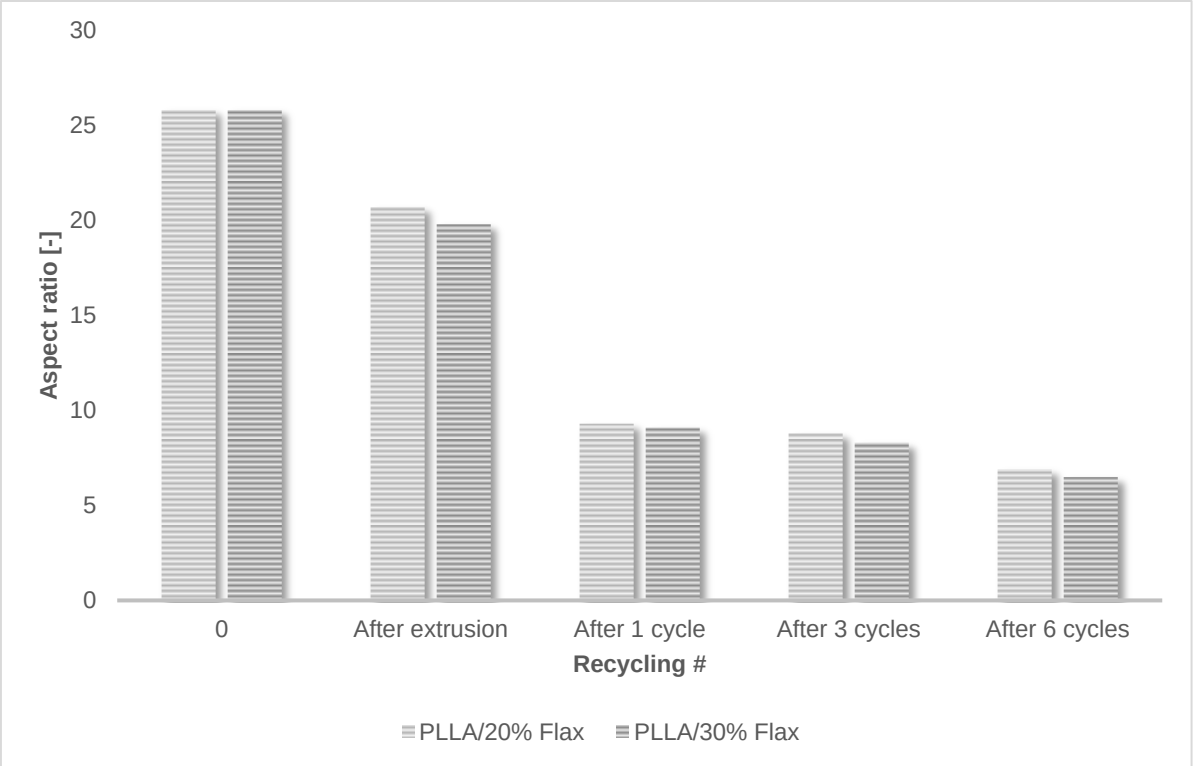

Figure 2-12: Effect of recycling number on the aspect ratio of flax fiber [Le 08]

2.4.3 Impact on thermal properties

Recycling is known to affect the results of the fiber reinforced composites taken out of thermal gravimetric analysis (TGA), differential scanning calorimetry (DSC) and dynamic mechanical analysis (DMA). These properties are namely the glass transition temperature (T_g), crystallization temperature (T_c), melt temperature (T_m), crystallization enthalpy (ΔH_c), melting enthalpy (ΔH_m), crystallinity index (χ), in addition, storage and loss moduli.

Effect of recycling on DMA moduli values for biopolymer matrix (BioFlex) and wood flour is not significant as reported by [Mor12]. The T_g values prove to decrease by recycling of PLLA/flachs as stated in [Le 08] with a significant increase in the crystallinity index. The TGA test of PP/flachs, in presence of a maleic anhydride grafted PP (MA-PP) as a coupling agent, shows a positive effect of recycling.

On the other side, the crystallization enthalpy (due to initiation of more surfaces from fibers or impurities as a result of recycling reduce the critical energy required for nucleation) and the melting temperature decrease by more reprocessing steps. On the contrary, melting enthalpy and crystallization temperature did not show a clear trend by recycling. Similarly, in [Gal95], the crystallization enthalpy for PP decreases as a result of the decrease of the nucleation density of the matrix due to the shortening of the polymer chains. This leads to an increase in the amorphous region on account of the crystalline region in the matrix promoting a better dimensional stability of the PP matrix during solidification.

2.4.4 Impact on mechanical properties

To discuss the impact of recycling on the mechanical properties, the results of [Kur15] will be recalled. The effect of recycling on the tensile strength of the PBT/PC blend with 10% glass fibers in the presence of 5% maleic anhydride compatibilizer is compared to unreinforced blend as shown in Figure 2-13. The reduction in strength in case of the reinforced blend is more prominent. The decrease in strength for the reinforced blend after 5 cycles of recycling is from 84 to 55.7 MPa (33.5%) while the decrease in case of un-reinforced blend is just from 52 to 47.8 MPa (7.8%).

There are two theories to explain this result. First one is the formation of free fiber surfaces without adhesion with the polymer matrix and thus a worse load transfer from matrix to fiber and vice versa is attained [Kur15]. The second theory [El-14a] is the lower effective load transfer due to the shortening of the average fiber length. More fibers will lie below the critical fiber length as shown in Figure 2-14. The effect of fiber length (below and above) the critical length on the fiber length efficiency term ($\eta_{l\sigma}$) is shown in Equation 2-1.

This will affect finally the composite overall strength *as defined in Equation 2- 3.*

$$\eta_{l\sigma} = \begin{cases} 1 - \frac{l_c}{2l} \cdots l \geq l_c \\ \frac{l}{2l_c} \ldots l < l_c \end{cases}$$

Equation 2- 1

'l_c' is the critical fiber length at which the fiber loading efficiency is maximized. It is defined in Equation 2- 2.

$$l_c = \frac{\sigma_f d}{2\tau}$$

Equation 2- 2

σ_f is the fiber strength, d is the fiber diameter and τ is the interfacial shear strength.

$$\sigma_c = \sigma_m (1 - v_f) + \eta_{oE} \eta_{lE} \sigma_f v_f$$

Equation 2- 3

Where subscripts '$_c$', '$_m$' and '$_f$' stand for composite, matrix and fiber respectively, v_f is the fiber volume fraction, 'σ' is strength, 'o' and 'l' stand for orientation and fiber length.

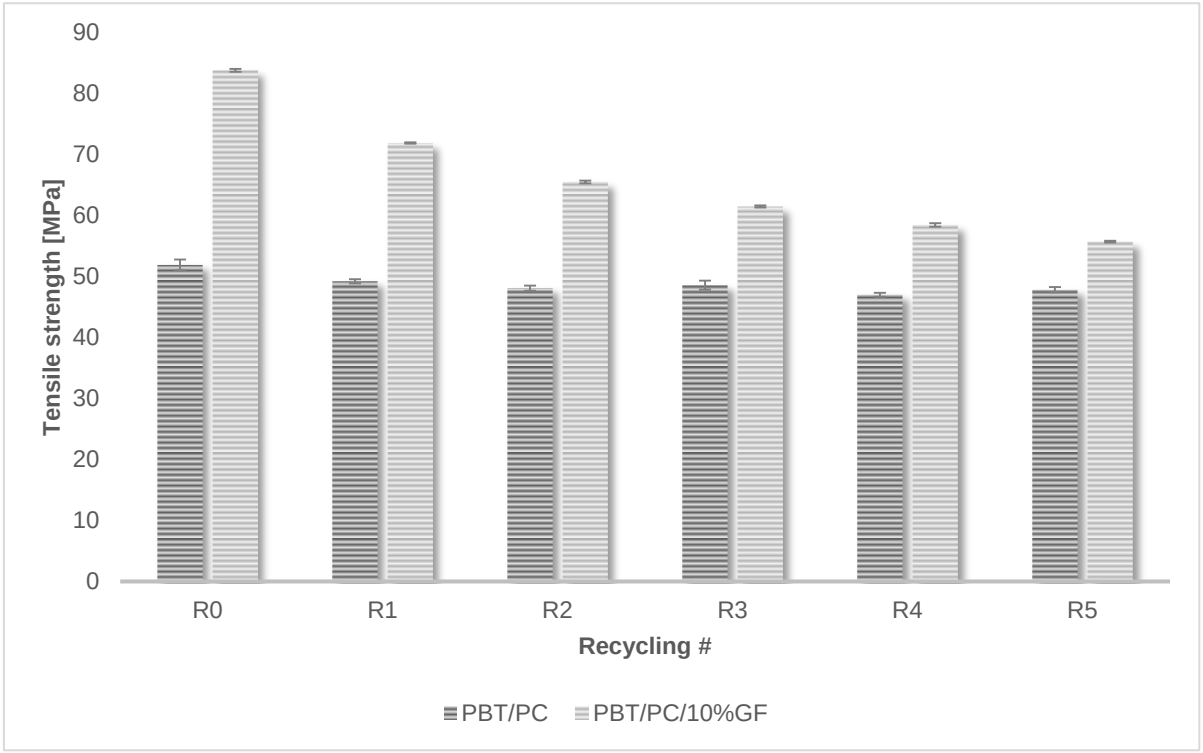

Figure 2-13: Effect of recycling number on the tensile strength of PBT/PC and PBT/PC/10%GF [Kur15]

As explained above and in a series of publications [Ber16], [Ber16], [Fu96], [Pee98], [Cre04], [Ber16], [Amu13], [Amu13], [Yip01], [Nor03], this relation between the fiber length and the resulting mechanical properties are already discussed and proved.

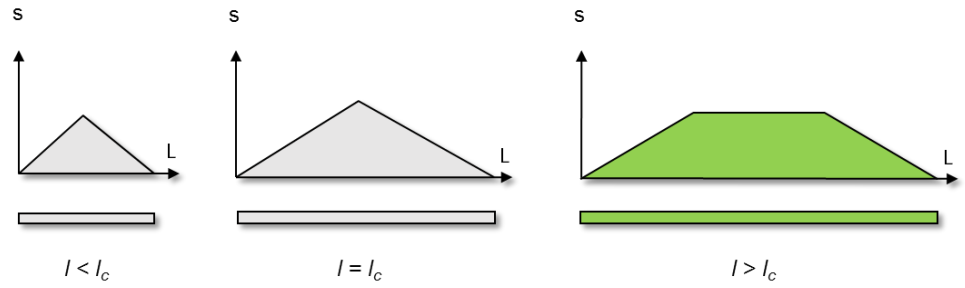

Figure 2-14: Effect of fiber length on the mechanical properties

Concept of the effect of fiber length is generalized by the aspect ratio. Aspect ratio (AR) is the quotient of fiber length to diameter as shown in Equation 2- 4. However, there was no much difference between length and AR concepts because fiber diameter in case of synthetic fibers shows almost consistency.

$$AR = \frac{L_{fibre}}{d_{fibre}}$$ Equation 2- 4

The analytical modeling developed to include the effect of the fiber geometrical distributions in length and diameter and not being limited to certain mean dimensions. This approach has explained the deviation between the experimental results and the expected modeling ones. For instance, Fu [Fu96] found out that to enable the polymer composite reaching the theoretical strength, the mean fiber length should exceed the critical fiber length with the factor of five or greater. Even more and for the sake of durable behavior, the mean fiber length should exceed the critical one with the factor of almost ten [Pee98].

As previously mentioned, the effect of recycling synthetic short fibers on shortening the fiber length can be described relatively easy, modeled and predicted. That is due to the fact fibers normally show one sort of breaking namely the fragmentation (fiber breaking with the same diameter). Besides, the fibers are considered straight and not flexible without curving or even tangling as shown in the straight glass fibers [Chr96]. It is interesting to notice that the fiber shortening due to recycling is not corresponding to a linear reduction in the measured mechanical properties. The mean fiber length is almost reduced to 50% of its original value, but the strength remains almost the same, the bending strength decreases only 3% and the impact strength reduces by almost 15%, [Chr96]. The same notice of non-affected mechanical properties under recycling is also reported by [Cic17] and [Le 09].

Flexibility of fibers, as shown in Figure 2-15, changes the efficiency of load transferred through the matrix to the fiber as well as the fiber fracture behavior. In [Bér08], the relative strength of the fiber against the flow induced stress is the criterion for fiber breaking as defined by the ratio (E-modulus / viscosity. Shear rate).

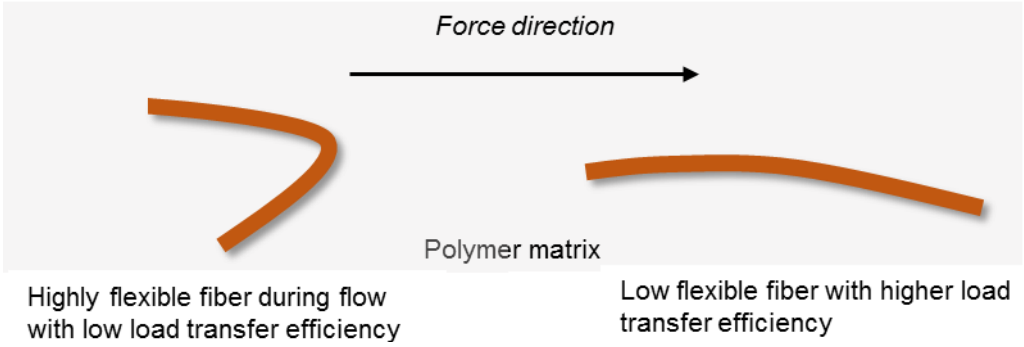

Figure 2-15: Effect of fiber flexibility on the load transfer efficiency

On the contrary to stiff synthetic fibers, natural fibers possess a unique nature and behavior under extreme mechanical stresses due to the applied shear. As described in Figure 2-7 and section 2.4.2, natural fibers in the compound when re-melted and re-injected, suffer from more splicing and fragmentation. The newly generated surfaces due to recycling are in the case of natural fibers more than those generated in case of glass fibers. This results in new coupling sites between the natural fibers and the polymer matrix. Therefore, the mechanical properties are enhanced after the first cycle as reported in [El-13], [Cic17] and [Le 08] and then stabilize or even decrease after the second or the third cycle.

Studying the recycling of natural fiber thermoplastic composites in this sense is not limited to the usual meaning of Reduce-Reuse-Recycle, but it can be thought of as a technique to reach better mechanical or physical performance. Also, understanding the recycling effect on the fiber morphology, fiber structure and fiber-matrix interaction will enlighten some non-explained deviations between the available modeling techniques and the experimental results [Vel12] [El-09].

2.5 Conclusion

Recycling of NFTC comprises polymer matrix, natural fibers and additives. Matrix recycling and additives compensation have already stable code of practice. The remaining candidate is the fiber. Issues related to the recycling of synthetic fibers are almost settled like fiber length reduction. However, in natural fibers, the recycling imposes new aspects like change in fiber size (agglomeration, branching, length, and diameter) and change in fiber composition due to thermal degradation.

Studying the recycling of natural fiber thermoplastic composites in this sense is not limited to the usual meaning of Reduce-Reuse-Recycle, but it can be thought of as a technique to reach better mechanical or physical performance. Also, understanding the recycling effect on the fiber morphology, fiber structure and fiber-matrix interaction will enlighten some non-explained deviations between the available modeling techniques and the experimental results.

3 Research Strategy

The methodical approach followed in this work shown in Figure 3-1 aims to study the effect of recycling on the rheological, thermal properties and morphology of the NFTC and relate them to the evolution in the mechanical properties. The characterization discusses these effects in terms of the changes in both fiber and polymer matrix. The change in fiber deals with the change in fiber dimensions and composition whereas the change in the matrix corresponds to flow behavior, thermal properties and molecular weight.

Two compounds with different fiber types namely Sisal Hemp are selected to show the potential of recycling on these two main fibers' types:

- Straight leaf fiber: Sisal
- Flexible curled bast fiber: Hemp.

The gained knowledge is then used to model the flow behavior of the recycled NFTC according to the fiber type.

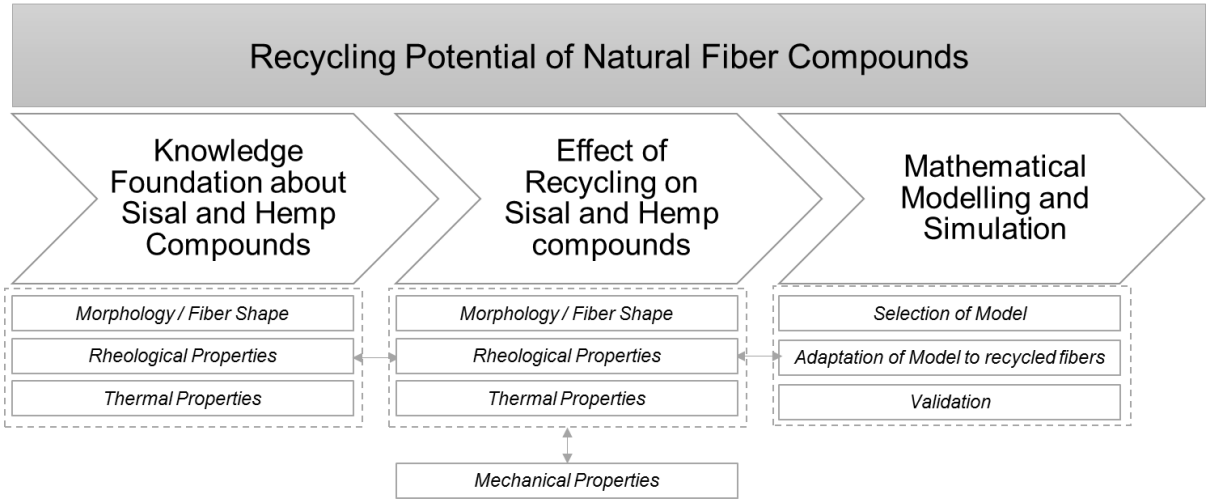

Figure 3-1: Research strategy

3.1 Materials and Methods

3.1.1 Thermoplastics

The selected matrix material for this research is Polypropylene Moplen EP500V which is widely used for injection molding applications, with Density of 0.9 g\cm³, Melt flow rate (230°C\2,16Kg) of 100 g\10min and Tensile Modulus of 1450 MPa, notched Izod of 5.9 kJ/m² at room temperature and 3 kJ/m² at 0°C.

Another commercial high flow polypropylene, made out of 50% recycled PP with 20% prime PP [FAO11] in Voerde company, is also used in the spiral flowability tests in order to reduce the recycling effect on the matrix and just consider the effect of natural fibers.

3.1.2 Natural fibers

The natural fibers used in the whole study are listed below in Table 3-1. Sisal and hemp are the fibers selected for the recycling study and consequently characterization tests such as rheological behavior, injection flowability and thermal tests. Hemp belongs to bast fibers which are extracted from the Cannabis plants from phloem tissues and are known for their soft structure due to their higher lignin content.

Table 3-1. The used natural fibers and their data

Natural fiber type	Supplier	Notices
Sisal fibers	Cayetano Garcia Del Moral S.L., Cabra del Santo Cristo, Spain	Chopped fiber slivers prepared in (BaVe Badische Faserveredelung GmbH, Malsch)
Sisal fibers*	APAEB, Bahia, Brasil	Slivers of fibers in chopped form
Hemp fibers*	AFT Plasturgie, Fontaine-lès-Dijon, France	Slivers of fibers in chopped form

*These fibers are compounded commercially with the commercial PP mentioned in 3.1.1 and supplied by Voerde and AFT (PF3 434A) respectively

On the contrary, Sisal fibers which are leaf fibers are stiffer in nature and are extracted from Agave Sisalana plants and are distinguished by their high cellulose content. More detailed illustration of the two fibers is discussed in section 4.3. As previously mentioned, these two types of fibers are the reinforcing fibers used in the NFTC in this study which are listed in Table 3-2.

Table 3-2. The used natural fibers composites and their data

Compound Name	Matrix	Fibre	Fibre Content
PP-S	Commercial Polypropylene	Sisal 1	30%
PP-H	Commercial Polypropylene	Hemp 1	30%
PP-30%Sisal	Moplen EP 500V High flow	Sisal 2	30%

3.1.3 Coupling agent

Maleic anhydride grafted polypropylene (MA-g-PP) is used as a coupling agent [FNR14] between the hydroxyl group in the natural fiber and the functional group in the polypropylene matrix [Kee04], [Li07]. To get such coupling, a double bond is needed to bind to the polypropylene and carboxylic acid (or anhydride) to form the ester linkage between the cellulosic fiber and the coupling agent [Era09] as shown in Figure 3-2. The needed amount of the MA-g-PP coupling agent for 30 wt% natural fiber is 3 wt% in accordance to Keener [Kee04]. This meets also the 1:10 rule of coupling agent: natural fiber ratio as reported in [El-14b]. Stabilizer is added internally in the supplying compounding company.

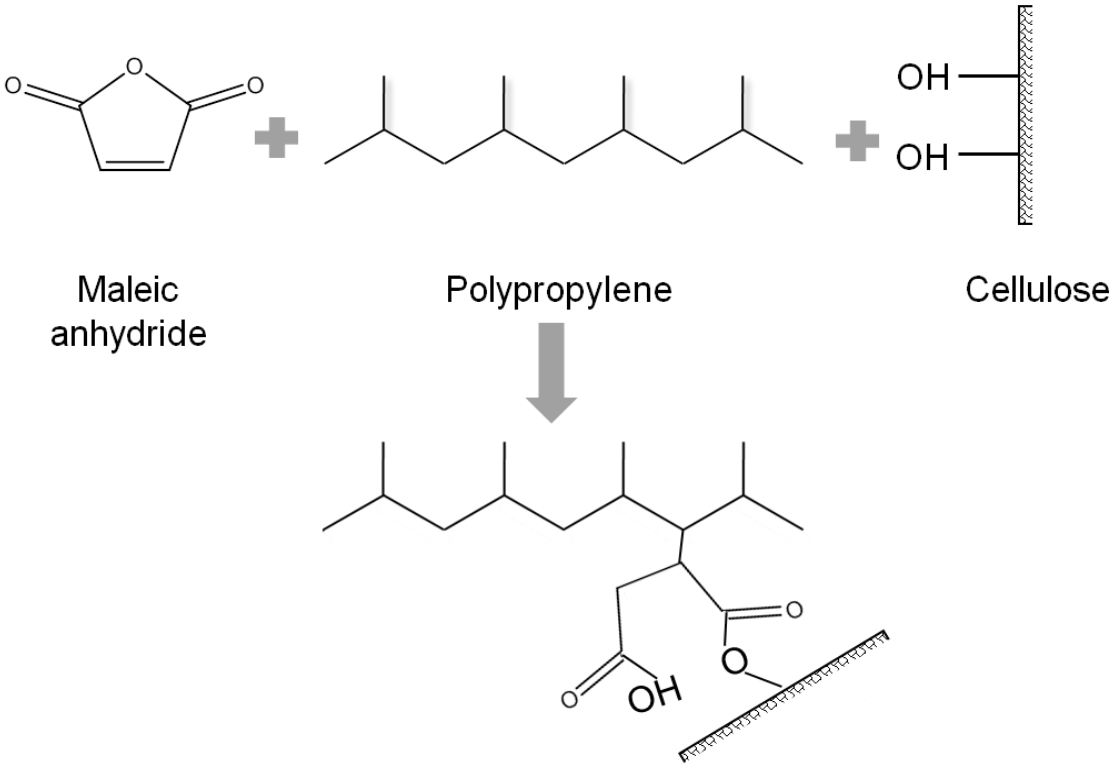

Figure 3-2: Schematic representation of the coupling between cellulose fiber and PP with the aid of maleic anhydride coupling agent [Era09].

3.2 NFTC preparation

Polypropylene and the other additives like the coupling agent and the stabilizer are added to the extruder. The fibers /pellets are added from a side opening. The atmospheric and vacuum degassing ports are used to get rid of the evolving gases from the natural fibers under heating.

As mentioned before, two commercial compounds of PP/Sisal and PP/Hemp with 30% fiber weight content. Both compounds are supplied by Kunststoffwerk Voerde and AFT (PF3 434A) respectively. Hereafter, the both NFTC samples are called PP-S and PP-H for PP/Sisal and PP/Hemp respectively. The compounding of PP, additives and all types of natural fibers are carried out using a twin-screw extruder [FNR14].

Although compounds used in this research are supplied by external suppliers as previously mentioned, it is important here to mention briefly the process followed internally to produce similar compounds according to [El-14a]. The used extruder for these purposes is from Berstorff of ZE 25 model (twin co-rotating extruder). This means that the body housing diameter is 25 mm. Number of heating chambers are nine. The extruder speed is variable from zero to 1200 revolution/min with a rotating torque of almost 90 Newton meters. The heating temperature reaches 400°C. The design of the extruder can be adjusted for governing the shear rate.

The extruder layout includes the zones of feed, compression and metering. Fiber mixing takes place after the feed and compression of PP. Second step of compression zone takes place on the PP/ natural fiber before the final metering of the compound as shown schematically in Figure 3-3.

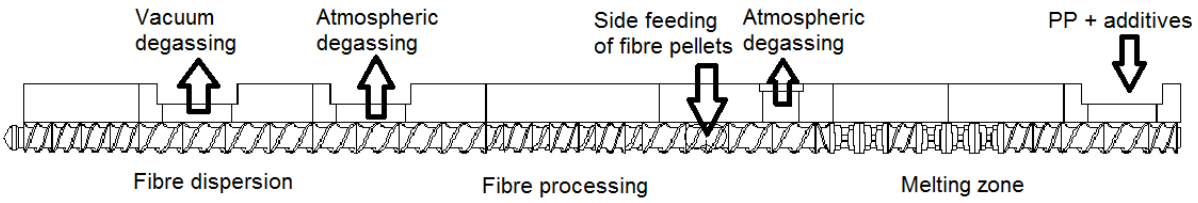

Figure 3-3: Extrusion procedure of PP with natural fibers [El-14a]

3.3 Recycling

The primary recycling experiments in this study are carried out by injection molding. Two injection molding machines with different capacities are used. The first one is Arburg Allrounder 220S 150-60 which is used to produce test samples and the recycling process.

The second machine is Arburg Allrounder 320C 600-250. It is used in producing 10 spirals samples for the flowability tests. The parameters of injection molding for both machines are listed in Table 3-3.

As mentioned above, the recycled material, out of the machine Allrounder 220S, is to be shredded and used in further cycles. By injection and material shredding to new pellets, a recycling cycling is considered complete. The pellets are afterwards dried overnight at 100°C.

Number of implemented recycling cycles is up to five. Hereafter, the samples are named with respect to the recycling cycle number (C0, C1, C2, C3, C4 and C5). C0 represents the original product.

Table 3-3. Parameters of Injection molding for Arburg Allrounder 220S 150-60

Parameters	**Arburg Allround 220S 150-60**	**Arburg Allround 320C 600-250**
Injection pressure (bar)	500	500
Injection flow (ccm/s)	20	20
Dosage volume (ccm)	8	40
Switch over point (ccm)	1,5	38
Time of holding Pressure (s)	7,5	7,5
Temperature (°C)	200	200

3.4 Characterization Techniques

3.4.1 Flow Length

Spiral flow length test is one of the most important methods to assess the flowability of a certain compound to predict its mold filling behavior in injection molding process. The spiral has a half circular cross section with 6 mm diameter and 9.5 mm pitch as seen in Figure 3-4a.

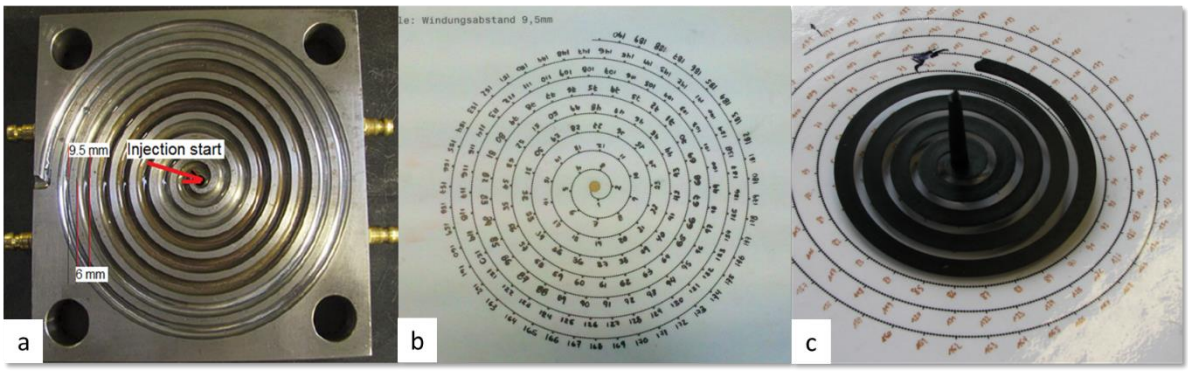

Figure 3-4: a-Spiral injection mold b- Template used to measure the flow length of the spirals samples c- Measurement of the spiral flow length against the template [Ram14a]

The spirals are injected in spiral forms conforming to ASTM D3123-09 and the corresponding flow lengths are measured. A special template is used to measure the spiral flow length as shown in Figure 3-4b & c. As mentioned in 3.1.1, to consider only the effect of recycling on the natural fibers, recycled PP is used as the thermoplastic matrix.

3.4.2 Viscosity measurements

Viscosity is simply a measure principle for the resistance of the polymer against flow under applied force. Viscosity of the compounds before and after recycling is measured using two different rheometer equipment. Rheometer is the equipment used to measure rheology of fluids in response to applied forces.

Since not all rheometers can cover all the required shear rates for the characterization, two rheometers were utilized to cover all the required shear rate range.

3.4.2.1 Rheometer for measurements at low shear rates

A rotational / oscillatory rheometer AR 2000ex from TA Instruments measures the viscosity of the compound using circular plate geometry type and with shear rates of 1E-3 up to 1E3 1/s. at an oscillation frequency sweep from 0,1 – 100Hz, strain of 1% and the viscosity was measured in function of low shear stress. The operating concept of the rheometer is schematically illustrated in Figure 3-5.

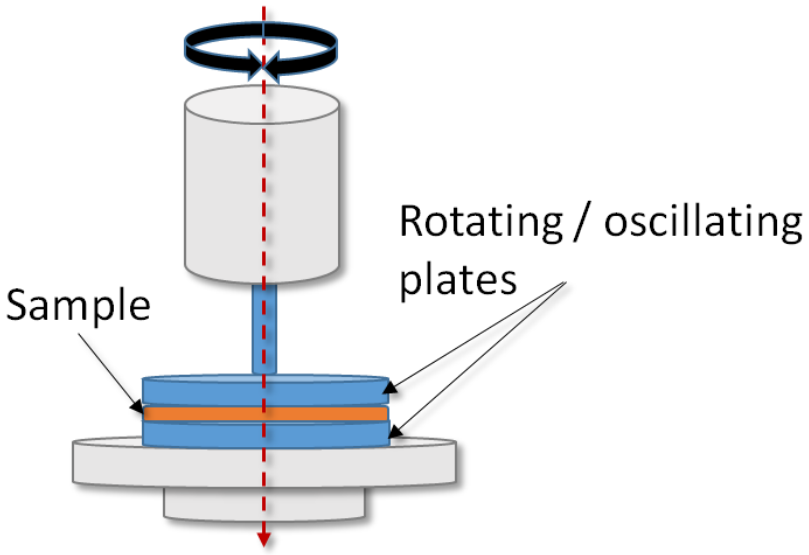

Figure 3-5 Schematic of rotational / oscillatory rheometer

3.4.2.2 Rheometer for measurements at high shear rates

The high-pressure capillary rheometer, named Rheograph 75, supplied by Göttfert with two canals of 15 mm diameter ending with dies of length / diameter of 0/1 and 15/1 mm. Its speed is 0.00005 - 40 mm/s which can impart shear rate up to 1E6 1/s. Such shear rate simulates the injection molding shear conditions. The pellets were put inside the Rheometer channel to be melted at the required temperature and the viscosity was measured against the applied high shear stress. Rabinowisch correction for non-parabolic velocity profile and Bagley correction for exit flow are implemented for corrected viscosity. A schematic illustration is shown in Figure 3-6.

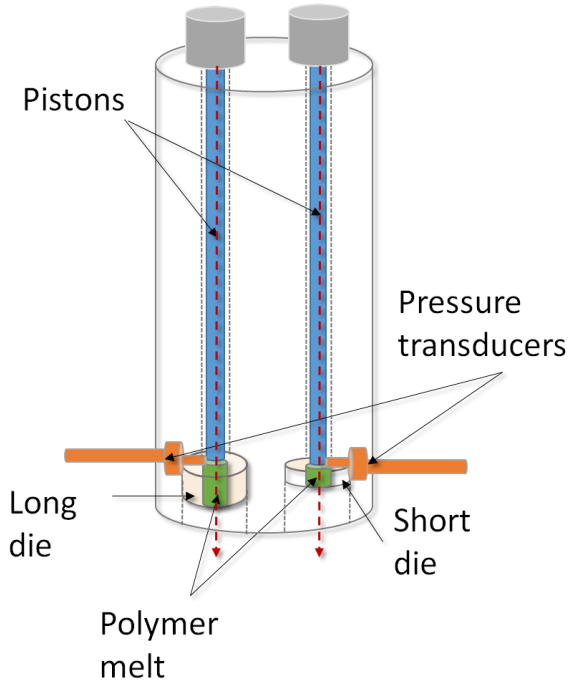

Figure 3-6: Schematic illustration for high pressure capillary rheometer

Both measurements were made at 200°C (the same temperature as the injection molding).

3.4.3 Extraction of natural fibers from the composites

The effect of recycling on the development of the fiber size (length and diameter) is studied. However, measurement of fiber size after recycling requires in the first step fibers extraction. In polymer composites, ashing the polymer is a known technique for extracting glass fibers. However, it is not suitable for extracting natural fibers due to their degradation and low thermal stability. Therefore, it is required to dissolve the polymer matrix chemically at a suitable temperature to avoid natural fiber degradation and hence the natural fibers can be extracted and further characterized or measured. Decalin as a solvent is used as suitable way for separating the fibers again [Ram14a], [El-14a].

Extraction procedure is done by weighing approximately 0.75 g of the composite material (such as the sprue of the injected spiral sample) in a test tube. Then the material is added to 30ml of Decalin solvent inside a volumetric flask. This mixture is stirred by the help of a magnetic stirrer and heated up to 165°C in an oil bath, as shown in Figure 3-7. A condenser is coupled to the flask to avoid the release of Decalin vapor. After two hours, the flask is taken and the solution is rapidly filtered by the aid of a vacuum system. The filtered fibers are then washed with acetone and afterwards placed in an oven at 105°C for drying. The same procedure is repeated for 3 samples of each cycle for the sprues taken from the injected spiral samples.

To check the effect of the recycling on the flow behavior of the fibers during injection, three pieces are cut from the injected spirals namely (the tip, the middle and the bottom), as shown in Figure 3-8. For each part, a similar procedure of fiber extraction was repeated three times for each cycle in three different spirals.

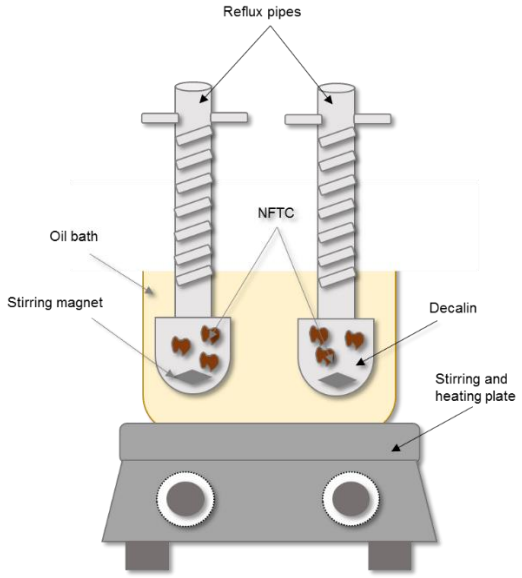

Figure 3-7: Fiber extraction using Decalin solvent at 165°C

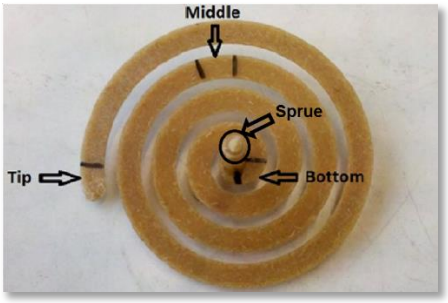

Figure 3-8: The pieces taken from the injected spiral for a following extraction process to get fibers

3.4.4 Measurement of fiber size

The effect of recycling on the development in fiber size (length and diameter) is studied by QICPIC. It is an instrument based on the image analysis sensor that combines particle size and shape analysis. There are two techniques of measurement. Firstly, is the dry technique (Rodos) which depends on the dispersion of the dry fibers/particles into a pressurized flow of air up to 4 bars in front of a high-speed camera. The camera has a high-performance data compression module which supports the acquisition of up to 450 images per second of 1024 x 1024 pixels. The particles are then sucked by a vacuum cleaner. However, this method is not suitable for natural fibers of small lengths because the images are not very accurate as shown in Figure 3-9 (left). The red line shows the acquired fiber length which is too short in relation to the real length due to the lack of sharpness and non-continuous fiber image. This technique is only applied for measuring the original fibers which have very large dimensions and could be measured without large errors.

The second technique is Lixell system where a wet dispersion for emulsions and suspensions (1 to 2,000 µm; with special flow-through cuvette also available for applications from 20 to 10,000 µm) is pumped and circulated in a closed loop. The required sharpness of the image is achieved by the Lixell system for the recycled natural fibers. The limited cavity thickness of the cuvette causes its blocking when measuring original fibers of large dimensions. Therefore, Lixell is used for fibers measurement starting cycle 1.

Figure 3-10 shows the Lixell system and its assembly of solution stirrer, pump, imaging system and connecting tubes. The dispersion of the fibers is carried out using isopropanol. Evaluation of the measured lengths and diameters is based on the fiber area accumulated distribution Q2.

For measuring the fibers' lengths, lens M8 (19-5000 µm) is used. Whereas for the fibers diameters, M6 (1-500 µm) is used according to ISO 13322-2. The results are displayed in graphs of Particle Size (µm) versus the accumulated distribution.

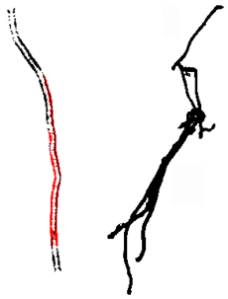

Figure 3-9: Fiber detected by the dry Rodos technique (left) and the wet Lixell technique (right). Source: http://www.sympatec.com/DE/ImageAnalysis/Fundamentals.html)

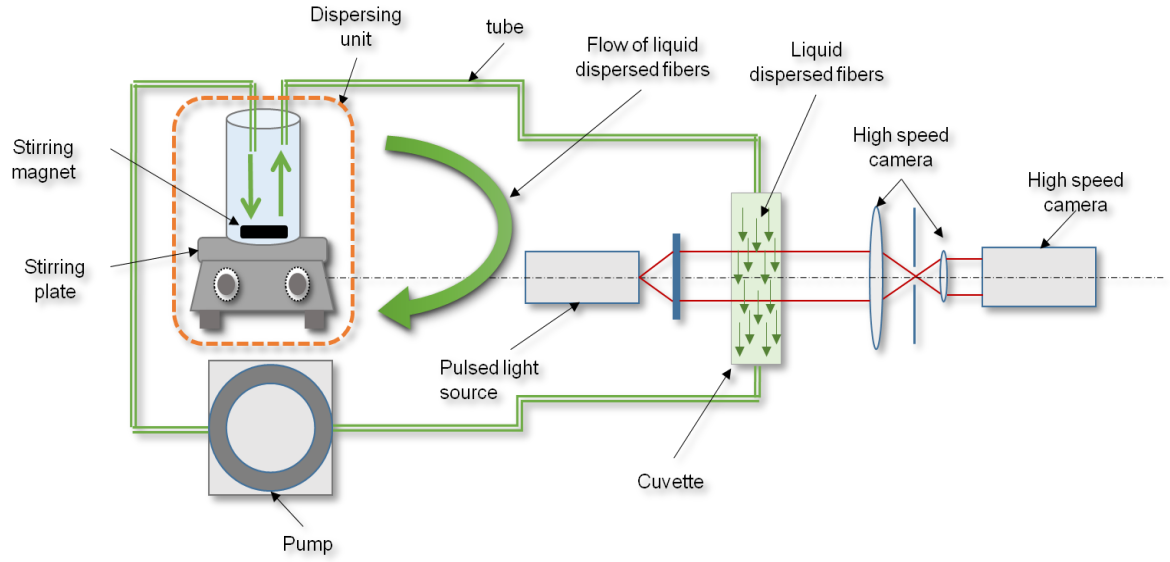

Figure 3-10: QicPic- Lixell method of operation

3.4.5 High pressure capillary rheometer

High-pressure capillary rheometer type Rheograph 75 from GÖTTFERT Werkstoffprüfmaschinen GmbH, Buchen is supplied with 75 KN load cell and measures within the temperature range RT – 400°C with accuracy of 0.02 K. Experiments with shear rates up to 40 mm/s and till 1400 bar can be measured. Thermal conductivity can also be measured using the hot wire method and provides accurate readings as a function in temperature and pressure.

For the investigations, the following tests were applied for selected samples:

- ***Viscosity*** is measured according to DIN 54811 at 180, 200 and 220°C at a shear rate range of 1 s^{-1} up to 1E6 s^{-1} where twin dies of dimensions L/D = 0.2 and 15 mm were used to generate pressure difference.

- ***Thermal conductivity*** is measured in temperatures from 40 – 220°C and pressures from 1 - 906 bar.

3.4.6 Moisture Absorption of Sisal and Hemp Fibers

Assessment of fibers affinity to moisture absorption is very important to be able to adjust processing parameters, understand the composite behavior and to evaluate the overall quality of the resulting composite.

Fibers are dried at 105°C for 24 h then directly placed in the conditioning chamber at 20°C and RH 65%. Weight readings are recorded over 180 min.

The moisture content is calculated according to the following Equation 3-1

$$\boldsymbol{Moisture\ Content} = (\frac{\boldsymbol{Wi}}{\boldsymbol{W0}} - \mathbf{1}).\mathbf{100}$$

Equation 3-1

W_0 = weight of dry fibers

W_i = weight of fibers at measuring time

3.4.7 Thermal gravimetric analysis TGA

TGA is conducted using Q5000 IR from TA instruments in oxygen or nitrogen atmosphere (as will be mentioned in each section) with 10 k/min rate from the room temperature up to 800°C.

3.4.8 Thermal gravimetric analysis with mass spectrometry TG-MS

This investigation was carried upon request from MEET - Münster Electrochemical Energy Technology Institut für Physikalische Chemie to specifically characterize the two commercial compounds. Spectrometer is ThermoStar model GSD 301 T.

3.4.9 Thermal gravimetric analysis with Fourier Transformation Infrared spectrometer TG-FTIR

This investigation was carried upon request from MEET - Münster Electrochemical Energy Technology Institut für Physikalische Chemie

The heating rate applied is 20 K/min within a temperature range RT – 1000°C for a 20-mg mass of sample. For the oxidation tests, a slower heating rate of 5 K/min was applied. FTIR is Thermo Scientific model Nicolet iS10.

3.4.10 Differential Scanning Calorimetry DSC

DSC is a thermo-analytical technique which measures the heat flow into or from a sample as it is either heated, cooled or under isothermal temperature. The objective of this test is the determination of the physical change in the tested polymer such as the endothermic melting, or the glass transition, or the exothermic recrystallization. Physical change is defined in term of temperature and enthalpy.

The selected procedure of the DSC test is heat-cool-heat process. The first heat aims to eliminate the previous thermal history of the polymer. Then by the cooling cycle, both the temperature and the enthalpy of the crystallization are determined from the

heat flow against temperature. The temperature is defined at the local minimum point of the curve and the enthalpy is calculated by integrating the area under the peak. All measurements are done using the software Universal Analysis 2000®.

The heat-cool-heat procedure is done in nitrogen medium and designed as in the following sequence illustrated in Figure 3-11:

1: Equilibrate at 20.00°C
2: Isothermal for 1.00 min
3: Data storage: On
4: Ramp 10.00°C/min to 175.00°C
5: Isothermal for 5.00 min
6: Mark end of cycle 1
7: Ramp 100.00°C/min to 124.50°C
8: Isothermal for 5.00 min
9: Mark end of cycle 2
10: Ramp 10.00°C/min to -50.00°C
11: Mark end of cycle 3
12: Ramp 10.00°C/min to 200.00°C
13: Mark end of cycle 4
14: Data storage: Off
15: End of method

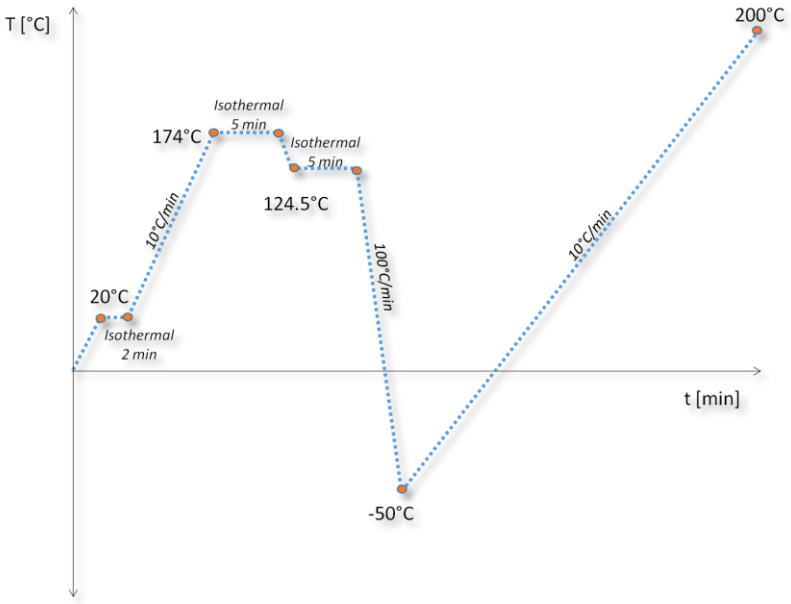

Figure 3-11: Heat-cool-heat cycle

3.4.11 Dynamic Mechanical Analysis DMA

DMA is a characterization technique to investigate the viscoelastic behavior of the polymer and its relaxation events. The test is carried out by applying a cyclic deformation at certain temperature and certain frequency in order to determine both storage and loss moduli and hence the glass transition temperature can be defined. Storage Modulus E' indicates the energy stored (can be recovered therefore real part) in the material during a loading cycle, in other words it represents the stiffness of the viscoelastic material. E'' on the other hand indicates the amount of energy dissipated (cannot be recovered and hence imaginary part) in the viscoelastic material during the same loading cycle. The ratio of E'' to E' gives the tan δ which is the loss factor representing the lost energy in friction or damping, this is shown in Figure 3-12. This means that materials with higher tan δ are less elastic than those with lower tanδ. Since the test is usually carried over a temperature sweep from below the T_g of the material till slightly above the operational temperatures. Phase

transitions in the materials are usually indicated by analyzing the peaks changes at tan δ especially T_g.

The glass transition (T_g) is a characteristic sign of amorphous materials, as polymers and glasses. Under the glass transition temperature, the polymer is hard and brittle; and above it the material is in a rubbery state.

The analysis is carried out with the injected sample (30 x 10 x 3 mm) for each cycle at four different frequencies (0.5; 1.0; 2.5 and 10.0 Hz) and oscillation amplitude of 15 µm. The sample was cooled to -100.0°C and maintained isothermal for 5 minutes; afterwards it was heated at a rate of 2.0°C\min until it reaches 140.0°C.

The ratio of the loss modulus to the elastic storage modulus represents the damping behavior of the polymer (known as tan delta). Tan delta is then plotted versus the temperature and the transition points represented as a peak in the curve can be defined using the software Universal Analysis 2000®.

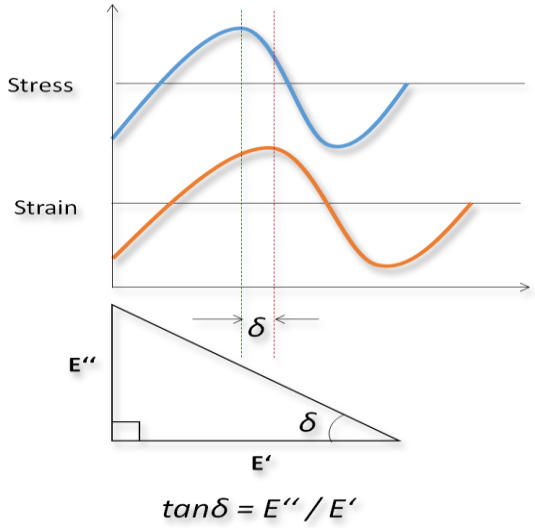

Figure 3-12: Theory of DMA test

3.4.12 Fiber orientation by digital microscope

To demonstrate the distribution of the fibers after injection and consecutive recycling steps, a rectangular sample is sliced and put on a slide to be observed using the Digital Microscope. Another objective of this microscopic analysis is to check the fiber homogeneity.

For this, an injected molded rectangular sample is cut in four pieces after that each piece needed to be embedded in resin for Microtome sections, as shown in Figure 3-13. The resin used in mounting the sample was Technovit 7100 (transparent one) and, after curing, it was covered by the resin Technovit 3040 (yellow one). After curing, using a Leica Microsystems Microtome type RM 2265, the samples embedded are cut in slices of thickness 10µm and 5µm and put on sample slides. All the slides are observed by Keyence digital microscope model VHX-500F and Helmut

Hund trinocular microscope with polarization filter and phase contrast enhancement and attached to a Panasonic color video camera.

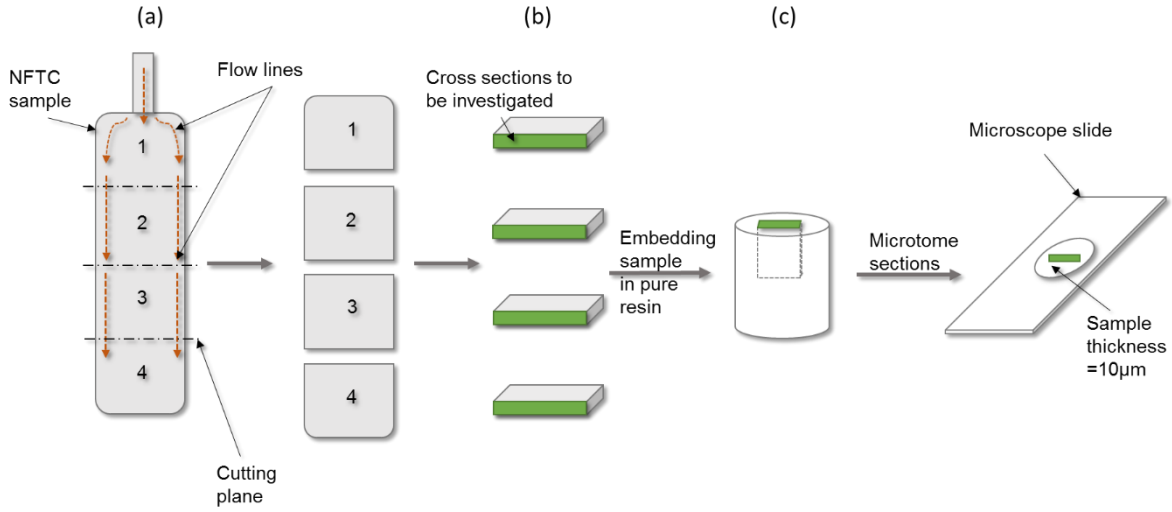

(a) injected sample for microscopic investigation (b) Four parts of the rectangular sample. (c) Sample after embedding and curing.

Figure 3-13: (a) injected sample for microscopic investigation (b) Four parts of the rectangular sample c) Sample after embedding and curing

3.4.13 Observation of crystal formation

To observe the nucleation and the formation of crystals of the polymer during a heating-cooling process, a heating machine and a polarized microscope (mentioned in 3.4.12) are used. The entire system is shown in Figure 3-14. The slides of samples are then subjected to the polarized microscopic analysis. The slide is put on the heating stage Polytherm D with a thermostat controlling the temperature. Temperature increases till it reaches the melting temperature measured by the DSC.

After that it is left to cool down slowly to the crystallization temperature (T_c) obtained from the DSC.

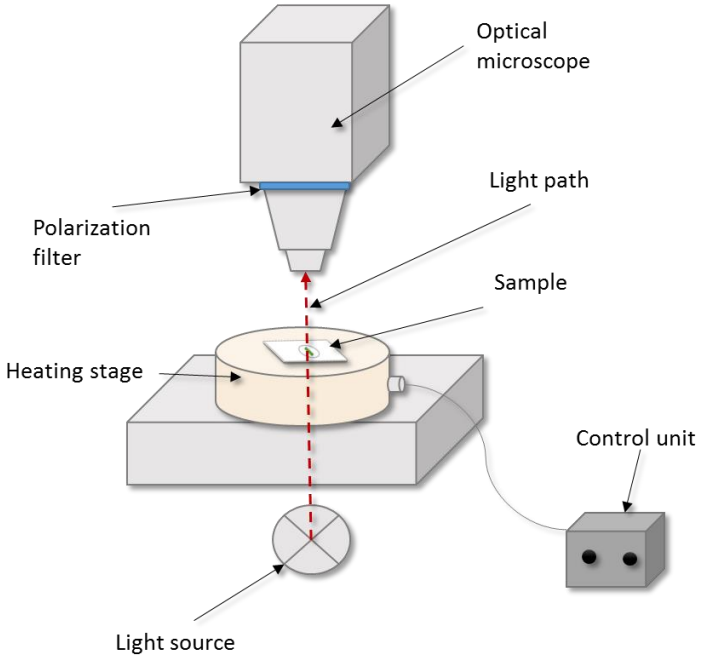

Figure 3-14: Polarized microscope, Heating Stage and their assembly

Temperature is then held isothermally at (T_c), for approximately 40 minutes. Pictures are taken during all cooling and isothermal process to monitor the development of the crystal formation.

For better identification of the crystal formation during cooling, the amorphous part is subjected to etching process. The tested samples are the samples coming out of the DSC test after heat-cool-heat process. The polarized microscopy samples are prepared as previously mentioned in 3.4.12. The sample is glued and put in an epoxy resin (EpoFix Resin) above the glass. Then it is left to cure over 24 hours.

Then a 10 µm slice is cut by the microtome and laid on a slide for further microscopic investigation using the through light assembly.

Etching of the samples is carried out by putting them in a solution of 40,0 g Chrome(VI)-oxide in 75,0 mL distilled water. The solution is heated up to 70 °C and etched for 4 minutes. The solution flask is coupled with a condenser to condense the released gases. Finally, the glasses are washed with distilled Water. The samples are then observed by the polarized and digital microscopes.

3.4.14 Mechanical Testing

Mechanical testing is performed on the Universal Testing Machine – Zwick Roell, Germany to investigate the evolution of the mechanical properties of NTFC in relation to the recycling cycles. For the characterization of the mechanical properties of the recycled compounds namely tensile properties, DIN EN ISO 527-2/1BB/2 is applied.

4 Characteristics of Sisal and Hemp Compounds

To be able to study the recycling behavior of Sisal and Hemp compounds, a full understanding of the compounds and the reinforcing fibers must be developed. To achieve this, a systematic characterization (as illustrated in Figure 4-1) is carried out to determine rheological, thermal and mechanical properties in addition to the morphology of the virgin compounds.

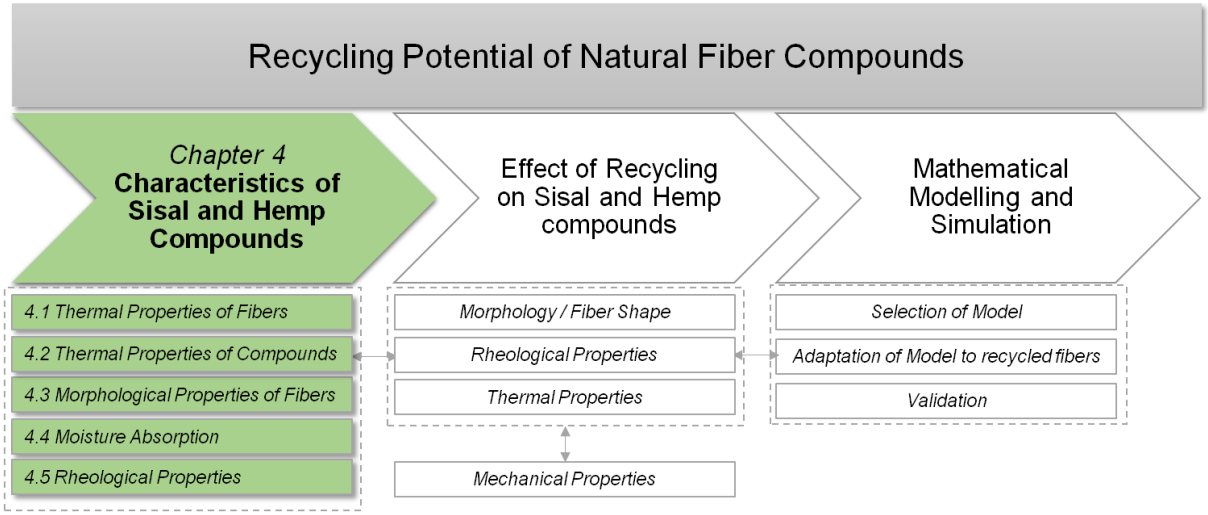

Figure 4-1: Chapter 4 flow chart

4.1 Thermal Properties of Sisal and Hemp Fibers

During injection moulding, natural fibers undergo severe combined mechanical and thermal stresses. Understanding the behavior of sisal and hemp fibers thermal decomposition is a key aspect to understand the changes in the characteristics of the NFTC after recycling.

As mentioned in 3.4.8 and 3.4.9, MS-TGA and MS-FTIR are applied to monitor the thermal decomposition behavior of the two fibers under study. Hemp and sisal fibers show a very similar decomposition behavior. The onset decomposition temperature of hemp is 269.5°C which is 8°C higher than that of the sisal, as shown in Figure 4-2. Figure 4-3 shows the FTIR-spectra for the absorption bands of the decomposition products such as acetic acid, water, carbon monoxide, carbon dioxide and methane.

The release of water, carbon dioxide and acetic acid takes place at different temperatures and the content of oxygen and hydrogen (CO-, H2-degassing) in the residual material is different as in Figure 4-2. Comparing the mass spectra and the FTIR spectra in Figure 4-3 and Figure 4-4, a difference in the amount of individual decomposition products for hemp and sisal could be noticed. The relationship between methyl alcohol and acetic acid is inversely proportional for both natural fibers as in Figure 4-5.

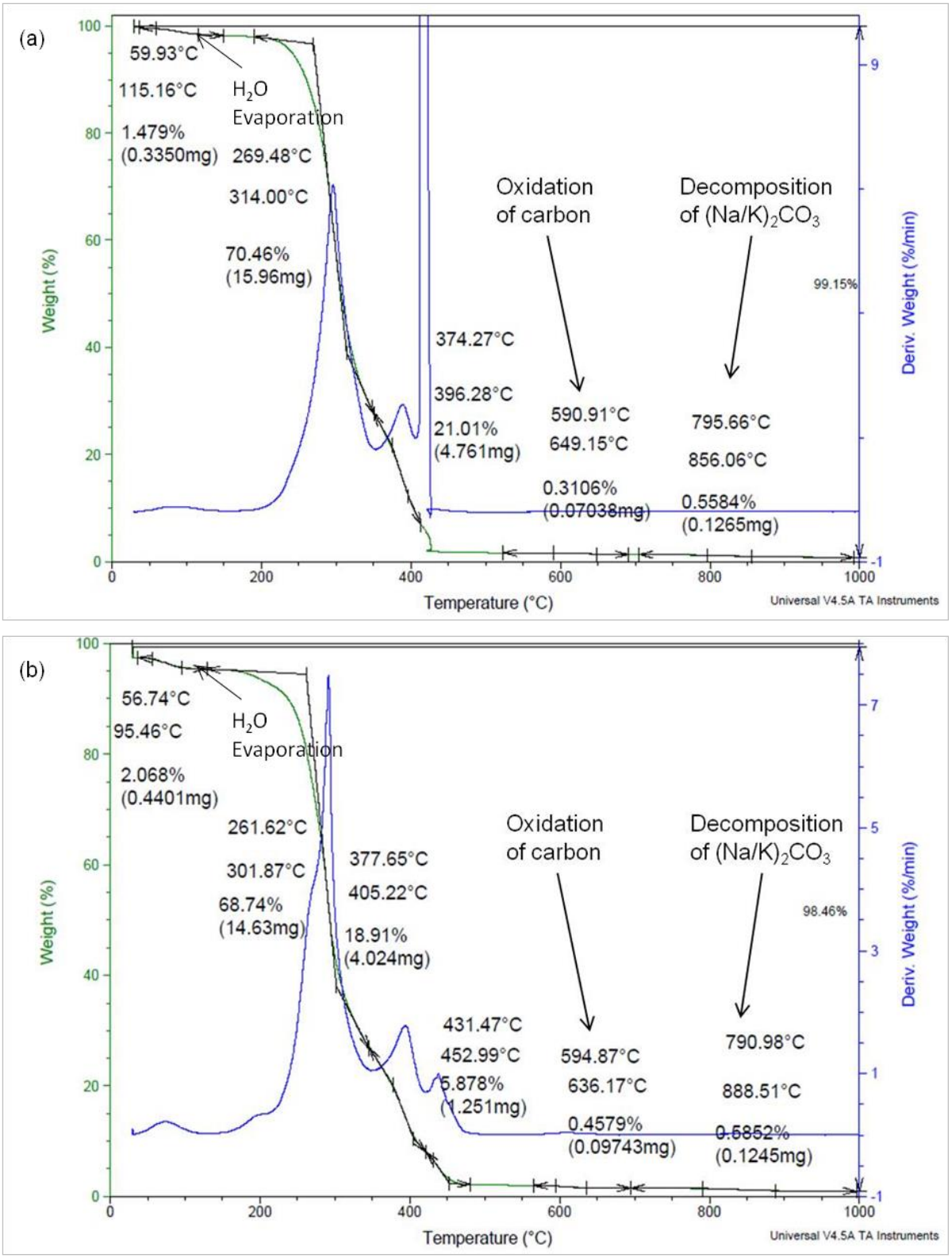

Figure 4-2: TGA of a) Hemp b) Sisal

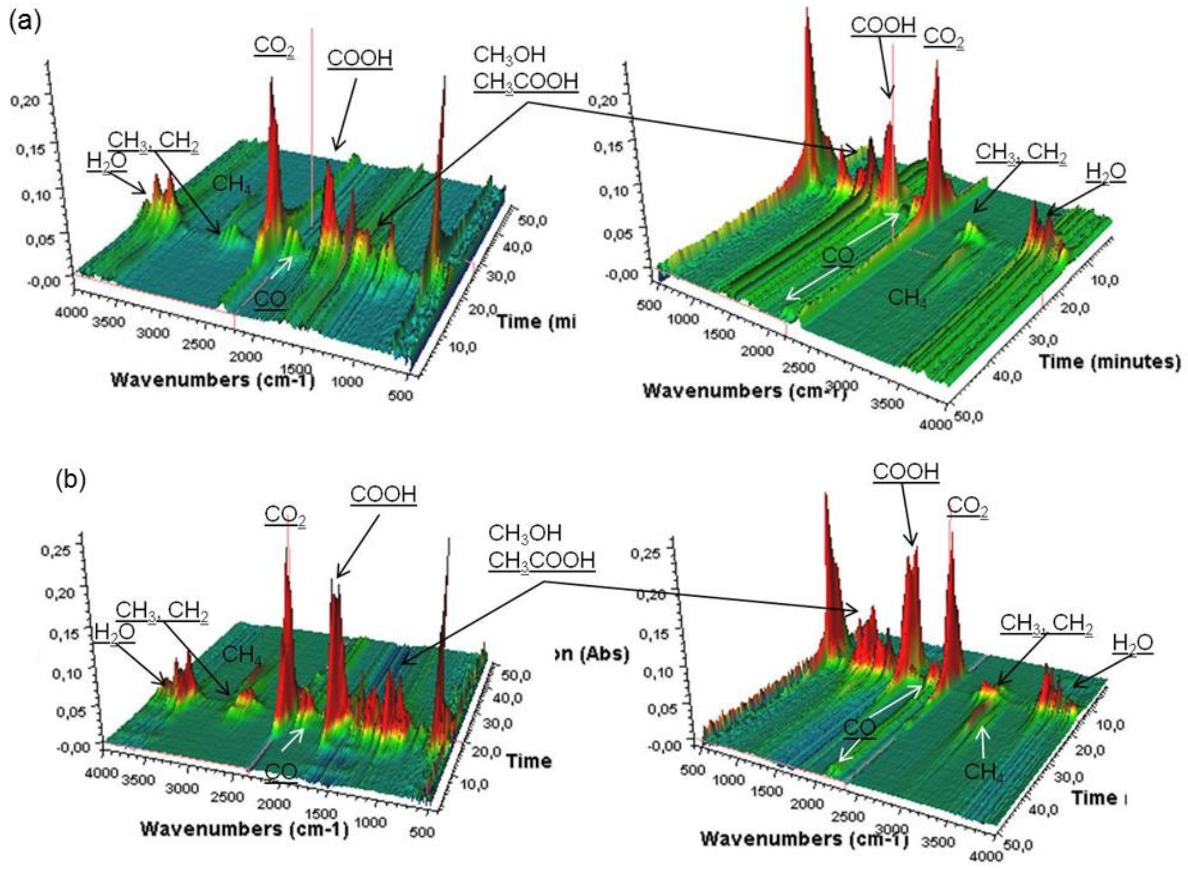

Figure 4-3: FTIR spectra of (a) Hemp (b) Sisal

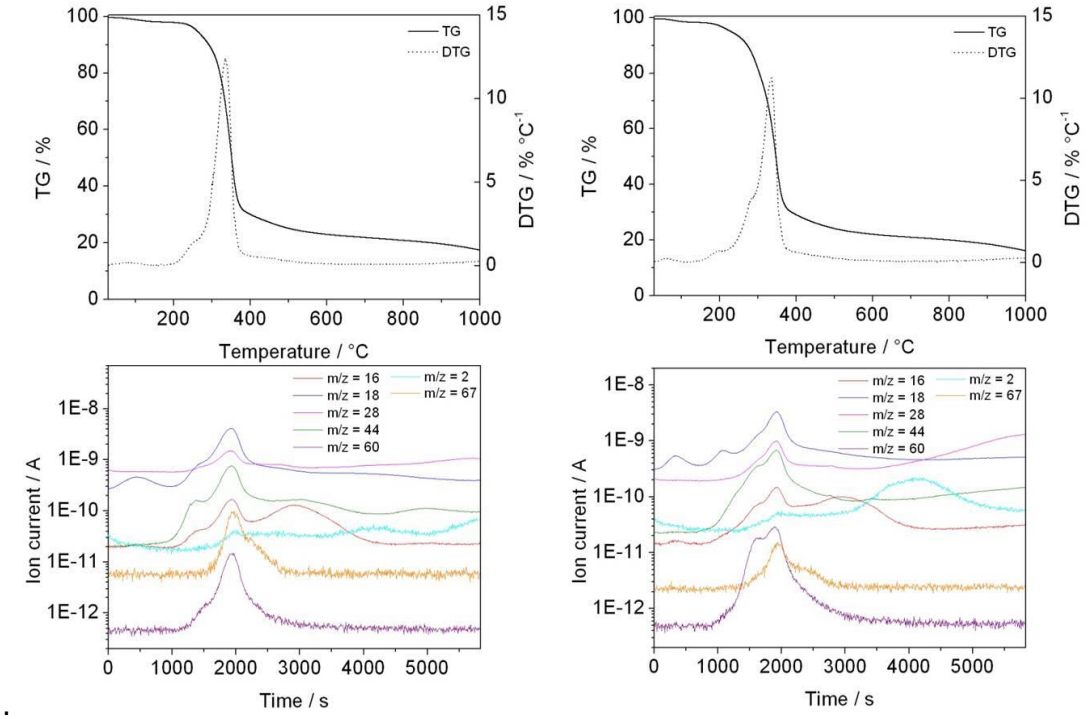

(a) Hemp (b) Sisal

Figure 4-4: Mass spectra of a) Hemp b) Sisal

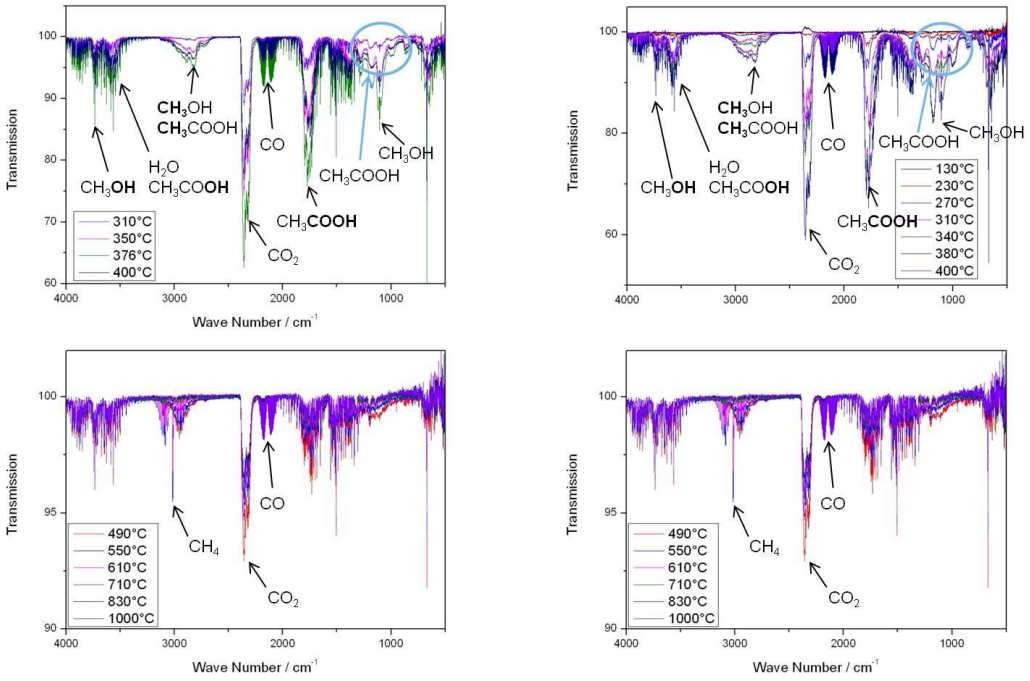

(a) Hemp (b) Sisal

Figure 4-5: FTIR spectra of (a) Hemp (b) Sisal

4.2 Thermal Properties of Sisal and Hemp Compounds

4.2.1 Compounds thermal decomposition behavior

A mutual interaction between fibers and matrix is shown in Figure 4-6. The natural fibers release carbohydrates with a high boiling point (Tbp. > 160 °C) which could not be detected by FTIR. The polymer “PP” releases also long-chain oligomers with a high boiling point. These oligomers clogged the transfer-line to the mass spectrometer and the KBr-Window is fogged as shown in Figure 4-6.

It is here very interesting to notice that the decomposition of natural fibers is not affected by the host polypropylene matrix. All decomposition products of the pure fibers were detected in the mass spectra of PP-H and PP-S (Figure 4-7).

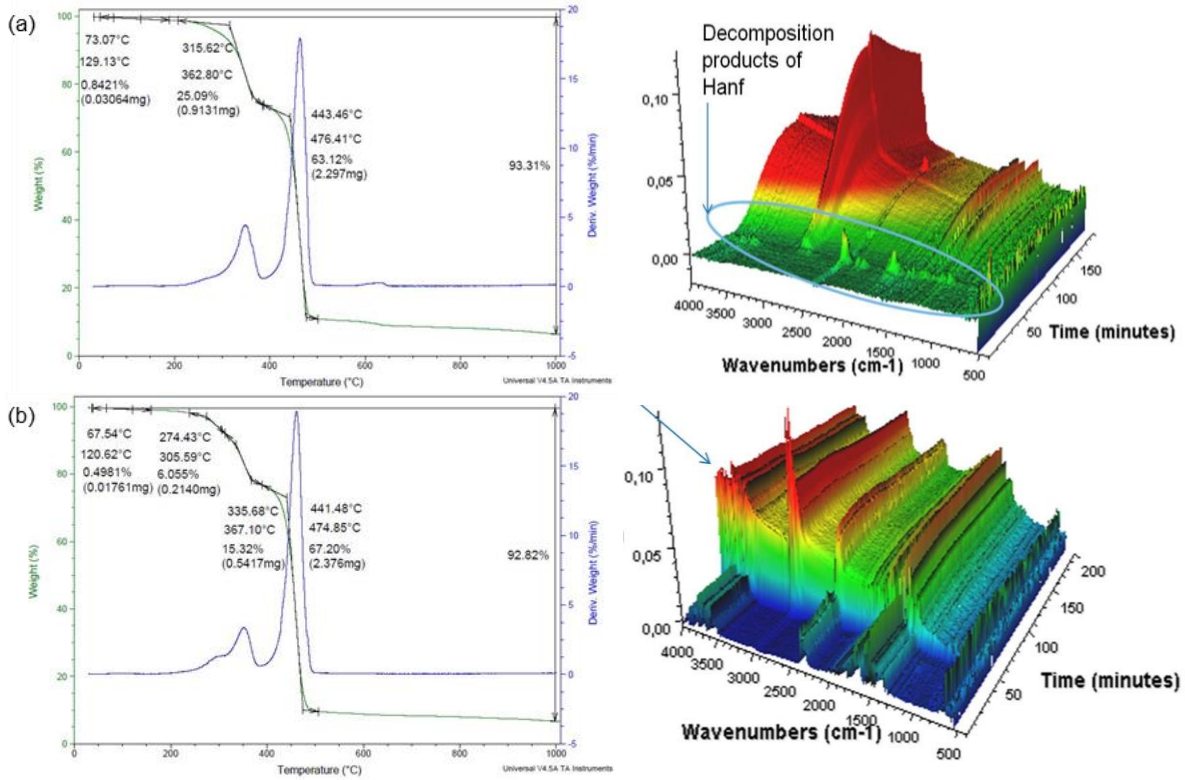

Figure 4-6: TG and FTIR spectra of a) PP-H b) PP-S

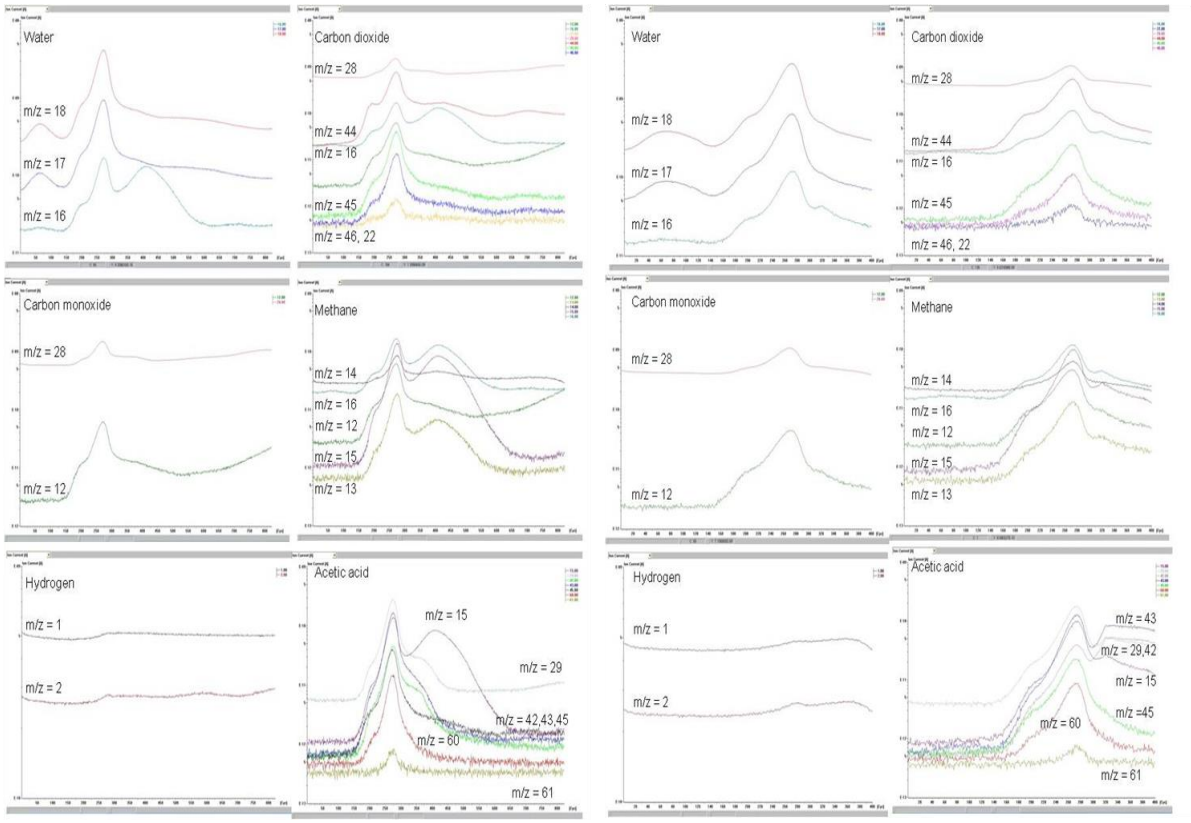

Figure 4-7a: Completed mass spectra of original Hemp fibers (left) and PP-H (right) (see Appendix A-7)

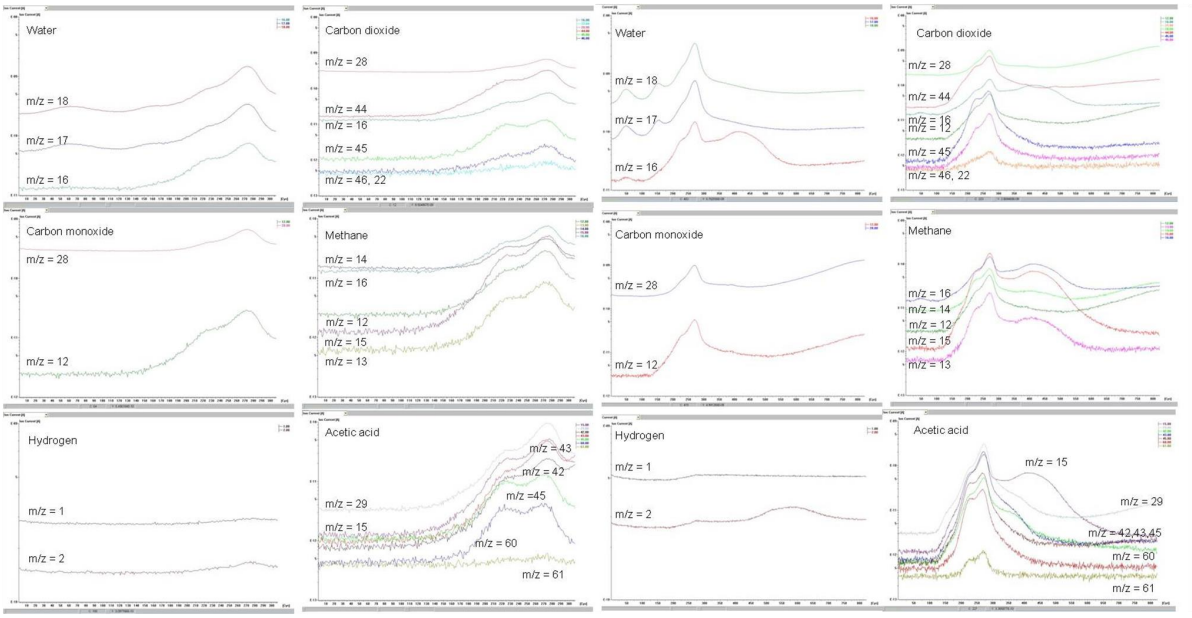

Figure 4-7b: Completed mass spectra of original Sisal fibers (left) and PP-S (right) (see Appendix A-8)

4.2.2 Compounds enthalpy changes

To study the endothermic and exothermic changes in the compounds at physical and chemical transitions, the differential scanning calorimetry analysis (DSC) is applied as mentioned in section 3.4.10. Compound characteristics namely melting point and heat of fusion are taken only from the second heating cycle to avoid the effect of thermal stresses from the manufacturing process on the readings (see Figure 4-8).

It is obvious from Table 4-1 that all compounds induce an increase in the melting temperature in comparison to the pure polymer matrix. On the other side, the recrystallization temperature of the compounds is 2-3°C lower than that of PP. This could be attributed to the addition of the coupling agent co-polymer MAPP to the PP matrix in the compounds. MAPP has a lower molecular weight and therefore a lower melting point than pure PP which lowers the melting point of the whole compound.

In addition, the recrystallization Enthalpy (ΔH_c) shows the same decreasing trend. Since the fibers represent only 30% of the total compound weight, and since recrystallization occurs only in the PP matrix, therefore each measured enthalpy has to be divided by 0.7 to obtain the representative ΔH_c of the PP.

By following this method, the following enthalpies are deduced:

$\Delta H_{c(PP\text{-}H)} = 77.48$ [J/g]

$\Delta H_{c(PP\text{-}S)} = 71.82$ [J/g]

$\Delta H_{c(PP\text{-}30\%Sisal)} = 94.61$ [J/g]

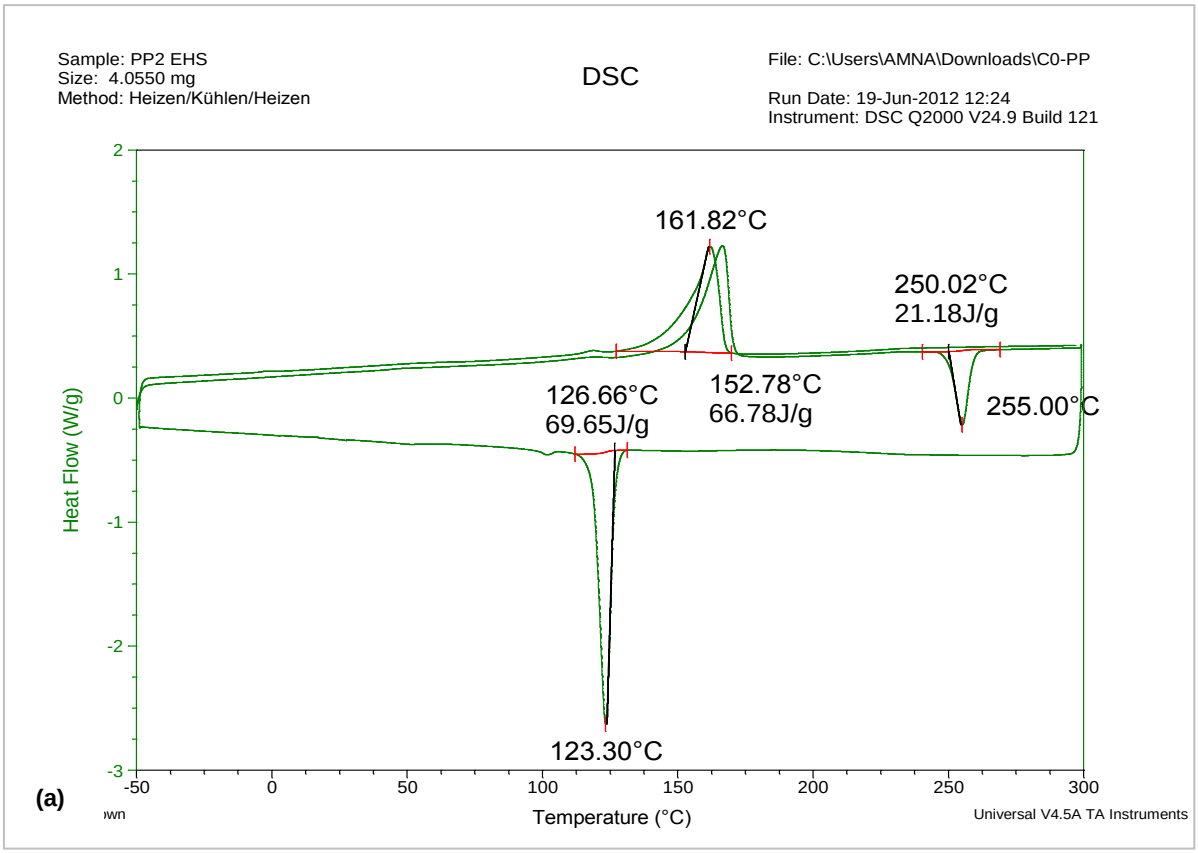

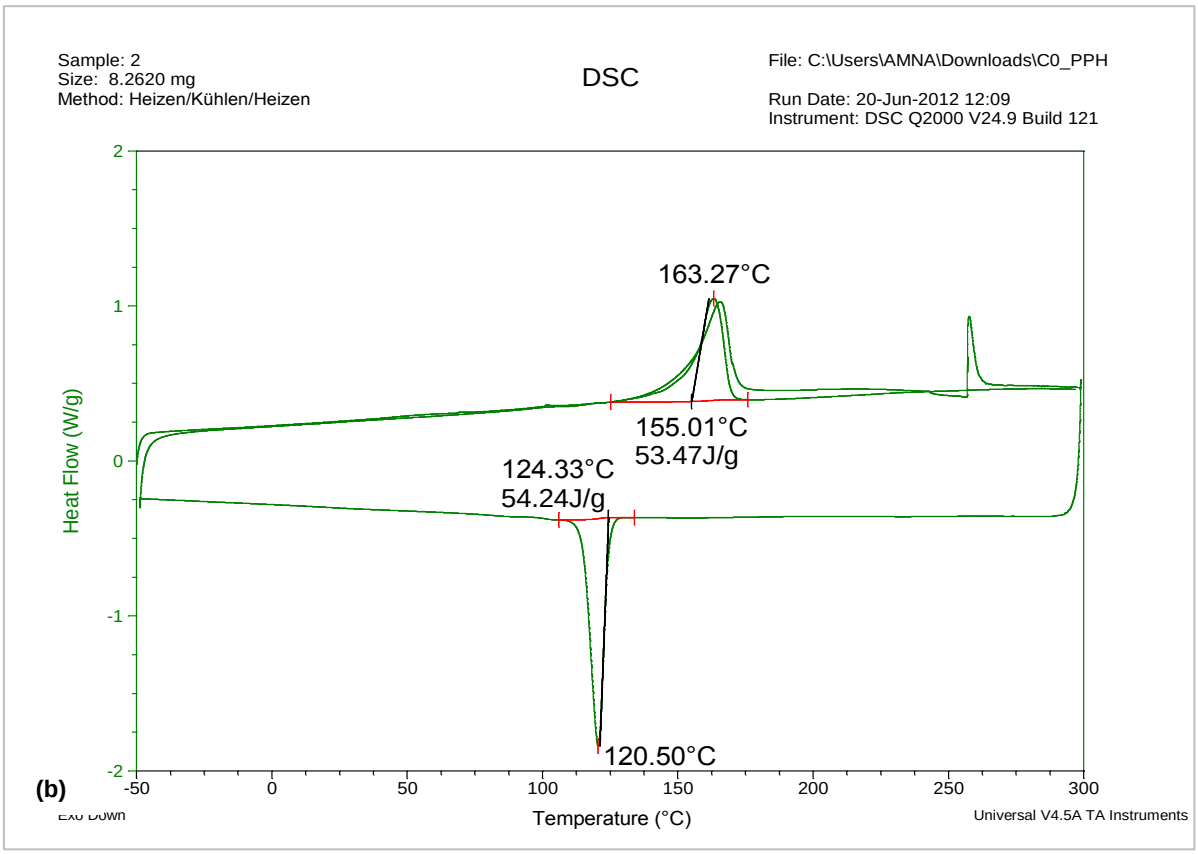

Figure 4-8: DSC of (a) PP (b) PP-H

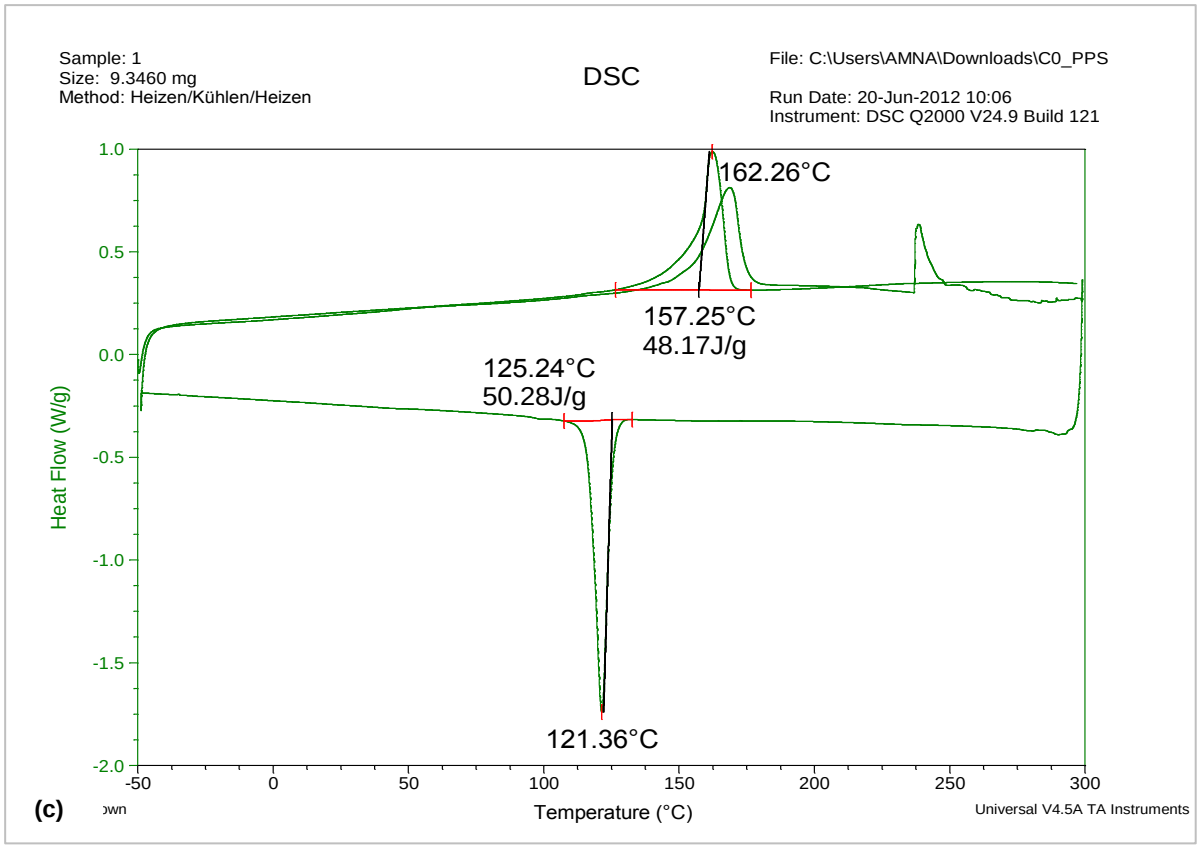

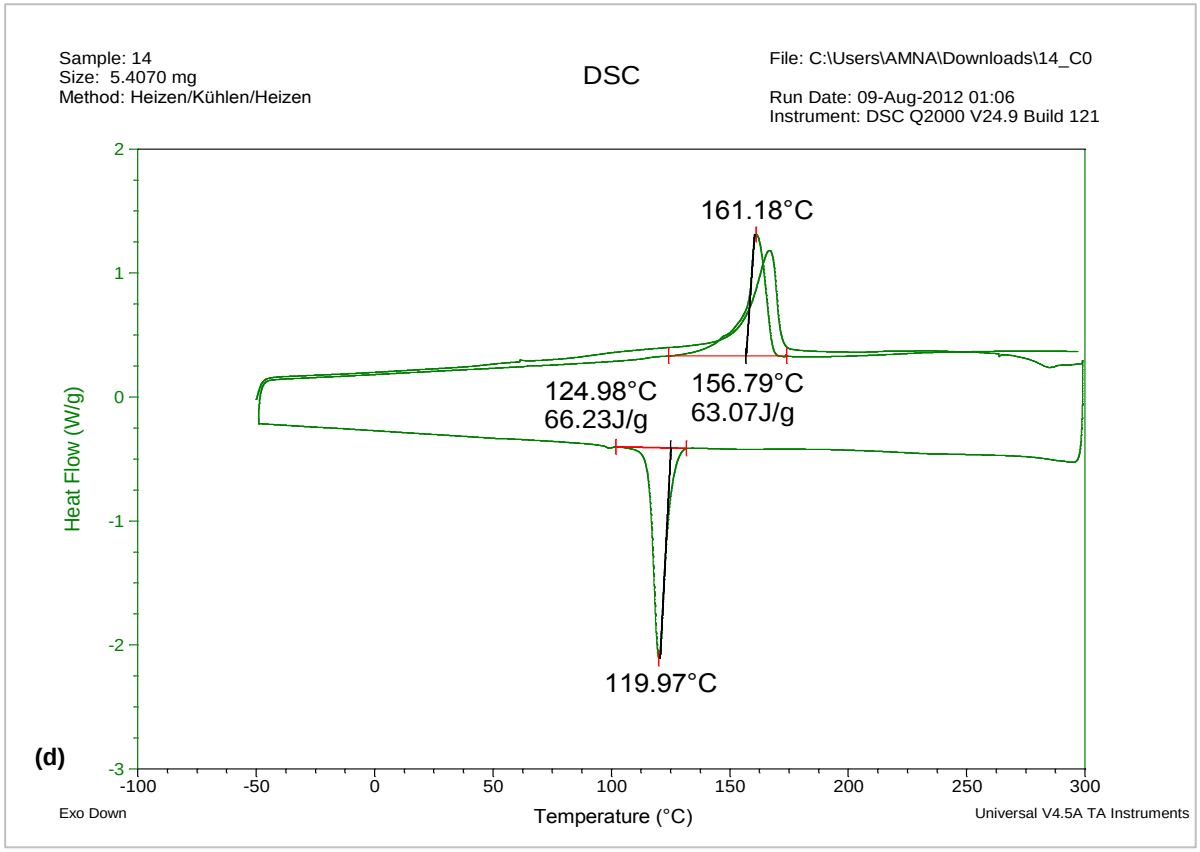

Figure 4-8: (c) PP-S (d) PP-30% Sisal

Table 4-1. DSC results of PP, PP-H, PP-S and PP-30%Sisal

Material	Melting Temp [°C]	Fusion Enthalpy [J/g]	Recrystallization Temperature [°C]	Recrystallization Enthalpy [J/g]
PP	161.82	66.78	123.3	69.65
PP-H	163.27	53.47	120.5	54.24
PP-S	162.26	48.17	121.36	50.28
PP-30%Sisal	161.18	63.07	119.97	66.23

This indicates that addition of fibers (regardless of type) enhances crystallization (reflected in the increase of ΔH_c). This is attributed to the action of fibers (foreign bodies in matrix) as nucleation initiators in the PP matrix.

4.2.3 Compounds thermal conductivity and heat capacity

After determining the melting temperatures of the compounds and the pure matrix, thermal conductivity is to be determined and correlated with the melting behavior. It is expected that most of fluctuations to happen around the melting temperature where a phase change takes place due to breakage of internal chain bonding under the supplied energy as a preparation to the melting step. Free moving molecules are known to have better ability to conduct energy which is obvious from the peaks in Figure 4-9. Maximum thermal conductivity is attained at the crystallization temperature of 120°C. After that, the increase of amorphous share releases the contact pressure of the sample which in turn decreases the thermal conductivity. The behavior of thermal conductivity is similar to that of the reverse specific heat capacity 'C_p'. C_p increases till the 150-160°C range before it decreases again with the start of melting.

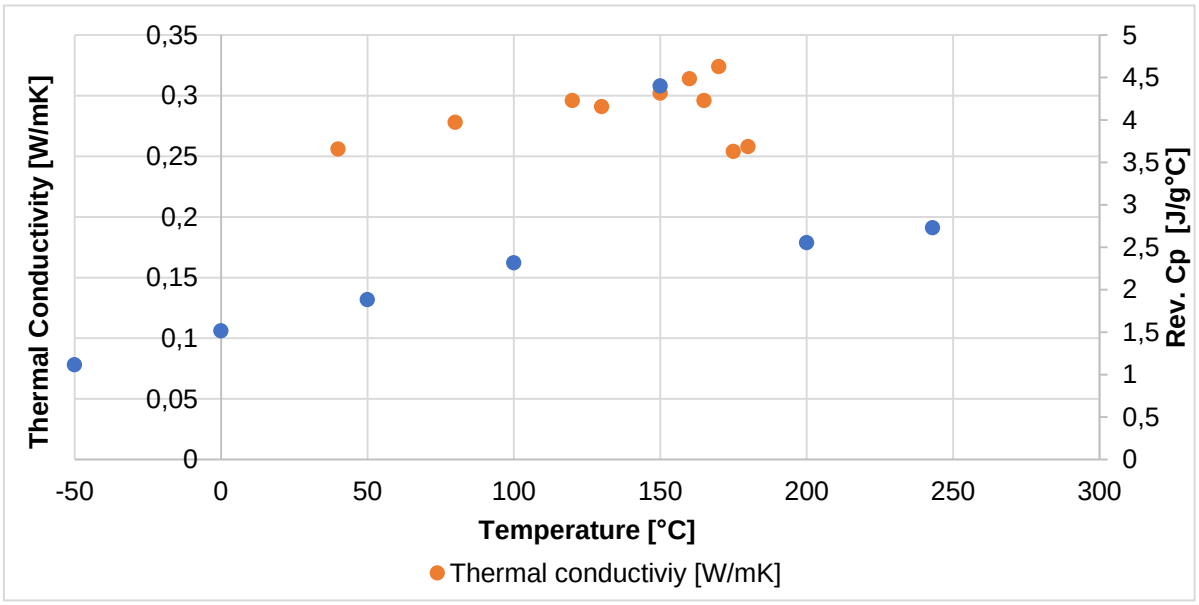

Figure 4-9: Effect of temperature on the thermal conductivity of PP-S

4.3 Morphological Properties of Hemp and Sisal fibers

Hemp and sisal fibers are natural fibers gained from Cannabis and Agave sisalana respectively. Hemp is usually extracted from the bast of the plant whereas sisal is extracted from the leaves of the Agave. In nature, leaves perform a total different function than the bast tissues which reflects on both physical and chemical structure of the fibers. Plant leafs unlike the stem undergo severe torsional and flexural stresses which require superior mechanical properties. Since cellulose, hemi cellulose, lignin and pectin are the main components of natural fibers, they are responsible of defining the properties of the natural fiber according to their percentages.

In Hemp, cellulose represents 61 wt.-% whereas hemicellulose and lignin have shares of 24 and 10 wt.-% respectively [Pan06]. On the other hand, sisal contains 73 wt-% cellulose, 13 wt.-% hemicellulose and 11 wt.-% lignin [Mwa02]. Since cellulose is the main constituent of the fiber, the variation in cellulose percentage (around 10% between sisal and hemp) and the orientation of its micro-fibrils are significant to the fiber properties.

Cellulose is distinguished by its high crystallinity which gives the stiffness to the structure. Hemicellulose on the other hand, is amorphous cellulose which provides the fiber with flexibility, elongation and increased reactivity.

Reviewing the previous composition of each fiber, it is expected that the hemp fiber will act differently than the sisal fiber. Hemp fiber is more flexible, and has a very irregular curled form due to the presence of large amount of hemicellulose. Sisal on the contrary is stiffer with a defined straight form.

To be able to understand the effect of the fibers' type on the resulting compound properties, fibers' morphology is investigated in order to understand the differences between fibers regarding the shape and size distribution. Table 4-2 illustrates hemp and sisal original fibers (before compounding) using different techniques.

As mentioned before in 2.4.4, the fiber stiffness is significant to the behavior of fiber in the polymer melt. Sisal fibers being stiff, tend to splice and break under stress depending on the diameter with less affinity to form agglomerations. Flexible hemp fibers on the contrary bend under stresses and have high affinity to agglomerate and build fiber clusters. The behavior of both fibers in the polymer melt can be easily adapted to the fibers behavior illustrated in figures 2-15 and Table 4-2.

QicPic measurements using the dry system RODOS at applied pressure 1 bar are listed in Table 4-3. It can be noticed that sisal fibers prove a narrower distribution for both length and diameter measurements in comparison to hemp fibers. In addition, considering sisal nature being stiffer than hemp and twice larger in size will reflect on both mechanical and rheological behavior of its compound compared to hemp as discussed later in section 4.5

The difference in the stiffness between sisal and hemp fibers has also a significant effect on the resulting fiber shape after compounding. Before entering the compounding process where natural fibers are introduced to the matrix in the kneading machine to produce the required compound, both sisal fibers and hemp fibers show no agglomerations as shown in the photos extracted from the photo gallery of the QicPic measurements (RODOS and LIXELL) in Figure 4-10.

Table 4-2. Morphology of extracted fibers

	Hemp	**Sisal**
Schematic	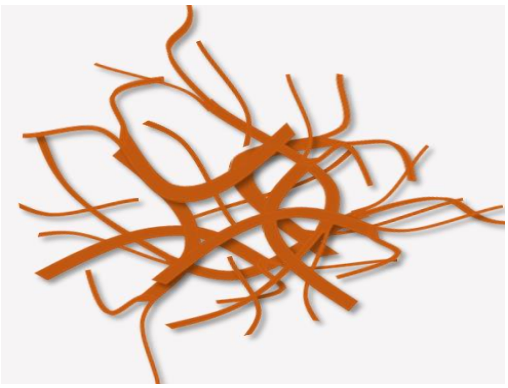	
Microscope	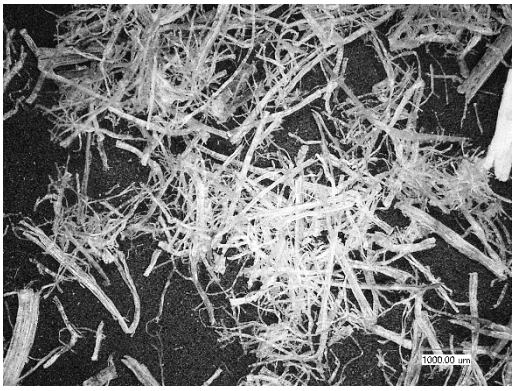	
REM	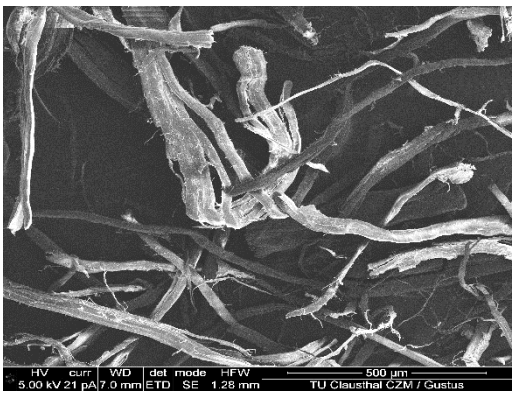	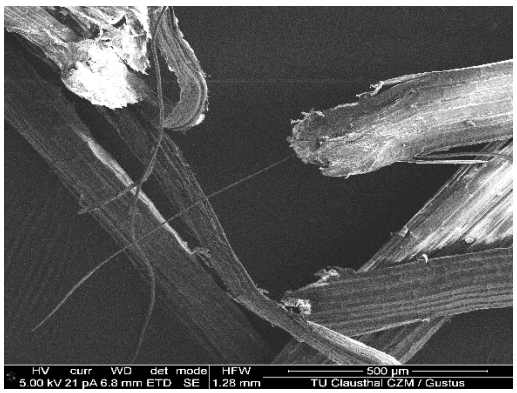
QicPic Photo gallery		

After compounding, sisal being stiff does break and splice under the applied shear forces between the extruder screws forming separate fiber fragments. Hemp fibers on the contrary, being flexible tend to tangle and agglomerate together forming clusters of fibers after undergoing relative reduction in length and diameter in comparison to sisal as shown in the same figure.

Table 4-3. Measurements of fiber size using QicPic

	Sisal		Hemp	
Q1	Original	Compounded	Original	Compounded
Length [µm]	4709	1860	3293	2200
Diameter [µm]	223	99	72	43
QicPic distribution diagram	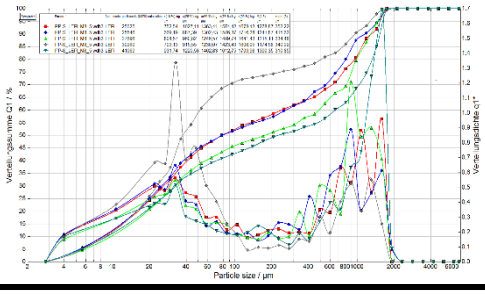		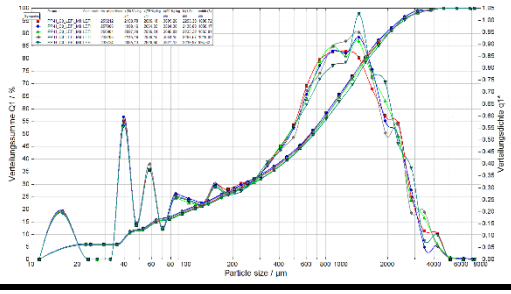	

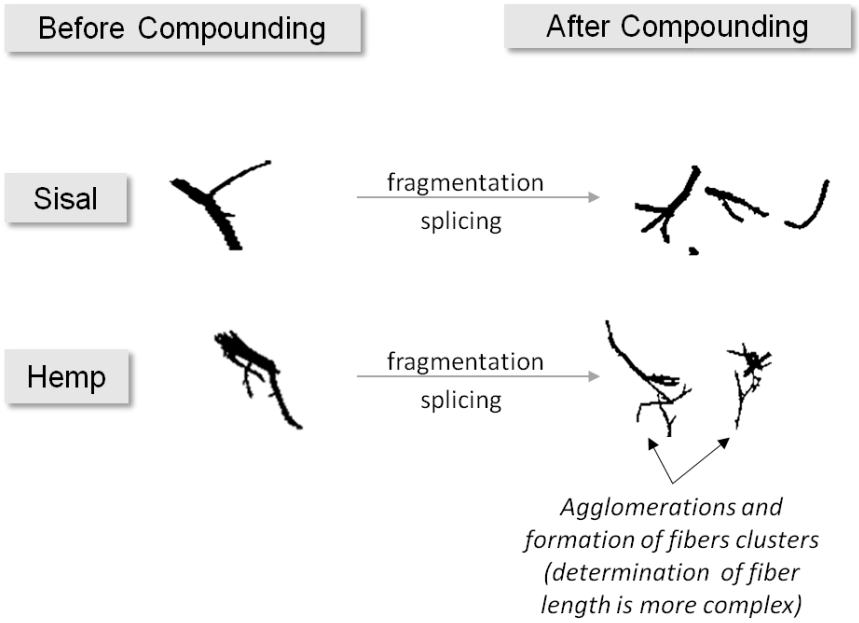

Figure 4-10: Development of fiber shape after compounding for both sisal and hemp

4.4 Moisture Absorption of Sisal and Hemp Fibers

Moisture absorption tests are very important to characterize both fibers and compounds to be able to set the processing conditions to assure a good quality of

the injected compound. In this case, the injected products are all samples which will be further tested, so the quality of the samples is very important to give conclusive results and representative analysis. Moisture absorption tests are performed on both neat sisal and hemp fibers and their compounds. Literature values show an average moisture content for sisal of around 9% whereas hemp around 10% As shown in Figure 4-11, neat fibers of sisal and hemp follow almost identical course in moisture absorption whereas hemp lands at a slightly higher moisture content than sisal. After 180 min, sisal and hemp reached 9% and 9.5% moisture contents respectively. This difference in the absorbed moisture contents is attributed to the content of hemicellulose in each fiber type. As previously mentioned in 4.3, hemp possesses up 10% higher amount of hemicellulose which are responsible of the moisture absorption [Cel13].

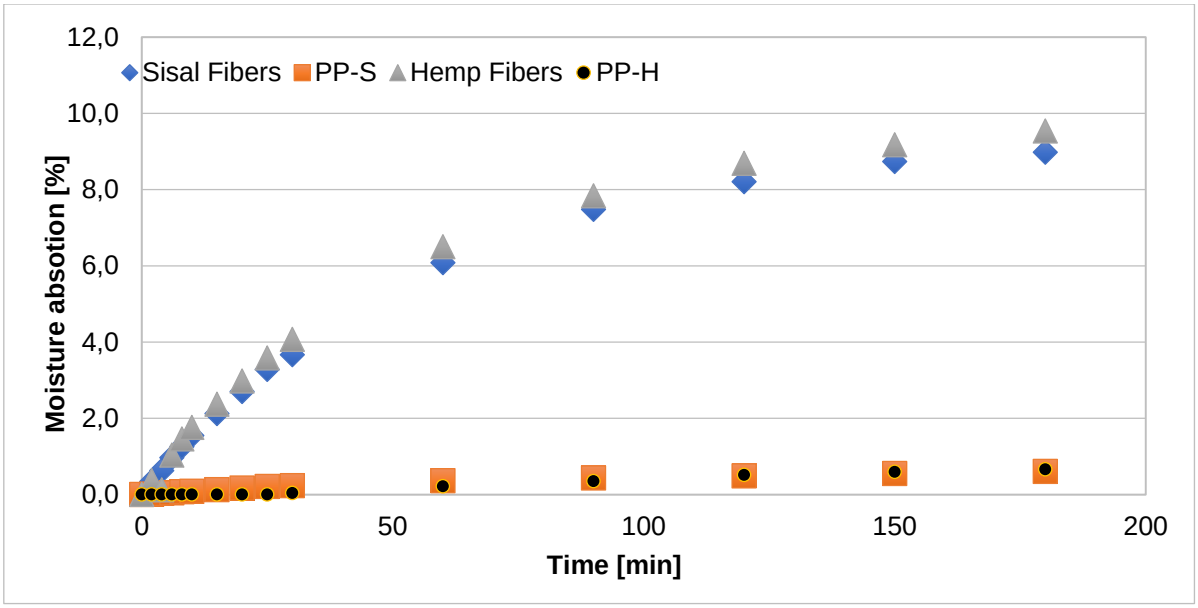

Figure 4-11: Effect of time on moisture absorption for different composites

On the contrary to neat fibers, both sisal and hemp compounds show very low levels of moisture content where after 3 hours, both sisal and hemp compounds reach only 0.7% moisture content. This result was expected due to the hydrophobic nature of the surrounding PP matrix which prevents the moisture absorption by fibers in case there is no open cut.

Understanding the hydrophilic behavior of sisal and hemp fibers and its influence on the properties of the compound especially in the characterization phase is very important for the quality of this research. Moisture absorption leads to volumetric nonconformance and instability inside the compound. Moisture absorption at room temperatures leads to the swelling of the fibers embedded in the PP matrix which in turn generate internal stresses. At temperatures, higher than 100°C such as common processing temperatures for injection molding of around 200°C for PP matrix compounds, evaporation of the trapped humidity inside the compounds occurs. This in turn leads to several uncontrolled effects such as shrinkage of fibers and simultaneously formation of internal pores in the injected sample [Cel13].

This volumetric change between the fiber and the matrix cause the de-bonding of the fibers from the matrix PP which in turn leads to the drop of the mechanical properties due to failure in the load transmission. Figure 4-12 illustrates these effects schematically.

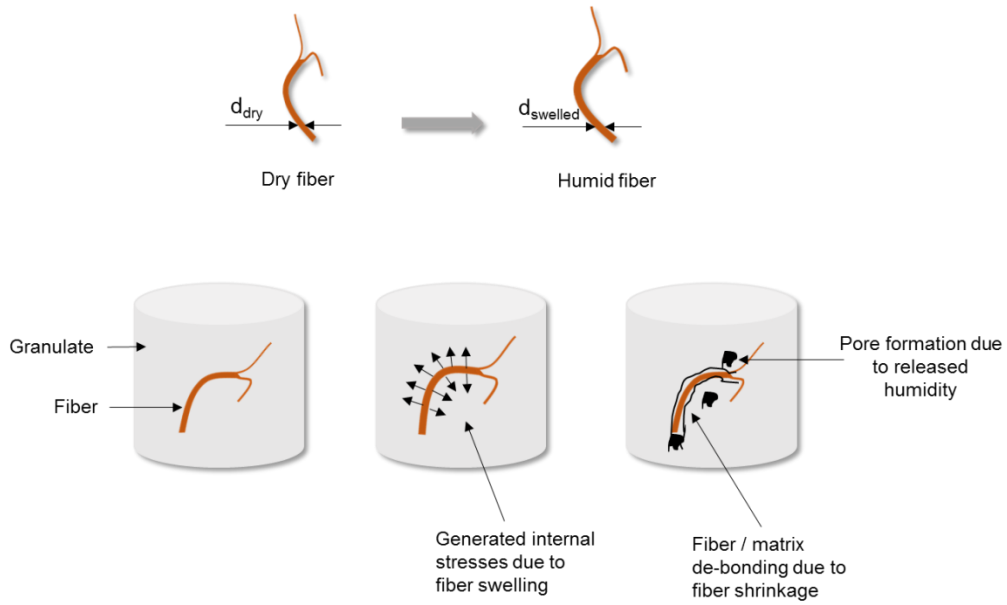

Figure 4-12: Effect of volumetric change between the fiber and the matrix on fibers' debonding

To avoid these effects, all the compounds and samples under examination are dried in oven at 100°C for 24 h before injection.

4.5 Rheological Properties of Sisal and Hemp Compounds

Rheology is one of the most important characteristic aspects when studying the flow of non-Newtonian fluids such as NFTC, especially for injection molding applications. It gives direct and indirect information about the flow behavior of the filled polymer melt under application of temperature and different shear rates. This is very important to develop an understanding about the behavior of the polymer melt during injection and during mold filling. Although the viscosity of NFTC is dependent on the matrix properties, fillers – especially natural fibers – play a very important role in influencing the melt viscosity. Natural fibers being a natural product unlike synthetic fibers have a wide span of geometries within the polymer melt. Being flexible, curly and having rough surface, natural fibers possess the ability to form agglomerations and fiber clusters within the polymer melt. Applying low shear rates, can give the clusters the needed time to de-agglomerate and to distribute among the matrix and hence cause higher rheological readings. By applying high shear rates simulating that of the injection molding process, the fiber clusters are forced in the flow direction without de-agglomerating and thus the matrix properties dominate the compound viscosity. To better understand this effect all materials under study are measured at both low and high shear rates.

4.5.1 Viscosity of Sisal and Hemp Compounds

In Figure 4-13a, the variation in the viscosity of the compounds is significant. The sisal fibers with the lower tendency to agglomerate are better distributed in the matrix and hence increase the overall viscosity of the compound. The two sisal compounds PP-S and PP-30%Sisal have identical behavior and represent the highest viscosity followed by the pure PP matrix (457 Pa.s with respect to the 381 Pa.s of PP at 100 1/s using the plate rheometer).

Hemp compound (PP-H), shows an unexpected behavior where its viscosity value drops below the value of the pure matrix. This could be attributed to the formation of several fiber clusters which are not distributed over the matrix and hence only the PP properties dominate. The lower viscosity value than the pure PP matrix could be explained by two factors:

- Presence of fiber clusters within the matrix cause the development of micro flow in the polymer melt which induces excess internal shear forces and cause the thinning of the compound [Ram14b]. This unexpected behavior matches with the flowability results after recycling for PP-H as discussed later in chapter 5.
- As previously mentioned in section 4.1 for the thermal properties, at 200°C – which is the testing temperature – as proven previously, the hemp starts to degas and produce volatile compounds which cause the decrease of the overall compound viscosity.

Under very high shear rates up to 10000 [1/s] (using the high-pressure capillary rheometer), the influence of the fibers demolishes and only the matrix rheological properties dominate as seen in Figure 4-13b.

It can be noticed that all compounds although having different reinforcing fibers possessing different properties in addition to the pure PP matrix, show parallel trends of viscosity. Here it is worth mentioning that some differences in the readings are present because of the difference in the method of operation between plate rheometer and high-pressure capillary rheometer. For the plate rheometer (measuring low shear rates, a simple correction is to be applied for non-Newtonian fluids to compensate the difference in shear rate from the center to the edge of the plate. This correction is mainly based on the measured rotational moment of the plate and characteristic local shear rate.

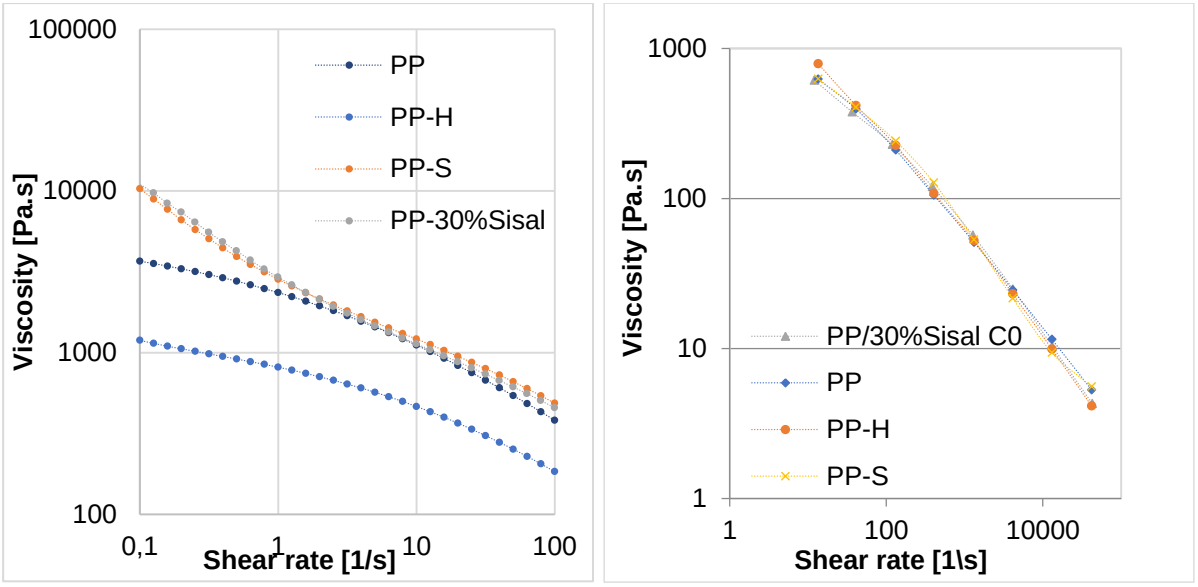

(a) (b)

Figure 4-13: Rheological behavior of NFTC compounds (a) Rheometer at T=200°C (b) High pressure capillary rheometer at T=200°C

The high-pressure capillary rheometer measures the viscosity indirectly by measuring the pressure difference at two dies at which the polymer melt flows. In this case two corrections should be applied: Weißberg-Rabinowitch-Correction and Bagley correction. Rabinowitch correction is used to compensate the error in reading caused by flow of non-Newtonian fluids where a valid shear rate could be calculated.

Bagley correction is applied to compensate the error in pressure reading due to die entrance effect to obtain the true shear stress and consequently calculate the true viscosity of the measured fluid.

4.5.2 Flowability of Sisal and Hemp Compounds

As mentioned in 3.4.1, the flowability of the compounds is investigated by measuring the flow length using the spiral flow method to determine the mold filling behavior of the compounds during injection molding. Pure PP represents the highest flowability in comparison to the other PP-S and PP-H as shown in Figure 4-14. The least flowability of PP-H is attributed to the agglomeration of the branched hemp (before recycling).

Contradictorily to the viscosity results, PP-H which has the lowest viscosity shows less ability to flow in the spiral mold than the PP-S with the higher viscosity. To be able to understand this phenomenon a better understanding of the flow and the distribution of the fibers along the spiral length is required [Ram14a]. Literature report several cases of a non-single-phase flow due to phase separation between reinforcing fibers and polymer matrix during injection molding specifically at mold entrance [Syk09].

This phase separation occurs due to the difference between the densities of the reinforcing fibers and the polymer matrix. Under high pressure and injection rate, the fibers with higher densities flow faster than the polymer matrix and hence phase

separation occurs. This multi-flow system is best studied using the spiral test which represents a one-dimensional flow.

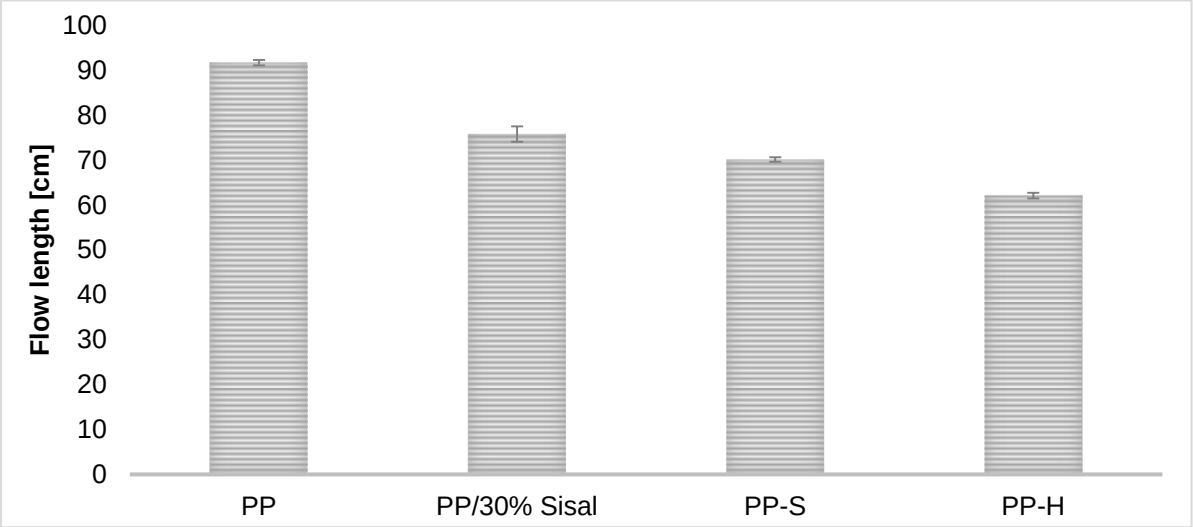

Figure 4-14: Spiral flow length of NFTC compounds

Phase separation is not only limited to the difference in the densities, it extends also to the fibers shape and size where longer flexible fibers behave differently than the stiff fibers. Development of a deep understanding of the flow of the hemp and sisal compounds is essential to construct a scientific foundation to further study the effect of recycling on these compounds. In order to achieve this, a qualitative assessment of the fibers distribution along the spiral length is performed as described in 3.4.3 and 3.4.4.

By analyzing the original granules, a deviation of the fiber weight content from the nominal 30 wt-% value could be determined where PP-S and PP-H have 26.7 wt-% (0.5 std. dev.) and 31.3 wt-% (0.8 std. dev.) respectively. However, these values of fiber content are not constant along the spiral length. As seen in Figure 4-15a, fiber content at position 10 cm shows the lowest values over all spiral positions besides the original granules. For PP-S the fiber content ranges between 22.1 – 40.4 wt.-%, whereas PP-H ranges between 28 – 36.3 wt.-%. By neglecting the fiber content value of the original granulates, an increasing linear trend could be easily detected for both PP-S and PP-H.

It is also noticed that the minimum and maximum fiber content values for both compounds balances nearly around the spiral midpoint. The fiber content value at this point corresponds to the fiber content of the original granulates as illustrated in Figure 4-15b. This finding was also reported in several studies where Kubat [Kub74] detected the presence of a fibers concentration gradient along the flow axis of the reinforced polymer melt. Kubat reported a reduction in the fiber content after entering the spiral mold followed by a linear increase till reaching a maximum at the tip of the spiral passing by the average (original) fiber content.

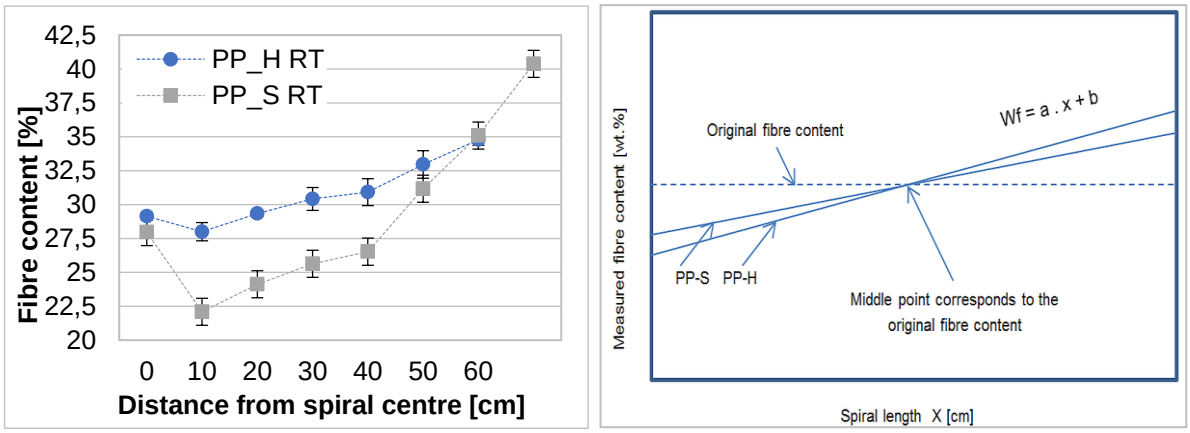

(a) (b)

Figure 4-15: Change of fiber content along the spiral length (a) Experimental (b) Trend lines [Ram14a]

This can be explained as follows: at first, the polymer melt undergoes turbulent flow conditions at mold entrance. This flow disturbance in addition to the difference in densities between fibers and matrix causes phase separation where matrix and fibers flow at different velocities.

This phase separation causes the fibers to agglomerate together forming fiber clusters. Secondly, the formation of a solidified layer of polymer of the surface of the mold cavity causes extra shearing stresses between the flowing melt and the surface of the solidified layer. In addition, the solidified layer causes the shorter fibers to attach to it where the longer and larger diameter fibers continue to move along with their inertia. Disturbed by the turbulences and the shearing forces, these long fibers tangle together and form fiber clusters. These fiber clusters move as one body with a reduced surface area in comparison to single homogenously distributed fibers. According to the principal of energy conservation, the reduced polymer interfacial surface of the fiber clusters leads to better flow conditions (longer flow distances) due to the reduced matrix resistance. This in turn results in obtaining higher fiber content at the tip of the spiral. Formation of flowing fiber clusters within the polymer melt is highly dependent on the fibers' shape and dimensions. Table 4-4 lists the fibers' lengths and diameters at different distances along the flow axis. It can be easily noticed that for hemp and sisal fibers, the longest fibers and the largest diameters are found at the end of the flow length, which emphasizes this theory.

Table 4-4. Fiber dimensions at certain positions along the spiral of PP-S and PP-H

	Flow [cm]	length		Average	std	diameter		Average	Std
		l1	l2			d1	d2		
PP-H	10	445,77	339,49	**392,63**	75,15	20,04	17,78	**18,91**	1,60
	30	434,05	392,21	**413,13**	29,59	43,68	12,46	**28,07**	22,08
	60	525,84	383,42	**454,63**	100,71	44,81	14,21	**29,51**	21,64
PP-S	10	753,38	329,21	**541,30**	299,93	62,07	21,84	**41,96**	28,45
	40	673,69	900,15	**786,92**	160,13	31,06	72,04	**51,55**	28,98
	80	927,02	570,50	**748,76**	252,10	77,98	19,98	**48,98**	41,01

The fiber length increased by 27% for PP-S and 14% for diameter. For PP-H, 14% increase in the length and 37% increase in diameter is also recorded. This means that fiber shape quantitative analysis is essential to explain the difference between PP-S and PP-H in terms of fiber content distribution along the flow axis.

4.6 Conclusion

Decomposition of natural fibers is not affected by the host polypropylene matrix. All decomposition products of the pure fibers (Carbohydrates, water, carbon dioxide and acetic acid) are detected in the mass spectra of PP-H and PP-S.

Addition of fibers enhances nucleation and crystal growth. Also leads to the increase of viscosity, decrease of spiral flowability and the increase of water absorption. Sisal compounds present relative higher viscosity with respect to the pure PP matrix, with values 457 Pa.s and 381 Pa.s respectively at 100 1/s. Hemp compound (PP-H) has a lower viscosity. This is attributed to the fiber branching which induces agglomeration at least in the first compound form before recycling.

Fiber morphology shows the branching flexible nature of hemp fibers in comparison to the straight and stiff nature of sisal fibers. This will help in modeling the effect of fiber type on the flowability and afterwards on the mechanical properties. The qualitative description of the fiber morphology is validated by the QicPic images.

5 Effect of Recycling on Characteristics of Sisal and Hemp Compounds

Recycling influences the behavior of the compound in several ways depending on the resulting properties of both matrix and fibers as a result of applying extensive shear and thermal stresses. Within this chapter, the effect of the recycling on the resulting compounds' properties will be discussed based on the change in the fibers morphology and compounds' rheological behavior after recycling. The discussion will focus mainly on the first four to five cycles according to the discussed property. In some particular cases where some emphasis is required, further cycles could be included for justification purposes.

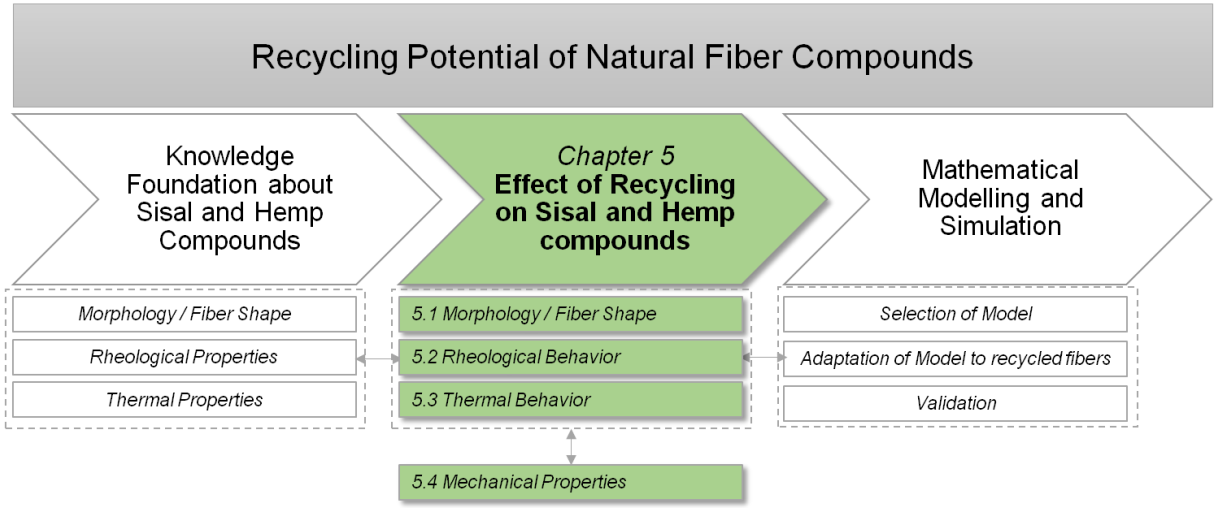

Figure 5-1: Chapter 5 flow chart

As shown in Figure 5-1, the effect of recycling on fibers' shape and size will be thoroughly discussed in 5.1 and will serve as a basis for understanding the change in the rheological behavior and flowability presented in 5.2. Afterwards in 5.3, effect of recycling on thermal properties of the compounds will be presented. Since crystallization behavior is a very important aspect when dealing with thermoplastics especially for injection molding processes, crystallization behavior of recycled compounds is also discussed in this section. Enlightened by the previous knowledge, the change in mechanical properties in relation to recycling which will be explained in 5.4. Information gathered from these results will serve as an input for the modeling of fiber flow behavior and mechanical properties under recycling which is to be discussed in chapter 6.

Finally, the knowledge gained from the discussions is summarized in an informative conclusion.

5.1 Effect of recycling on fibers' morphology and polymer structure

As mentioned in 2.4.4 and illustrated in Figure 2-14, it is assumed that the mechanical properties of the composite are dependent on the development of the fiber size, shape and coupling with the PP matrix. In order to verify this assumption, dynamic image analysis (QicPic) and microscopic investigations in addition to electron scanning microscope investigations are performed.

5.1.1 Fiber size

The reduction in fiber size (length and diameter) is detected by QicPic and key results are listed in Table 5-1 below with supporting pictures.

Table 5-1. Fiber dimensions and fiber gallery at different cycles of PP-S and PP-H

	[µm]	Original	C0	C1	C4
Sisal	Length	4709	1860	1358	837
	Diameter	223	99	95	16
	QicPic Photo Gallery	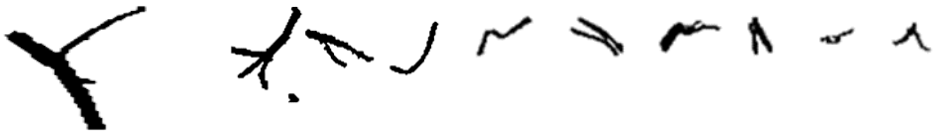			
	Microscopic Pictures	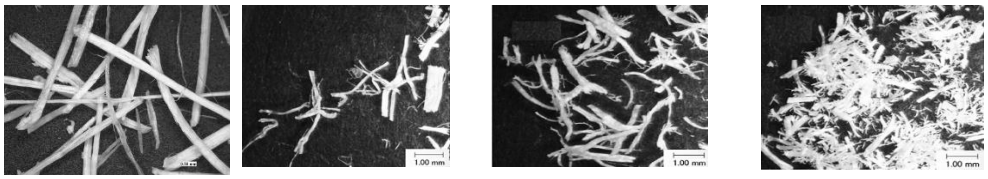			
Hemp	Length	3293	2200	2085	686
	Diameter	72	43	37	27
	QicPic Photo Gallery				
	Microscopic Pictures	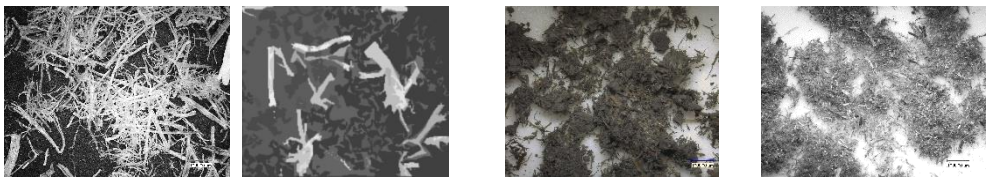			

From Table 5-1, it is obvious that sisal fibers undergo successive reduction in length till cycle 4. On the other hand, the diameter remains constant with a value around 100 µm for the first cycles, afterwards a significant reduction in diameter at C4 occurs. This could be attributed to the effect of the severe shear forces in the extruder screws which cause the fragmentation and splicing of the stiff large sisal fibers till the critical length/diameter is achieved where the fibers could easily flow in between the cavities of the two screws without being affected by further recycling. On the other hand, hemp fibers show a slightly different behavior where a significant reduction in size occurs in the first compounding step C0. Afterwards hemp fibers length and diameter remain almost constant till cycle 4 where a second significant

size reduction occurs. To evaluate the influence of the multiprocessing steps, the fiber length and diameter are determined via dynamic image analysis sensor QICPIC using the wet method LIXELL. The effect of recycling on the fiber dimensions and fibrillation in both hemp and sisal is obvious. The fiber shape in Table 5-1 resembles the theory of fiber size deterioration during multi-processing cycles schematically shown in Figure 2-7. The results are statistically evaluated using the second moment Q2 using Equation 5-1.

$$\boldsymbol{Q_2 = \frac{\sum_{i=1}^{n} X_i^2}{n}}$$

Equation 5-1

Where “X” is the fiber size (diameter or length) and “n” is the number of measured fibers. The second moment is selected for the evaluation because it gives more weight for the fiber with larger lateral surface area and consequently the effect of small fibers which do not impart in reinforcing and load transfer is reduced. Figure 5-2 shows selected frames taken from the dynamic imaging.

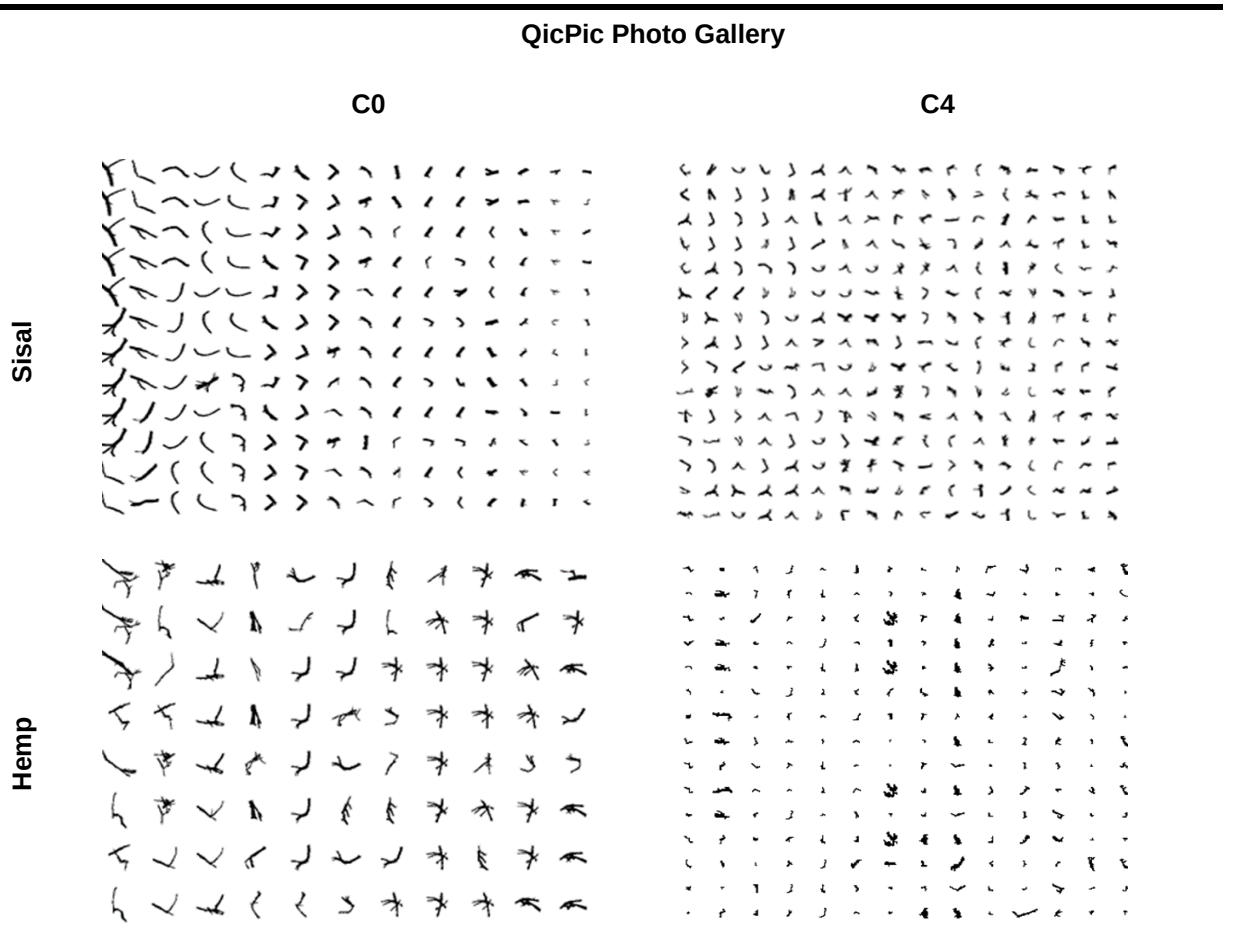

Figure 5-2: Dynamic image system of sisal and hemp fibers at C0 and C4 using QICPIC (M8 lens)

Figure 5-3 shows the results of length measurement for C4 for extracted sisal (a) and hemp (b) using the image analysis software which analyzes the fibers regarding the continuous length and diameter. Each graph shows five successive length measurements for the same sample.

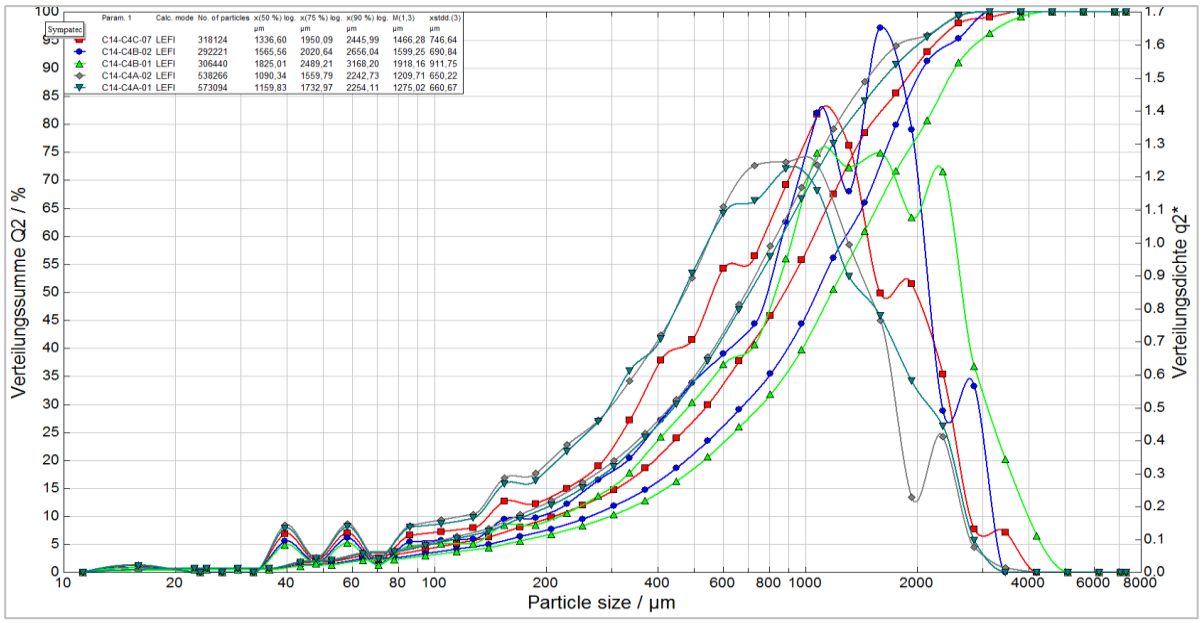

(a)

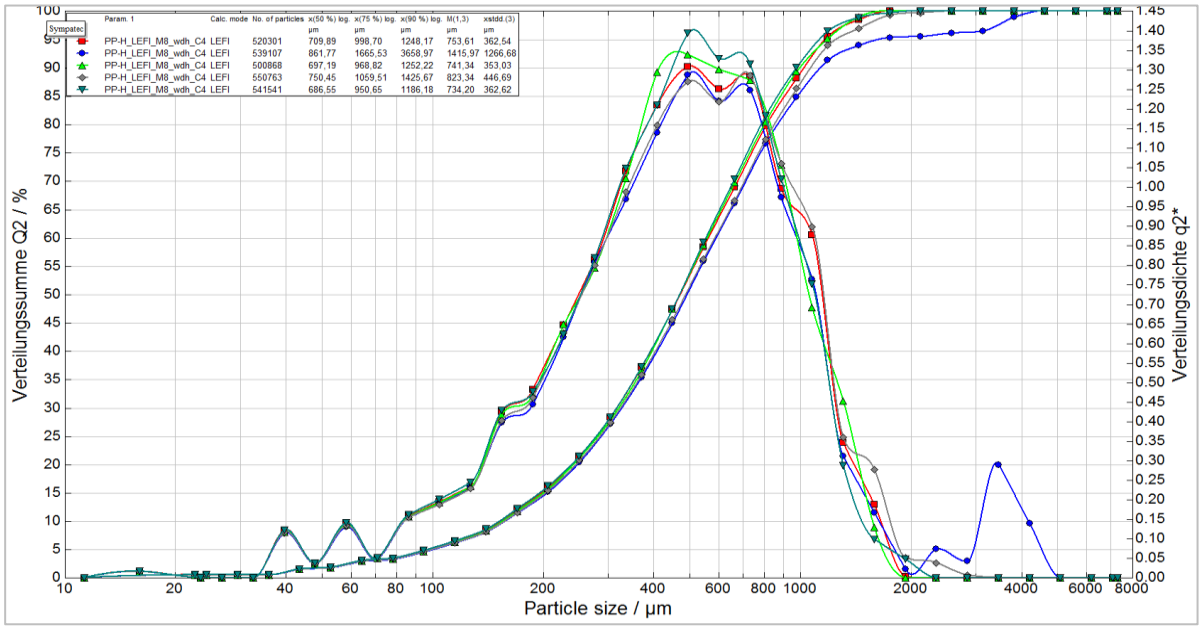

(b)

Figure 5-3: An example of the results taken from QICPIC showing the fiber length distribution of (a) PP-S and (b) PP-H at C4

For the investigated cycles, the sprue position is considered the original situation before being subjected to further shearing and fibers separation during spiral injection. This is justified by Figure 5-4, where fiber lengths were measured for all positions in the injected spiral. It is obvious that the fiber length for the sprue position represents the average fiber length for all positions.

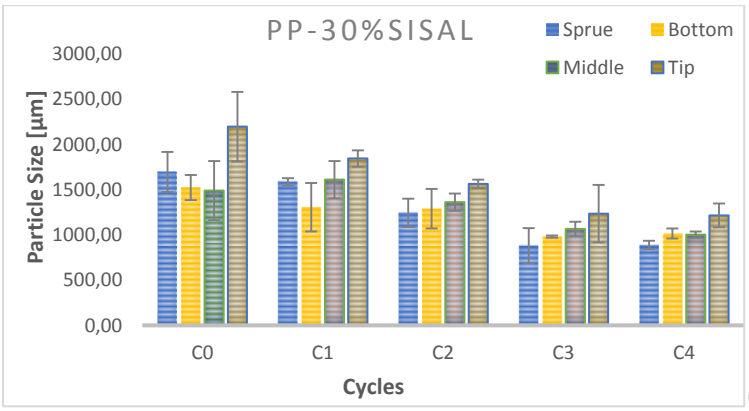

(a)

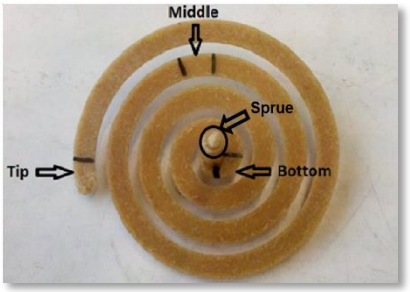

(b)

Figure 5-4: Effect of recycling on fiber length (a) Fiber length at C0 and C4 (b) positions of fiber extraction for QicPic measurement

Figure 5-5 presents the median fiber length of the extracted hemp and sisal fibers from the sprue position. The fiber length decreases in a negative logarithmic function. Stable values are reached starting from the second and third cycle according to fiber type. On the other side, Figure 5-6 shows the change in fiber diameter for both fibers. It is obvious that the first cycle has the largest influence on the fibers size reduction (length and diameter) afterwards; the reduction follows a very steep slope.

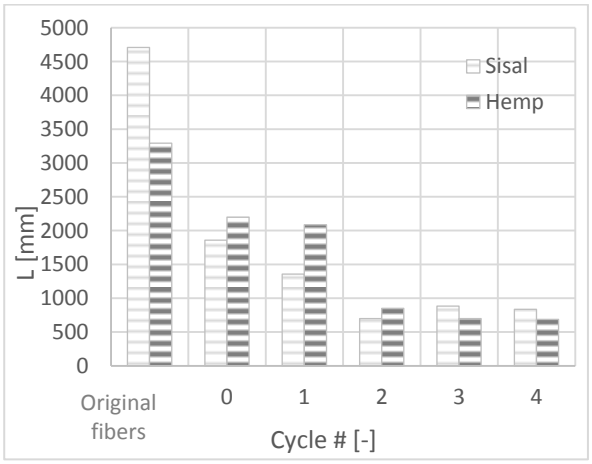

Figure 5-5: Median fiber length of PP-S and PP-H taken from the sprue extracted fibers at different cycles

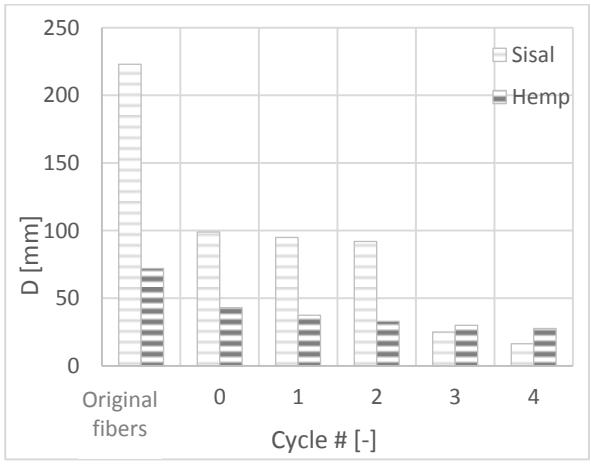

Figure 5-6: Median fiber diameter of PP-S and PP-H taken from the sprue extracted fibers at different cycles

It is important here to mention that diameter measurements must be carefully considered. QicPic numerical analysis system based its calculation on the measuring the fibers transversal size and consider it the diameter of the fiber. This is correct in case of synthetic fibers which have standard circular cross section. However, natural fibers being a natural product have different cross sections varying from circular to oval to flat for the same fiber type in the same compound as illustrated in the microtome sections in Figure 5-7. A microscopic investigation of the microtome slices is carried out to determine the fiber shape and orientation. The injected samples of PP-30%Sisal and PP-H at C0 (shown in Figure 3-13) are cut to four positions at even distances. The structure shows long fibers concentrated at the end of the rectangular

sample which also matches with the results from the spiral test for sisal sample. Additionally, the edge of the sample has more cross-sections of fibers. This indicates that the fibers are oriented with the direction of the flow. The reason is that the high shear at sidewalls helps in the orientation of the stiff sisal fibers. Hemp fibers show different behavior, where much less orientation could be detected. This is attributed to the flexible nature of hemp fibers which tend to bend under stresses rather than orient to a special position. The orientation of hemp fibers could only be detected at the upper edge of the sample where the injection flow occurs.

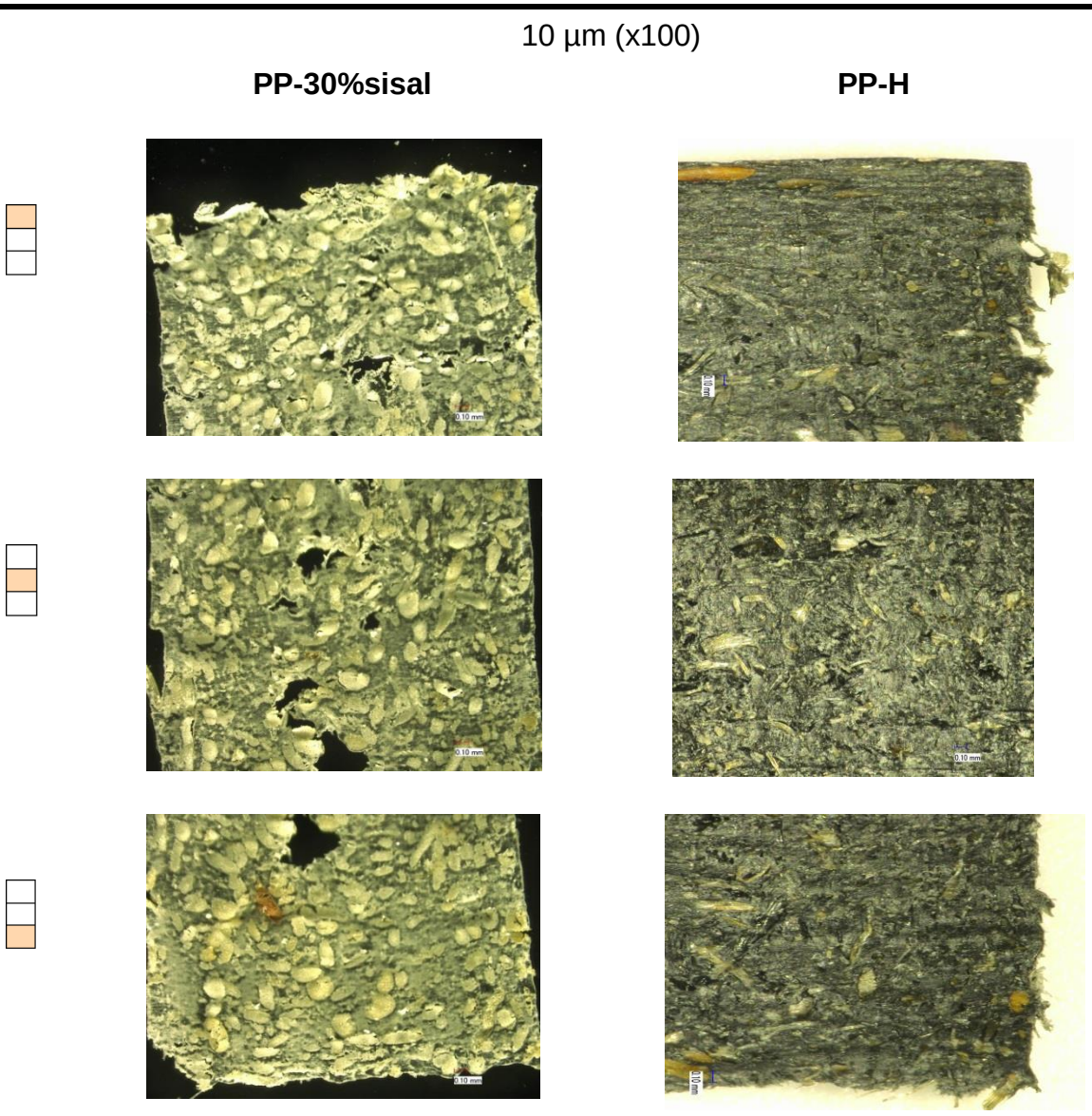

Figure 5-7: Microscopic pictures of microtome sections taken from four cross sections of PP/30% sisal and PP-H at C0

5.1.2 Fiber aspect ratio

Critical aspect ratio is the minimum fiber length to diameter ratio required to reach the maximum adhesion shear strength. Based on the results of lengths and diameters, the aspect ratio of the fiber can be calculated as in Equation 5-2.

$$\boldsymbol{AR = \frac{L}{D}}$$

Equation 5-2

Where '$\boldsymbol{L}$' represents fiber length, '$\boldsymbol{D}$' is the fiber diameter and '$\boldsymbol{AR}$' is the aspect ratio.

Results of the aspect ratio are then illustrated in Figures 5-8 and 5-9. AR values decrease from 18 at C0 to 7.4 at C2 for sisal fibers. Afterwards, an increasing trend till C4 is observed where AR reached 50. Hemp fibers show a different behavior where the aspect ratio remains almost constant till C3 (51.1) then drops at C3 to almost the half (24). Taking into consideration that not only fiber length decreases due to recycling, but also a decrease in the fiber diameter occurs, the increase of AR after C2 could be easily comprehended.

According to [Bos04], the critical aspect ratio for flax (L=400 µm, D= 15 µm) is 26. Pickering [Pic16] investigated the critical length of Hemp and sisal fibers in PP matrix with MA-PP coupling agent and reported values of 0.67 and 2.3 mm respectively.

In another research [Bou07] reported lower values for sisal and hemp aspect ratios where for the original compounds' AR values. For PP-Hemp treated with maleic anhydride, aspect ratios of 8.5 and 7.5 for C0 and C4 respectively are reported. PP-Hemp compound without malice anhydride recorded lower values of 11 and 2.5 for C0 and C4 respectively. For PP-Sisal, values of 9 and 4 for the aspect ratio of the original compound and after 4 processing cycles are reported.

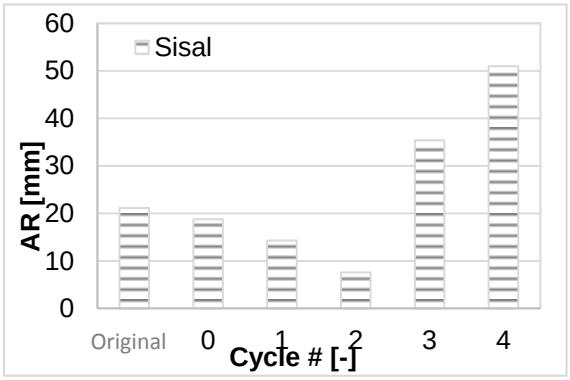

Figure 5-8: Aspect ratio of extracted sisal fibers taken from the sprue extracted fibers at different cycles

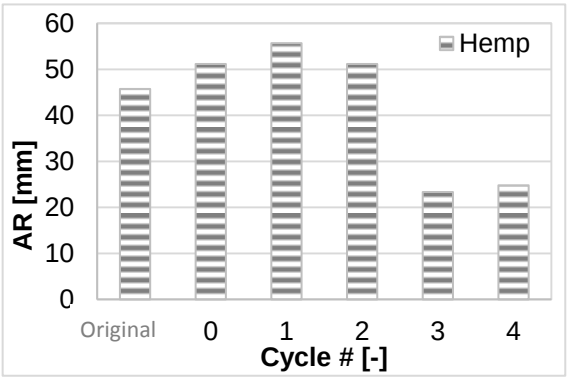

Figure 5-9: Aspect ratio of extracted hemp fibers taken from the sprue extracted fibers at different cycles

This enormous difference in values between the researchers is attributed to the method of determination of fiber length. [Pic16] used the digital microscope to measure the fibers length where only a few number of fibers (av. 50 fibers / sample) are measured. Smaller fibers could be ignored during measurement due to the magnification limits. In this thesis, the QicPic method gives statistically reliable results (av. 300000 fibers / sample) where all fibers in range are measured. Therefore, the results of fibers especially sisal in Figure 5-8 are very promising since AR is above

the value 26 after recycling. This demonstrates that sisal fibers are more suitable for recycling since their load transfer ability is not critically affected.

5.1.3 Fibers distribution

As previously discussed in Figure 5-4, the fiber lengths vary along the spiral length where longer fibers are always found at the tip position and shorter fibers are found at the bottom. The effect of recycling on this behavior is studied in this section on PP-S. Trend lines of different cycles are shown in Figure 5-10, Figure 5-11 and Figure 5-12 for fiber length, diameter and aspect ratio respectively. Samples taken from sprue are plotted at -10 mm for illustration purposes. The following information could be concluded from both figures:

- The slope of fiber length with respect to position is positive for all cycles. This means that longer fibers can be injected for longer distances,
- Fiber length decreases by recycling where fiber length of C0 is the longest and C4 is the shortest
- The decrease in fiber length due to recycling is minimized after C3. Therefore, the fiber length along the spiral after C3 is close to that after C4
- Fiber diameter decreases along the spiral length especially in the first cycles like C0 and C1
- The magnitude of the slope describing the diameter reduction is significant at the original batch C0. Then the magnitude is decreased at C1 and then it almost vanishes at C4. This means that the fiber size is reduced enough so that it is not anymore able to be spliced (smallest diameter)
- Aspect ratio increases by the increase of the cycle number.

Comparing these results with [Els17], equivalent results are obtained. For instance, Elsabbagh [Els17] has shown also that the longer fibers are injected for longer distances. However, he described the fiber length as well as fiber content analytically in non-linear empirical equations.

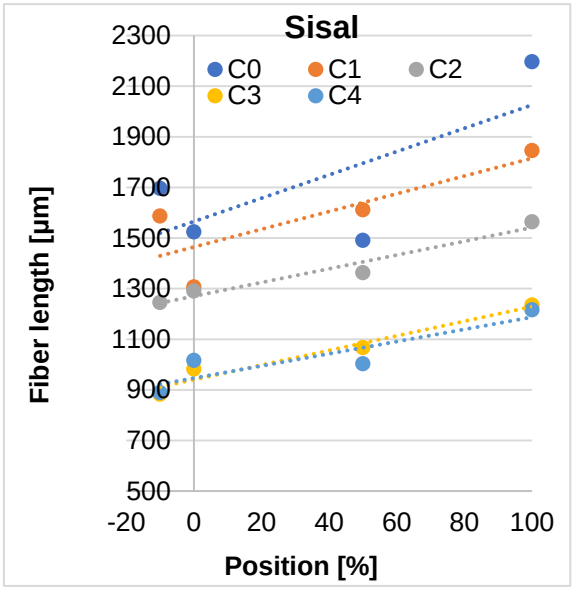

Figure 5-10: Development of the median extracted fiber length along the spiral length at different cycles

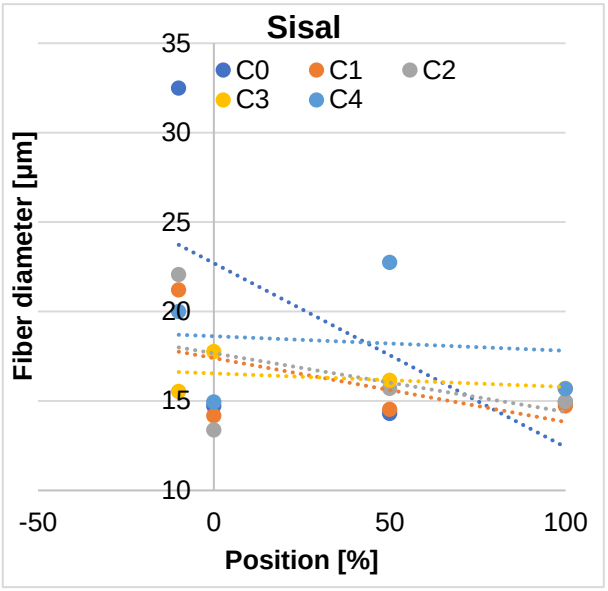

Figure 5-11: Development of the median extracted fiber diameter along the spiral length at different cycles

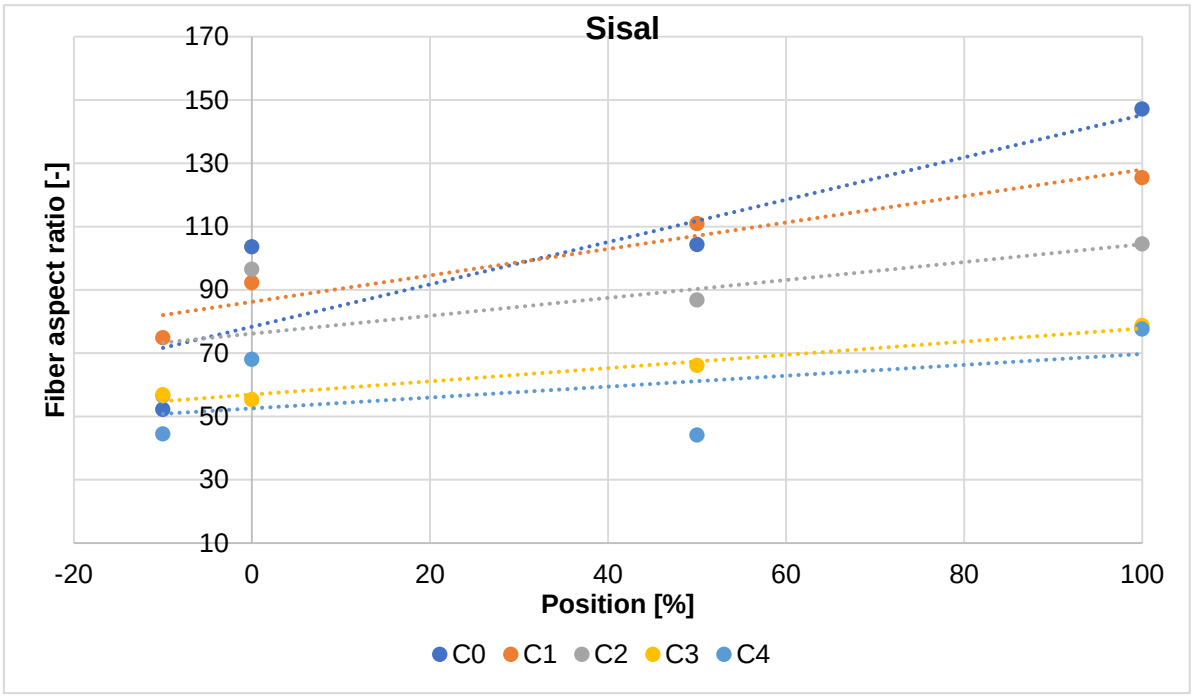

Figure 5-12: Development of the fiber aspect ratio along the spiral length at different cycles

Another effect of recycling on fiber structure and distribution could also be concluded from Figure 5-13a&b. It is remarkable that larger and longer fibers are present at C0 more than C4. It also can be noticed that at C4, the fibers are more homogeneously distributed over the matrix, whilst at C0, the fibres form more agglomerations. This leads to the conclusion that recycling has a positive effect on the homogeneity of the resulting compound which reflects afterwards on the mechanical properties as will be later discussed in 5.4.

C0

10µm (x100) 5µm (x600)

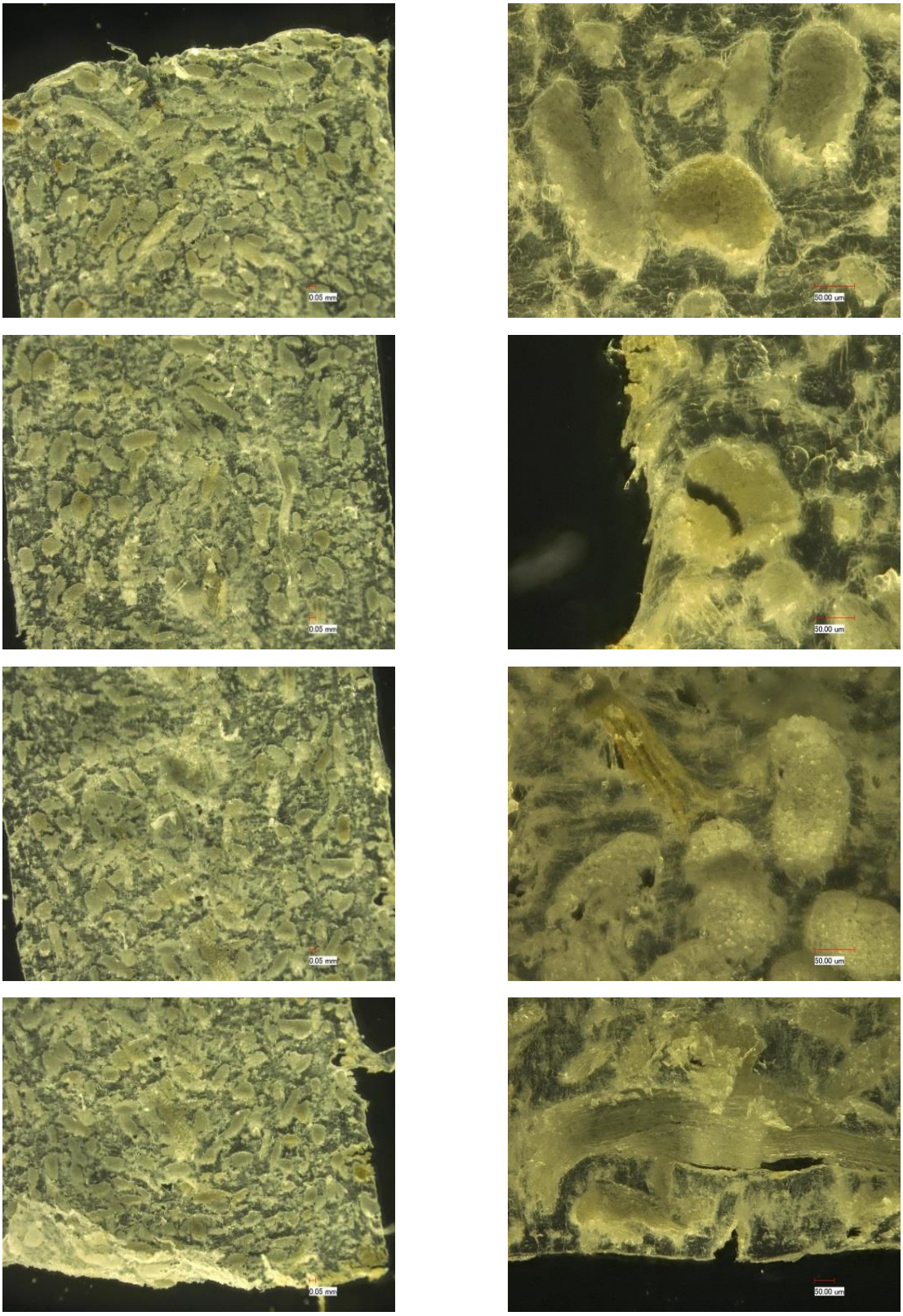

Figure 5-13a: Microscopic structures taken from four cross sections of PP/30% sisal at C0

C4

10µm (x100) 5µm (x600)

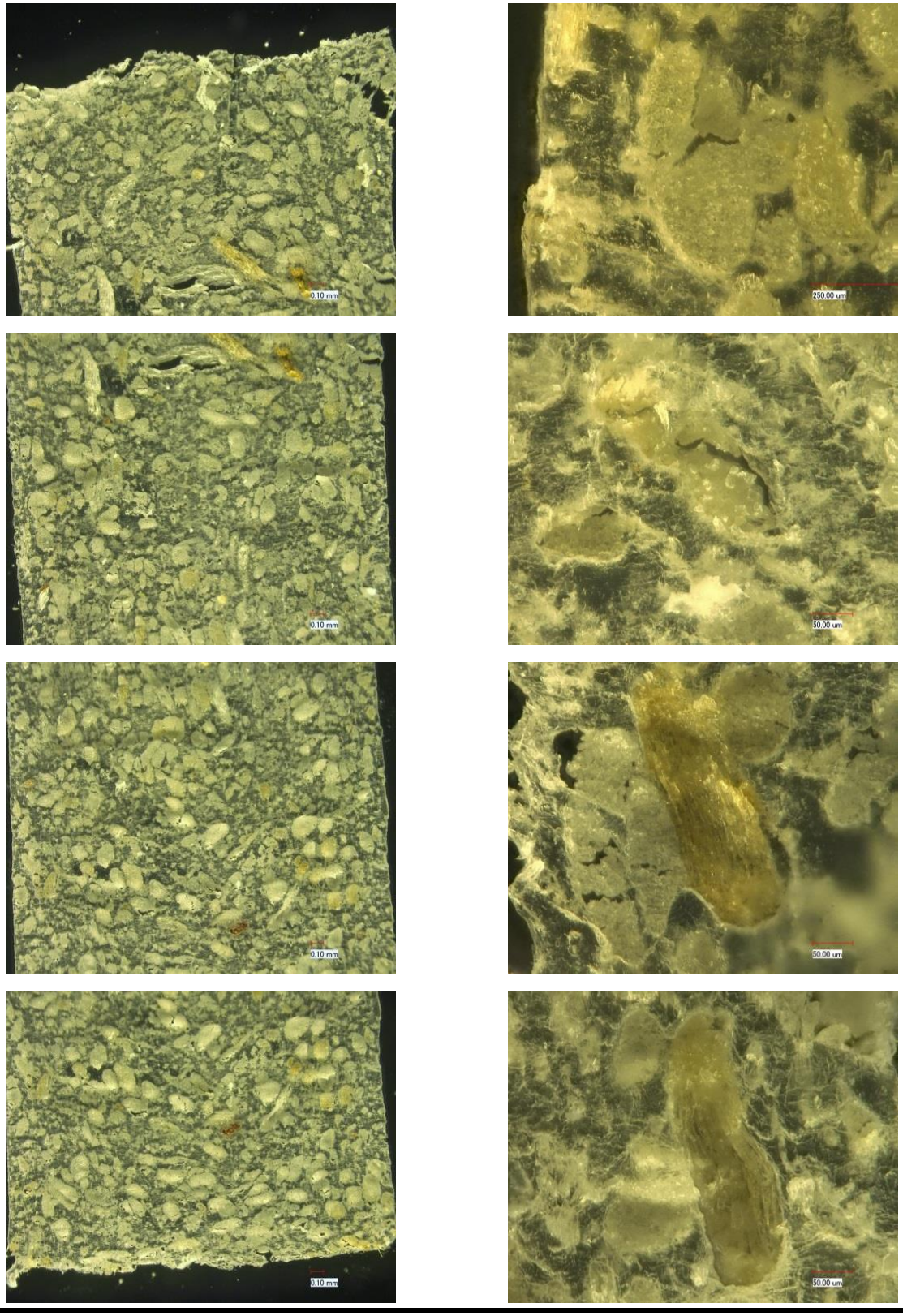

Figure 5-13a: Microscopic structures taken from four cross sections of PP/30% sisal at C4

5.2 Effect of recycling on rheological behavior of sisal and hemp compounds

5.2.1 Flowability

Recycling of NFTC affects not only the molecular weight of PP and the fiber length, but also the rheological aspects of the material. Rheological properties correspond to some aspects such as the viscosity and the flowability of the material. Viscosity describes the material flow quantitatively. Flowability measurement, by the injection of spirals, is a qualitative description for how long the material can flow through a spiral mold with certain dimensions under certain process parameters (Pressure, mold temperature, polymer temperature…).

Based on the discussions in the previous section 5.1especially figures 5-8 and 5-9, a theory about the expected flow behavior of the compounds after recycling could be crystallized. Hemp and sisal fibers are selected to investigate the effect of the fiber type and shape on the flowability of NFTC and hence verify the theory. Evolution of compounds flowability is expected to pass by three main stages which comply with the changes in the fibers dimensions.

- Stage 1 (C0): Fibers are still long and thick in case of sisal or are tangling together forming agglomerations in case of hemp which leads to a lower flowability than expected.
- Stage 2 (C1 – C2): Where a massive reduction in both length and diameter of fiber occurs leading to a significant positive change in the flowability.
- Stage 3 (> C3): A slight change in flowability could be detected due to the homogeneous distribution of the fibers in the matrix after size reduction and successive shear stresses during recycling.

Study of fiber discusses the effect of the shape (straight or branched) and the effect of the type (stiff or flexible). Sisal represents the type of short stiff fiber without branching while the hemp fiber represents the flexible branching type of fibers.

Based on the morphology of both fibers (hemp and sisal), it is expected that both PP-S and PP-30% Sisal will perform better flowability results than PP-H due to the straight form and stiffness of the reinforcing sisal fibers which hinder the formation of agglomerations.

To verify this theory, spirals are injection molded as described in section 3.4.1 and the lengths of the spirals are measured in cm. The average length is used as an indicator for the spiral flowability. Number of samples is 10 samples per each cycle. Flowability tests are also carried out on PP samples as reference.

Figure 5-14 presents the average spiral flow length for each cycle. The flowability behaviors are presented in continuous form although they are out of discrete and integer number of cycles. But for better illustration, continuous curves are used. The following remarks can be deduced out of the flowability results:

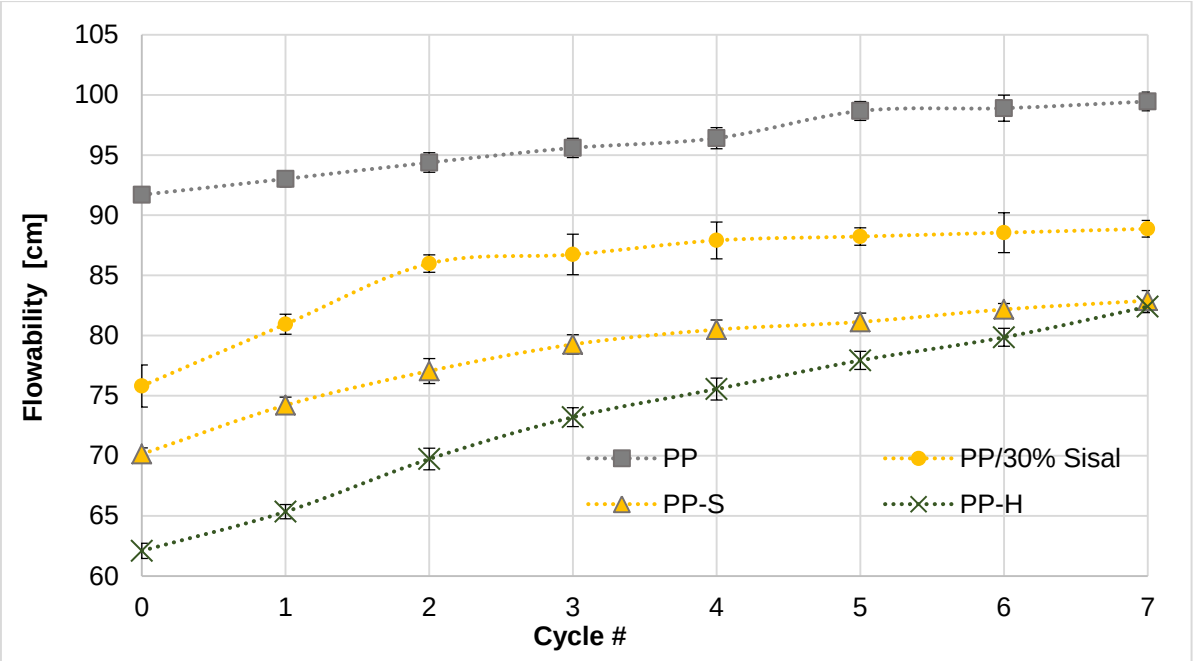

Figure 5-14: Effect of recycling number on the flowability for PP and different compounds (spiral test)

- Generally, Increasing the number of recycling times increases the flowability length,
- The increase in flowability does follow more than single linear trend. The flowability increases remarkably in one or two cycles. Then, the flowability increases slightly in a logarithmic trend. Logarithmic trend is more suitable in describing the breaking events of fibers along the consequent reprocessing cycles. The slope of the logarithmic function decreases with more cycles which is not the case with linear functions,
- The presence of fibers with PP affected the flowability of the composite negatively in comparison to the flowability of the pure PP. Flowability values of both types of NFTC at any cycle are less than that of the flowability of PP by 15-25% depending on the fiber type and the cycle number,
- By increasing the number of cycles, the flowability of both fibers are coming closer to each other. This can be explained by the fiber length relation with the total viscosity and flowability [Els17]. The fiber length after each cycle can be correlated with fiber breakage. This can be attributed to the quick breaking of sisal fibers after one cycle. Further cycles do not induce much breakage of fibers and hence flowability is not significantly enhanced. Hemp fibers due to flexibility and branching are also broken to smaller ones after the first and the second cycles but further cycles still induce relatively significant fibers breakage,
- PP-H has flowability values less than that of PP-S and PP- 30% Sisal. This can be attributed to the fiber shape. The effect of fiber type is discussed in [Els15a]. Figure 5-15 shows previous results obtained on non-recycled NFTC injection molded at the same parameters (1000 bar and 200°C). Different fiber

types are used such as cellulose, flax, wheat straw, wood fiber, hemp and sisal. Flax and hemp belong to the bast fibers where fibers are branched and flexible. Sisal fibers are leaf fibers whereas wheat straw are grass fibers. Cellulose fibers are regenerated fibers acting like sisal but with higher aspect ratio and more flexible behavior (lower bending modulus).

- The flowability of PP-H after one cycle does not change significantly. This indicates the presence of fibers still tangling or agglomerating. Afterwards, the flowability increases steeply indicating meaningful change in fiber size. It is obvious that the flowability behavior does not follow the pattern of E-modulus or tensile strength with respect to cycle number shown later in 5.4.

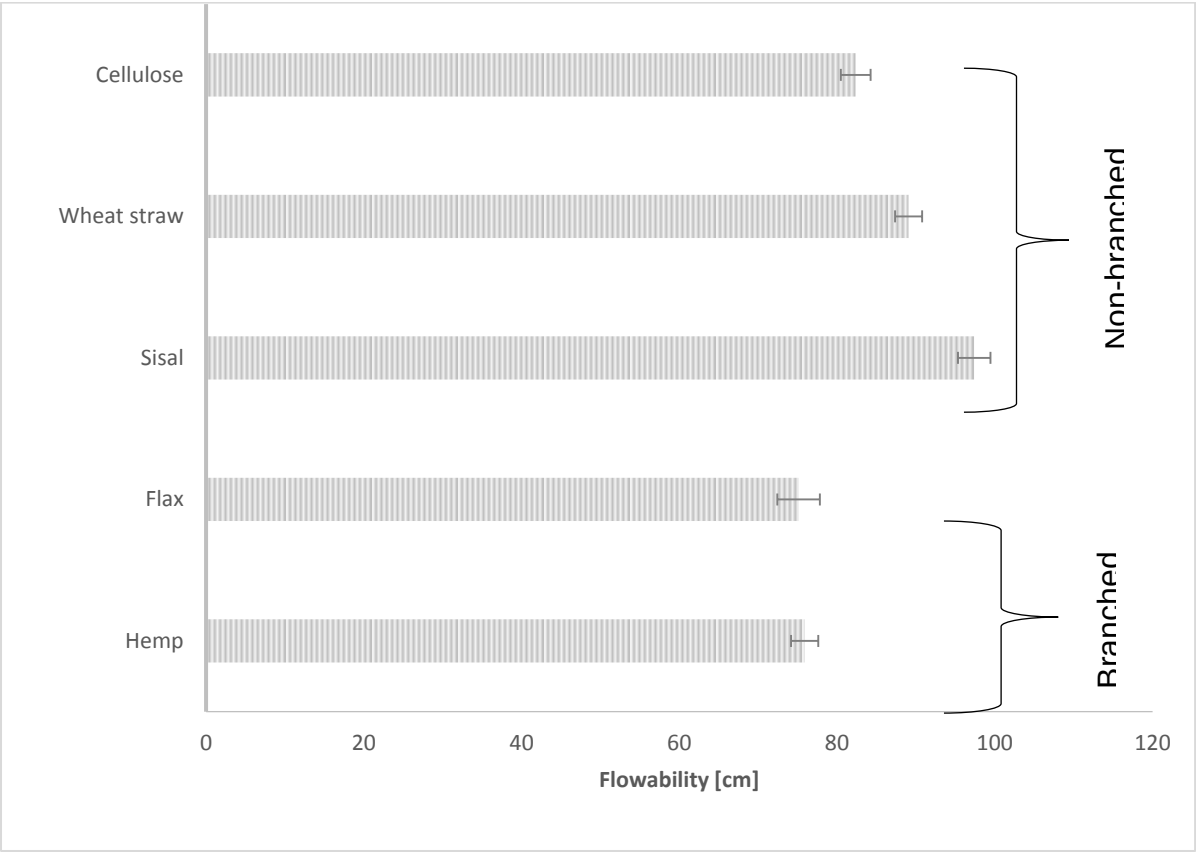

Figure 5-15: Effect of fiber type on the spirals' flowability at 1000 bar injection pressure [Els15a]

The theory of the flowability behavior can be justified in a quantitative manner to three stages as follows:

a- Threshold shearing (in terms of cycle number) is required before a significant improvement in flowability is noticed. This stage is assumed to be characterized with tangling or agglomerating fibers. This is most likely to occur in the branched fibers like flax and hemp,

b- The second stage is characterized with a sensitive flowability behavior. Flowability is remarkably enhanced with more recycling. The enhancement here can be interpreted theoretically in terms of fiber splicing and thinning besides to less agglomeration,

c- Third stage shows relatively slow improvement in flowability. This implies less effect of fiber change in size combined with the decrease in the molecular weight of the PP matrix.

The three stages of flowability behavior are then dominated by three factors. The first stage is governed by the required threshold shear to loosen the entanglements. The second stage is controlled by the fiber branching whereas the third stage is finally controlled by the degradation of PP molecular weight. However, these assumptions of the three stages cannot be validated without microscopic evidences and fiber measurement.

A schematic diagram illustrates the three stages theory in Figure 5-16, where the flowability is controlled by the fiber agglomeration, fiber shape and length. At stage 1, fibers are thick and may be tangling especially the hemp fibers. At stage 2, fibers start to be split, getting thinner and shortened. Stage 3 assumes fiber thinning and more shortening. This assumption of fiber's sizing is validated by the QicPic measurements Figure 5-17.

The viscosity measurements of the NFTC after several recycling will be helpful in explaining the flowability results. Thus, viscosity measurement can give a quantitative description for the spirals' injection molding. This description can be further used in modeling and simulation of the NFTC flow.

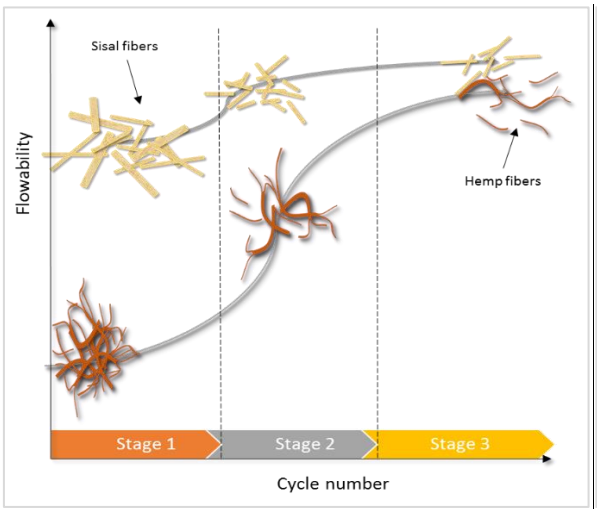

Figure 5-16: The presumed three stages of flowability at different cycle numbers showing the corresponding fiber shape and size.

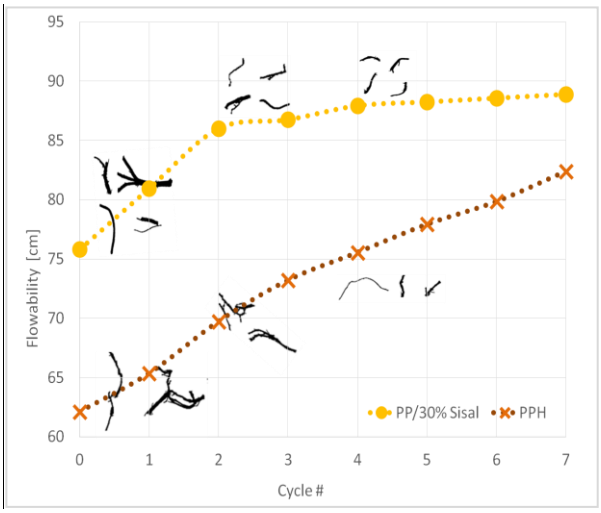

Figure 5-17: Effect of the number of cycles on the spirals' flowability for PP, PP-H and PP/30% Sisal

5.2.2 Viscosity

To measure the resistance of the molten compound to the shear stress, viscosity measurements on the rotational rheometer with the low shear rate range of 0.01 up to 100 1/s at 200°C are performed.

Graphs comparing the viscosity between all cycles are illustrated for better visualization of the results and to be able to deduce correlations. As discussed in 5.2.1, the main changes happen in the first three cycles. Therefore, just the original material C0 and the first subsequent cycles till C5 are presented. Figure 5-18 shows the decrease of PP viscosity by reprocessing. Figure 5-19 and Figure 5-20 show the following remarks in comparison with the behavior of PP:

- Viscosity of PP does not change significantly after the third cycle (C3) indicating that there is no more remarkable molecular scissions,
- Viscosity of filled polymers is higher than the unfilled PP.
- The non-Newtonian range in filled PP is larger than unfilled PP.
- Viscosity of PP-S and PP-H is reduced under the effect of recycling. However, the viscosity of the NFTC is magnified more than ten times in comparison with PP at the very small shear rates [0.01-40] 1/s. Afterwards, higher shear rates show that NFTC have close or even lower viscosity than PP.
- The viscosity of PP, PP-S and PP-H at 100 1/s are 343, 197 and 192 respectively,
- It is important also to highlight the decreasing trend of PP-S viscosity regardless the shear rate,
- The reduction in viscosity in case of PP-S follows a decreasing exponential function. PP-H shows oppositely a non-systematic trend. For instance, C0 and C1 have low viscosities with respect to C2 and C3 at least till 40 1/s shear rate approximately,
- PP-H acts normally starting C2. C3 has lower viscosity than C2. This implies that the hemp fiber homogeneity within PP is not consistent and the viscosity of PP dominates the whole NFTC viscosity. However, the effect of hemp is still present because the viscosity behavior is not the same of PP at the investigated shear rate spectrum.

Figure 5-21 shows the recycling effect on PP/30% Sisal (longer length and lower aspect ratio). The decrease of viscosity under the effect of recycling is relatively small in PP/30% Sisal in comparison with PP-S of Figure 5-19.

The effect of fiber type on the measured viscosity is shown in Figure 5-22. Therefore, only the results of the original compounds (C0) are considered. PP-S has higher viscosity at C0 indicating a significant effect of fiber type. On the other side, both types of sisal fibers show similar viscosity results at C0. It should be recalled that the effect of the fiber dimensions is proved to be significant with the further recycling as shown in Figure 5-22, to Figure 5-27.

At C0, PP-H shows relatively lower viscosity with respect to PP reinforced with sisal (PP-S and PP/30% Sisal). At higher cycle numbers, PP-H has viscosity higher than the sisal compounds as shown in Figure 5-24. Starting from C3, PP-H has high viscosity but then decreases rapidly with increasing shear rate, Figure 5-24, Figure 5-25 and Figure 5-26.

The viscosity measurement using rotational / oscillatory rheometer is limited to small range of shear rates. However, this small range can better represent the effect of fiber type, shape and cycle number on the viscosity. According to a recent research in SPE [SPE16], it is proved that highly filled polymers undergo a special behavior under shearing as shown in Figure 5-28. At very low and very high shear rates the polymer compound shows a Newtonian behavior where the measured viscosities are considered the compounds' η_0 (zero shear viscosity) and η_∞ (infinite shear viscosity) respectively.

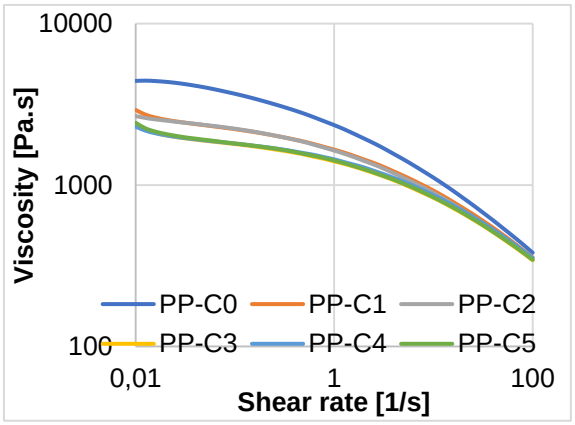

Figure 5-18: Effect of the number of cycles on PP viscosity using rotational rheometer at 200°C

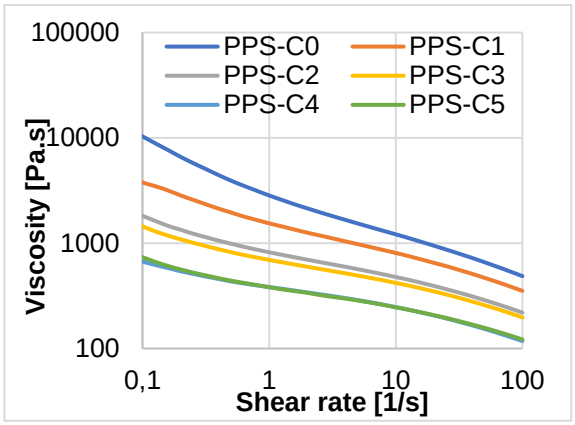

Figure 5-19: Effect of the number of cycles on PP-S viscosity using rotational rheometer at 200°C

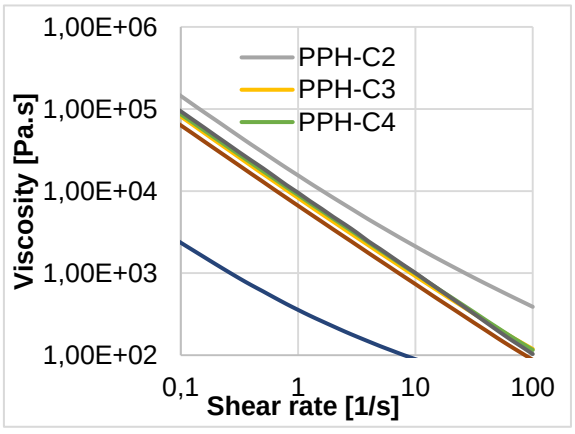

Figure 5-20: Effect of the number of cycles on PP-H viscosity using rotational rheometer at 200°C

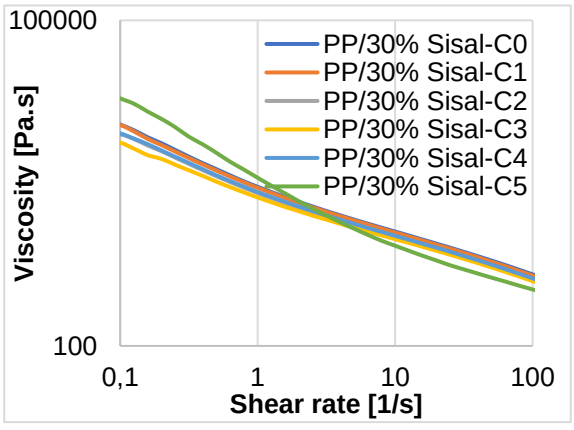

Figure 5-21: Effect of the number of cycles on the viscosity of PP/30% Sisal using rotational rheometer at 200°C

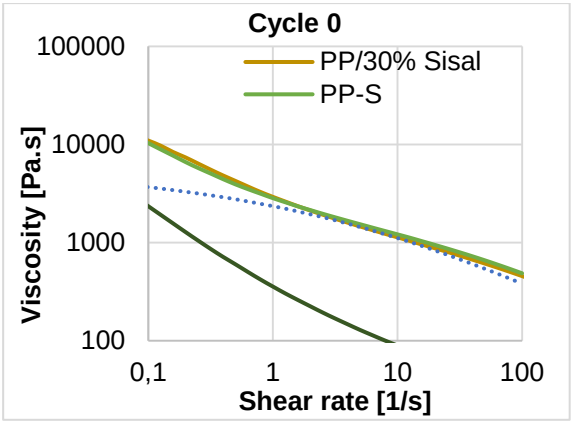

Figure 5-22: Effect of the fiber type on NFTC viscosity at C0 using rotational rheometer at 200°C

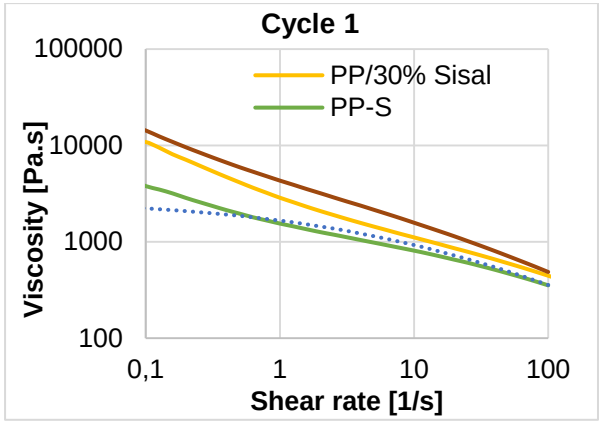

Figure 5-23: Effect of the fiber type on NFTC viscosity at C1 using rotational rheometer at 200°C

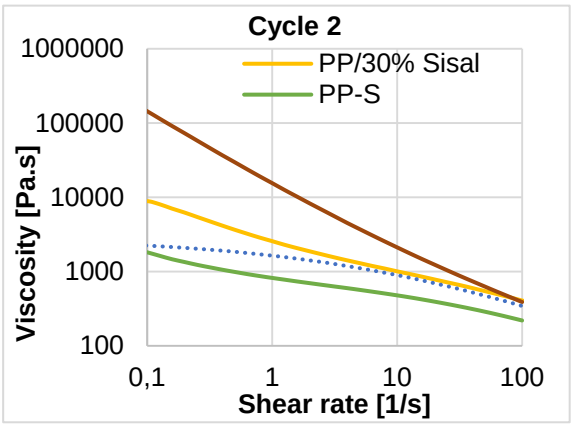

Figure 5-24: Effect of the fiber type on NFTC viscosity at C2 using rotational rheometer at 200°C

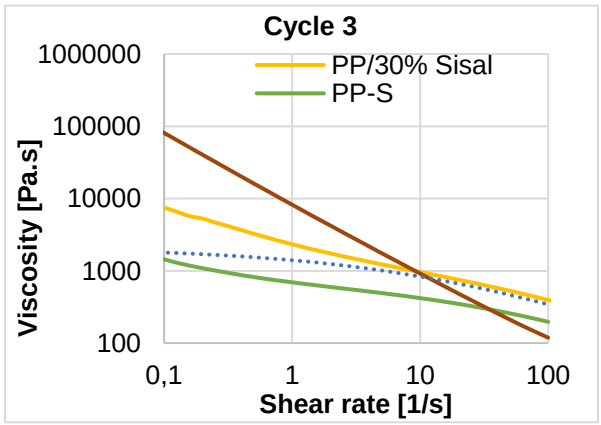

Figure 5-25: Effect of the fiber type on NFTC viscosity at C3 using rotational rheometer at 200°C

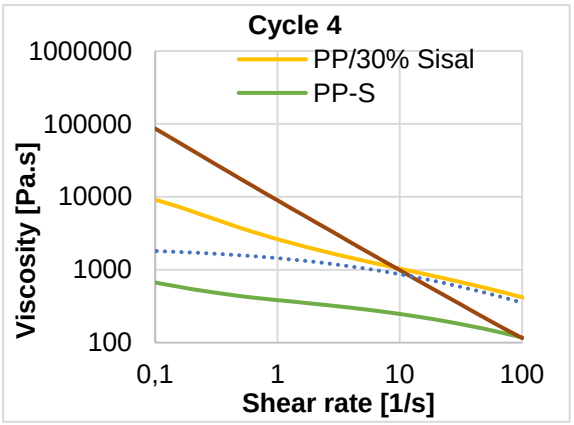

Figure 5-26: Effect of the fiber type on NFTC viscosity at C4 using rotational rheometer at 200°C

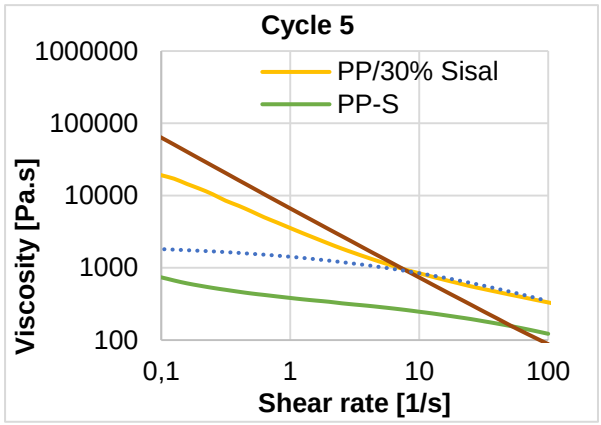

Figure 5-27: Effect of the fiber type on NFTC viscosity at C5 using rotational rheometer at 200°C

The non-Newtonian region lies between these two areas and is named Power-law region. This region describes the behavior of the compound especially the shear thinning phenomena under higher shear rates as shown in the same figure.

Fibers interact together due to its hydrophilic nature and attract together causing the increase of the non-Newtonian range by inducing high shearing stresses as a result of its friction with the matrix during motion resulting in the shear thinning effect. Thus, causing it to occur at lower shear rates than for the unfilled polymer melt. [TA 13]

This theory is adapted to understand and analyze the rheological behavior and results of the studied compounds in this theory.

The results shown in Figures 5-22 to 5-27comply with this model where the behavior at low shear rates is dominated by the fillers. Oppositely, the viscosity behavior at high shear rate is dominated by the polymer matrix behavior [TA 13].

The shear rate / viscosity behavior, as shown in Figure 5-28a, can be classified to three stages matching with the suggested 3-stage model of cycle number / flowability shown in Figure 5-28b. This relation between the two behaviors can be explained by means of energy conservation taking into consideration the inverse proportionality between flowability and viscosity. Absorbed energy at higher shear rates which causes thinning of the compounds, is proportional to the absorbed energy after repetitive cycles which also causes the increase in the flowability till a plateau is reached.

The disadvantage of rheometer measurement is that the shear rate range does not meet the expected shear rates during the injection molding process. High capillary rheometer is more capable of implementing higher shear rates (>1E4 1/s).

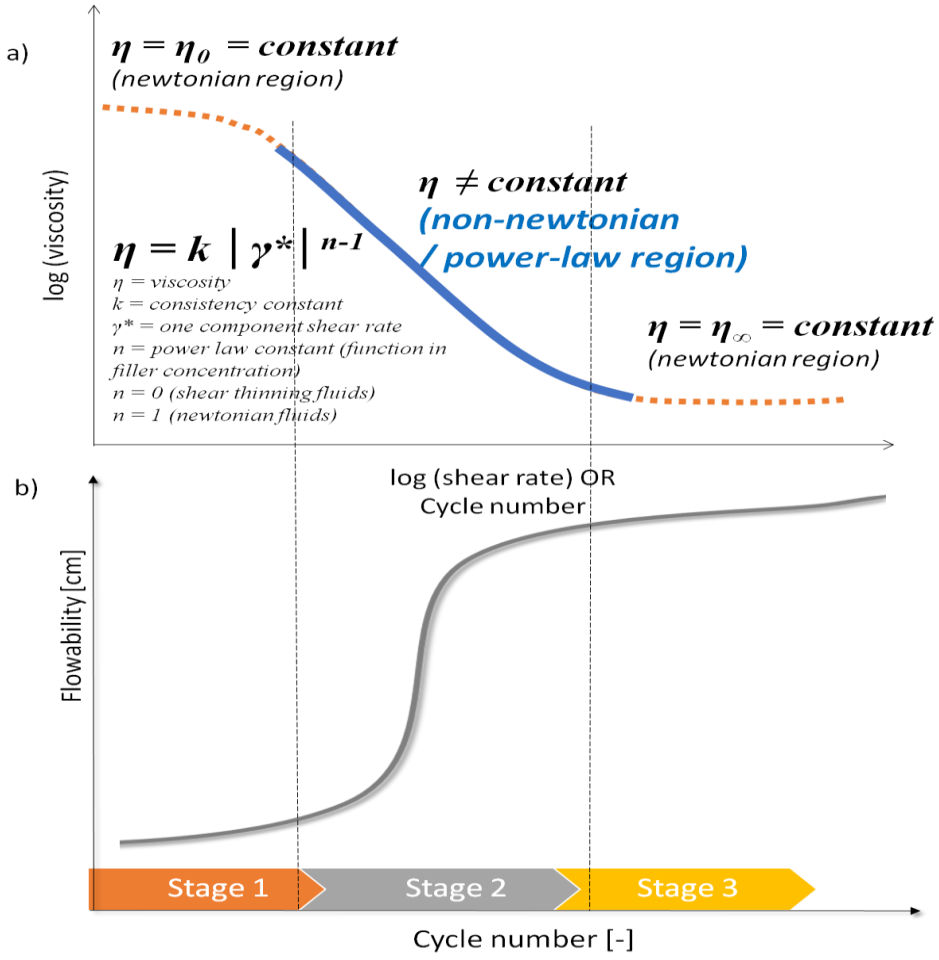

Figure 5-28: Power-Law model vs. 3-Stage Model [SPE16]

The objective of this wide range of shear rates is not only to measure the viscosity but also to check fibers coalescence when the compound is subjected to aggressive shearing. Fibers coalescence takes place when the fibers are not homogeneously distributed in the PP matrix [TA 13].

Figure 5-29 illustrates the recycling effect of PP/30% sisal on the viscosity at high shear rates up to 1.0E5 1/s. The measurements at different cycle numbers are getting close to each other by increased shear rate. These results match with the closeness of viscosities measured by the rheometer for the same material compound (PP/30% Sisal) in Figure 5-21.

The results of both rheometer and high capillary for PP/30% sisal (C0 and C4) are plotted together to check their similarity. As seen in Figure 5-30, the rheometer results are almost 5% more than those of high pressure capillary technique. But the trends are parallel. The higher rheometer measurements trends meet those reported by Kirchberg [Kir11] and Khan [Kha09].

The difference is attributed firstly to the use of the raw data without considering Bagley and Rabinowitch corrections regarding the pressure drop at entrance and the non-Newtonian flow respectively.

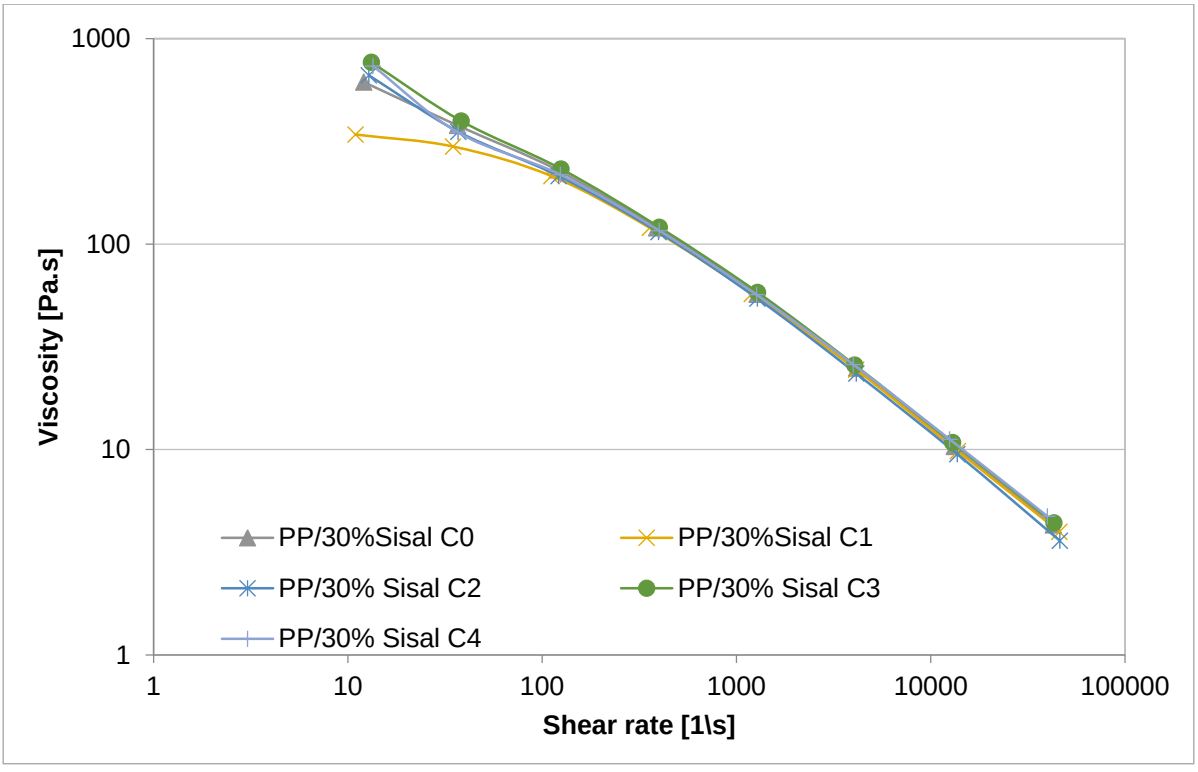

Figure 5-29: Effect of the number of cycles on the viscosity of PP/30% Sisal using high capillary rheometer at 200°C

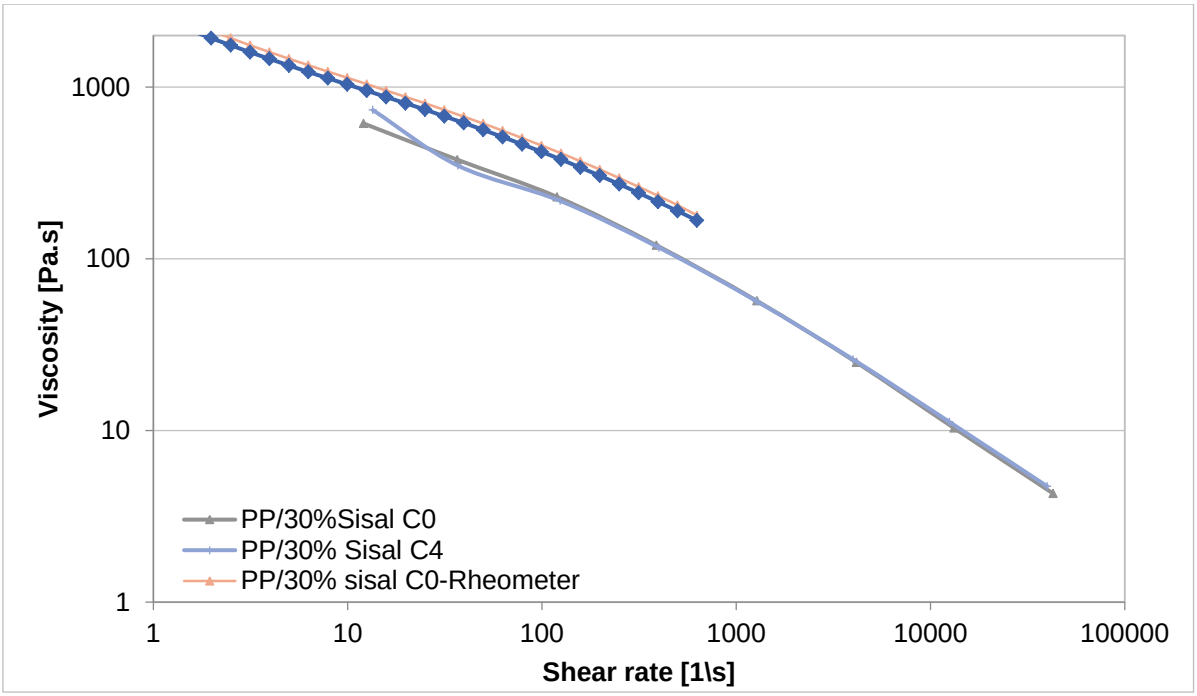

Figure 5-30: Measured viscosity using rotational rheometer against viscosity of high capillary rheometer for PP/30% Sisal at C0 and C3 at 200°C

5.2.3 Analysis of flowability versus viscosity measurements

Sections 5.1 and 5.2 presented besides the morphology of fibers, the rheological aspects, namely flowability and viscosity, under the effect of different cycles. The logical question which should be addressed now would be:

‘’Is there a consistent relation linking the flowability with the measured viscosity?’’

It is understood that the increase of flowability is a measure of decreasing the viscosity. Therefore, an index is proposed as following in Equation 5-3:

$$\boldsymbol{Index = Flowability\ x\ Viscosity}$$

Equation 5-3

Where:

Flowability is the average spiral length in cm

Viscosity is measured at shear rate 1 1/s

The index values are plotted in Figure 5-31 for PP as a reference material and both PP-H and PP-S compounds. As obvious, PP and PP-S are showing almost constant values. This indicates an evidence of the proposed relation between the flowability and viscosity according to the model proposed by Elsabbagh in [Els17]. This is attributed to the simple straight shape of the sisal and so its results fit perfectly in the model.

On the contrary, PP-H values show fluctuating results before stabilization after the third cycle. This is due to the complex branched nature of the hemp fibers which does

not support a simple inverse proportionality relation between viscosity and flowability at the studied flow rate (1 1/s) and 200°C temperature and consequently doesn't fit in the model.

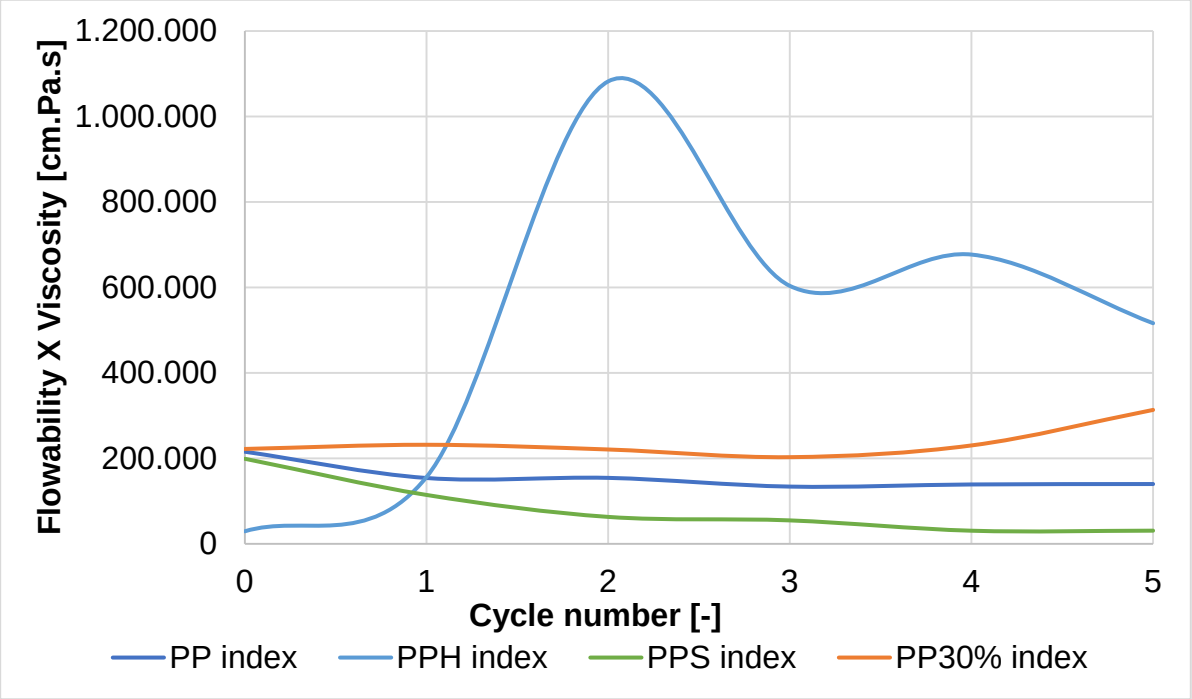

Figure 5-31: Calculated index values (Equation 5-3) for PP, PP-H and PP-S compounds

5.3 Effect of recycling on the thermal behavior characteristics

This section discusses the effect of the recycling on the thermal characteristics of NFTC. The thermal tests are designed to monitor the thermal degradation of the polymer composite as well as the constituents of the lignocellulosic fiber. This understanding will help in predicting the sequence of thermal decomposition and hence the composite can be better designed [Yao08].

5.3.1 Thermal gravimetric analysis

As mentioned before, recycling of the compounds under study is performed by shredding the injected parts to granulate then re-injecting them again in the injection molding machine. This leads to the application of several thermal stresses on the compounds during the injection process because of melting the compounds at temperatures around 200°C and application of high shear forces inside the machine between the screws. Despite of that, both natural fibers and the PP matrix proved to sustain their thermal stability during recycling at acceptable levels.

Figure 5-32 shows the effect of recycling on PP (original PP and five cycles). A zoom in is made around the maximum decomposition rate. Evaluation of the midpoint decomposition process (peak derivative thermal gravimetry DTG) is carried out according to ISO 11358. The temperature does not change excessively. However, it shows a decreasing trend of almost 3.3°C (from 458 to 454.7°C) after 5 cycles.

This decreasing trend is significant since the analysis is based on measuring 3 samples of each compound and obtaining the average with a standard deviation of less than 5%.

Similarly, Figure 5-33 shows the recycling effect on PP/30%Sisal. Humidity is the source of water vapor released at 100°C. Then as shown in the zoom Figure 5-33b, there are three degradation peaks at 295, 354 and 459°C. The first decomposition is related to the degradation of pectin and hemicelluloses, i.e. acetyl 4-O-methylglucuronoxylan. Second decomposition stage at 354°C is attributed to the degradation of α-cellulose which is the main fiber constituent that is responsible for load bearing. Here the amount of degradation is a function of the dehydration process. In addition, cellulose chain breaks-up to smaller chains which in turn release flammable volatiles and solid char. Most likely, lignin decomposition takes place also in the same second stage. The third decomposition range is attributed to the pyrolysis of the host PP matrix [Doa07].

It is also observable in Figure 5-33b, that there are two opposite trends for the change of the peak temperatures under the recycling effect. The first and the second stages show that the peaks slightly decrease from 297 to 295°C and 358 to 354°C respectively. On the other hand, the third stage shows an increasing trend of peak temperature from 435 to 459°C.

The decreasing trend in the first and second stages meets the results of Stehle [Ste16]. This is attributed to the relative depolymerization of hemicellulose and cellulose after recycling. Stehle [Ste16] has carried out further TGA experiments on the extracted fibers out of the compound after dissolving the PP. The extracted fibers show the same decrease of the decomposition temperatures.

The increase of the peak temperature in the third stage from 435 to 459°C matches with the results of [El-09]. The results are explained by the following points of view:

- Recycling develops new fiber surfaces ready for coupling with PP [El-09] in the presence of the coupling agent,
- Recycling gives chance for more number of carbonyl groups to share in increasing the coupling of the hydroxyl group with the PP matrix by the help of the grafting agent [Fon15] and consequently the decomposition temperature of the compound could be delayed.

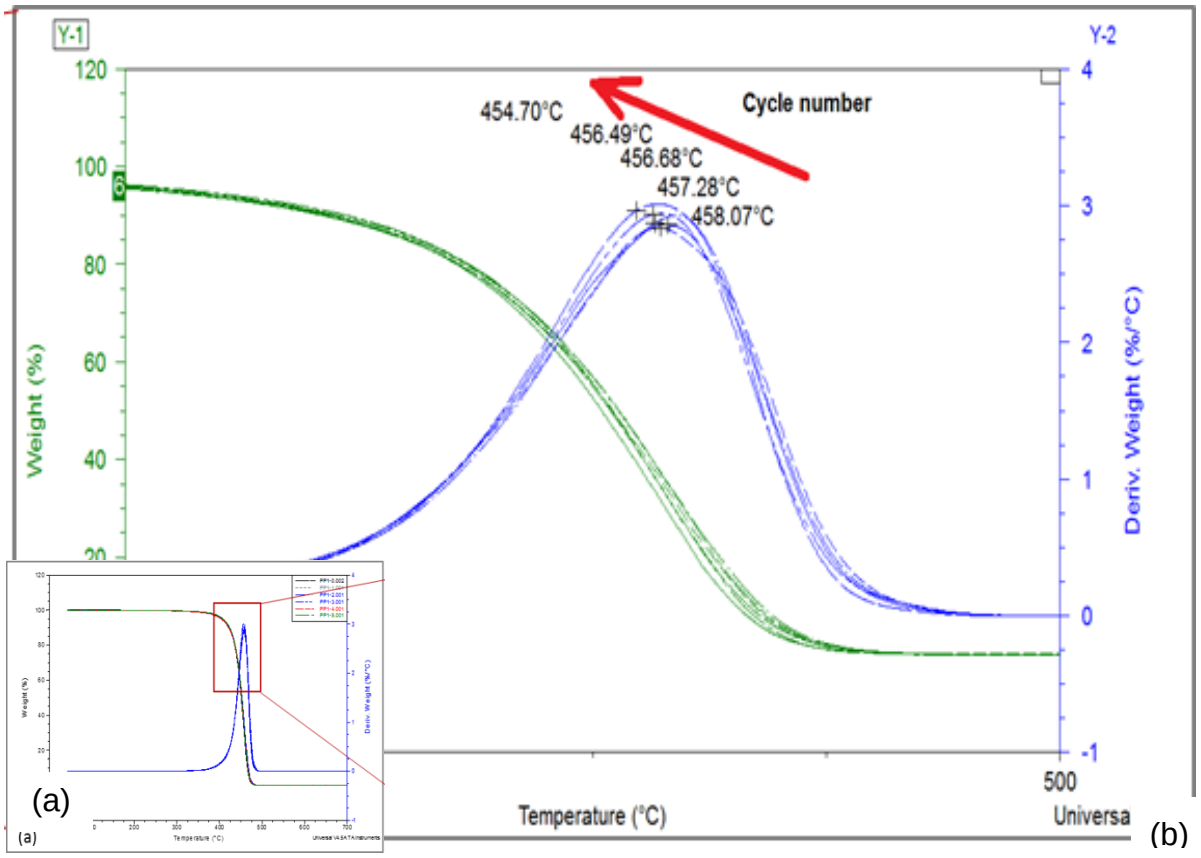

Figure 5-32: TGA and DTG of PP (a) Whole spectrum (b) Zoom

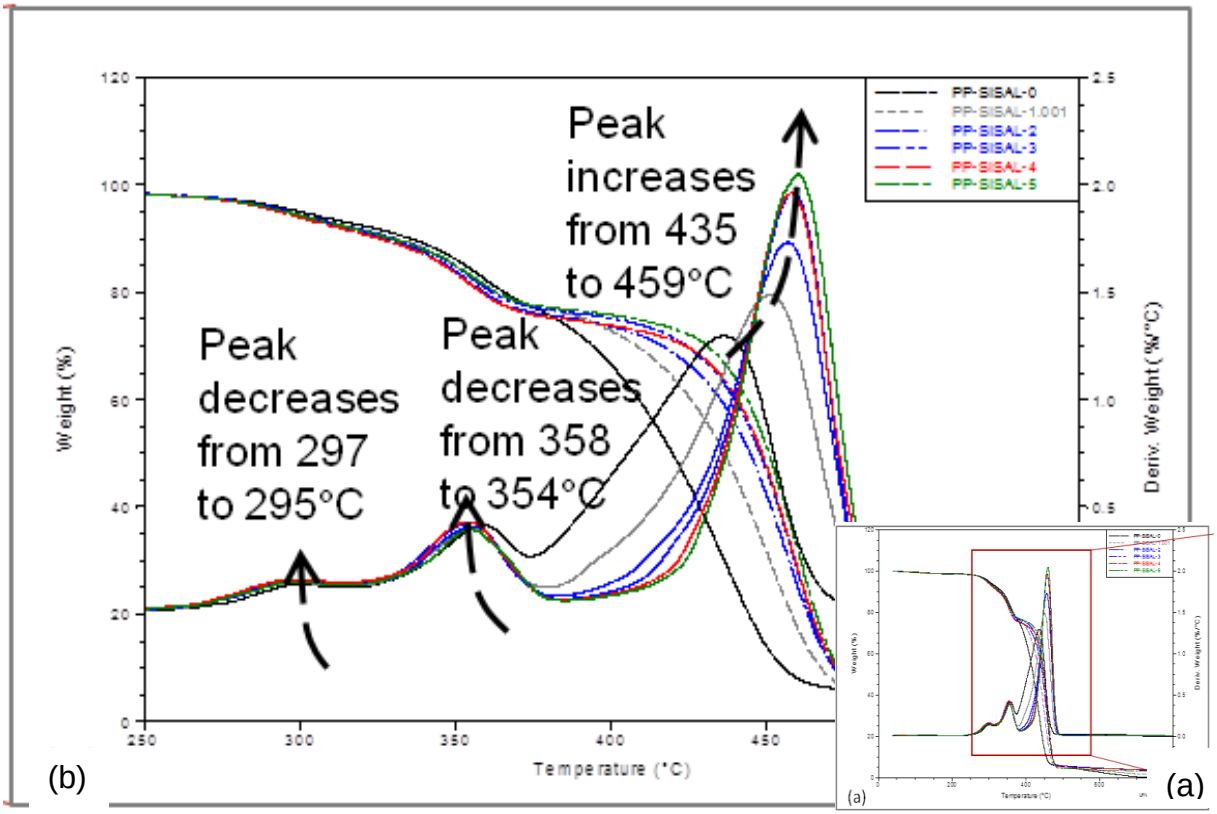

Figure 5-33: TGA and DTG of PP/30% Sisal (a) Whole spectrum (b) Zoom

The effect of the fiber type regarding the cycle number on the TGA results is also studied, namely sisal and hemp in PP-H and PP-S compounds. Figure 5-34a illustrates the TGA and DTG of PP-S commercial compound. For illustration, the original compound, the fifth cycle and the eighth cycles are considered. A zoom-in is made on the temperature range of 300-500°C. The effect of the cycle number is obvious from C0 to C5 and from C5 to C8. The behavior is like that of PP/30% Sisal in Figure 5-33b.

On the contrary, PP-H shows less sensitivity to recycling regarding the thermal properties. As seen in Figure 5-34b, the TGA curve of the fifth cycle is close to that of the original material. Whereas the eighth cycle shows a clear difference. This remark infers that hemp has consistent coupling efficiency with PP matrix even after five cycles. In other words, the efficient surface areas of the hemp fibers seem that they are not too much increased by the recycling. But as seen in the eighth cycle, the decomposition temperature is offset to higher temperature indicating more coupling sites. Regarding the previous stage above 300°C, the peak temperature of PP-H is around 347°C which is 7°C less than that detected in PP-S or PP/30% Sisal. But the peak temperature in PP-H in this stage (around 347°C) is almost constant and not decreasing as reported in PP/ sisal composites. At the end of the TGA experiment of PP-S in Figure 5-34b, the remaining char is almost constant (15%) for the original compound in comparison with the fifth cycle. The eighth cycle shows less char (10%) remaining at the end. Similar behavior is found with PP-S. This remark meets exactly what reported in [Fon15] who concluded that no significant changes occur till the fifth cycle.

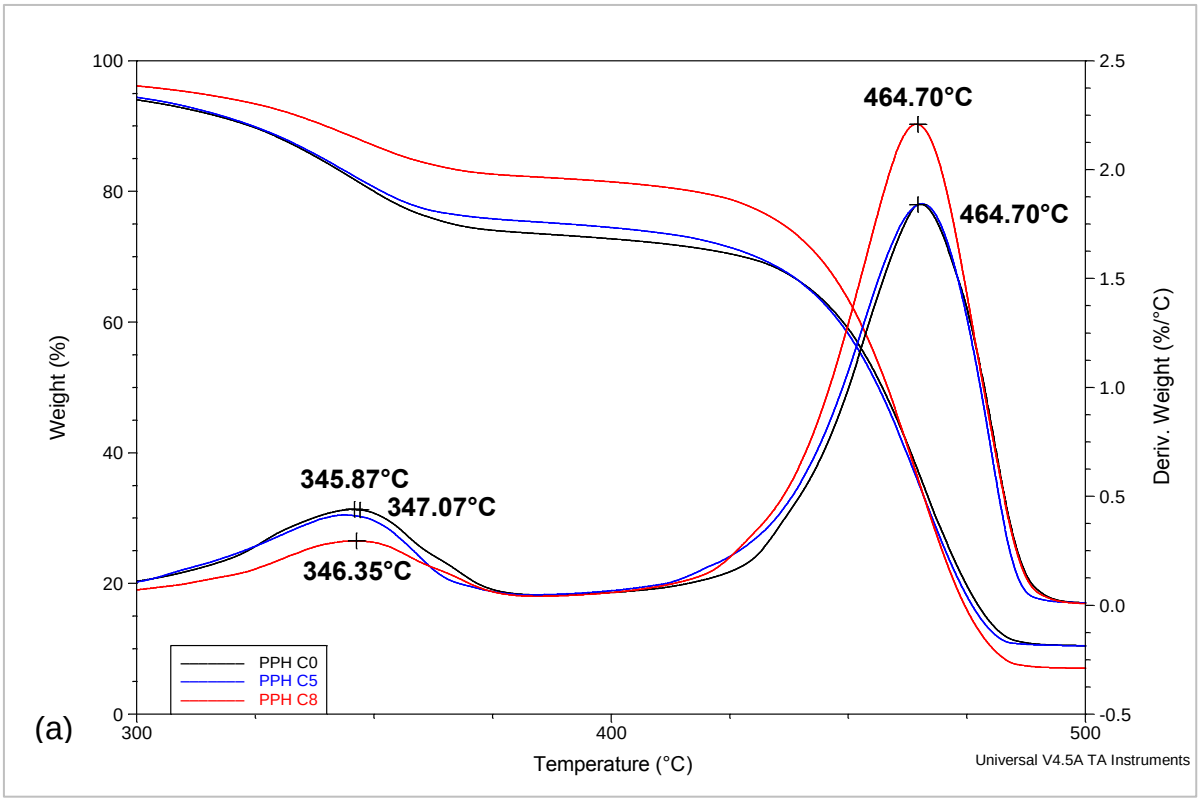

Figure 5-34: TGA and DTG of (a) PP-H

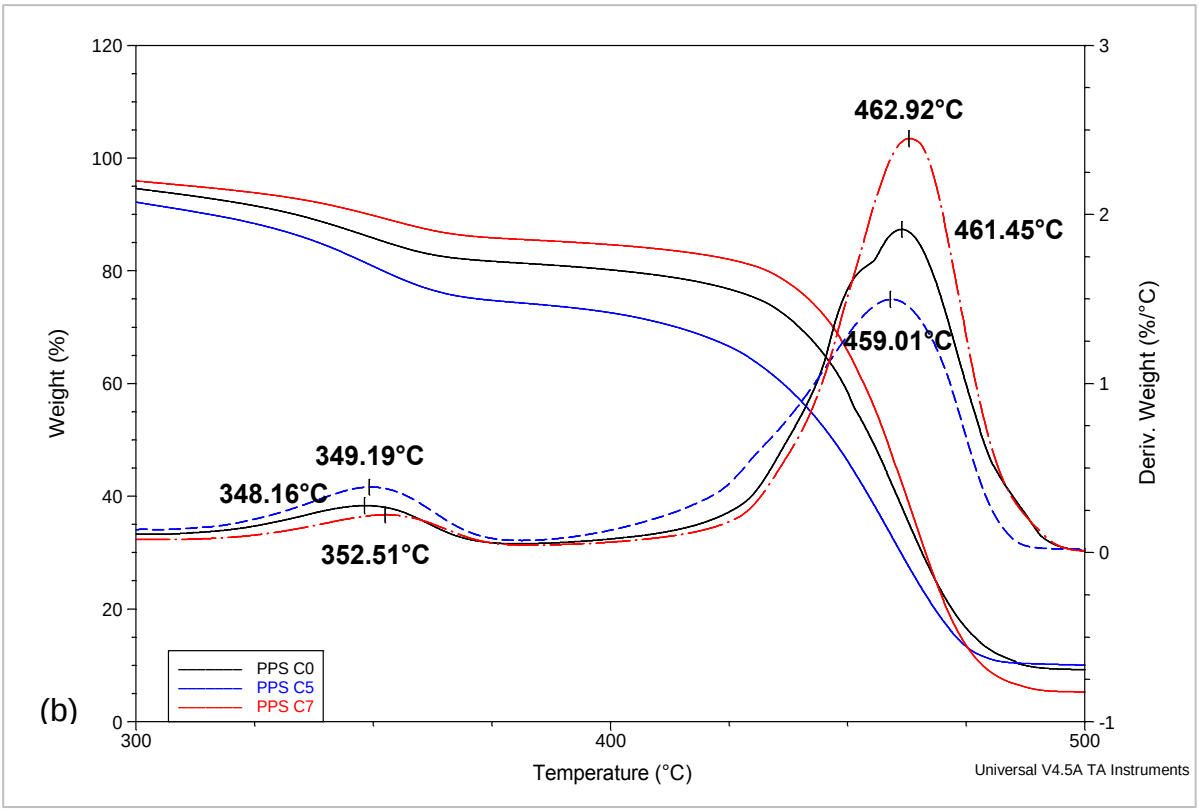

Figure 5-34: TGA and DTG of (b) PP-S

5.3.2 Differential scanning calorimetry

As mentioned in 3.4.10, heat-cool-heat procedure is followed in the DSC experiments to investigate the thermal transitions in the compounds during melting and solidification phases. Polymer characteristics can be taken out the second heat cycle avoiding the thermal history of the polymer sample [Hut84]. Therefore, the difference in the determined temperatures and enthalpies between the first and second cycles is meaningful. First cycle defines the compound properties. The second heat cycle defines the inherent properties of the material.

An example of DSC experiment is shown in Figure 5-35, cycle 3 shows a narrower peak in melting zone at the second heat cycle (cycle 3) in comparison to the first heat cycle (cycle 1). From the DSC experiments, melting, recrystallization and second melting temperatures are collected.

Similarly, the enthalpies of melting and recrystallization along the heat/ cool/ heat stages are calculated using the software of the universal analysis software for the TA instruments.

DSC results for the original PP matrix, the commercial PP-sisal and PP-hemp and finally the PP/30% Sisal compounds are presented in Table A-1 to Table A-5 in the Appendix. The results cover the temperature and the enthalpy (melting or recrystallization) for the three stages of heat-cool-heat procedure. The melting point taken out from the first heat stage is measured for PP, PP-S and PP-H at different cycle numbers. The results are plotted in Figure 5-36.

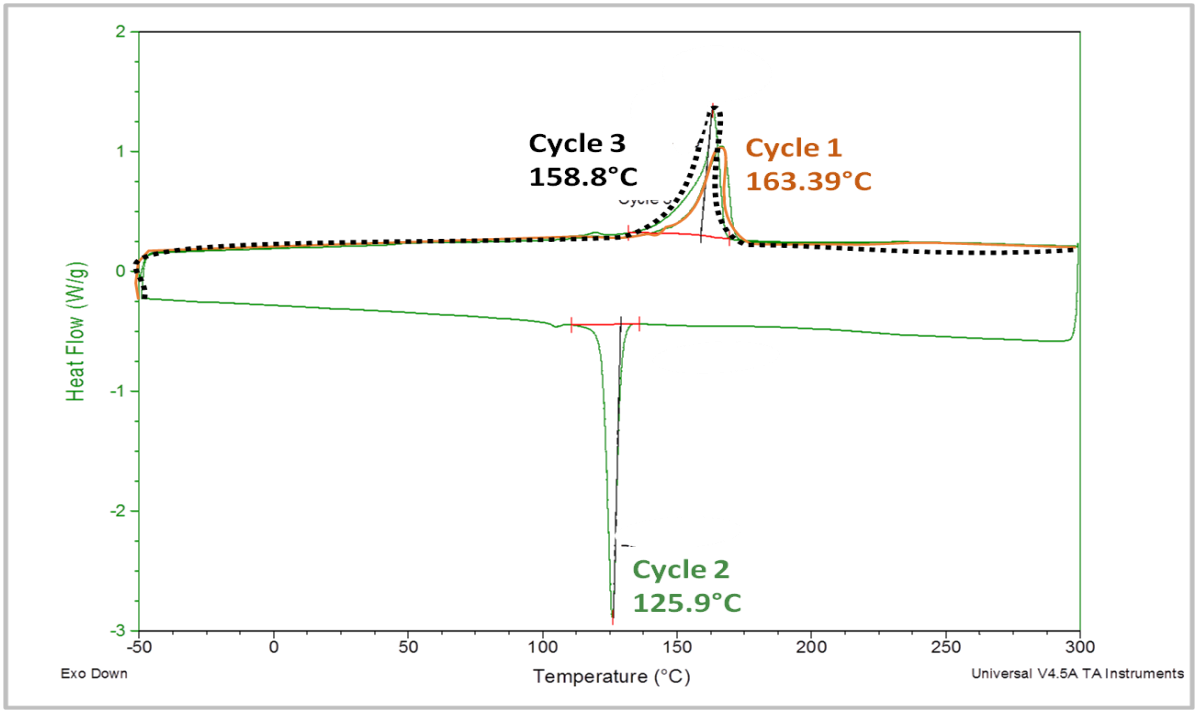

Figure 5-35: DSC curve showing the heat-cool-heat cycles (Cycle 1: heat in orange, cycle 2: cool in green, cycle 3: heat in green) and both melting and crystallization characteristics

The melting points of all materials change within 4°C maximum. The range of deviation in case of PP-H is greater than that of PP-S. PP has an almost constant melting temperature till the fifth cycle. Afterwards, it decreases one degree in average. For the commercial PP compounds reinforced with sisal and hemp PP-S and PP-H, the melting temperature decreases with increasing the cycle number. To illustrate the effect of recycling on the melting temperature of the NFTC compound, a relative index is calculated as in Equation 5-4. The results are plotted in Figure 5-37 for both heat cycles.

It is obvious that the cycle number has a linear trend effect on the difference between the compounds melting temperature with respect to PP. Additionally, the second heat cycle has lower temperature difference than that of the first heat cycle. This is attributed to the removal of the compounding history of the thermal stresses during the re-melting process.

$$\boldsymbol{Difference\ in\ melting\ temperature} = \boldsymbol{Tm}\ (\boldsymbol{PP}) - \boldsymbol{Tm}(\boldsymbol{PP-S})$$

$$\boldsymbol{Difference\ in\ melting\ temperature} = \boldsymbol{Tm}\ (\boldsymbol{PP}) - \boldsymbol{Tm}(\boldsymbol{PP-H})$$

Equation 5-4

Where T_m= melting temperature

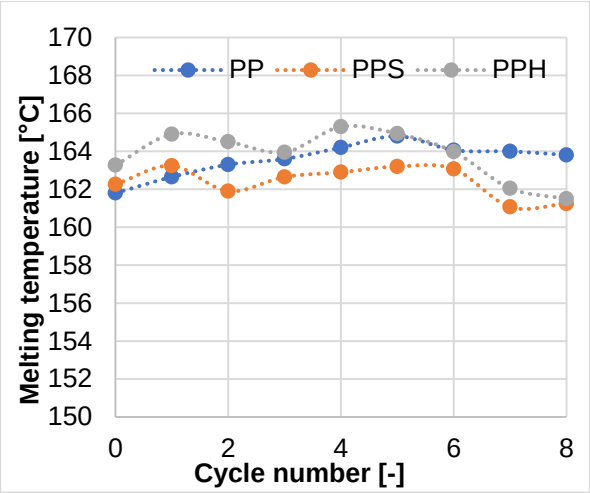

Figure 5-36: Melting point of PP, PP-S and PP-H at different cycle numbers

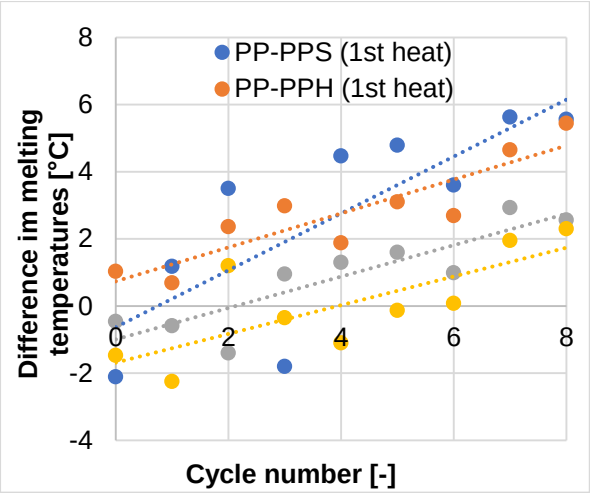

Figure 5-37: Difference in melting temperature between PP and both PP-S and PP-H at different cycle numbers

Figure 5-38 shows the melting enthalpy development along the cycle number. It is noticed that the melting enthalpy of the compounds is less than that of the pure PP. This is attributed to lower polymer fraction due to the fiber presence (30 wt.%). However, for justified comparison, the enthalpies of the compounds are normalized by dividing it to the PP weight fraction as in Equation 5-5 [Mor15].

$$\boldsymbol{Normalised\ Hm = Hm/(1 - fibre\ wt.\%)}$$

Equation 5-5

Where H_m is the melting enthalpy of the compound in j/g

After normalization as shown in Figure 5-39, the enthalpies of both compounds are found to be close to PP melting enthalpy till the sixth cycle. Afterwards, the melting enthalpies of the compounds are greater than the original PP.

The increase of composites' enthalpies at the late cycles is partially explained in [Fon15] where the fiber content is reduced from the theoretical value (30 wt.-%) to lower values especially after five cycles. Another reason for the increased melt enthalpy at the late cycles is that the generated fibers' surfaces by recycling are maximized. Hence the efficiency of coupling between the fibers and PP is also maximized giving the maximum enthalpy and hence better nucleation. Here it is worth mentioning that although the sisal fibers from the two compounds PP-S and PP/30% sisal are from different suppliers, but no significant difference is noticed in their thermal effect in the compound.

Looking through Table A-5 (Appendix) it is obvious that the melting enthalpy develops almost constantly with small variation and relative maximization at the fifth cycle.

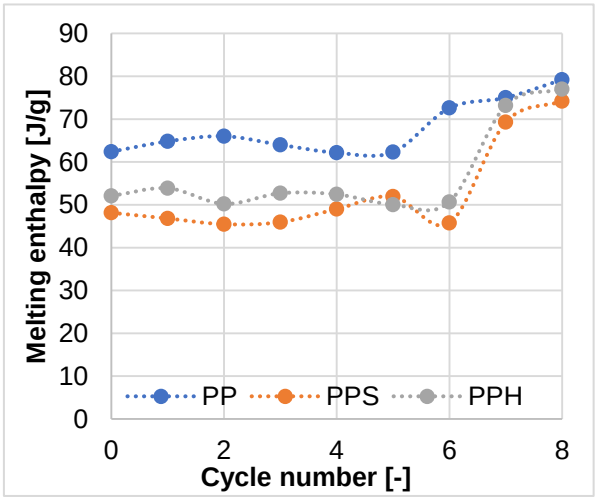

Figure 5-38: Melting enthalpy of PP, PP-S and PP-H at different cycle numbers

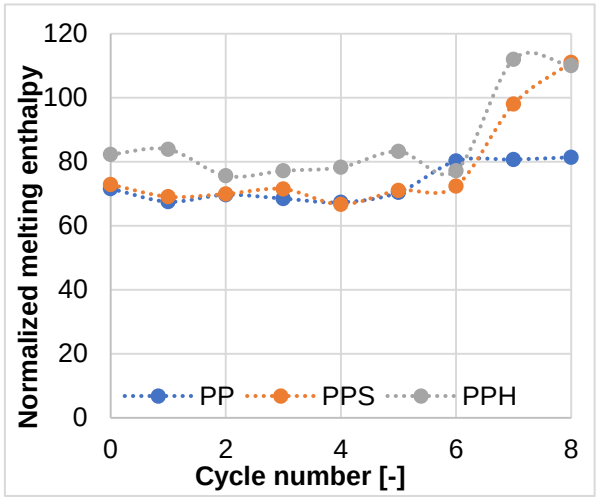

Figure 5-39: Normalized melting enthalpy of PP-S and PP-H w.r.t. PP at different cycle numbers

The difference between the attained melting points at the first and the second heating DSC cycles, as mentioned earlier, corresponds to the thermal history of the compound. Therefore, this difference in temperature is plotted against the cycle number of PP and both compounds PP-S and PP-H as shown in Figure 5-40.

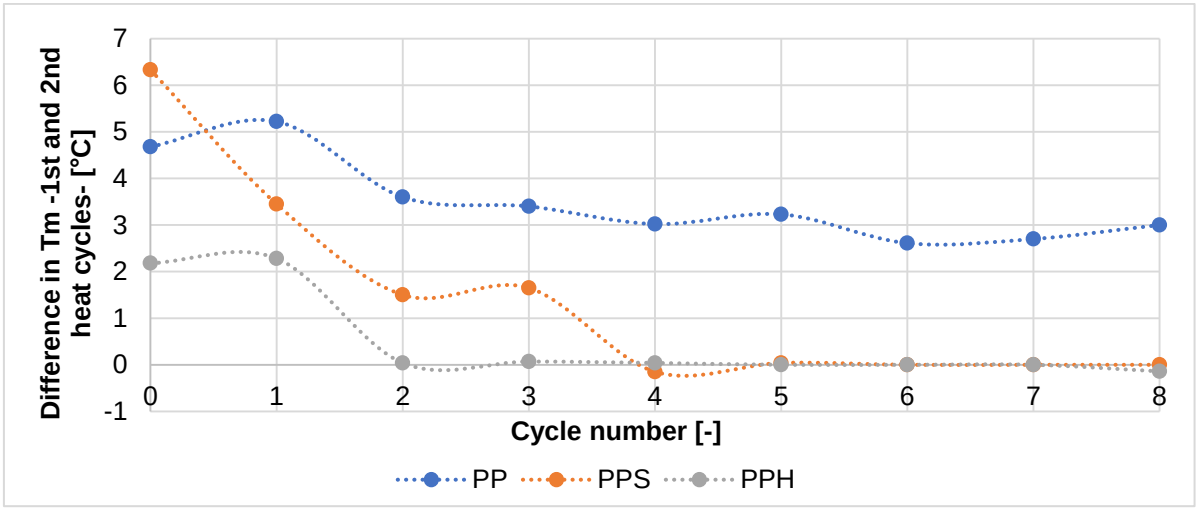

Figure 5-40: Difference in melting points between the both heating cycles (T_{m1}-T_{m2}) of PP, PP-S and PP-H at different cycle numbers

It is obvious that all curves show reduction of the difference in melting points ($T_{m1} - T_{m2}$) between first and second heating cycles which stabilizes starting the fourth cycle. On the other side, the difference in melting points of PP-S starts with 6°C difference and then decreases to almost zero ($T_{m1} = T_{m2}$) starting from the fourth cycle. As mentioned before, the difference between the two melting points of the two heating cycles originates from the thermal stresses in the compound which is removed by the second heating cycle. Based on this, highly homogeneous compounds tend to build less thermal stresses and therefore the difference between the two heating cycles tends to zero.

Since $T_{m1} - T_{m2}$ = zero for PP-S after four cycles, this indicates that an optimum combination of PP structure and fiber size is reached in which no more thermal history is developed. Similarly, PP-H starts at low level of temperature difference of 2°C then just after two cycles, this optimum combination of structure and fiber size is attained and the difference in melting temperatures is reduced to zero.

Recrystallization temperature (T_c) behaves like melting temperature, as shown in Figure 5-41. T_c of PP continues its increasing trend with more cycles whereas T_c of both PP-S and PP-H increases first starting the third cycle and remains at a relatively elevated level till the sixth cycle. Recrystallization enthalpy shows the same course observed in the behavior of the melting enthalpy against the cycle number, as illustrated in Figure 5-42. This could also be correlated with the fibers' breakage at the late cycles producing more fibers of shorter lengths which act as nucleation enhancers and promote crystallization.

For better illustration, original material and eighth cycle are just shown in Figure 5-43 and Figure 5-44.

It is obvious that:

- The crystallization temperature is shifted to relatively higher temperatures,
- There is no significant change from C0 to C8 in case of PP,
- Crystallization enthalpy increases from C0 to C8 for PP-S and PP-H,
- In case of compounds, crystallization rate increased because the area under the curve increases significantly while the time of crystallization (complete – onset time) is not aptly increased.

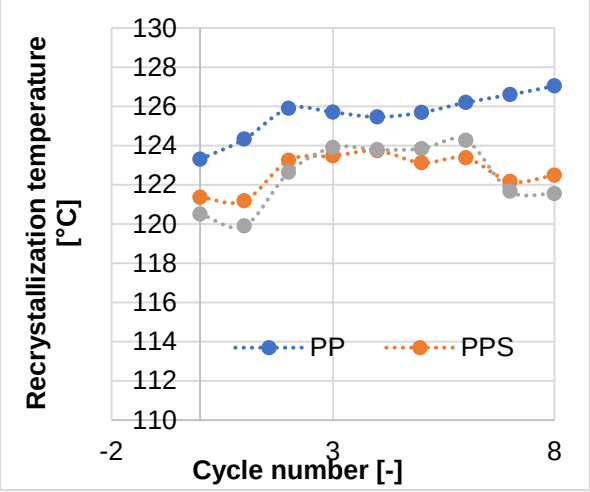

Figure 5-41: Recrystallization temperature of PP, PP-S and PP-H at different cycle numbers

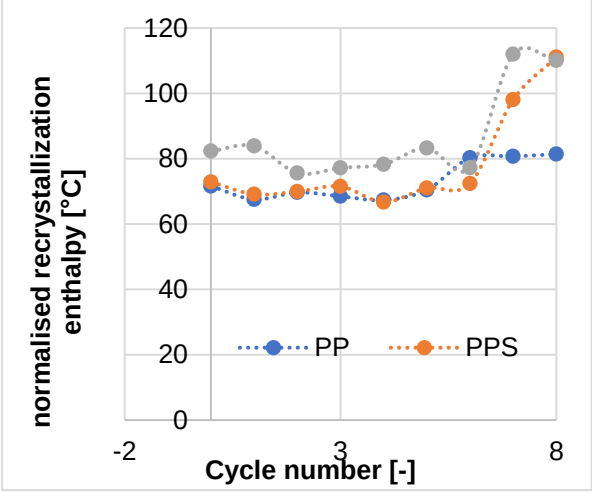

Figure 5-42: Norm. Recrystallization enthalpy of PP, PP-S and PP-H at different cycle numbers

These results imply that the inclusion of fibers in polypropylene accelerate the crystallization onset. Oppositely, recycling results in the retardation of the enthalpy release maximum but the crystallization enthalpy itself is enhanced.

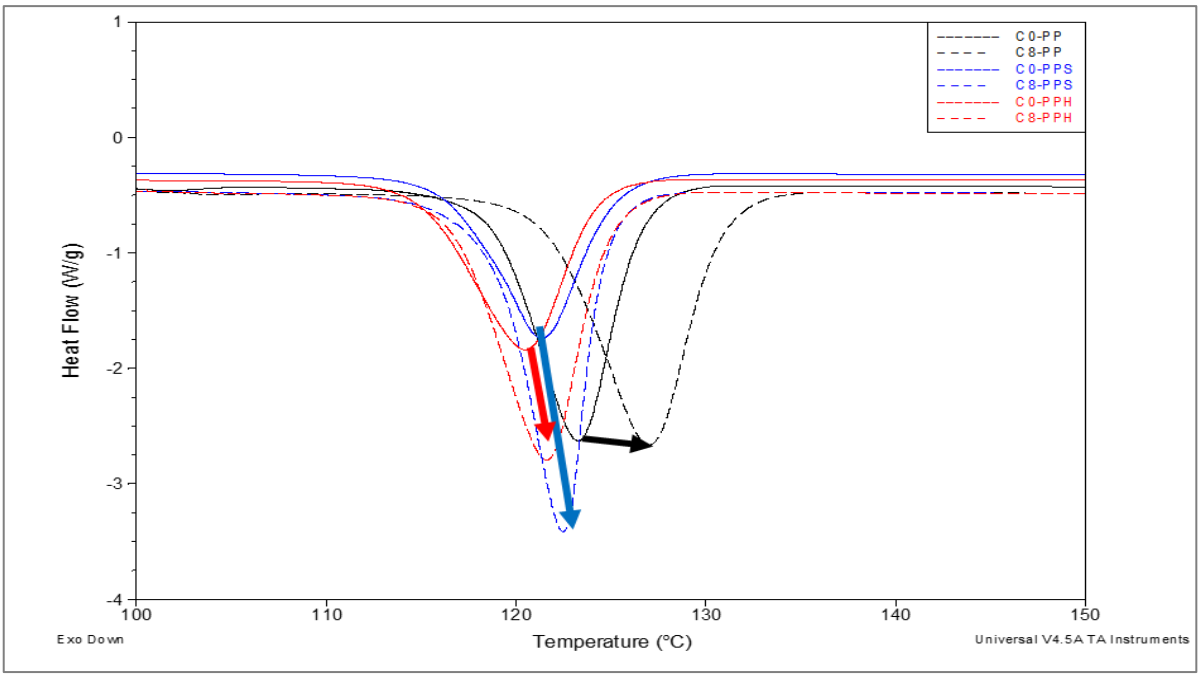

Figure 5-43: Recrystallization enthalpy of PP, PP-S and PP-H at C0 and C8 (Temperature as X-axis)

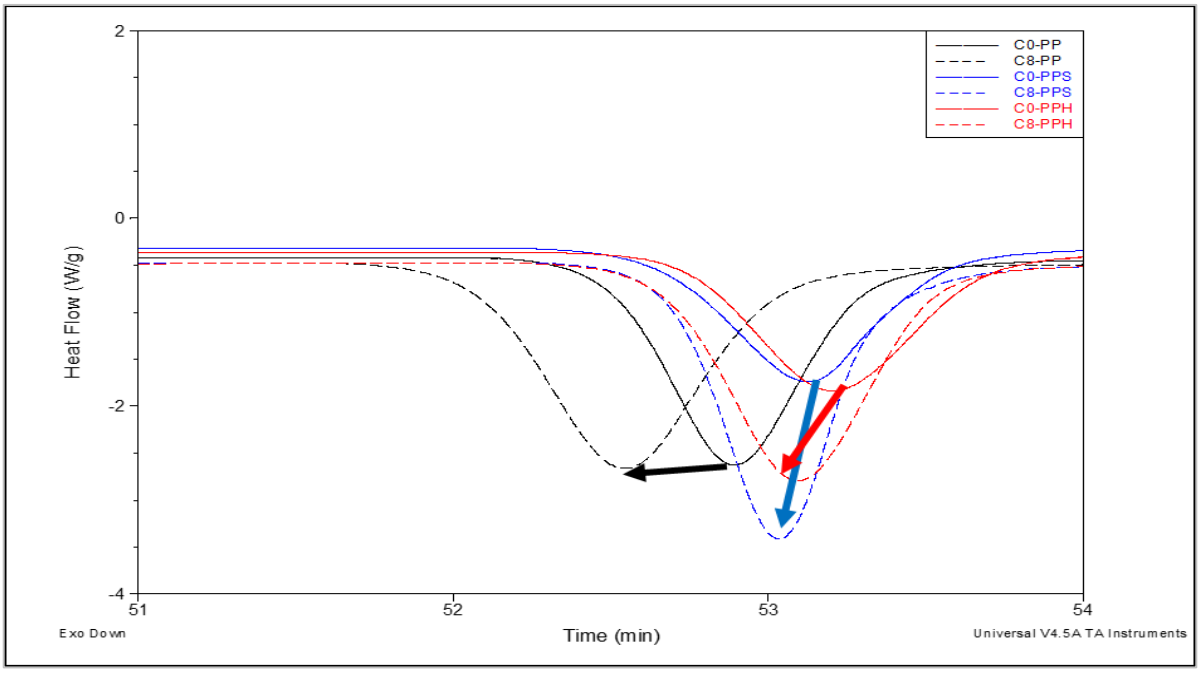

Figure 5-44: Recrystallization enthalpy of PP, PP-S and PP-H at C0 and C8 (Time as X-axis)

From the measured melting enthalpies, it is possible to calculate the Degree of Crystallinity, using the Equation 5-6. The degree of crystallinity is plotted for the three different materials in Figure 5-45. As followed in enthalpy, the degree of crystallinity is normalized by considering the fiber content as followed in Equation 5-6 [Che07]. The increase in crystallinity at late cycles is assumed to be, due to the expected lower molar mass because of the shortened molecular chains after successive recycling.

This assumption is validated in several literature sources; Rust et al. measured the MFI index and calculated the Molecular weight PP after recycling several cycles. He

reported a linear decrease in the molecular weight as the number of reprocessing cycles increase as shown in Figure 5-46 [Rus06].

$$X_C = \frac{\Delta H_m}{\Delta H_m^o (1 - wf)} \cdot 100\%$$

Equation 5-6

Where:

X_C: Degree of crystallization [%]

ΔH_m: Melting enthalpy [J\g]

$\Delta H^o{}_m$: Reference value [J\g]

W_f: Fiber content [%]

For polypropylene, the value of $\Delta H^0{}_m$ is 207.1 J\g.

Figure 5-46 shows also that the PP-S and PP-H have higher degrees of crystallinity in comparison to PP. The reason is that the fibers act like nucleating agents. Also, it is obvious that the crystallinity degree of PP-H is relatively higher than that of PP-S.

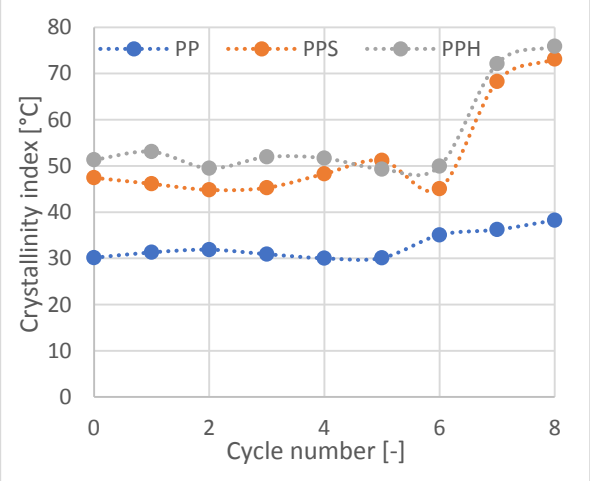

Figure 5-45: Crystallinity degree of PP, PP-S and PP-H at different cycle numbers

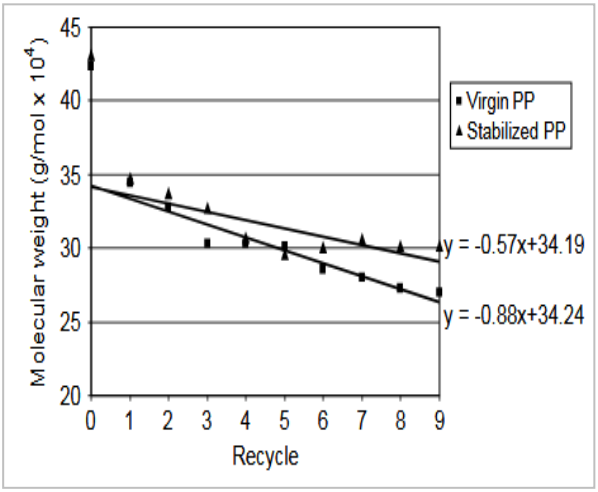

Figure 5-46: Calculated Molecular weight vs. cycle numbers [Rus06]

The superiority of PP-H crystallinity can be explained in terms of the fiber dimensions and surface area. Sisal fibers are thicker and longer than the branched hemp fibers. But both fibers have the same loading in the composites (theoretically 30 wt.-%). This means that the hemp fibers have greater surface areas, as schematically illustrated in Figure 5-47. Two factors affecting the crystallinity after recycling. First is the shortening and splicing of the fibers, and secondly is the breaking of the polymer chains. The first factor helps in increasing the crystals initiation and hence the crystallinity. There are more short fibers enhancing nucleation, which is expected to initiate the formation of more crystals.

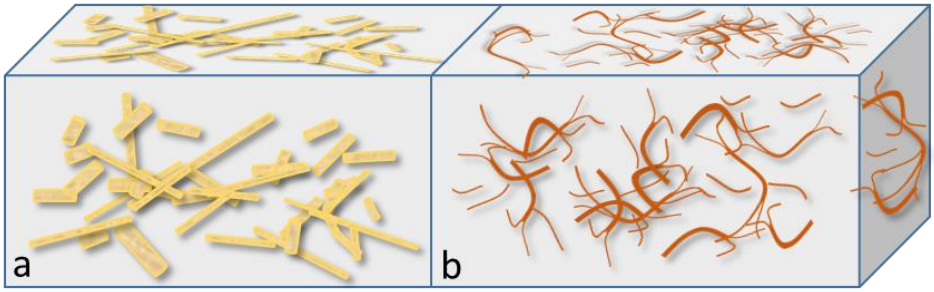

Figure 5-47: Assumed fiber shape: (a) Sisal fibers in a polymer matrix. (b) Hemp fibers in a polymer matrix.

On the other hand, the second factor leads to smaller crystals, since the polymer chains are shortened during recycling. Here it is also important to consider that shorter chains have a higher moving ability and can freely fold and align to form the crystal lattice. This is also reported by [Gal95] where the increase of crystallinity due to recycling is attributed to the shortening of the molecular chains and the diminishing of the molecular weight. The chains are hence more mobile and can crystallize in a more ordered pattern. This is reflected in a higher crystallinity value. Also during recycling, more impurities are introduced in the thermoplastic matrix. These impurities act as foreign surfaces which reduce the free enthalpy needed for the formation of critical nucleus and hence the nucleus size is reduced. Thus, the crystallization temperature is increased and crystallization starts at higher temperatures. All these factors interact with each other. By analyzing the results, the first factor has more effect on increasing the crystallization. A microscopic investigation using polarized microscope and heating stage is carried out. During the cooling time in the cool step (heat-cool-heat procedure), the crystals are prone to nucleate at the fiber surface. By recycling, there are more surface areas due to the fibrillation. Figure 5-48 shows the crystals nucleating on the fiber surface area and then growing and hence the crystallinity degree can be increased. In Figure 5-48a, the sample is investigated using a ring illumination. The sisal fiber surrounded by PP spherulites can be easily identified. Fig 5-48b represents a sample with etched surface where only PP crystals could be determined by light reflection through a polarization filter. For illustration purposes, a zoom in for a selected area is shown in 5-48c.

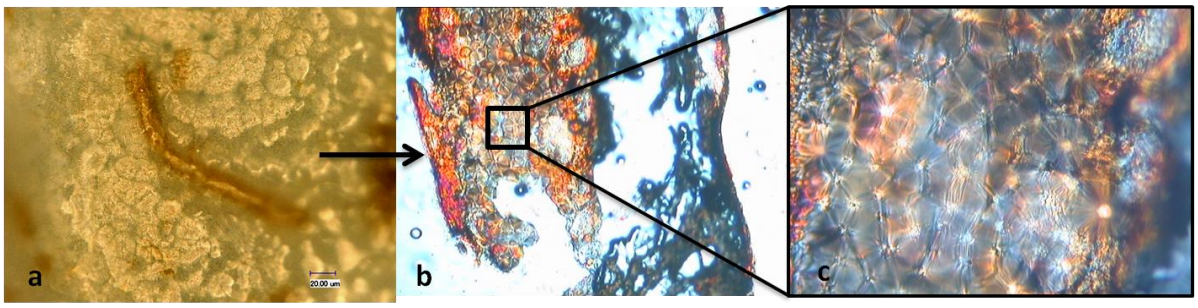

Figure 5-48: Crystals nucleating around and on fiber surface area during the cooling time in the cool step

5.3.3 Dynamic mechanical analysis

The dynamic mechanical properties of PP and both compounds PP-S and PP-H is evaluated in the longitudinal flow direction of the injection molding (0° direction). DMA studies the response of the sample subjected to small sinusoidal oscillation, as a function of time and temperature. Definition of T_g using DMA is more convenient because the change in the moduli is much more pronounced in DMA than change of specific heat C_p in DSC measurement [Ehr11].

Figure 5-49 shows DMA test for PP. The testing frequency of the sinusoidal loading has four levels of 0.5, 1.0, 2.5 and 10.0 Hz. The temperature changes from -100°C to 140° to cover all the expected structure transformations like T_g. Evaluation of DMA yields information about the components of the complex E-modulus (Storage modulus E' representing the real part and loss modulus E'' representing the imaginary part) besides the loss factor tan δ (representing the ratio E'' to E') as mentioned in 3.4.11. As shown in Figure 5-49, the peak temperatures are shifted towards higher transitional temperatures by increasing the applied frequency.

DMA storage modulus curves show a clear transition near to 0°C. But the tan δ curves show three peak values indicating transition states. The first peak takes place at around -50°C. In some curves, there are two overlapping peaks at the first position around -50°C. This transition cannot be simply named γ transition because the used reference PP is a blend of PP with other additives. Therefore, this peak is assumed to be due to the additives for plasticization such as ethylene co-vinyl acetate (EVA) according to [Liu10] [TA 17]. The second peak is just above 0°C and represents the glass transition temperature of the amorphous part in PP (β transition). The third maximum is above 60°C. This is the α transition, which results from the remaining 'rigid' amorphous molecular segments in the crystals and the material turns from solid to rubbery state [Doa07].

Figure 5-50 presents the effect of recycling on the E', E'' and tan δ for PP at 1 Hz. A trend of increasing storage modulus by increasing the cycle number is clear. The increase in the E' indicates an increase in the stiffness of the polymer, which may be the result of a restriction in the segmental motion of the molecular chains as schematically illustrated in Figure 5-51. Double bonds are broken and cross-linking starts [Ehr11]. This is also confirmed by the observably higher T_g of the recycled samples.

It is important here to consider two counteracting factors affecting the viscosity of the compounds: the restriction to segmental motions due to building new links as a result of recycling increase the viscosity of the compound from one side. On the other hand, the reduction in fibers' length after recycling leads to the release of the agglomerations and so the viscosity of the compound drops. The interaction of these two factors determines the resulting viscosity of the compound.

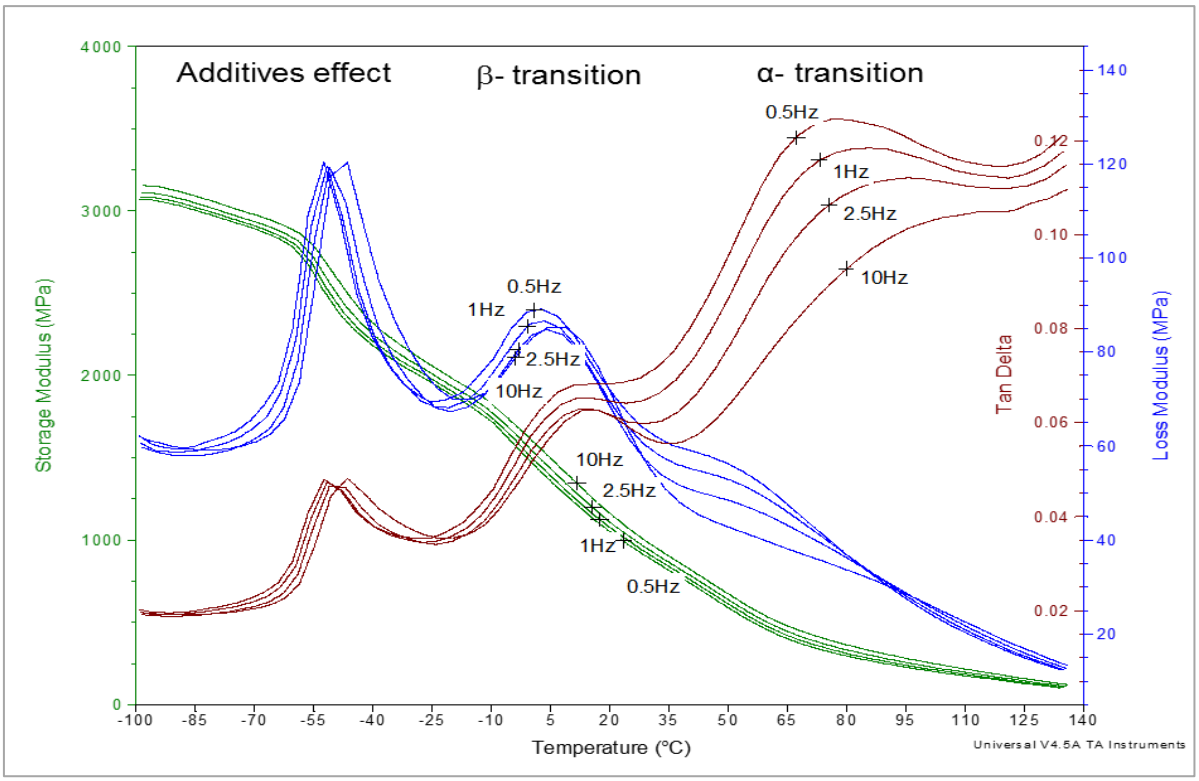

Figure 5-49: DMA results of the original PP (E', E'', tan δ)

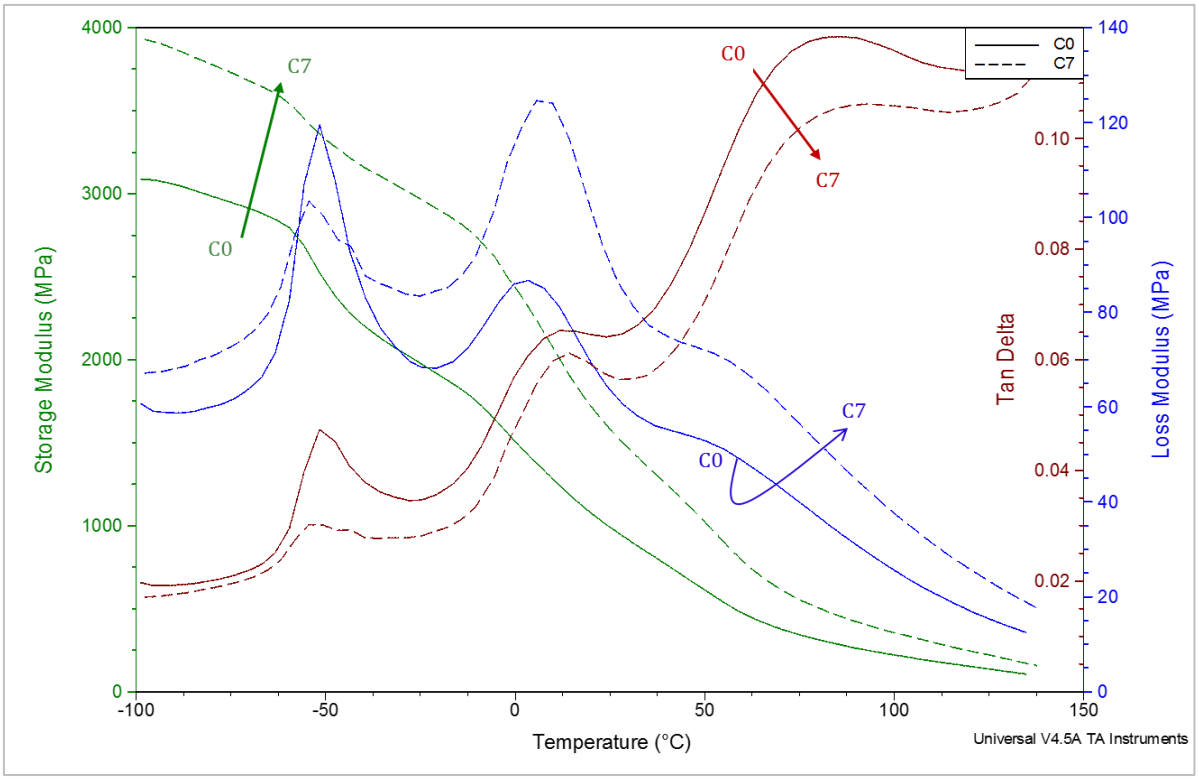

Figure 5-50: Effect of recycling on DMA (E', E'', tan δ) for PP at 1 Hz

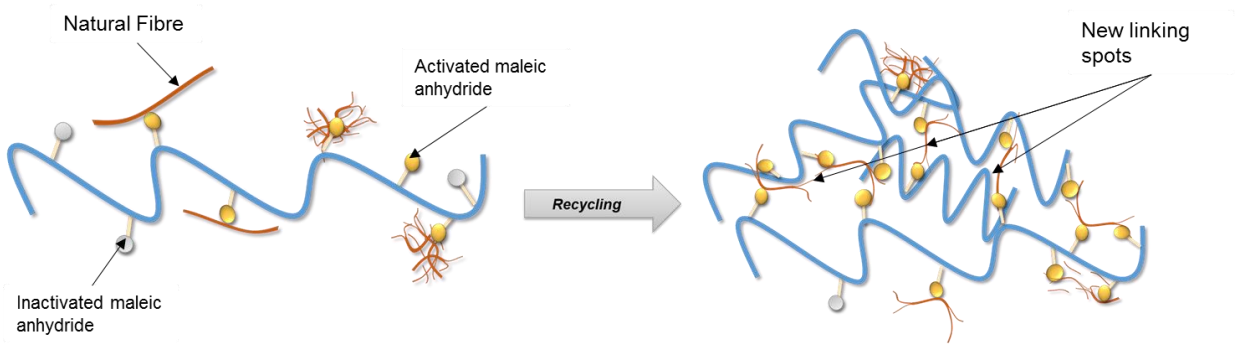

(a)

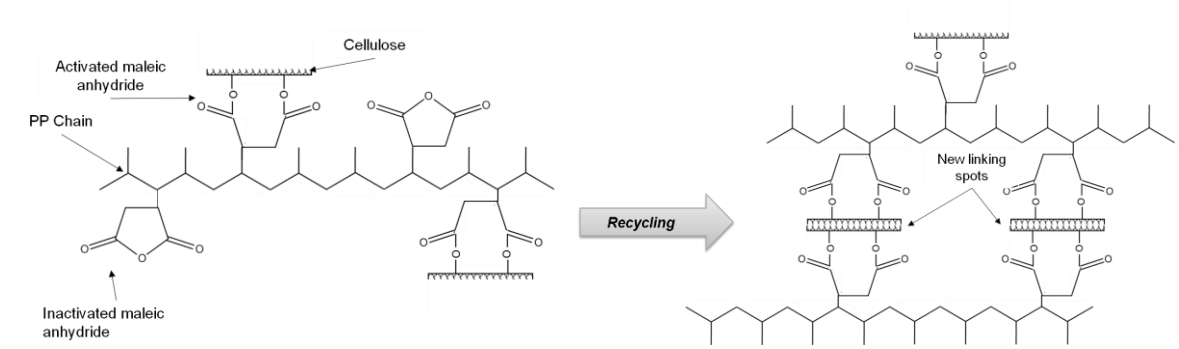

(b)

Figure 5-51: Restriction in segmental motion due to new reactive sites (a) Schematic (b) Structure

The derivative of E' with respect to cycle number is positive. This means that the increase of E' is not linear with cycle number. Increasing the temperature leads to decreasing E' from 3.1 GPa at -100°C to 0.5 GPa at 140°C. The loss modulus E'' shows a different behavior for the effect of cycle number. E'' decreases after the first cycle then it increases again. tan δ also shows a similar behavior of E''. The damping factor (in terms of tanδ) decreases by increasing the cycle number because of the restriction to the mobility of PP molecules in the relaxation process. On the other hand, the loss factor, tanδ, does not change linearly with respect to the cycle number. Rather it fluctuates as shown in Figure 5-52. It drops after the first cycle then starting from the fourth cycle, the loss factor increases again indicating the stiffening of the matrix.

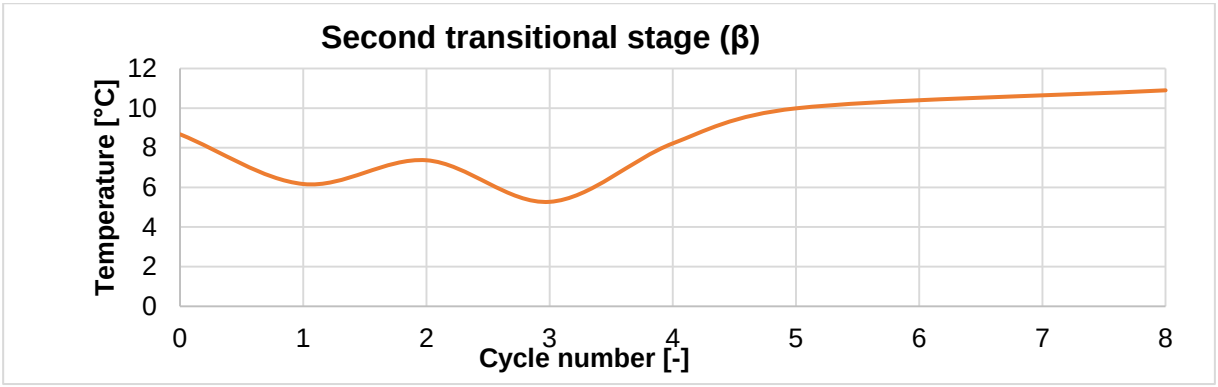

Figure 5-52: Effect of recycling on the transitional temperature for PP at 1 Hz

Figure 5-53 and Figure 5-54 show the effect of recycling on E', E'' and tan δ for both composites PP-S and PP-H in comparison to the neat PP in Figure 5-50. It is obvious that both the composites have high storage and loss modului. The rank of storage modulus for the investigated materials is [PP, PP-S, PP-H] ascendingly. This matches with the results of [Mof12] who worked with PP/Sisal system and proved that the presence of fibers shifted both storage and loss moduli to higher values.

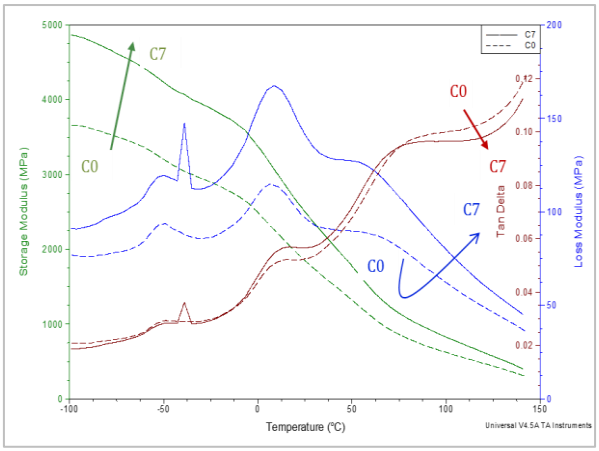

Figure 5-53: Effect of recycling on DMA (E', E'', tan δ) for PP-S at 1 Hz

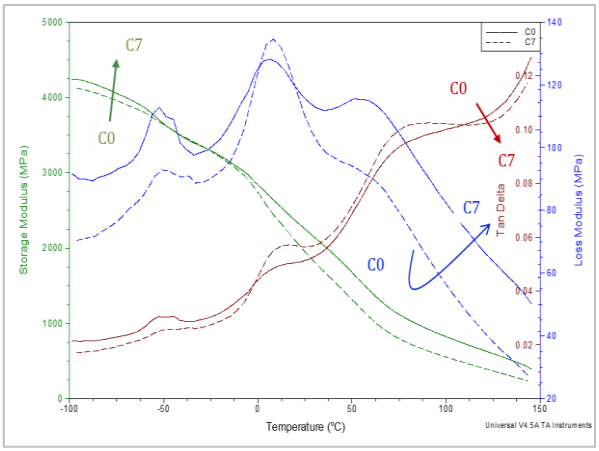

Figure 5-54: Effect of recycling on DMA (E', E'', tan δ) for PP-H at 1 Hz

For more specific comparison, E', E'' and tanδ are illustrated in Figure 5-55 (a-c) and Figure 5-56 (a-c) for the three materials (PP, PP-S and PP-H) at C0 and C8 respectively. Important values for storage and loss moduli are listed in Table 5-2 and Table 5-3 respectively.

Some remarks can be depicted from this comparison in Figure 5-55 at C0 as following:

- ***Storage modulus E':*** At -100°C, PP-H, PP-S and PP have 4250, 3700 and 3100 MPa respectively. At room temperature they decrease to 2100, 1900 and 1000 MPa. At the end of the test, they decrease to 500, 400 and 120 MPa.
- ***Loss modulus E'':*** The three materials show the same behavior. At room temperature, they show maximization of E''. PP has the least modulus of around 60 MPa whereas PP-H and PP-S have 91.61 and 77.57 MPa respectively. It is obvious that the transitional temperature, especially at β and α stages, increases with 4°C by the addition of fibers in comparison to PP. This is attributed also to the lack of mobility by the addition of fiber to the PP chains [Mof12].
- ***Loss factor (tanδ):*** PP shows the highest damping factor with respect to PP-S and PP-H. Both composites show almost identical behavior. Reduction of the loss factor means that, at certain same temperature, the increase of E' with increasing fiber content is greater than that of the E''. Additionally, the decrease of tan δ is considered a sign for improving the fatigue resistance as well as the elasticity of the composites due to the high elasticity of the natural fibers [Doa07].

Table 5-2: Storage Moduli PP, PP-S and PP-H

Material	Storage Modulus (-100°C) [MPa]		Storage Modulus (RT) [MPa]		Storage Modulus (140°C) [MPa]	
	C0	C8	C0	C8	C0	C8
PP	3100	4000	1000	1750	120	130
PP-S	3700	4800	1900	2500	400	430
PP-H	4250	4130	2100	2050	500	280

Table 5-3: Loss Moduli of PP, PP-S and PP-H

Material	Loss Modulus (-100°C) [MPa]		Loss Modulus (RT) [MPa]		Loss Modulus (140°C) [MPa]	
	C0	C8	C0	C8	C0	C8
PP	60.67	67.17	65.87	94.2	12.48	17.68
PP-S	77.57	91.12	98.74	145.1	37.62	45.73
PP-H	91.61	70.44	116.9	113.6	54.51	29.51

The same procedure is followed in the comparison at C8 out of Figure 5-56 and the remarks are depicted as follows:

- ***Storage modulus:*** At -100°C, PP-S, PP-H and PP have 4866, 4116 and 3929 MPa respectively. At room temperature they decrease to 2566, 2008 and 1633 MPa. At the end of the test, they decrease to 410, 260 and 157 MPa.
- ***Loss modulus:*** The three materials show the same behavior. At room temperature, they show maximization of E''. PP has the least modulus of 94.2 MPa whereas PP-S and PP-H have 145.1 and 113.6 MPa respectively. It is obvious that the transitional temperature, especially at β and α stages, increases with 3°C by the addition of fibers in comparison to PP.
- ***Loss factor:*** PP shows the highest damping factor with respect to PP-S and PP-H. Both composites show almost identical behavior.

Two very important differences between C0 and C8 are concluded from Figure 5-55 and Figure 5-56:

- The ranking is changed. In C0, the ascending ranking of the storage and loss moduli at C0 is [PP, PP-S, PP-H]. While at C8, the ranking became [PP, PP-H, PP-S]. This means that after 8 cycles, the strengthening per unit cycle for sisal is higher than that of hemp. This can be explained regarding the fiber

dimensions along the number of the reprocessing cycles as previously explained in 5.1.1.

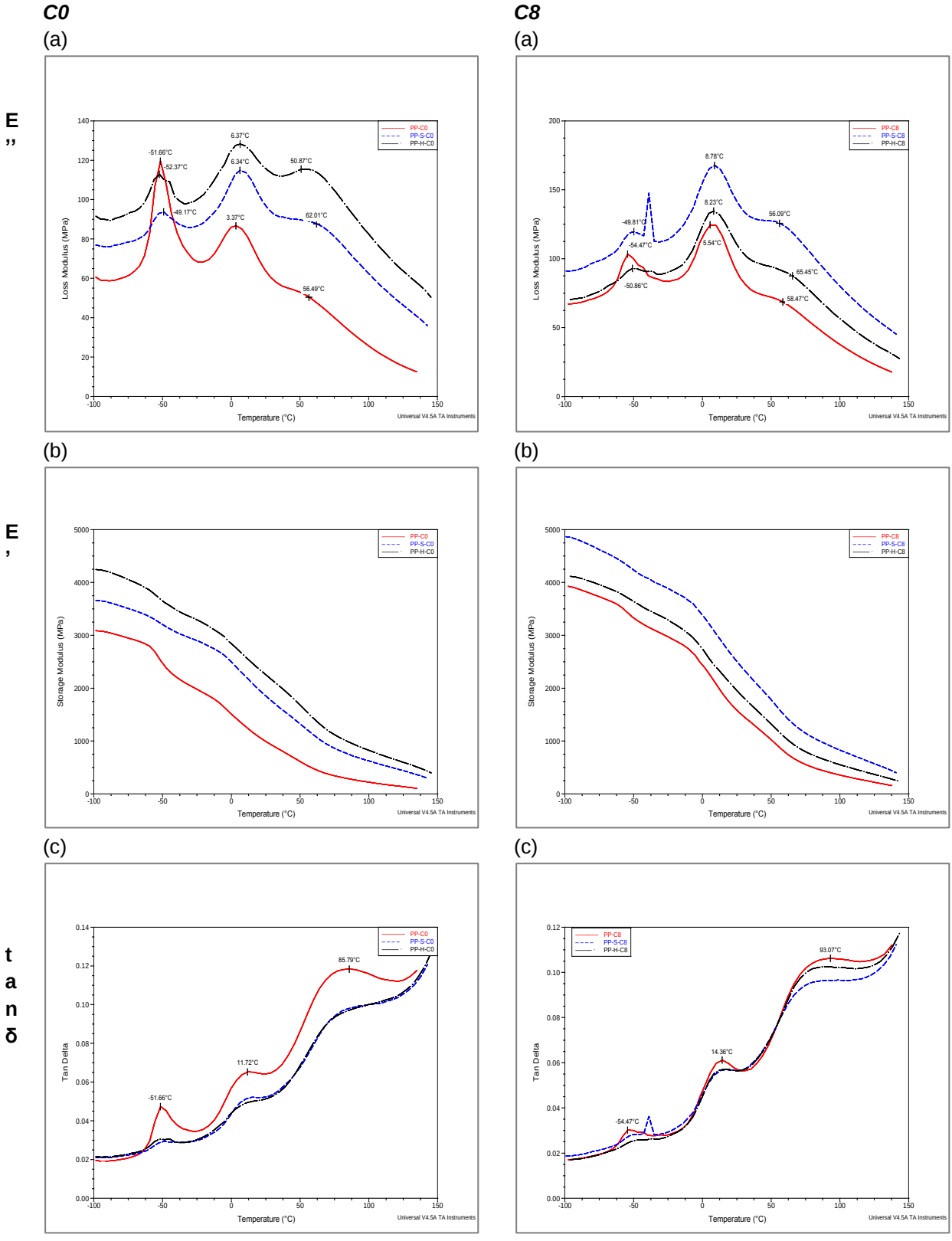

Figure 5-55: DMA results (E', E'', tan δ) for PP, PP-S and PP-H at 1 Hz for C0

Figure 5-56: DMA results (E', E'', tan δ) for PP, PP-S and PP-H at 1 Hz for C8

- The strengthening of sisal after 8 cycles is prominent with respect to the hemp fibers. Therefore, the gap between PP-S and PP-H is significant whereas the

curves of PP and PP-H are close to each other. This depicts that the hemp fibers are losing their role in strengthening after this number of cycles.

DMA results can be further processed to define other thermal and mechanical indices describing the effect of the reprocessing cycles. These indices are namely the activation energy and the modulus of retention ratio.

Activation energy (E_{act}) is an important quantity for describing the glass transition. E_{act} is the amount of energy needed by a polymer structure to impart a glass transition and switch from a quasi-stable state to another stable glassy state. It is calculated using the modified linear form of Arrhenius formula in Equation 5-7 and Equation 5-8.

$$\boldsymbol{f = f_0 e^{\frac{-E_{act}}{RT}}}$$

Equation 5-7

$$\boldsymbol{\ln(f) = \ln(f_0) - \frac{E_{act}}{RT} = \ln(f_0) - \frac{E_{act}}{R}\frac{1}{T} = A - B\frac{1}{T}}$$

Equation 5-8

where f is the applied frequency, f_o is the frequency when the temperature (T) approaches infinity. R is the gas constant of 8.314 j/mol.k.

According to Arrhenius equation, a plot of log f against $1/T$ should give a straight line with slope proportional to the activation energy for the relaxation process. For reasons of clarity and comprehensibility only C0 and C8 are considered in the plot of these Arrhenius formulae shown in Figure 5-57 to Figure 5-62 beta and alpha transitions of PP, PP-S and PP-H. Plots from C0 to C8 could be reviewed in the Appendix in Figures A-1 to A-6.

The regression equations describing these trend lines are also shown in these figures. The coefficients of the ‘X: reciprocal of the temperature” represent the slopes of these trend lines.

These coefficients are then multiplied by the gas constant to obtain the activation energies for the neat PP, PP-S and PP-H in the both alpha and beta transitions at different cycles.

It is obvious that the last cycle is characterized by two points:

- The trend line describing the last cycle is offset back to the left side (as an indication of higher transitional temperature),
- The slope of the last cycle is steeper than the first cycles. Thus, indicates higher activation energies.

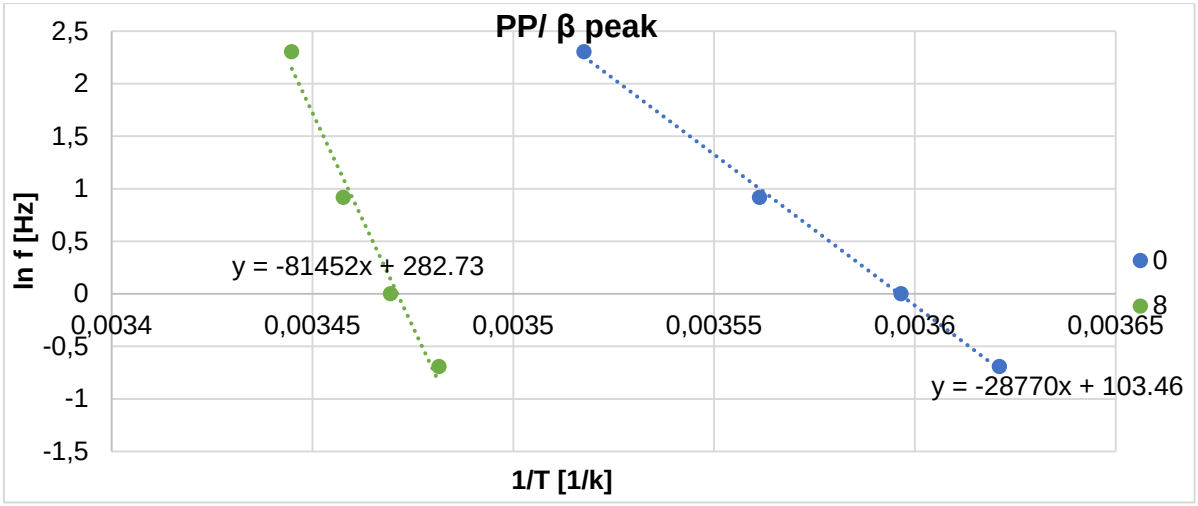

Figure 5-57: Arrhenius formula presentation for PP/ β transition at different cycle number taken from frequencies 0.5, 1.0, 2.5 and 10 Hz.

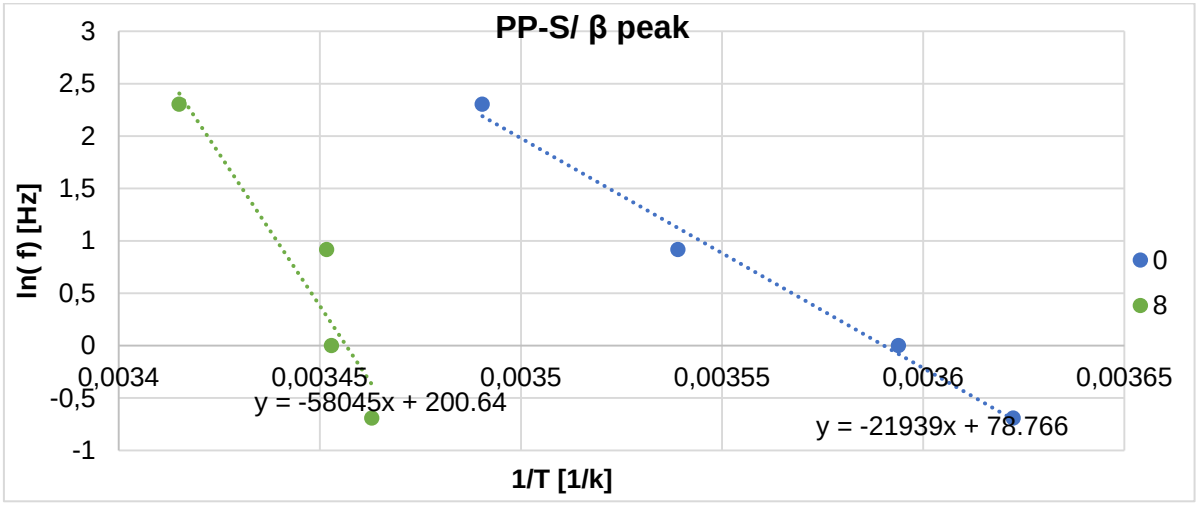

Figure 5-58: Arrhenius formula presentation for PP-S/ β transition at different cycle number taken from frequencies 0.5, 1.0, 2.5 and 10 Hz.

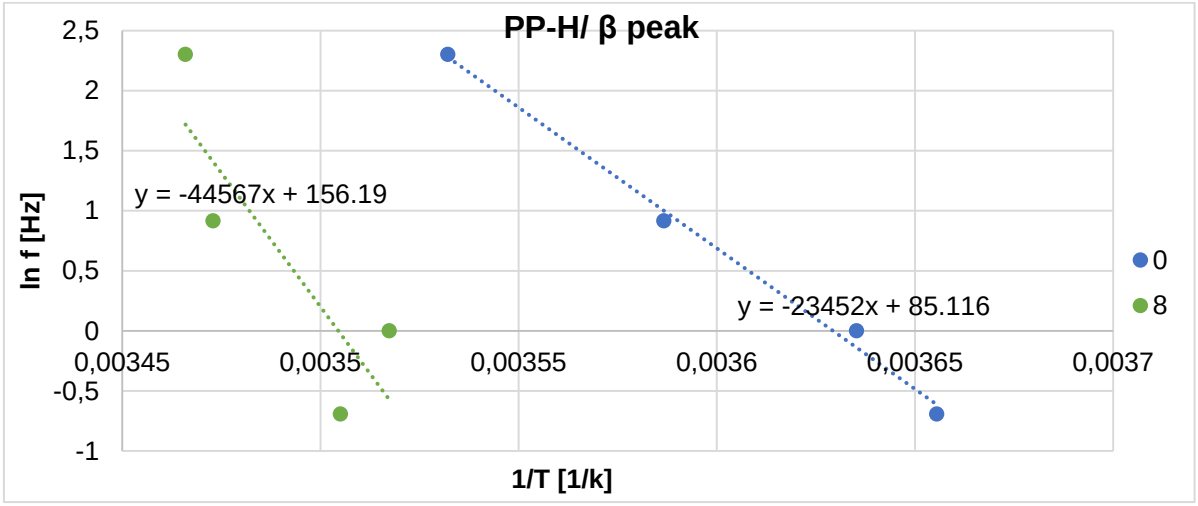

Figure 5-59: Arrhenius formula presentation for PP-H/ β transition at different cycle number taken from frequencies 0.5, 1.0, 2.5 and 10 Hz.

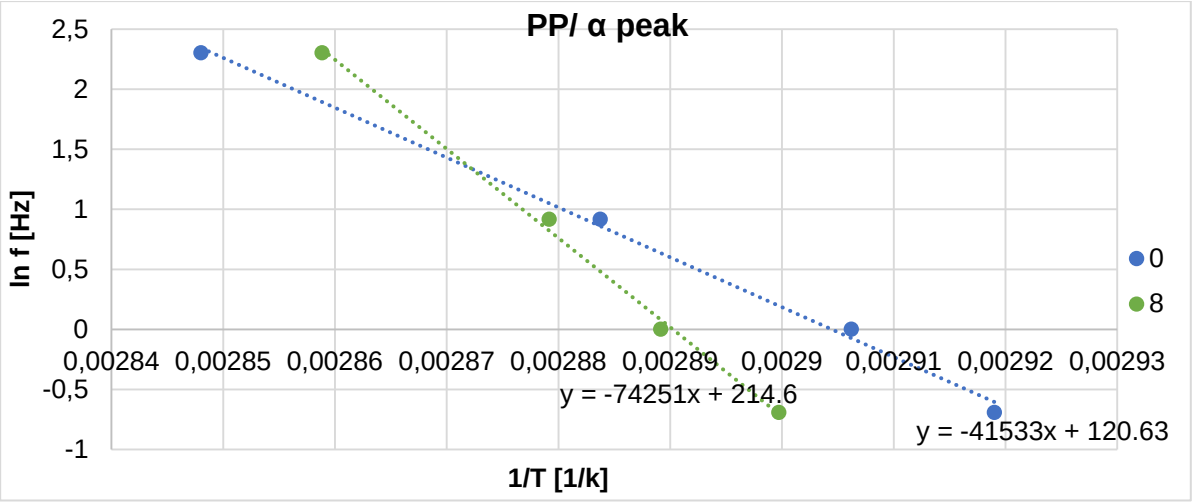

Figure 5-60: Arrhenius formula presentation for PP/ α transition at different cycle number taken from frequencies 0.5, 1.0, 2.5 and 10 Hz.

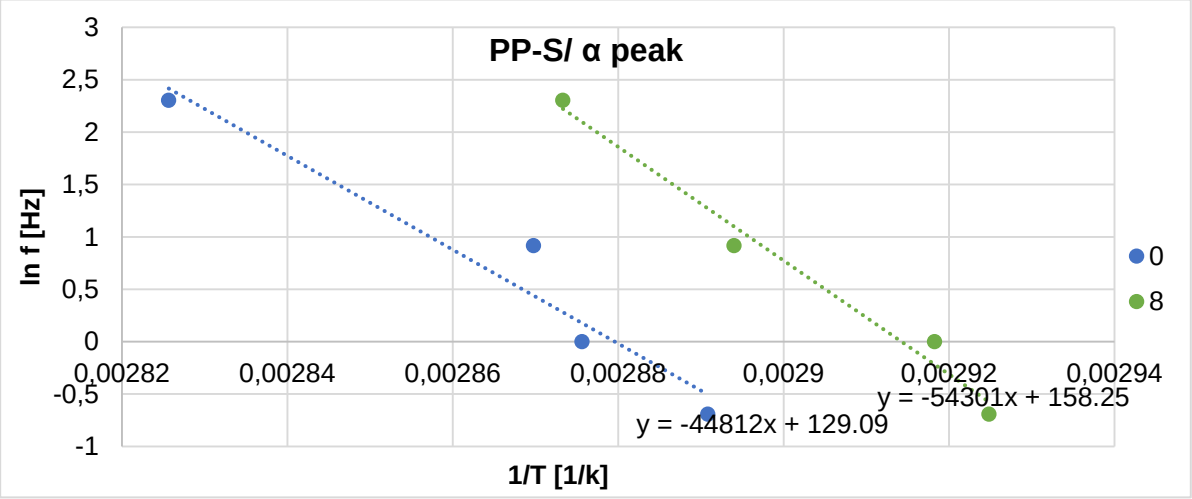

Figure 5-61: Arrhenius formula presentation for PP-S/ α transition at different cycle number taken from frequencies 0.5, 1.0, 2.5 and 10 Hz.

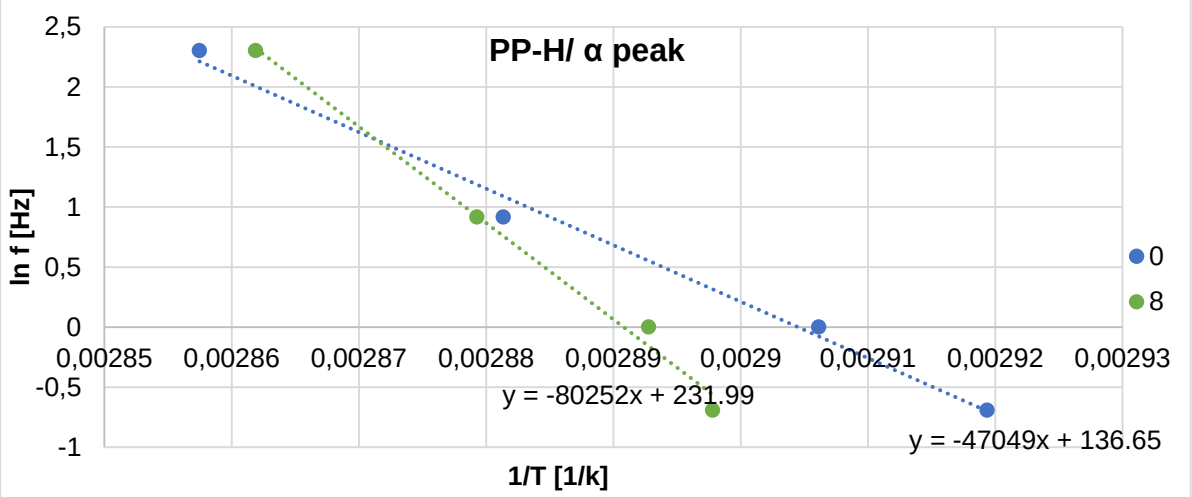

Figure 5-62: Arrhenius formula presentation for PP-H/ α transition at different cycle number taken from frequencies 0.5, 1.0, 2.5 and 10 Hz.

After calculating the activation energy, according to Equation 5-9, Figure 5-63 and Figure 5-64 are plotted to present the effect of the reprocessing cycle on the activation energy at alpha and beta transitions respectively.

$$E_{act} = Gas\ constant(R)\ x\ Slope\ of\ the\ trend\ line$$

Equation 5-9

The activation energy is reduced after the first cycle and remains stable till the fourth one before it starts again to increase at the last cycles. Also, it is remarkable that PP has the highest activation energy in the alpha transition, whereas the difference is not so significant in the beta transition.

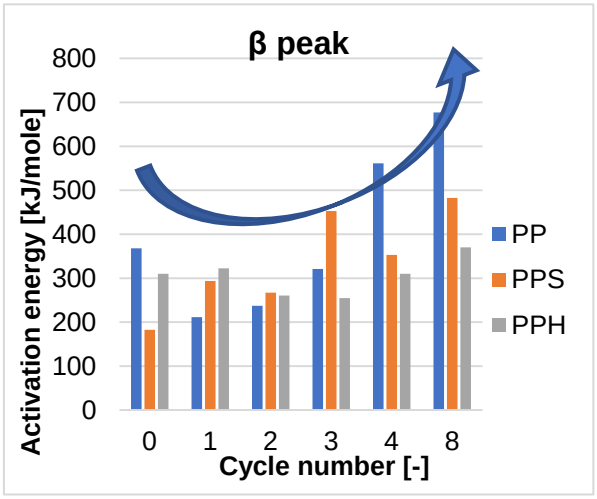

Figure 5-63: Activation energy of PP, PP-S and PP-H for different cycles at β transition

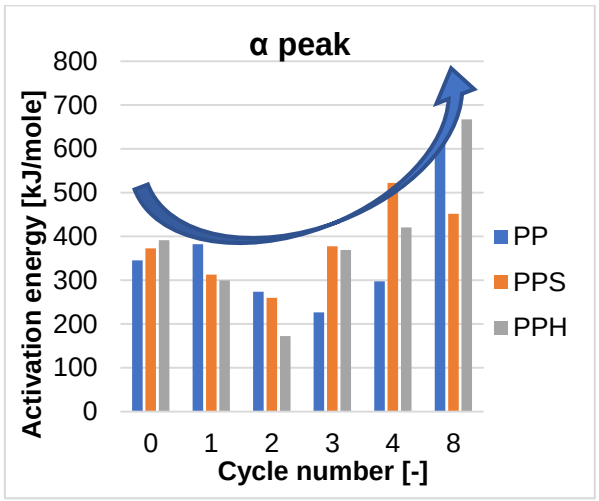

Figure 5-64: Activation energy of PP, PP-S and PP-H for different cycles at α transition

To be able to go deeper in the analysis, the effect of the fiber size on the activation energy should be considered as well. The same procedure is followed to calculate the activation energy for PP/30%Sisal (Longer length and larger diameter resulting in lower AR). Figure 5-65 shows the Arrhenius plot. It is clear how much the regression of the trend lines is better than the regression of the commercial PP-S or PP-H. However, Figure 5-66 shows that the activation energies of both PP-S and PP/30% Sisal are close to each other.

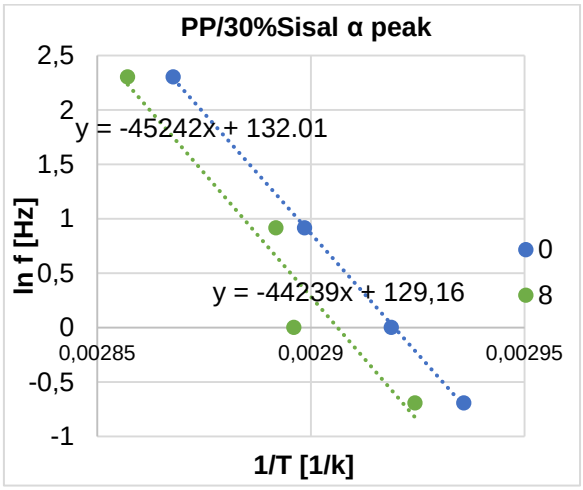

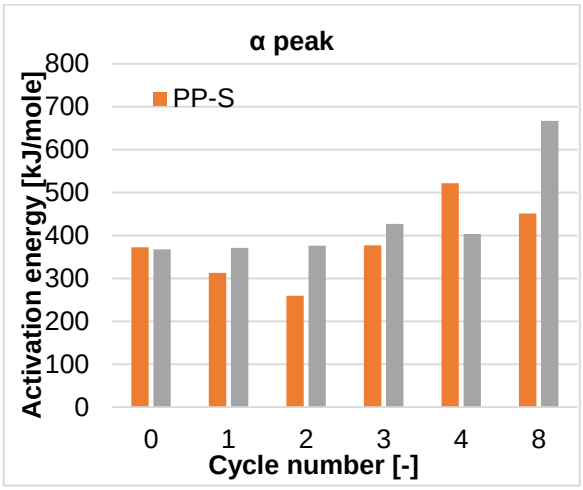

Figure 5-65: Arrhenius formula presentation for PP/30% Sisal α transition at different cycle number taken from frequencies 0.5, 1.0, 2.5 and 10 Hz.

Figure 5-66: Activation energy of PP-S and PP/30% Sisal for different cycles at α transition

Modulus of retention ratio (MRR) is an index which describes the effectiveness of a certain parameter in reinforcing the composite system [Pau10]. In the current study, this parameter can be the fiber content or the number of cycles. MRR is the ratio of the modulus of retention (MR) of the composite divided by MR of the polymer matrix. Modulus of retention itself is the storage modulus of the material at the glass state divided by the storage modulus at the rubbery state. Therefore, MRR is calculated as shown in Equation 5-10.

$$\boldsymbol{MRR} = \frac{\left(\boldsymbol{E'_G}/\boldsymbol{E'_R}\right)_{\boldsymbol{Composite}}}{\left(\boldsymbol{E'_G}/\boldsymbol{E'_R}\right)_{\boldsymbol{Polymer}}}$$

Equation 5-10

where E'_G and E'_R are the storage modulus values in the glassy and rubbery region, respectively. The higher the value of MRR is, the lower the effectiveness of the parameter (either the fiber content or the cycle number). Higher MRR means that there is a higher ratio between the E modulus at glassy state to the E modulus at rubbery state as shown in Figure 5-67. Since most materials operate within temperatures above their T_g i.e. in the rubbery phase, therefore a material which sustains its E modulus during the transition from glassy to rubbery states is more convenient for industrial applications.

The measurement of E' values are taken around alpha and beta transitions (E'_G) and (E'_R) for both composites and the host polymer matrix at 1 Hz as shown in Figure 5-68.

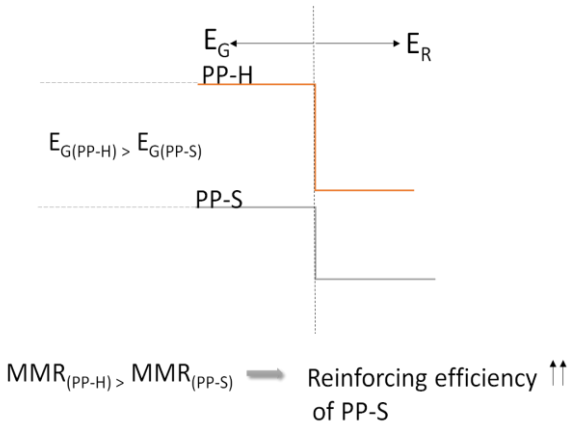

Figure 5-67: Determination of the Storage moduli E'_G and E'_R around beta transition

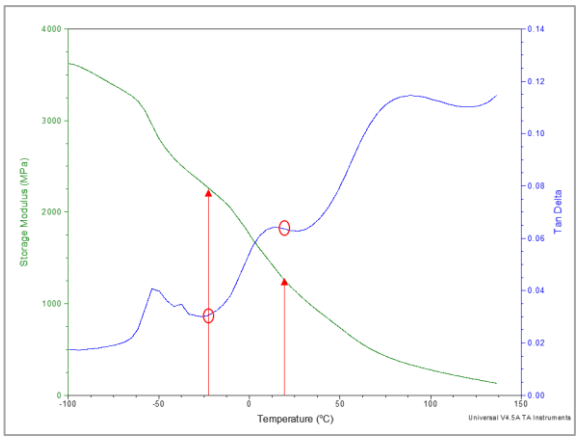

Figure 5-68: MMR of both PP-H and PP-S in comparison to their storage moduli

The trends of MRR for both PP-S and PP-H are mixing with each other at the first cycles. Then at the last cycles, PP-H proves to have lower efficiency in reinforcing (higher MRR) in comparison to PP-S as shown in Figure 5-69. However, this index is suitable for defining the effect of fiber type or content because PP before recycling is taken as the reference material.

But to consider the effect of the cycle number, the MRR index can be modified to be referred to the PP at the corresponding cycle. Therefore, a modified modulus of retention (MMRR) at certain cycle number (i) is used shown in Equation 5-11. Figure 5-70 shows clearly that PP-S has lower MMRR for both alpha and beta transitions for the different cycles. This means that PP-S has higher efficiency in reinforcing after structure transitions.

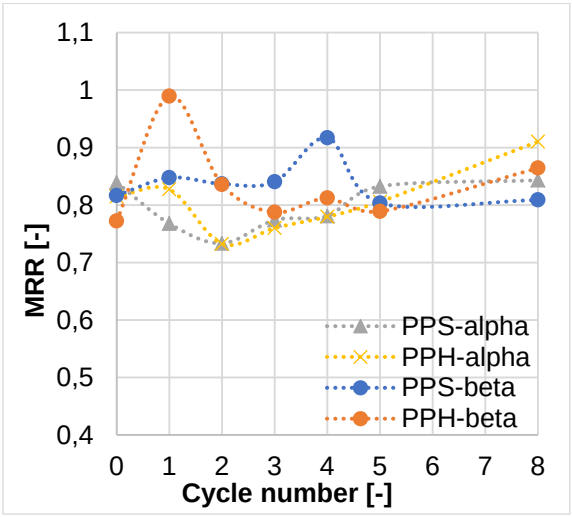

Figure 5-69: Modulus of retention ratio for PP-S and PP-H at alpha and beta transitions

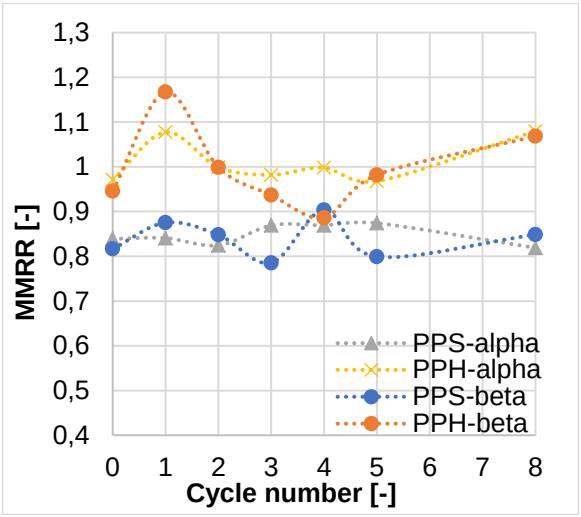

Figure 5-70: Modified modulus of retention ratio for PP-S and PP-H at alpha and beta transitions

This concept of better reinforcing efficiency (modulus of retention) is not contradicting with the superiority of PP-H storage modulus at C0 in Figure 5-55. Although the PP-H starts with E_G larger than PP-S, but the reinforcing efficiency of PP-H through the transformation from Glassy to Rubbery state remains limited when compared with

PP-S. As explained previously in the fibers morphology discussed in 4.3, this could be attributed to the straight fiber form of the Sisal fibers which participate in load transmission better than hemp (see Figure 5-67).

$$MMRR_{cycle\ i} = \frac{\left(E'_G / E'_R\right)_{Composite,cycle\ i}}{\left(E'_G / E'_R\right)_{Polymer,cycle\ i}}$$

Equation 5-11

5.4 Effect of recycling on the mechanical properties of sisal and hemp compounds

As discussed in the previous sections, it is proved that recycling leads to the splicing and shortening of the fibers and hence a better distribution of the fibers in the matrix is achieved. In addition, not only recycling enhanced the homogeneity of the compounds but it was also proved by dynamic mechanical analysis that recycling leads to the enhancement of the thermo-mechanical characteristics of the compounds to different degrees depending on the number of processing cycles. Thermal analysis also proved no critical deterioration of the natural fibers after recycling. Based on these facts, it is also to be expected that NFTC recycling would improve selected mechanical properties of the compounds.

The effect of the executed number of cycles on the E-modulus, tensile strength, elongation and impact strength of PP/30% Sisal composite against the behavior of PP through recycling is shown in Figures 5-71 till 5-74. All mechanical results of both PP and PP/30% Sisal from C0 till C8 are listed in Table A-6 (Appendix).

E-modulus of PP/30% sisal improves by 1.3% from 3033 to 3075 MPa after two cycles, then it starts to decrease by 6.8% to 2914 MPa after 8 cycles as shown in Figure 5-71. Oppositely, the recycling of PP shows the behavior seen in Figure 2-13. The E-modulus decreases 13% after two cycles then the values stabilize. This highlights the effect of the first cycles on the fibers. Fibers recycling helps in strengthening, even the composite of PP/30% Sisal after two recycling increased whereas the polypropylene twice recycled decreased. More analysis will be given in Figure 5-75. The tensile behavior of both PP/30% Sisal and PP at C8 is illustrated in Figure 5-72. Here, it is noticed that the same behavior shown in Figure 5-71 is repeated. Tensile strength of PP/30% Sisal decreased from 40 MPa to 36 MPa after 8 cycles. But it is obvious that this reduction is not linear. The decrease in strength is almost
0.5 MPa/cycle for the first three cycles then it drops to 37 MPa and continues decreasing with a lower gradient till the eighth cycle. For PP, it decreases rapidly from 29 to 26.7 MPa from the first cycle then it stabilizes.

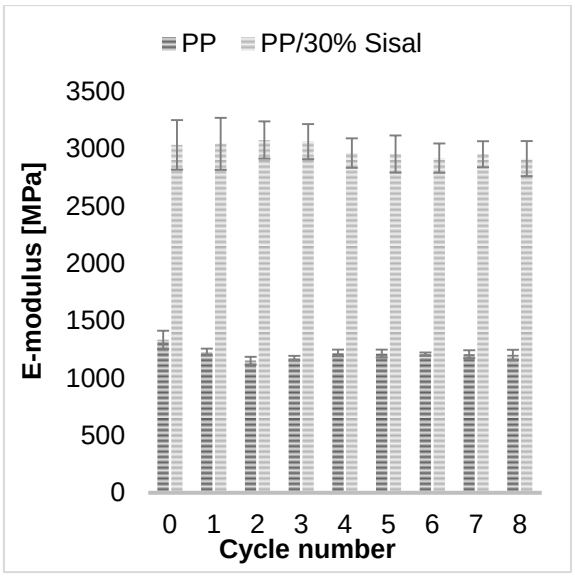

Figure 5-71: E-modulus of PP and PP/30% Sisal at after different number of cycles

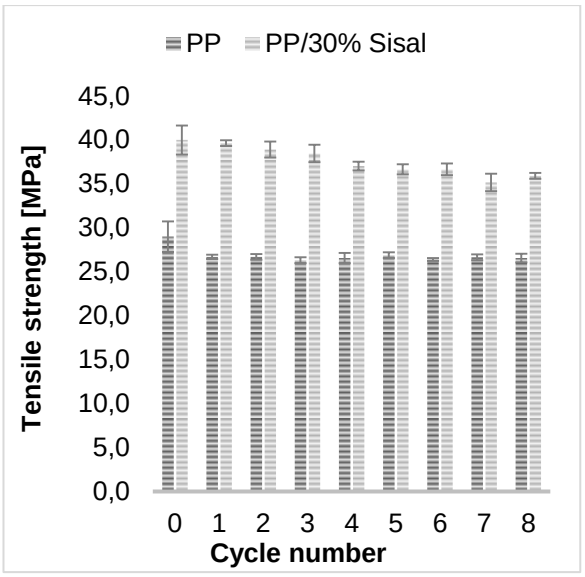

Figure 5-72: Tensile strength of PP and PP/30% Sisal at after different number of cycles

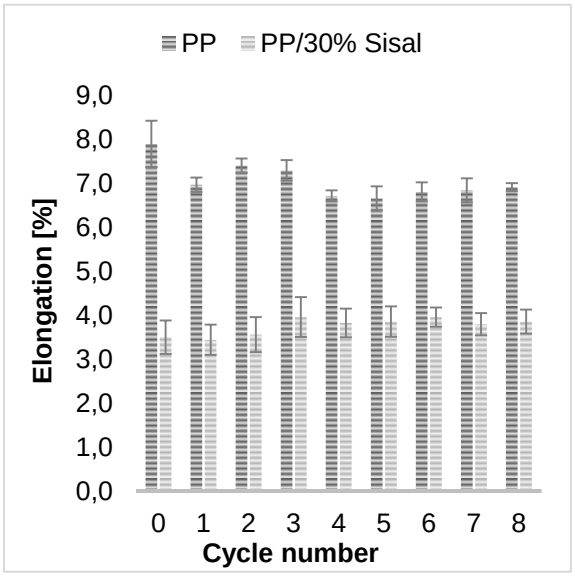

Figure 5-73: Elongation of PP and PP/30% Sisal at after different number of cycles

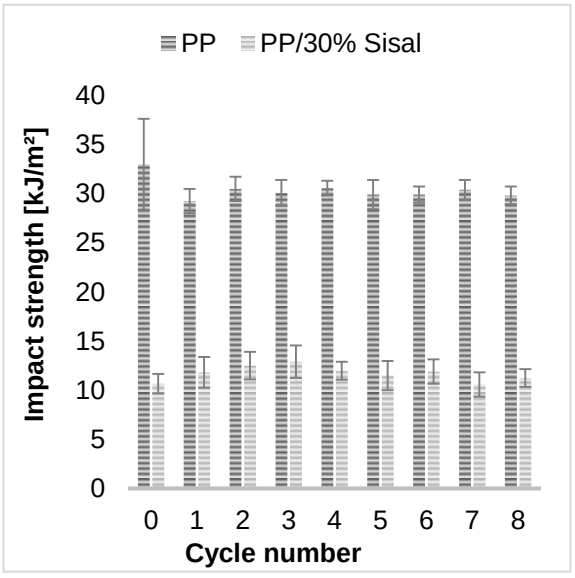

Figure 5-74: Impact strength of PP and PP/30% Sisal at after different number of cycles

Similar trends of results are attained by [Ste16] [Mah13]. Stehle [Ste16] has reported greater drop in strength after the first cycle. This decrease after the first cycle cannot be only attributed to the decreasing chain size. But it can also be contributed to the need of antioxidant formulations to stabilize the polymer during reprocessing [Mar02], [Mah13]. The breaking elongation of PP/30% Sisal with respect to PP is represented in Figure 5-73. As expected, the fibers affect the elongation negatively because they act as crack propagation motivators. The elongation of PP/Sisal shows a parabolic behavior with a maximum after three cycles. This implies that the expected deterioration of elongation due to the chain scission is counteracted by another positive factor. Recycling of PP results in decreasing trend of elongation. The results are again like those of virgin PP having undergone three cycles [Mah13].

Figure 5-74 shows the impact strength of the recycled PP and PP/30% Sisal. Although the mechanical strength and E-modulus of PP/Sisal are better than those of PP, the impact strength of PP/Sisal is less than the counterpart PP sample at the same number of cycles. The impact strength of PP/Sisal shows again a maximum value after three cycles. That is the same as in the elongation development in Figure 5-73. The difference here lies in the almost constant impact strength of PP after the reduction observed at first cycle.

The analysis of Figure 5-71 till Figure 5-74 shows different peak cycles according to the mechanical property under investigation. Thus, for better understanding, a reprocessing of the data is given by calculating the relative properties for each value (Table A-7 in Appendix).

For easy comparison, normalization functions are constructed as in Equation 5-12, Equation 5-13, Equation 5-14 and Equation 5-15 for E-modulus, tensile strength, and elongation at break and impact strength respectively at cycle (i) where *'i'* is the cycle number. The normalized functions are illustrated together in Figure 5-75 and listed in details In Table A-8 in the Appendix.

$$E-modulus_{Normalised} = \left(\frac{Rel.Emodulus_i - Rel.Emodulus_0}{Rel.Emodulus_0}\right) * 100$$

Equation 5-12

$$\sigma_{Normalised} = \left(\frac{Rel.\sigma_i - Rel.\sigma_0}{Rel.\sigma_0}\right) * 100$$

Equation 5-13

$$Elongation_{Normalised} = \left(\frac{Rel.Elongation_i - Rel.Elongation_0}{Rel.Elongation_0}\right) * 100$$

Equation 5-14

$$Impact\ strength_{Normalised} = \left(\frac{Rel.Impact\ strength_i - Rel.mpact\ strength_0}{Rel.Impact\ strength_0}\right) * 100$$

Equation 5-15

Figure 5-16 is added to Figure 5-75 to visualize the direct effect of the evolution of the fiber size on the resulting mechanical property. The tensile strength improvement is maximized with 7% after one cycle while E-modulus is maximized after two cycles and the impact strength after three cycles with 30% relative improvement following the exact course of the flowabilty. Away from them, the elongation at break shows the maximum improvement after six cycles which is correlated to the deterioration of the fibers length in addition to the relative reduction in fiber content at late cycles as previously explained.

It is also observed that the normalized change % in E-modulus, elongation at break and impact strength ended after eight cycles with positive stable value. Whereas the

normalized change % in tensile strength is close to zero. The important thing is the trend of these curves and not the number of cycles itself. Because the thermal and shear loading per each cycle depends on the reprocessing parameters (temperature, compounding element form, speed…).

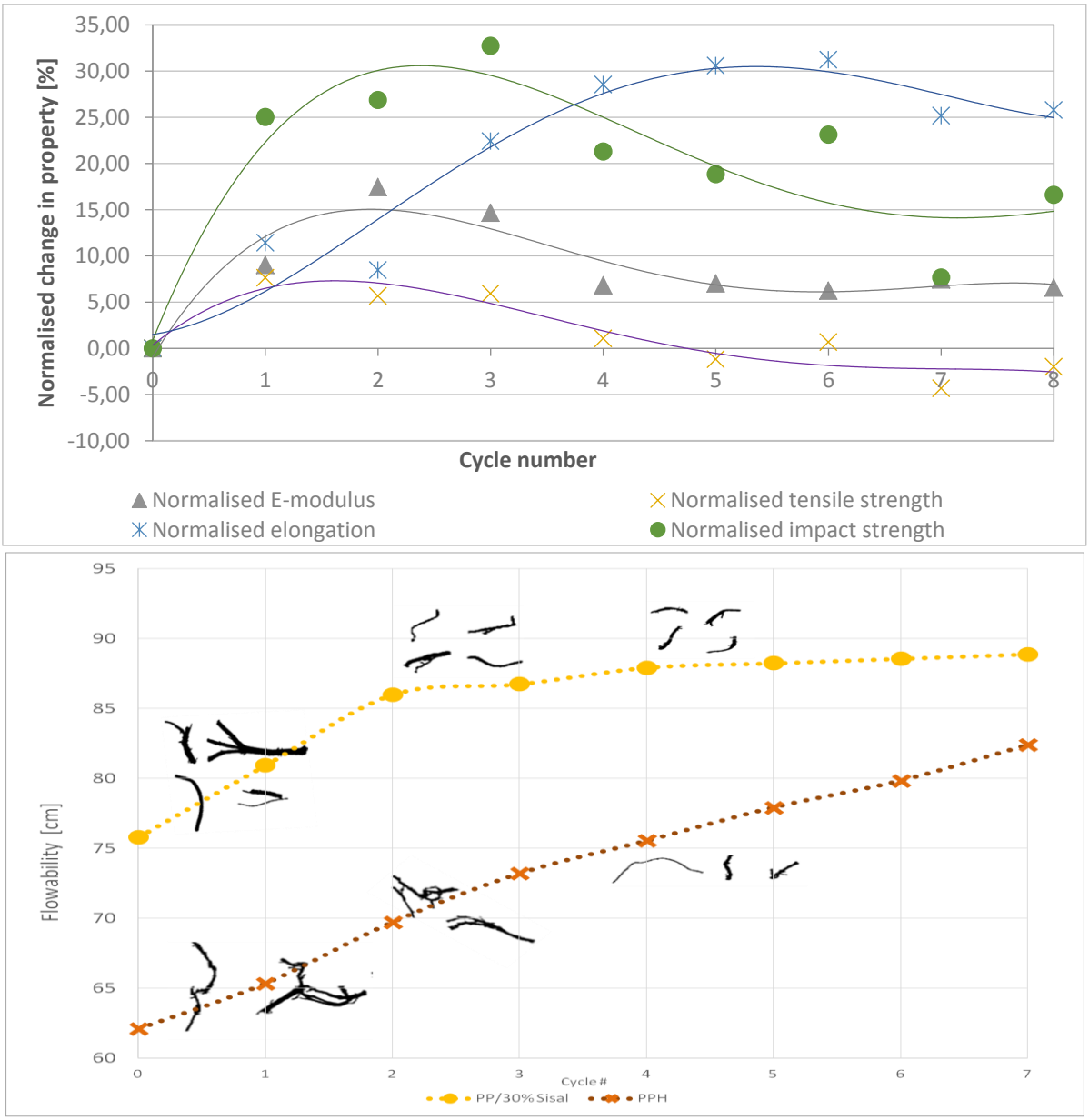

Figure 5-75: Effect of the number of cycles on the normalized property (PP/30% Sisal with respect to PP)

5.5 Conclusion

Considering the recycling of NFTC, the following main points could be deduced:

- Recycling causes the deterioration of fiber length and diameter. Reduction of fiber length is significant at the first cycle. Reduction in diameter is significant at the first cycle then diameter size stabilizes afterwards. Since diameter also decreases by recycling, the aspect ratio remains at acceptable values and the fiber sustains its ability to transfer load in case of sisal.

- Recycling causes general reduction in fiber size which causes the agglomerations to de-entangle and a better distribution of fibers in the matrix is achieved. Longer fibers are injected to longer distances and are usually found at the tip of the injected spiral
- Recycling increases the flowability in the spirals indicating break-up of molecular chains as well as the break-up of the agglomerated fiber clusters.
- Viscosity behavior at low shear rates is significantly affected by the presence of the fibers and their shape. On the contrary, the viscosity behavior at high shear rate is dominated by the polymer matrix behavior.
- Viscosity of NFTC is reduced by recycling. The effect of fiber type and preparation is significant where the viscosity reduction is more remarkable in case of PP-H and PP-S than the PP-30%Sisal as well as PP.
- Mechanical testing shows an improvement of (E-modulus, strength, elongation and impact strength) at the first cycle then these properties start to decrease differently. For example, strength decreases even lower than its original value while the reduction in E-modulus and impact strength is relatively small. This different behavior is assured by the normalization curves.
- TGA shows that the temperature corresponding to the first peak of decomposition decreases with the recycling, in case of PP-S. However, for PP-H, the decomposition temperature does not decrease as PP-S. This is due to the fact the coupling improves by defibrillation of hemp agglomerated fibers by developing new fiber surfaces.
- The main DSC result is that cycle number has a linear trend effect on the difference between the compound melting temperature with respect to that of PP. Since, the melting temperature of PP is almost constant at different cycles, therefore the NFTC show almost linear reduction in their melting points.
- Degree of crystallinity increases by recycling especially at the last cycles due to the presence of short lower molar mass.
- Storage modulus of NFTC increases by recycling as result of the restriction to the segmental motion of the molecular chains.
- Ranking of storage and loss moduli are varying between the original compound and after the eighth cycle. The ascending ranking of the storage and loss moduli in the original compound is [PP, PP-S, PP-H]. While after eight cycles, PP-H behavior is too close to PP and the ranking became [PP, PP-H, PP-S]. This is attributed to the decreasing efficiency of hemp fibers in reinforcing after excessive recycling.
- The activation energies are reduced in NFTC in comparison to PP. The activation energy is reduced after the first cycle and remains so till the fourth one before it starts again to increase at the last cycles.

Regarding the previous points, it is highly recommended to develop a standardized legend for all NFTC products defining the maximum allowable number of reprocessing cycles according to the material properties.

In addition, compounders and NFTC products producers should issue protocols to help evaluating the incoming recycled NFTC and allocate them to the relevant cycle number according to the material condition.

6 Mathematical Modeling and Simulation

6.1 Correlation between fiber dimensions, recycling and flowability

This section studies an analytical model that describes the flowability in terms of cycle number. To find out this link between the cycle number and the flowability, the effect of recycling on the fiber distribution in dependence on its size is also investigated. Back to Figure 5-16, the QICPIC analysis shows the image size and shape after extraction from selected cycles. This assumption of the three stages can be validated by the QICPIC dynamic images shown in Figure 6-1. The hemp fibers start branched at C0 and continue branched in C1. The fibers are then defibrillated and spliced to less branched ones at further cycles. In sisal, the branching is much less as shown in C0. Afterwards, the lengths decrease significantly with almost straight less branched fibers and uniform diameter (see Table 5-1).

To understand the relation between fiber length (due to successive recycling) and the flowability, the change of fiber lengths against cycle number is plotted in Figure 6-2. Two trends are observed: A linear negative trend at the first cycles and a constant trend for advanced cycles. Linear trend is taken for simplicity but second-degree polynomial or more can also be selected for more accuracy especially in case of hemp compounds. After a certain fiber length, a quasi-constant value is attained.

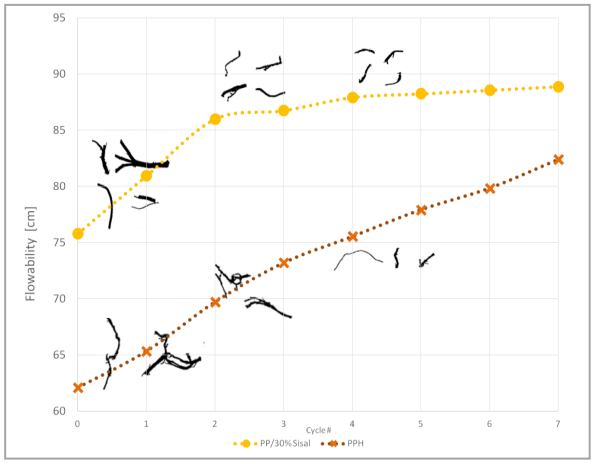

Figure 6-1: Effect of the number of cycles on the spirals' flowability and fiber shape for PP-H and PP-S

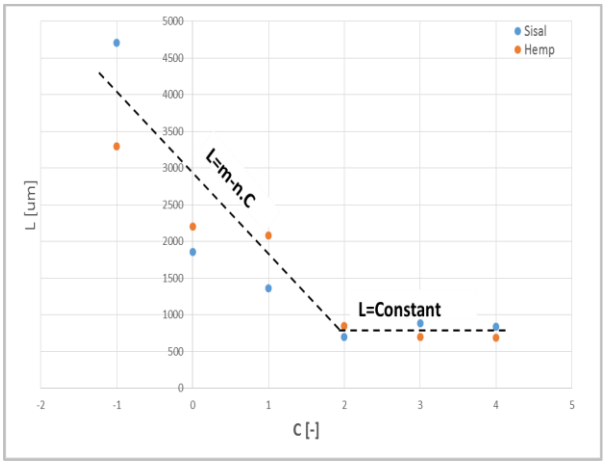

Figure 6-2: Effect of cycle number on fiber length for extracted hemp and sisal fibers

The flowability development with respect to the cycle number can be interpreted by understanding the flow regimes and the transition from heterogeneous flow to homogeneous flow specifically slurry flow regimes as named by [Bre05] which deal with solid flowing in a liquid as the case of the NFTC in the molten phase. The fluid is understood to flow homogeneously when the volume fraction of the solids (sizes must lie within the micron region) is relatively low and the solids are well mixed in the matrix liquid.

Heterogeneous flow occurs when larger particles present at the liquid mixture –in this case the polymer melt– start to precipitate under the force of gravity and hence flow

with different velocity and a vertical concentration gradient starts to build up as shown in Figure 6-3.

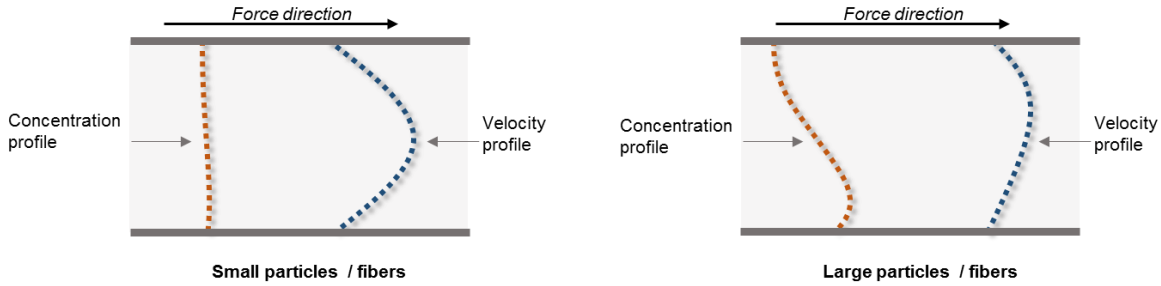

Figure 6-3: Effect of particle/ fiber size: a) small particles b) large particles on concentration and velocity profiles across a horizontal flow [Che09]

Separation speed of particles with average radius *'R'* from a carrier fluid is denoted by *'Vs'* as in Equation 6-1 and Equation 6-2 for small and big particles respectively, where '$\Delta\rho$' is the difference in densities between that of the carrying fluid *'ρ'* and that of the particles. *'η'* is the fluid kinematic viscosity. 'v' is the flow velocity.

In Equation 6-1, the kinematic viscosity is a function of the fiber volume fraction in the composite [Beh09] as in Equation 6-3. The viscosity *'η'* increases with the increase of fiber volume fraction *'ϕ'*. This interprets why the flowability offsets downwards from PP to PP-S in Figure 6-4.

$$\boldsymbol{V_s = \frac{2R^2 g}{9\eta}.\frac{\Delta\rho}{\rho}} \quad \textit{if} \quad \boldsymbol{\frac{2vR}{\eta} \ll 1}$$

Equation 6-1

$$\boldsymbol{V_s = \sqrt{\frac{2Rg}{3Cd}\frac{\Delta\rho}{\rho}}} \quad \textit{if} \quad \boldsymbol{\frac{2vR}{\eta} \gg 1}$$

Equation 6-2

$$\boldsymbol{\eta = \eta_{fluid}(1 + \eta_{\varphi} + 5\varphi^2 + 53\varphi^3)}$$

Equation 6-3

'Cd' is the drag coefficient and is calculated as shown in Equation 6-4, [Bre05].

$$\boldsymbol{Cd = \frac{24}{R}(1 + aR^b)}$$

Equation 6-4

'a' and ***'b'*** are constants <1

Therefore, for simplicity, Equation 6-4 can be simplified to Equation 6-5

$$\boldsymbol{Cd = \frac{24}{R}}$$

Equation 6-5

The separation velocities, in Equation 6-1 and Equation 6-2, can be rewritten after excluding the constant parameters or values as shown in Equation 6-6 and Equation 6-7.

$$\boldsymbol{V_s \propto R\ (big\ particles)}$$

Or

$$\boldsymbol{V_s \propto \sqrt{L}(long\ fibres)}$$

Equation 6-6

$$\boldsymbol{V_s \propto R^2\ (small\ particles)}$$

Or

$$\boldsymbol{V_s \propto L\ (short\ fibres)}$$

Equation 6-7

Determining the separation velocity helps in defining the concentration and velocity profiles of multiphase flows (i.e. fibers in PP matrix). As seen in Figure 6-3, large particles show heterogeneous flow compared to the homogeneous flow of the small particles. This depicts that there is a critical size at which the flow pattern changes its regime.

Considering that the kinetic energy of a particle at certain position is constant then the summation of kinetic energy in both directions (flow and separation) is constant and hence the sum of the squared velocities (V_f and V_s) in both directions is constant as in Equation 6-8. Thus, the flow velocity can be described as in Equation 6-9.

By merging Equation 6-6 and Equation 6-7 into Equation 6-9, Equation 6-10 and Equation 6-11 are concluded:

$$\boldsymbol{V_s^2 + V_f^2 = Const}$$

Equation 6-8

$$\boldsymbol{V_f^2 = Const - V_s^2}$$

Equation 6-9

$$\boldsymbol{V_f^2 = Const - k.L \quad for\ long\ fibres}$$

Equation 6-10

$$\boldsymbol{V_f^2 = Const - k'.L^2 \quad for\ short\ fibres}$$

Equation 6-11

Where $\boldsymbol{k}$ and $\boldsymbol{k'}$ are proportionality constants.

Referring to Bernoulli's equation on a horizontal mold with constant cross section as in Equation 6-12 where 'h_l' is the head loss due to friction which can be replaced by the flowability spiral length 'F', as in Equation 6-13. This equation simply describes the head loss as a linear function of flowability.

$$\frac{P}{\rho g} + \frac{V_f^2}{2g} = Const + h_l$$

Equation 6-12

$$h_l = Const \,.\, F$$

Equation 6-13

Equation 6-10 and Equation 6-11 can be again rewritten after replacing 'V_f' with 'F' as shown in Equation 6-14 and Equation 6-15. Where 'F' is the spiral flow length and 'L' is the length of fibers.

$$F = Const - k.L \quad for\ long\ fibers$$

Equation 6-14

$$F = Const - k'.L^2 \quad for\ short\ fibers$$

Equation 6-15

Recalling the relation between the fiber length and the cycle number as shown in Figure 6-2, Equation 6-14 and Equation 6-15 will be transformed to Equation 6-16 and Equation 6-17.

$F = Const - k.(m - n.C)$ for first cycles (long or agglomerated fibers)

Equation 6-16

$F = Const - k'.Const^2 = Const'$ for further cycles (short defibrillated fibers)

Equation 6-17

Equation 6-16 is a linear equation and Equation 6-17 is a constant value. However, the main separation equations, Equation 6-1 and Equation 6-2, assume that the carrying fluid is not function of recycling cycles. So, the flowability of the polymer has to be considered with respect to the cycle number. Figure 5-13 is redrawn in Figure 6-4 after the addition of trend line for PP to know the (cycle number-flowability) relation of the host carrying polymer. As shown, the trend line is a linear equation. The overall flowability will be then a combination of this trend line (flowability of polymer) with the flowability due to fiber flow regime in Equation 6-16 and Equation 6-17. This combination can be described as in Equation 6-18. This means that the overall flowability for both situations (beginning and further cycles corresponding to

long and short fibers respectively) will be second-degree polynomial equation as in Equation 6-19 and first-degree polynomial equation as in Equation 6-20.

$$\boldsymbol{F = F_{Polymer} \cdot F_{fiber\ effect}}$$

Equation 6-18

$$\boldsymbol{F_1 = (1st\ order\ linear).(1st\ order\ linear) = a_1 + b_1 C + c_1 C^2}$$ → for long fibers

Equation 6-19

$$\boldsymbol{F_2 = (1st\ order\ linear).(Constant) = a_2 + b_2 C}$$ → for short fibers

Equation 6-20

Recalling that $b_2 = b_{PP} = 1.1595$ cm/cycle

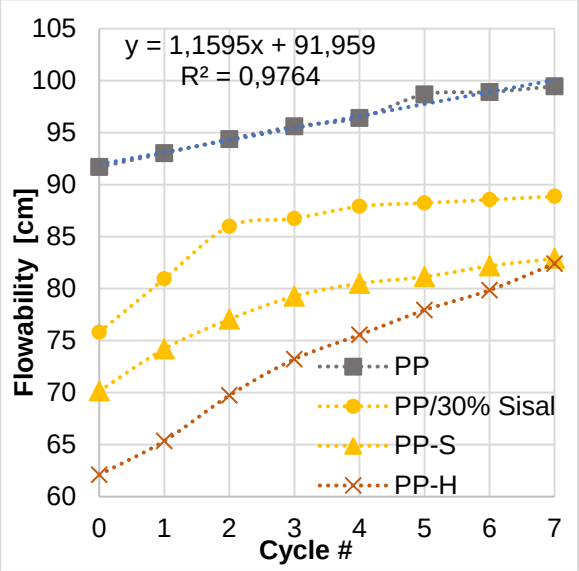

Figure 6-4: Effect of recycling number on the flowability for PP and different compounds (Trend line of PP is shown)

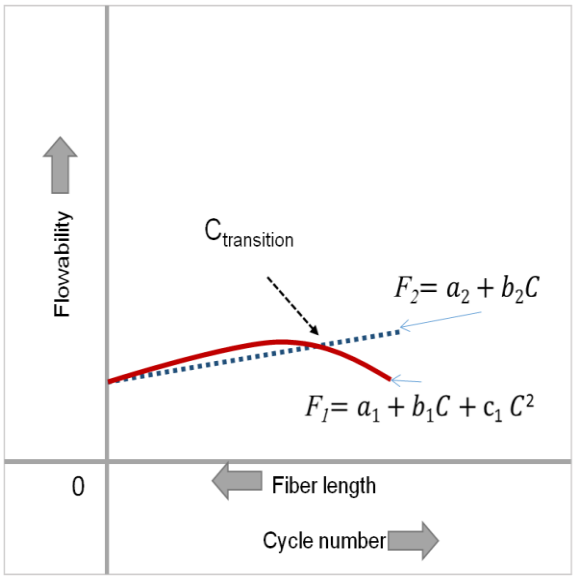

Figure 6-5: Effect of the number of cycles as well as the fiber length on the spirals' flowability

A schematic representing these equations is shown in Figure 6-5 to illustrate the effect of the cycle number as well as the fiber length on the flowability of the composite material. The two equations are continuous and differentiable. 'a_2' can be determined from Equation 6-20 using the known 'b_2' and 'F_2' in case of PP-S. By equating Equation 6-21 and Equation 6-22, we find out the critical '$C_{transition}$'.

Now, the coefficients of Equation 6-20 are all defined. Afterwards, coefficients of Equation 6-19 are solved. "a_1" is the flowability at cycle 0. To find out 'b_1' and 'c_1'; two equations are to be solved simultaneously. The flowability at first and second cycles is applied in Equation 6-23 and Equation 6-24. After finding all the coefficients and by equating Equation 6-19 and Equation 6-20 (note that the known values are in blue), the point of transition from the model 1 to model 2 could be determined.

$$\boldsymbol{F_1' = b_1 + 2c_1 C}$$ *for long fibers*

Equation 6-21

$$F_2' = b_2 \qquad \textit{for short fibers}$$

Equation 6-22

$$F_1^{C=1} = a_1 + b_1.1 + c_1.1^2 = a_1 + b_1 + c_1$$

Equation 6-23

$$F_1^{C=2} = a_1 + b_1.2 + c_1.2^2 = a_1 + 2b_1 + 4c_1$$

Equation 6-24

Figure 6-6 shows the model versus experimental results for PP-H. The assumption of polymer dominant behavior at high cycles (b_2=1.1595) is implied. However, a difference is attained. The transition from one flow regime to another takes place after C3. If another adjusted b_2 value is used, for example b_2=2.2, a better matching as in Figure 6-7 could be achieved, but this means that the single phase dominant behavior does not correspond to pure PP.

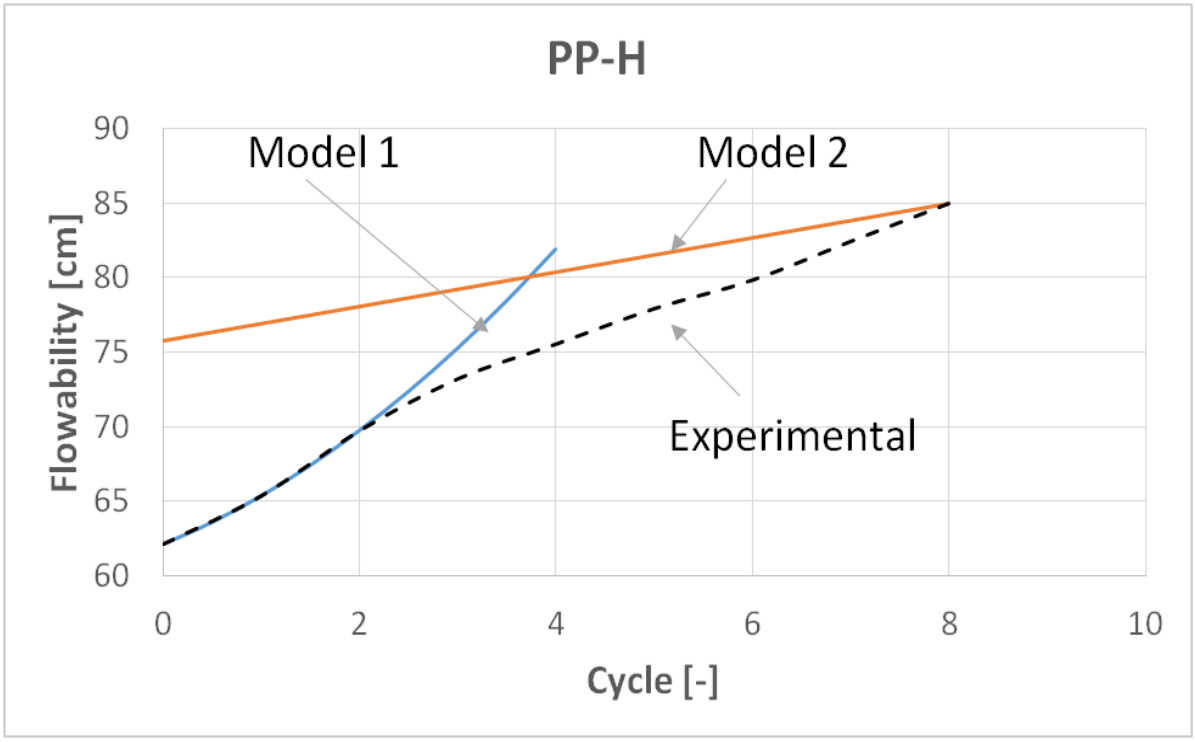

Figure 6-6: Model versus experimental for PP-H using the polymer dominant behavior at high cycles (b_2=1.1595)

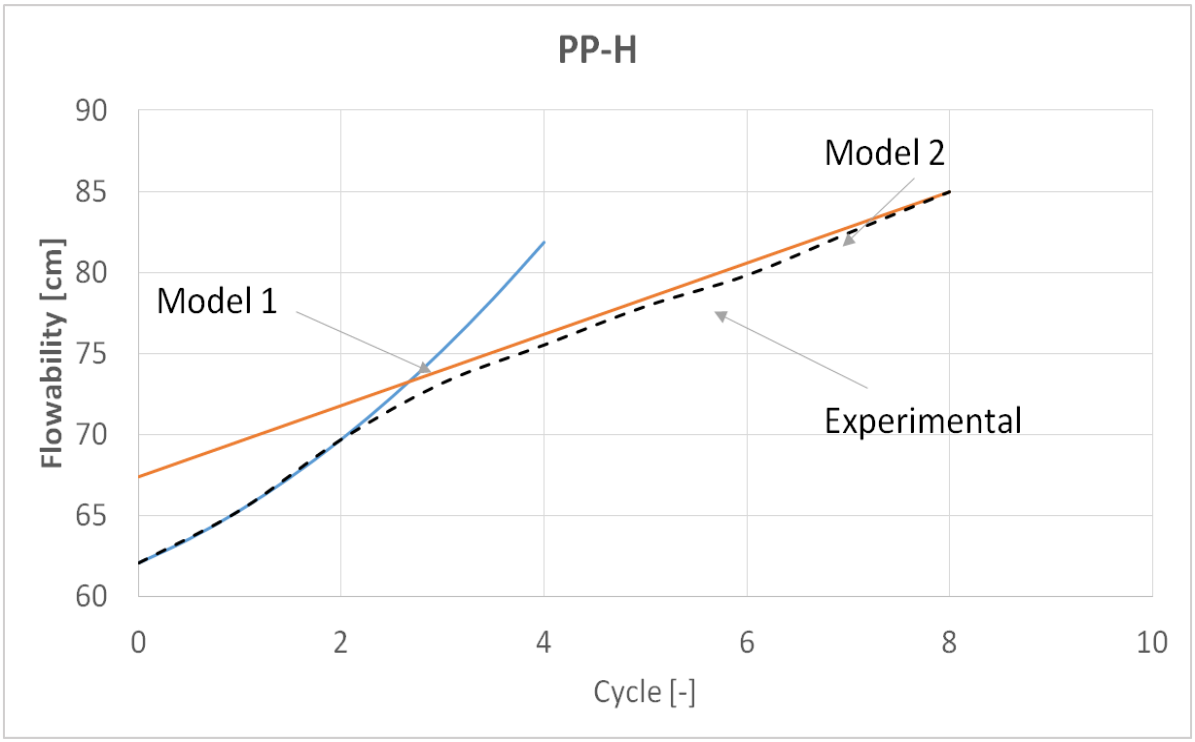

Figure 6-7: Model versus experimental for PP-H using the adjusted polymer dominant behavior at high cycles (b2=2.2)

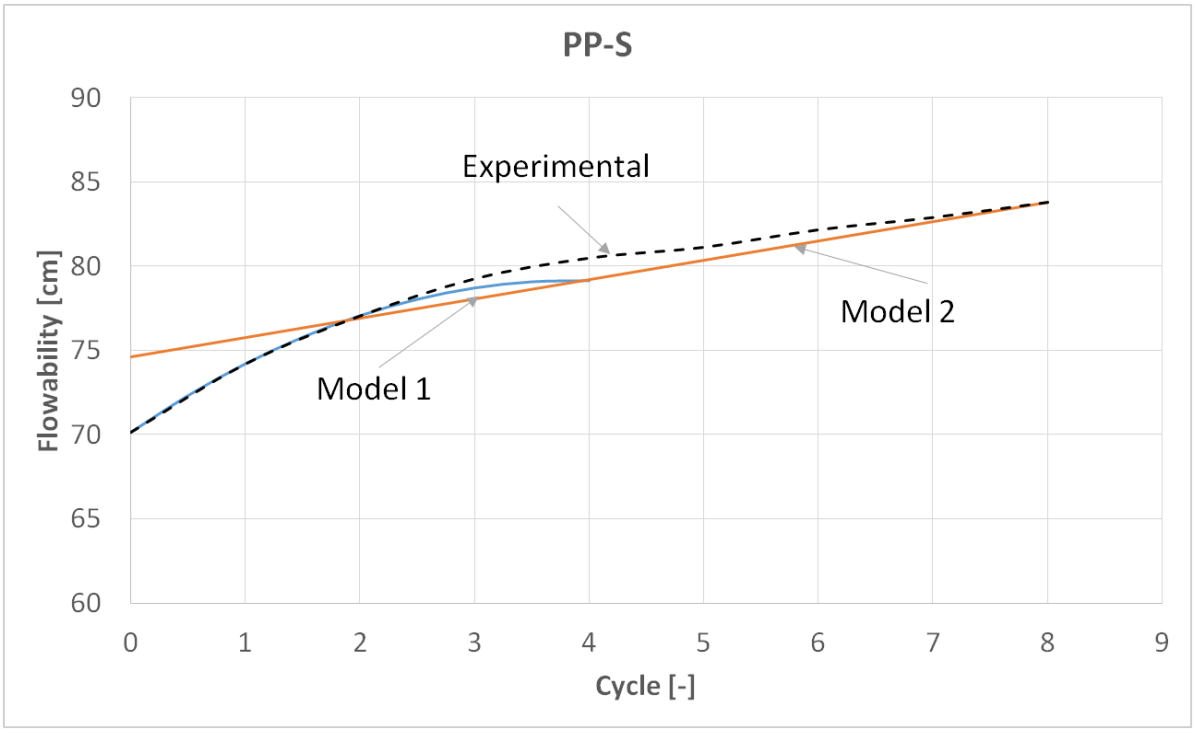

Figure 6-8: Model versus experimental for PP-S using the polymer dominant behavior at high cycles (b2=1.1595)

On the other side PP-S shows excellent matching even with the b2=1.1595 of PP. The transition takes place after C1 (Figure 6-8). The parabolic nature of the first model explains the first and the second stages of fiber size development. The second model corresponds to the assumed third stage of fiber final shape.

6.2 Correlation between fiber dimensions and mechanical properties

In [Els17], both fiber size and flowability are defined as functions of the processing parameters (pressure, injection temperature, mold temperature, fiber type and fiber content). Similarly, as previously mentioned in this work (Figure 5-75), it is assumed that there are dependent relations of fiber size and mechanical properties and flowability as functions of cycle number as in Equation 6-25 and Equation 6-26. Consequently, a relation can be derived to describe the property as a function of the fiber size as shown in Equation 6-27.

$$\because \boldsymbol{Fiber\ size} = \boldsymbol{f}(\boldsymbol{cycle\ number})$$

Equation 6-25

$$\because \boldsymbol{Mechanical\ property} = \boldsymbol{f}(\boldsymbol{cycle\ number})$$

Equation 6-26

$$\therefore \boldsymbol{Mechanical\ property} = \boldsymbol{f}(\boldsymbol{fiber\ size})$$

Equation 6-27

Based on the above methodology, non-linear functions of symmetrical sigmoidal type (4 PL) are assumed to correlate between the following pairs of fiber aspect ratio and the corresponding property namely:

- Relation of (Aspect ratio, E-modulus) as shown in Equation 6-28,
- Relation of (Aspect ratio, Tensile strength) as shown in Equation 6-29,

The model results, describing the mechanical properties and flowability of PP/30% sisal, are plotted in Figure 6-9 and Figure 6-10. A good matching in the trends of the curves, between the experimental and model results, is found. However, low regressions (in order of 68%) are present because the results seem to follow an alternating function.

$$\boldsymbol{Emodulus_{model}} = \mathbf{3051.3} - \mathbf{193}/(\mathbf{1} + \left(\frac{\boldsymbol{AR}}{\mathbf{43}}\right)^{\mathbf{6}})$$

Equation 6-28

$$\boldsymbol{UTS_{model}} = \mathbf{39.6} - \mathbf{4.3}/(\mathbf{1} + \left(\frac{\boldsymbol{AR}}{\mathbf{50}}\right)^{\mathbf{7.3}})$$

Equation 6-29

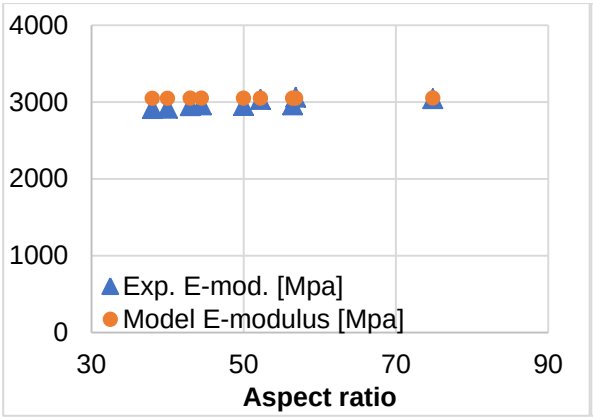

Figure 6-9: Experimental versus model E-modulus as functions of aspect ratio (AR)

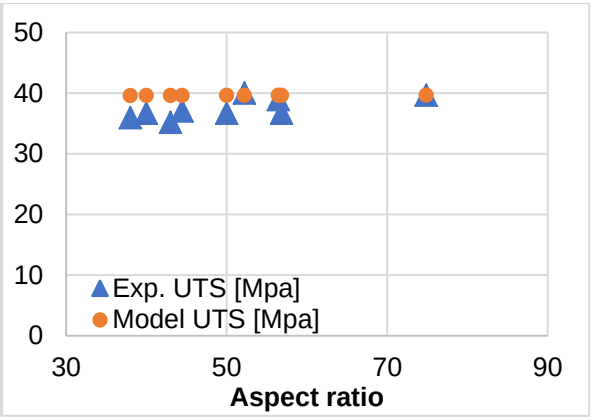

Figure 6-10: Experimental versus model tensile strength (UTS) as functions of aspect ratio (AR)

6.3 Conclusion

- Analytical model is constructed to correlate the flowability with the cycle number by interpretation of the changing fiber length. The model describes the three assumed stages using two power equations. The model sets the conditions of using both equations (in case of branched tangled hemp fibers) or just the second equation (in case of straight sisal fibers)

- Using fitting curve models, mechanical properties of the NFTC are described in terms of both the cycle number and fiber length.

7 Conclusions and Future Work

Primary mechanical recycling of natural fiber reinforced polypropylene is studied and evaluated in this work. The experimental work studies different parameters, namely, the number of the reprocessing cycles of injection molding, fiber type, fiber form and fiber shape. The characterization covers the effect of previously mentioned parameters on various aspects (rheological, flowability, thermal and mechanical properties) of the composites. The main findings of this study are listed in the following points:

7.1 Characterization of original compounds

Addition of natural fibers to PP induces an increase in the melting temperature in comparison to the pure polymer matrix. On the other side, the recrystallization temperature of the compounds is 2-3°C lower than that of PP. This indicates that addition of fiber (regardless of its type) enhances nucleation and crystal growth. Thus, leads to the increase of viscosity, decrease of spiral flowability and the increase of water absorption. Hemp composite has lower viscosity due to the fiber branching which induces agglomeration at least in the first compound form before recycling.

Decomposition of natural fibers is not affected by the host polypropylene matrix. All decomposition products of the pure fibers (Carbohydrates, water, carbon dioxide and acetic acid) are detected in the mass spectra of PP-H and PP-S.

Sisal fibers prove a narrower distribution for both length and diameter measurements in comparison to hemp fibers. In addition, considering sisal nature being stiffer than hemp and larger in size reflects on both mechanical and rheological behavior of its compound compared to hemp.

In contradiction to the viscosity results, PP-H which has the lowest viscosity shows less ability to flow in the spiral mold than the PP-S with the higher viscosity. This is attributed to the branching and tangling of hemp fibers which leads to the domination of the matrix viscosity.

7.2 Potential of recycled NFTC

7.2.1 Mechanical properties

The main concern about recycling the polymer composites is the drop of the mechanical properties because of the scissions in the molecular chains. However, both E-modulus and tensile strength attained their levels at the first two cycles and then they decreased 7 and 10% respectively after eight cycles.

Reprocessing of the data collected from the recycled composite and PP shows that the composite mechanical properties (E-modulus, tensile strength, impact strength and elongation) improve gradually till a certain cycle before decreasing again.

The maximum improvement is dependent on the mechanical property under investigation. For example, E-modulus and tensile strength maximize at the second cycle, while the impact strength maximizes at the third cycle and further, the elongation maximizes after six cycles.

This improvement after two cycles is attributed to the increased efficiency of coupling between the newly developed surface areas of the reinforcing fibers and PP. The new areas are generated because of the fibrillation during recycling.

7.2.2 Flowability properties

Flowability increased by recycling with different modes. First a critical level of material homogeneity is needed to impart improvement in flowability. This mode takes place in PP-H because of the fiber shape. Second mode, a rapid improvement in flowability is observed. Third mode takes place starting at the third or fourth cycles where the flowability improvement is dominated by PP.

Fibers affected the flowability of the composite negatively in comparison to the flowability of the pure PP. Flowability values of both types of NFTC at any cycle are less than that of the flowability of PP by 15-25% depending on the fiber type and the cycle number.

Fiber shape plays a very important role in the flowability of composite during injection molding. Straight stiff fibers of sisal have better flowability values than that of hemp reinforced PP.

7.2.3 Rheological properties

Viscosity of PP increased from 4300 Pa.s to eight times by adding 30% sisal (32400 Pa.s) and much more in case of 30% hemp (845000 Pa.s). The viscosity decreases significantly by increasing the shear rate (100 1/s), so that PP-S has close viscosity to PP (192 Pa.s) whereas PP-H is just 50% more than that of PP (343 Pa.s).

Recycling results in decreasing the viscosity. However, PP-H, filled with hemp, increased its viscosity after two cycles before it starts to decrease as other composites and PP. This sudden increase in viscosity of PP-H is attributed to the branched fibers which results in agglomerating fibers without coupling with PP. Therefore, the viscosity at this stage is dominated by the matrix PP. Recycling enhances the coupling and hence the viscosity increases. This is not the case of sisal reinforced PP because sisal fibers are straight fibers without branching.

7.2.4 Thermal properties

The composites are subjected to thermal and thermo-mechanical tests, namely, TGA, DSC and DMA. Hot stage and microscopic investigations are also used to validate theories about crystal formation. In comparison to PP-S, PP-H shows less sensitivity to recycling regarding the thermal properties. TGA curve of PP-H does not change significantly till the fifth cycle. TGA of PP-S changes obviously from one cycle to another.

There are two opposite trends for the change of the peak temperatures under the recycling effect. The first and the second peaks in sisal reinforced PP show that the peaks slightly decrease from 297 to 295°C and 358 to 354°C respectively. On the other hand, the third stage shows an increasing trend of peak temperature from 435 to 459°C.

The overall improvement of thermal stability is attributed to the newly generated surfaces during recycling and hence more coupling between PP and fibers is attained. Recycling gives chance for more number of carbonyl groups to share in coupling the hydroxyl group with the PP matrix by the help of the grafting agent and consequently the decomposition temperature of the compound is delayed.

DSC results show that addition of fibers to PP decrease the melting point of the composite. DSC results go along with the mechanical and TGA results. The measured melting points increased after recycling almost 4°C after 3 cycles before they started to decrease again.

Normalized enthalpies of composites are close to PP melting enthalpy till the sixth cycle. Afterwards, the melting enthalpies of the compounds are more than the original PP. This excess of enthalpy, after the sixth cycle, is interpreted by the volatilization of some fiber constituents after six cycles and hence PP share is increased. Additionally, the newly generated coupling surfaces in the last cycles require also an increase in melt enthalpy. Crystallization enthalpy increased by recycling in case of the compounds PP-S and PP-H. Oppositely, recycling of PP does not prove such obvious change in crystallization temperature.

Degree of crystallinity increases by recycling especially at the last cycles due to the presence of shorter spliced fibers in addition to the lower molar mass of PP. PP-S and PP-H have higher crystallinity degrees in comparison with PP because fibers help in nucleating crystals. The crystallinity degree of PP-H is relatively higher than that of PP-S because it has more surface areas susceptible for crystal nucleation.

A proposal is assumed to describe the factors affecting the crystallinity during recycling. Fibrillation helps in increasing compounds' crystallinity. Simultaneously, smaller crystals are expected to be formed because of the shorter polymer chains during recycling.

DMA results of sisal reinforced PP highlight the increased storage modulus by recycling as result of the restriction to the segmental motion of the molecular chains. This statement is confirmed by the higher T_g of the recycled samples. Loss modulus E'' as well as tan δ decrease after the first cycle then they increase again.

The loss factor, tanδ, does not change linearly with respect to the cycle number. It drops after the first cycle then starting from the fourth cycle, the loss factor increases again indicating the stiffening of the matrix.

Effect of recycling on DMA appears remarkably between the original material and after being recycled eight cycles. In case of the original material, the ascending

ranking of the storage and loss moduli is [PP, PP-S, PP-H]. While after eight cycles, PP-H behavior is too close to PP and the ranking became [PP, PP-H, PP-S]. This means that the reinforcing efficiency of hemp fibers is severely inhibited after eight cycles of reprocessing.

The activation energies of all investigated materials are measured and it is found out that it is reduced in case of the composites. PP has the highest activation energy in the alpha transition, whereas the difference is not so significant in the beta transition. Similarly, modulus of retention ratio and its modification are calculated. PP-S has higher efficiency in reinforcing the composite after structure transition.

7.2.5 Fiber size measurement

Fiber measurement (length and diameter) and hence the calculation of fiber aspect ratio validates the assumed effect of fiber shape on the flowability of the injection molded samples. Finally, empirical relations are established to describe the composite mechanical properties as well as flowability as function of fiber aspect ratio.

7.3 Summary

The development of selected important characteristics of the recycled compounds in comparison to PP matrix is summarized in the spider chart shown in Figure 7-1. This chart serves as a “one-glance summary” for the selected key properties.

For comparison and illustration purposes, the specific values are calculated for each group (PP, PP-S, PP-H for C0 and C4) w.r.t. the maximum value. Since pure PP matrix is not reinforced with fibers, the aspect ratio for PP-C0 and PP-C4 are considered 0.

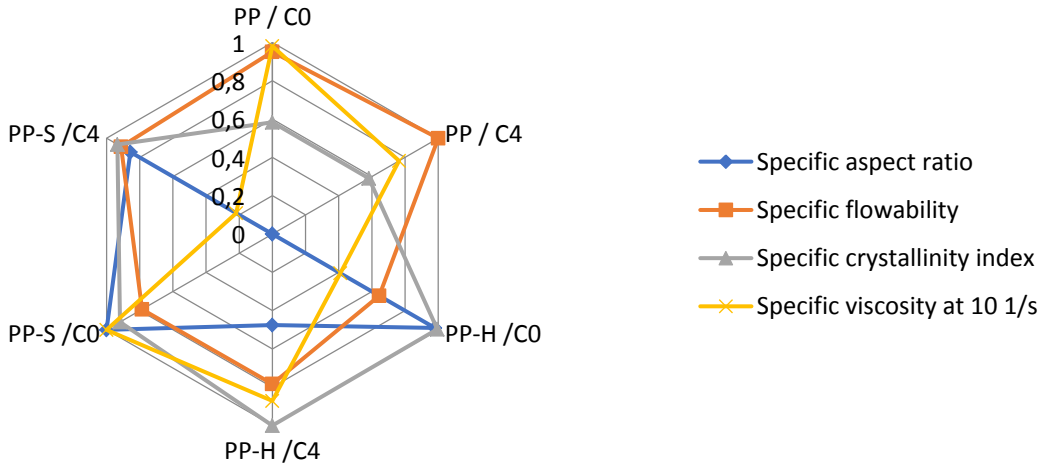

Figure 7-1: Summary of selected properties

7.4 Future work

This work portrays the potential of NFTC from the recycling point of view where certain compound mechanical properties are enhanced after applying primary mechanical recycling. Recycling of NFTC is limited to products having certain fiber type and fiber content in addition to specific polymer trademarks and coupling agents. This leads to the question: ‘’What are the required precautions in case of dealing with non-specific materials as will be the case in the real practice?’’

With this regard, the experimental work in the future should be expanded to study the recycling of consumed products (out of the manufacturer premises). The problem in dealing with consumed products lies in the uncertainties of the materials undergoing recycling. Therefore, certain procedures are needed to define the material composition. The solution suggests different approaches to characterize the materials before recycling namely: classification, purification and transformation to polymer and fiber with certain properties purification [Al-10a], [Bai11].

Classification means sorting (visual, density measurement, centrifugal…). Visual sorting deals with several aspects, for example:

- Sorting of packages with known producer indicating certain material,
- Sorting of products with respect to transparency or color change due to UV effect and stabilizer’s damage.

There are also other classification methods such as:

- Thermal tests to check the homogeneity of polymer molecular weight, degree of contamination, fiber constituents by mass spectrometry (Technical limitations such as spectral coverage and spectral resolution of the detectors are to be considered)
- Physical flowability test
- Fiber content by dissolving the polymer or by any other indirect method such as ultrasonic (UT)
- Mechanical testing of molded samples
- Microscopy to check the fiber shape

Transformation means the exclusion of certain polymers by purification or the break-up of matrix to certain molecular weight range and fibers to certain length. Solvents like toluene and petroleum ether [Had12] are implemented to dissolve polymers. In case of NFTC, purification is limited to polymers of low melting temperature because natural fibers thermally decompose at elevated temperatures. In the same context, pyrolysis is not acceptable for NFTC unless the waste composite contains a mixture of natural and synthetic fibers and only the synthetic fibers are targeted for recovery.

A flowchart, shown in Figure 7-2, displays the protocol required to define the waste materials undergoing recycling process.

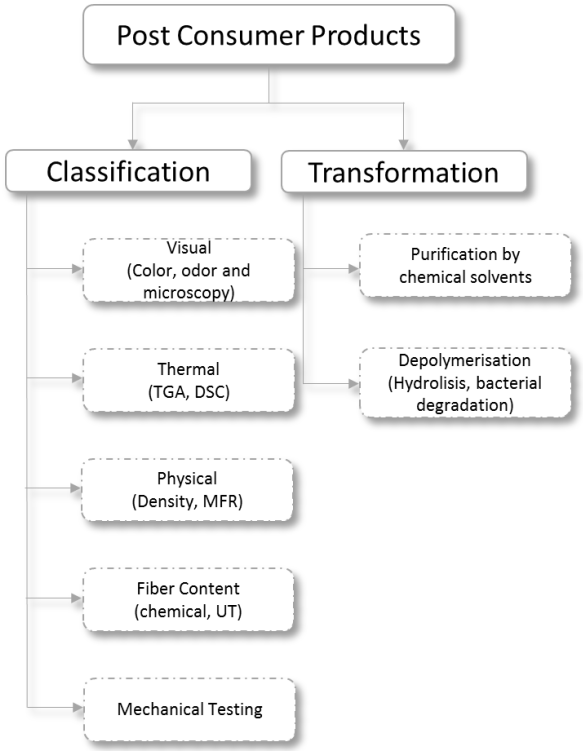

Figure 7-2: Suggested approaches for consumer products before recycling

Based on the results of the current study, it cannot be guaranteed that the waste consumer product has passed just one cycle or more than ten cycles. So, the schematic shown in Figure 7-3 suggests an adequate protocol to follow with consumer products. As in Figure 7-3, using some of the classification tests, consumer products could be allocated. However, this is not sufficient since other measures like colorants, stabilizers and anti-oxidants addition have to be considered.

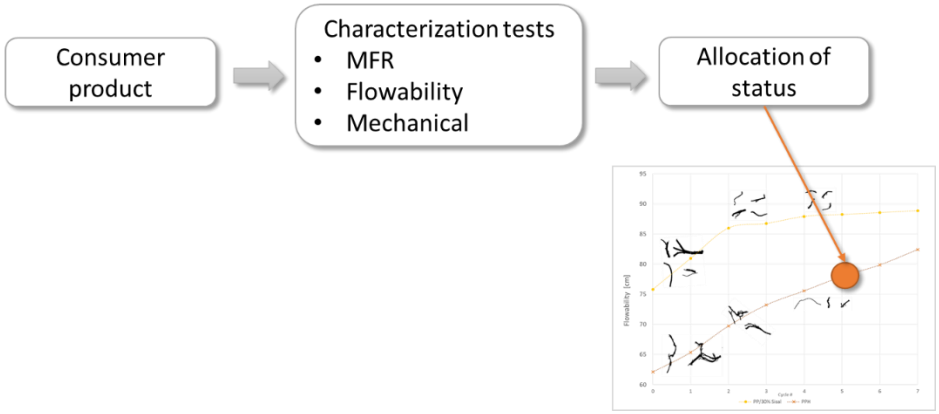

Figure 7-3: Suggested protocol to allocate the consumer products before recycling

Literature

[Agu99] Aguado J., Serrano D.P. Feedstock Recyc Hrsg.: Feedstock Recycling of Plastic Wastes, Cambridge, 1999.

[Al-10] Al-Salem, S. M.; Lettieri, P.; Baeyens, J.: The valorization of plastic solid waste (PSW) by primary to quaternary routes. From re-use to energy and chemicals. In Progress in Energy and Combustion Science, 2010, 36; S. 103–129.

[Al-10a] Al-Salem, S. M.; Lettieri, P.: Kinetics of Polyethylene Terephthalate (PET) and Polystyrene (PS) Dynamic Pyrolysis. In World Academy of Science, Engineering and Technology, International Journal of Chemical, Molecular, Nuclear, Materials and Metallurgical Engineering, 4; S. 402–410.

[Al-15] Al-Mosawi, A. I.; Abdulsada, S. A.; Rijab, M. A.: Mechanical Properties of Recycled Bamboo Fibers Reinforced CompositeComposite. Technical Solutions. In European Journal of Advances in Engineering and Technology, 2015, 2; S. 20–22.

[Amu13] Amuthakkannan, P. et al.: Effect of fibre length and fibre content on mechanical properties of short basalt fibre reinforced polymer matrix composites. In Materials physics and mechanics, 16; S. 107–117.

[Aur01] Aurrekoetxea, J.; Sarrionandia, M. A.; Urrutibeascoa, I.: Effects of recycling on the microstructure and the mechanical properties of isotactic polypropylene. In Journal of materials science, 36; S. 2607–2613.

[Aza03] Azapagic, A.; Emsley, A.; Hamerton, I.: Polymers. The environment and sustainable development. J. Wiley, West Sussex, England and Hoboken, NJ, 2003.

[Bai11] Baillie, C. et al.: Waste-based composites—Poverty reducing solutions to environmental problems. In Resources, Conservation and Recycling, 55; S. 973–978.

[Bal11] Baley, C.; Bourmaud, A.: Composites Feature: Recycling composite materials reinforced with plant fibres. In JEC Magazine, 2011, 55.

[Beh09] Behzadfar, E.; Abdolrasouli, M. H.; Sharif, F. and Nazockdast, H.: Effect of solid loading and aggregate size on the rheological behavior of PDMS/Calcium varbonate suspensions. In Brazilian journal of chemical engineering, 2009, 26.

[Bér08] Béreaux, Y.; Charmeau, J. Y.; Moguedet, M.: Modelling of fibre damage in single screw processing. In International Journal of Material Forming, 2008,1; S. 827–830.

[Ber16] Berthet, F. et al.: Behaviour and damage of injected carbon-fibre-reinforced polyether ether ketone. From process to modelling. In Journal of Composite Materials, 2016; S. 1–11.

[Bos04] Bos, H. L. Bos, H. L.: The potential of flax fibres as reinforcement for composite materials. Technische Universiteit Eindhoven, 2004.

[Bou07] Bourmaud, A.; Baley, C.: Investigations on the recycling of hemp and sisal fibre reinforced polypropylene composites. In Polymer Degradation and Stability, 2007, 92; S. 1034–1045.

[Bou08] Bourmaud, A.; Pimbert, S.: Investigations on mechanical properties of poly(propylene) and poly(lactic acid) reinforced by miscanthus fibers. In Composites Part A: Applied Science and Manufacturing, 2008, 39; S. 1444–1454.

[Bou09] Bourmaud, A.; Baley, C.: Rigidity analysis of polypropylene/vegetal fibre composites after recycling. In Polymer Degradation and Stability, 2009, 94; S. 297–305.

[Bre05] Brennen, C. E.: Fundamentals of multiphase flows, Cambridge university press, 2005.

[Bre12] Brems, A.; Baeyens, J.; Dewil, R.: Recycling and recovery of post-consumer plastic solid waste in a European context. In Thermal Science, 2012, 16; S. 669–685.

[Car14] Carus, M. et al.: WPC/NFC Market Study 2014-03.

[Cel13] Celino, A.; Freour, S.; Jacquemin, F. and Casari, P.: The hygroscopic behavior of plant fibers: a review. In Front Chem, 2013, 1.

[Che07] Chen, J.; Li, X.; Wu, C.: Crystallization Behavior of Polypropylene Filled with Modified Carbon Black. In Polymer Journal, 2007, 39; S. 722–730.

[Che09] Chemloul, N.; Chaib, K.; Mostefa, K.: Simultaneous measurements of the solid particles velocity and concentration profiles in two phase flow by pulsed ultrasonic doppler velocimetry. In J. of the Braz. Soc. of Mech. Sci. & Eng., 2009, XXXI; S. 333–343.

[Cho11] Cho, H. S. et al.: Biodegradability and biodegradation rate of poly(caprolactone)-starch blend and poly(butylene succinate) biodegradable polymer under aerobic and anaerobic environment. In Waste Management, 2011, 31; S. 475–480.

[Chr96] Chrysostomou, A.; Hashemi, S.: Influence of reprocessing on properties of short fibre-reinforced polycarbonate. In Journal of materials science, 31; S. 1183–1197.

[Cic10] Cicala, G.; Cristaldi, G. ;Recca, G.; Latteri, AComposites Based on Natural Fibre Fabrics, Woven Fabric Engineering, Polona Dobnik Dubrovski 2010 (Ed.), ISBN: 978-953-307-194-7, InTech, Available from: http://www.intechopen.com/books/woven-fabric-engineering/composites-based-on-natural-fibre-fabrics

[Cic17] Cicala G.; Tosto C., Latteri , A., La Rosa, A. D.; Blanco, :I., Elsabbagh, A.; Russo, P. Ziegmann, G.: ‘’Green Composites Based on Blends of Polypropylene with Liquid Wood Reinforced with Hemp Fibers: Thermomechanical Properties and the Effect of Recycling Cycles’’ Materials 2017, 10, 998; doi:10.3390/ma10090998

[Col15] Colucci, G. et al.: Effect of recycling on polypropylene composites reinforced with glass fibres. In Journal of Thermoplastic Composite Materials, 2015; S. 1–17.

[Cre04] Creasy, T. S.; Kang, Y. S.: Fiber Orientation during Equal Channel Angular Extrusion of Short Fiber Reinforced Thermoplastics. In Journal of Thermoplastic Composite Materials, 2004, 17; S. 205–227.

[Dam13] Dammer, L. et al.: Market Developments of and opportunities for biobased products and chemicals, 2013.

[Dav05] Davis, G. U.: Open windrow composting of polymers. An investigation into the operational issues of composting polyethylene (PE). In Waste Management, 2005, 25; S. 401–407.

[Doa07] Doan, T.; Brodowsky, H.; Maeder, E.: Jute fibre/polypropylene composites II. Thermal, hydrothermal and dynamic mechanical behaviour. In Composites Science and Technology, 2007, 67; S. 2707–2714.

[Ehr11] Ehrenstein, G.: Polymer-Werkstoffe. Struktur ; Eigenschaften ; Anwendung. Carl Hanser Fachbuchverlag, s.l., 2011.

[El-09] El-sabbagh, A.; Steuernagel, L.; Ziegmann, G.: Processing and modeling of the mechanical behavior of natural fiber thermoplastic composite. Flax/polypropylene. In Polymer Composites, 2009, 30; S. 510–519.

[El-13] El-sabbagh, A.; Steuernagel, L.; Ziegmann, G.: Low combustible polypropylene/flax/magnesium hydroxide composites. Mechanical, flame retardation characterization and recycling effect. In Journal of Reinforced Plastics and Composites, 2013, 32; S. 1030–1043.

[El-14a] El-Sabbagh, A. M. M. et al.: Effect of extruder elements on fiber dimensions and mechanical properties of bast natural fiber polypropylene composites. In Journal of Applied Polymer Science, 2014, 131; n/a-n/a.

[El-14b] El-sabbagh, A.: Effect of coupling agent on natural fibre in natural fibre/polypropylene composites on mechanical and thermal behaviour. In Composites Part B: Engineering, 2014, 57; S. 126–135.

[Els15a] Elsabbagh, A. et al.: owards the Flow Pattern Simulation of Cellulosic Fiber Thermoplastic Composites during Injection Molding: Material Characterization. In (Mondal, M. I. H. Hrsg.): Cellulose and cellulose composites. Modification, characterization and applications. Nova Science Publishers Inc, New York, 2015.

[Els15b] Elsabbagh, A. et al.: Towards the Flow Pattern Simulation of Cellulosic Fiber Thermoplastic Composites during Injection Molding: Material Characterization (pp. 173-210). Mondal (Ed.) 2015 – Cellulose and cellulose composites, Nova publisher, 2015.

[Els17] Elsabbagh, A.: Processing and optimising the mechanical and physical properties of natural fibre reinforced polypropylene composites. Dissertation, 2017.

[Era09] Erasmus, E.; Anandjiwala, R.: Studies on Enhancement of Mechanical Properties and Interfacial Adhesion of Flax Reinforced Polypropylene Composites. In Journal of Thermoplastic Composite Materials, 2009, 22; S. 485–502.

[FAO11] FAO - Global Materials Team Hrsg.: New technology for sustainability. FSAO. Ford, 2011.

[FNR14] FNR: Werkstoff- und Fließmodelle für naturfaserverstärkte Spritzgieß-materialien für den praktischen Einsatz in der Automobilindustrie. Abschlussbericht: Simulation NFK, 2014.

[Fon15] Fonseca-Valeroa, C. et al.: Mechanical recycling and composition effects on the properties and structure of hardwood cellulose-reinforced high density polyethylene eco-composites. In Composites Part A: Applied Science and Manufacturing, 2015, 69; S. 94–104.

[Fu96] Fu, S.-Y.; Lauke, B.: Effects of fiber length and fibre orientation distributions on the tensile strength of short-fiberreinforced-polymers. In Composites Science and Technology, 1996, 56; S. 1179–1190.

[Gal95] Galesky, A.: Nucleation of polypropylene. In (Karger-Kocsis, J. Hrsg.): Polypropylene. Structure, blends and composites. Chapman & Hall, London [u.a.], 1995; S. 4.

[Geb14] Gebrehiwot, S. Z.: Manufacturing and rheological analysis of spiral flow test piece. Dissertation, Finland, 2014.

[Had12] Hadi, A. J.; Najmuldeen, G. F.; Ahmed, I.: Polyolefins Waste Materials Reconditioning Using Dissolution/Reprecipitation Method. In APCBEE Procedia, 2012, 3; S. 281–286.

[Hop09] Hopewell, J.; Dvorak, R.; Kosior, E.: Plastics recycling. Challenges and opportunities. In Philosophical Transactions of the Royal Society B: Biological Sciences, 2009, 364; S. 2115–2126.

[Hut84] Hutchinson, J. M.; Kovacs, A. J.: Effects of thermal history on structural recovery of glasses during isobaric heating. In Polymer Engineering and Science, 1984, 24; S. 1087–1103.

[Ign14] Ignatyev, I. A.; Thielemans, W.; Vander Beke, B.: Recycling of Polymers. A Review. In ChemSusChem, 2014, 7; S. 1579–1593.

[Inc99] Incarnato, L.; Scarfato, P.; Acierno, D.: Rheological and mechanical properties of recycled polypropylene. In Polymer enginnering and science, 1999, 39; S. 749–755.

[Kar03] Kartalis, C. N.; Papaspyrides, C. D.; Pfaendner, R.: Closed-loop recycling of postused PP-filled garden chairs using the restabilization technique. III. Influence of artificial weathering. In Journal of Applied Polymer Science, 2003, 89; S. 1311–1318.

[Kee04] Keener, T.; Stuart, R.; Brown, T.: Maleated coupling agents for natural fibre composites. In Composites Part A: Applied Science and Manufacturing, 2004, 35; S. 357–362.

[Kha09] Khan, A.; Mahmood, N.; Bazmi, A.: Direct comparison between rotational and extrusion rheometers. In Materials Research, 2009, 12; S. 477–481.

[Kir11] Kirchberg, S. ; Ziegmann, G.: Effect of Spherical Iron Silicon (FeSi) Microparticles on the Viscosity Behaviour of Polypropylene Melt. Journal of Applied Rheology, 2011, 21 (3), 35495-7.

[Kub74] Kubat, J. and Szalanczi, A.: Polymer-glass separation in the spiral mold test. In Polymer Engineering and Science, 1974, 14; S. 873–877.

[Kur15] Kuram, E.; Ozcelik, B.; Yilmaz, F.: The influence of recycling number on the mechanical, chemical, thermal and rheological properties of poly(butylene terephthalate)/polycarbonate binary blend and glass-fibre-reinforced composite. In Journal of Thermoplastic Composite Materials, 2015.

[Le 08] Le Duigou, A. et al.: Effect of recycling on mechanical behaviour of biocompostable flax/poly(l-lactide) composites. In Composites Part A: Applied Science and Manufacturing, 2008, 39; S. 1471–1478.

[Le 09] Le Baillif, M.; Oksman, K.: The Effect of Processing on Fiber Dispersion, Fiber Length, and Thermal Degradation of Bleached Sulfite Cellulose Fiber Polypropylene Composites. In Journal of Thermoplastic Composite Materials, 2009, 22; S. 115–133.

[Li07] Li, X.; Tabil, L. G.; Panigrahi, S.: Chemical Treatments of Natural Fiber for Use in Natural Fiber-Reinforced Composites. A Review. In Journal of Polymers and the Environment, 2007, 15; S. 25–33.

[Liu10] Liu, L. et al.: Selective distribution, reinforcement, and toughening roles of MWCNTs in immiscible polypropylene/ethylene-co-vinyl acetate blends. In Journal of Polymer Science Part B: Polymer Physics, 2010, 48; S. 1882–1892.

[Mah13] Mahendrasinh M. Raj, Hemul V. Patel, Lata M. Raj and Naynika K. Patel: Studies on mechanical properties of recycled polypropylene blended with the virgin polypropylene. In International journal of science inventions today, 2013, 2; S. 194–203.

[Mar02] Martins, M. H.; Paoli, M. de: Polypropylene compounding with post-consumer material: II. Reprocessing, 2002, 78.

[Mar16] Markets and Markets: Natural Fiber Composites Market worth 6.50 Billion USD by 2021. http://www.marketsandmarkets.com/PressReleases/natural-fiber-composites.asp, 03.05.2016.

[Men92] Menges, G.; Michaeli, W.; Bittner, M. Hrsg.: Recycling von Kunststoffen. Carl Hanser Verlag, München Wien, 1992.

[Mof12] Mofokeng, J. P. et al.: Comparison of injection moulded, natural fibre-reinforced composites with PP and PLA as matrices. In Journal of Thermoplastic Composite Materials, 2012, 25; S. 927–948.

[Mor12] Morin, C. et al.: Near- and supercritical solvolysis of carbon fibre reinforced polymers (CFRPs) for recycling carbon fibers as a valuable resource. State of the art. In The Journal of Supercritical Fluids, 2012, 66; S. 232–240.

[Mor15] Morreale, M. et al.: Mechanical, Thermomechanical and Reprocessing Behavior of Green Composites from Biodegradable Polymer and Wood Flour. In Materials, 2015, 8; S. 7536–7548.

[Mül13] Mülhaupt, R.: Green Polymer Chemistry and Bio-based Plastics. Dreams and Reality. In Macromolecular Chemistry and Physics, 2013, 214; S. 159–174.

[Mwa02] Mwaikambo, L.Y., Ansell, M.P,; Chemical modification of hemp, sisal, jute, and kapok fibers by alkalization, Journal of Applied Polymer Science, 2002, 84, 12, 2222-2234

[Nor03] Norman, D. A.; Robertson, R. E.: The effect of fiber orientation on the toughening of short fiber-reinforced polymers. In Journal of Applied Polymer Science, 2003, 90; S. 2740–2751.

[Oli15] Oliveux, G.; Dandy, L. O.; Leeke, G. A.: Degradation of a model epoxy resin by solvolysis routes. In Polymer Degradation and Stability, 2015, 118; S. 96–103.

[Oth09] Otheguy, M. E. et al.: Recycling of end-of-life thermoplastic composite boats. In Plastics, Rubber and Composites, 2009, 9/10; S. 406–411.

[Pan06] Panthapulakkal, S.; Sain, M.; Injection-molded short hemp fiber/glass fiber-reinforced polypropylene hybrid composites—Mechanical, water absorption and thermal properties, Journal of Applied Polymer Science, 2006, 103, 4, 2432-2441

[Pan10] Panda, A. K.; Singh, R. K.; Mishra, D. K.: Thermolysis of waste plastics to liquid fuelA suitable method for plastic waste management and manufacture of value added products—A world prospective. In Renewable and Sustainable Energy Reviews, 2010, 14; S. 233–248.

[Pau10] Paul, S. A. et al.: Dynamic mechanical analysis of novel composites from commingled polypropylene fiber and banana fiber. In Polymer Engineering & Science, 2010, 50; S. 384–395.

[Pee98] Peebles, L. H. et al.: Mechanical properties of carbon fibers. In (Donnet, J. et al. Hrsg.): Carbon fibers, 1998; S. 312–369.

[Pic06] Pickering, S. J.: Recycling technologies for thermoset composite materials—current status. In Composites Part A: Applied Science and Manufacturing, 2006, 37; P. 1206–1215.

[Pic16] Pickering, K.L.; Aruan Efendy, M.G.; Le, T.M.: A review of recent developments in natural fibre composites and their mechanical performance. In Composites: Part A, 2016, 83; P. 98–112.

[Pla10] Plastics Europe: Association of plastics manufacturers: Plastics- The facts 2010, 2010.

[Pla12] Plastics Europe: Association of plastics manufacturers: Plastics – the Facts 2012. An analysis of European plastics production,demand and waste data for 2011, 2012.

[Pla15a] Plastics Europe: Association of plastics manufacturers: Plastics – the Facts 2014/2015: An analysis of European plastics production, demand and waste data. http://www.plasticseurope.org/documents/document/20150227150049-final_plastics_the_facts_2014_2015_260215.pdf, 08/10/2015.

[Pla15b] Plastics Europe: Association of plastics manufacturers; Consultic: Global production of plastics 2014 | Statistics. http://www.statista.com/statistics/282732/global-production-of-plastics-since-1950/, 11.03.2016.

[Ram14a] Ramzy, A. Y. et al.: Rheology of natural fibers thermoplastic compounds. Flow length and fiber distribution. In Journal of Applied Polymer Science, 2014, 131, 3, DOI: 10.1002/APP.39861

[Ram14b] Ramzy, A. et al.: Developing a new generation of sisal composite fibres for use in industrial applications. In Composites Part B: Engineering, 2014, 66; S. 287–298.

[Res14] Restrepo-Flórez, J.-M.; Bassi, A.; Thompson, M. R.: Microbial degradation and deterioration of polyethylene – A review. In International Biodeterioration & Biodegradation, 2014, 88; P. 83–90.

[Rus06] Rust, N., Ferg, E.E., Masalova, I.: A degradation study of isotactic virgin and recycled polypropylene used in lead acid battery casings, Polymer Testing, Volume 25(1), 2006, P. 130-139.

[Sch01] Scheirs, J.: Polymer recycling. Science, technology and applications. Wiley, Chichester [etc.], 2001.

[Sch06] Schnürer, A.; Schnürer, J.: Fungal survival during anaerobic digestion of organic household waste. In Waste Management, 2006, 26; S. 1205–1211.

[Sco02] Scott, G.: Why Degradable Polymers? In (Scott, G. Hrsg.): Degradable Polymers. Principles and Applications. Springer Netherlands, Dordrecht, 2002; S. 1–15.

[SPE16] Campbell, G., Wetzel, M.: Correlation between filler concentration and viscosity power-law for polymer slurries. SPE- Plastics Research Online; 10.2417/spepro.006560.

[Ste16] Stehle, M.: Charakterisierung des Abbauverhalten von Polypropylen und von sisalfaserverstärkten Polypropylenen nach dem Recycling. B.Sc., Clausthal, 2016.

[Syk09] Sykacek, E.; Hrabalova. M.; Mundigler, N.: Extrusion of five biopolymers reinforced with increasing wood flour concentration on a production machine, injection moulding and mechanical performance. In Composites Part A: Applied Science and Manufacturing, 2009, 40; S. 1272–1282.

[TA 13] TA Instruments: Understanding rheology of thermoplastic polymers, 2013.

[TA 17] TA Instruments: dynamic mechanical analysis polypropylene - Google Search. https://www.google.de/search?q=glass+transition+table+HDPE&ie=utf-8&oe=utf-8&client=firefox-b&gfe_rd=cr&ei=TULyWODbJ8Hi8AfIp5vwDA#q=dynamic+mechanical+analysis+polypropylene, 4/16/2017.

[The08] The european parliament and the council of the european union: on waste and repealing certain Directives, 2008.

[The13] The european parliament and the council of the european union: on a mechanism for monitoring and reporting greenhouse gas emissions and for reporting other information at national and Union levelrelevant to climate change and repealing Decision No 280/2004/EC. Regulation (EU) No 525/2013 of the european parliament and of the council of 21 May 2013, 2013.

[Tok09] Tokiwa, Y. et al.: Biodegradability of Plastics. In International Journal of Molecular Sciences, 2009, 10; S. 3722–3742.

[Vel12] Velez Garca, G. M. et al.: Improvement in orientation measurement for short and long fiber injection molded composites. SPE ACCE Conference, 2012.

[Wor14] Worrell, E.; Reuter, M.A. Hrsg.: Handbook of recycling. State-of-the-art for practitioners, analysts, and scientists. Elsevier, Waltham, Mass., 2014.

[Yao08] Yao, F. et al.: Thermal decomposition kinetics of natural fibers. Activation energy with dynamic thermogravimetric analysis. In Polymer Degradation and Stability, 2008, 93; S. 90–98.

[Yip01] Yip, H.; Pickering, S. J.; Rudd, C. D.: Degradation of fibre length during the recycling of carbon fibre composites using a fluidised bed process. In (ICCM Hrsg.), 2001.

Appendix

Table A-1. DSC results for PP at different cycle numbers

PP	1st heat cycle	Cool cycle	2nd heat cycle	1st heat cycle	Cool cycle	2nd heat cycle
Cycle	Melting temperature	Crystallization temperature	Melting temperature	Melting enthalpy	Crystallization enthalpy	Melting enthalpy
#	[°C]	[°C]	[°C]	[J/g]	[J/g]	[J/g]
0	166.48	123.30	161.8	61.26	71.60	62.40
1	167.87	124.33	162.65	59.28	67.52	64.82
2	166.90	125.90	163.30	58.63	69.70	66.02
3	167.01	125.71	163.60	54.01	68.50	64.01
4	167.22	125.46	164.20	49.18	67.32	62.16
5	168.03	125.69	164.80	50.93	70.43	62.30
6	166.67	126.20	164.06	64.30	80.25	72.61
7	166.70	126.61	164.02	68.01	80.70	75.02
8	166.80	127.04	163.80	72.64	81.40	79.20

Table A-3. DSC results for PP-S at different cycle numbers

PP-S	1st heat cycle	Cool cycle	2nd heat cycle	1st heat cycle	Cool cycle	2nd heat cycle
Cycle	Melting temperature	Crystallization temperature	Melting temperature	Melting enthalpy	Crystallization enthalpy	Melting enthalpy
#	[°C]	[°C]	[°C]	[J/g]	[J/g]	[J/g]
0	168.59	121.36	162.26	41.15	51.01	48.14
1	166.69	121.18	163.24	44.07	48.37	46.81
2	161.90	123.25	161.90	46.28	48.96	45.47
3	162.65	123.47	162.65	41.03	50.05	45.94
4	162.75	123.74	162.90	39.29	46.68	49.01
5	163.24	123.12	163.20	40.82	49.71	51.93
6	163.07	123.38	163.07	47.8	50.67	45.74
7	161.07	122.17	161.07	69.52	68.62	69.28
8	161.24	122.49	161.24	84.17	77.74	74.21

Table A-4. DSC results for PP-H at different cycle numbers

PP-H	**1st heat cycle**	**Cool cycle**	**2nd heat cycle**	**1st heat cycle**	**Cool cycle**	**2nd heat cycle**
Cycle	**Melting temperature**	**Crystallization temperature**	**Melting temperature**	**Melting enthalpy**	**Crystallization enthalpy**	**Melting enthalpy**
#	[°C]	[°C]	[°C]	[J/g]	[J/g]	[J/g]
0	165.45	120.50	163.27	42.25	57.61	52.08
1	167.18	119.90	164.90	55.74	58.73	53.88
2	164.54	122.63	164.50	56.68	52.93	50.21
3	164.02	123.90	163.95	57.02	54.03	52.71
4	165.34	123.79	165.30	41.22	54.79	52.44
5	164.93	123.84	164.93	44.89	58.28	50.03
6	163.98	124.27	163.98	54.79	54.04	50.67
7	162.05	121.67	162.05	75.67	78.38	73.18
8	161.36	121.55	161.50	64.01	77.04	77.02

Table A-5. DSC results for PP/30% Sisal at different cycle numbers

PP/30% Sisal	**1st heat cycle**	**Cool cycle**	**2nd heat cycle**	**1st heat cycle**	**Cool cycle**	**2nd heat cycle**
Cycle	**Melting temperature**	**Crystallization temperature**	**Melting temperature**	**Melting enthalpy**	**Crystallization enthalpy**	**Melting enthalpy**
#	[°C]	[°C]	[°C]	[J/g]	[J/g]	[J/g]
0	165.45	119.97	161.18	63.07	66.23	63.07
1	165.95	112.31	158.76	69.70	66.25	58.10
2	166.27	113.14	157.64	59.38	65.67	57.25
3	165.81	113.97	157.99	60.19	66.5	62.82
4	165.57	114.76	157.82	67.17	68.88	61.82
5	164.45	116.85	158.09	72.20	70.83	68.01
6	165.46	114.51	158.19	68.2	66.34	67.18
7	165.26	117.16	159.15	64.73	70.32	69.55
8	164.00	115.70	158.01	67.19	70.99	65.07

Table A-6: Results of the mechanical testing on PP and PP/30% Sisal

Cycle number	E-modulus [MPa]		Tensile strength [MPa]		Elongation at break [%]		Impact strength [kJ/m²]	
	PP	**PP/Sisal**	**PP**	**PP/Sisal**	**PP**	**PP/Sisal**	**PP**	**PP/Sisal**
0	1334	3033	29.0	40.0	7.9	3.5	33	10.7
1	1227	3043	26.7	39.6	7.0	3.4	29.2562	11.8
2	1152	3076	26.7	38.9	7.4	3.6	30.4959	12.5
3	1174	3062	26.3	38.5	7.3	4.0	30.0826	12.9
4	1220	2962	26.6	37.0	6.7	3.8	30.5785	12.0
5	1214	2954	26.9	36.7	6.7	3.9	29.9174	11.5
6	1208	2919	26.4	36.7	6.8	4.0	29.9174	11.9
7	1208	2952	26.7	35.2	6.8	3.8	30.4132	10.6
8	1203	2914	26.6	35.9	6.9	3.9	29.8347	11.2

Table A-7: Relative properties of PP/Sisal w.r.t. PP

Cycle number	Relative E-modulus $\frac{\sigma_{PP/Sisal}}{\sigma_{PP}}$	Relative tensile strength $\frac{\sigma_{PP/Sisal}}{\sigma_{PP}}$	Relative elongation at break $\frac{Elongation_{PP/Sisal}}{Elongation_{PP}}$	Relative impact strength $\frac{Impact\ strength_{PP/Sisal}}{Impact\ strength_{PP}}$
0	2.27	1.38	0.44	0.32
1	2.48	1.48	0.49	0.40
2	2.67	1.46	0.48	0.41
3	2.61	1.46	0.54	0.43
4	2.43	1.39	0.57	0.39
5	2.43	1.36	0.58	0.38
6	2.42	1.39	0.58	0.40
7	2.44	1.32	0.55	0.35
8	2.42	1.35	0.56	0.38

Table A-8: Normalized relative properties of Table 5-5 w.r.t. the values of cycle 0

Cycle number	**Normalized relative E-modulus [%]**	**Normalized relative tensile strength [%]**	**Normalized relative elongation [%]**	**Normalized relative impact strength [%]**
0	0.00	0.00	0.00	0.00
1	9.03	7.63	11.43	25.04
2	17.44	5.67	8.47	26.88
3	14.67	5.94	22.42	32.73
4	6.82	1.07	28.55	21.30
5	7.02	-1.18	30.60	18.85
6	6.23	0.67	31.24	23.13
7	7.44	-4.33	25.18	7.66
8	6.56	-1.99	25.80	16.61

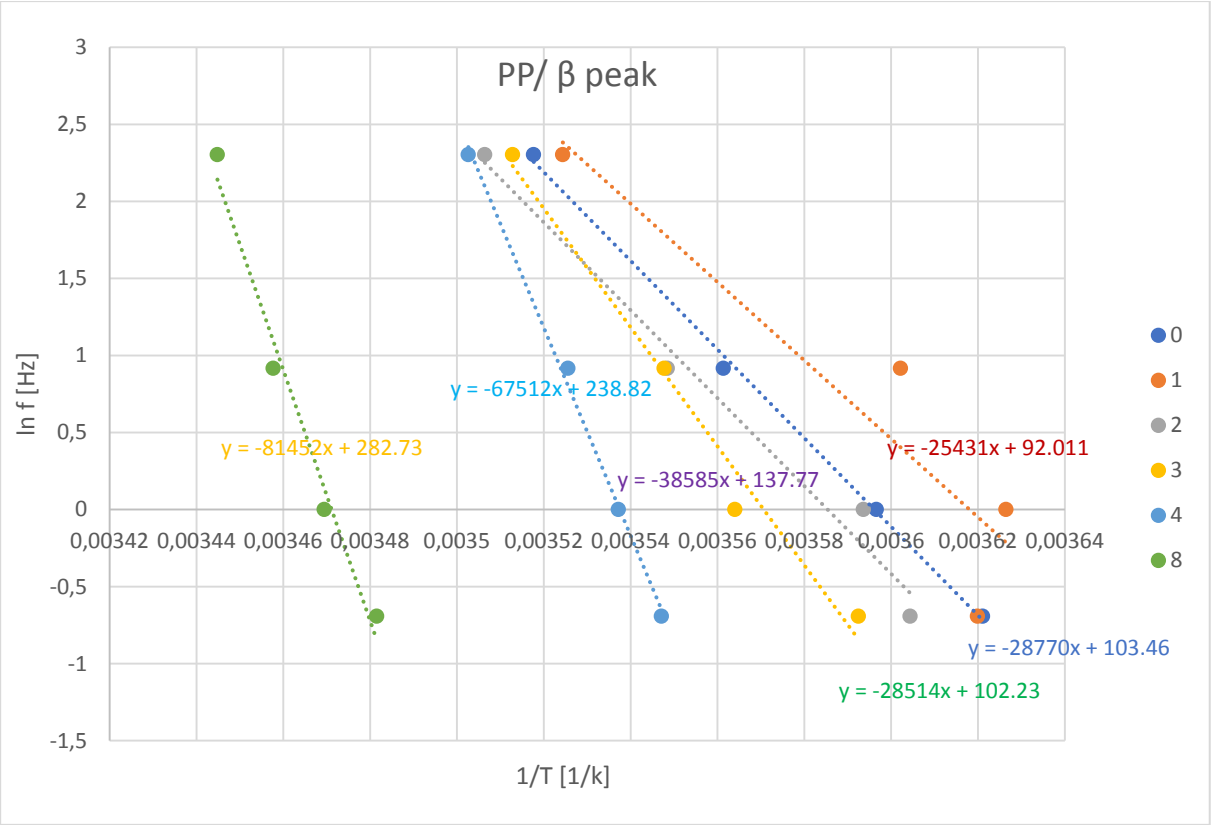

Figure A-1: Arrhenius formula presentation for PP/ β transition at different cycle number taken from frequencies 0.5, 1.0, 2.5 and 10 Hz.

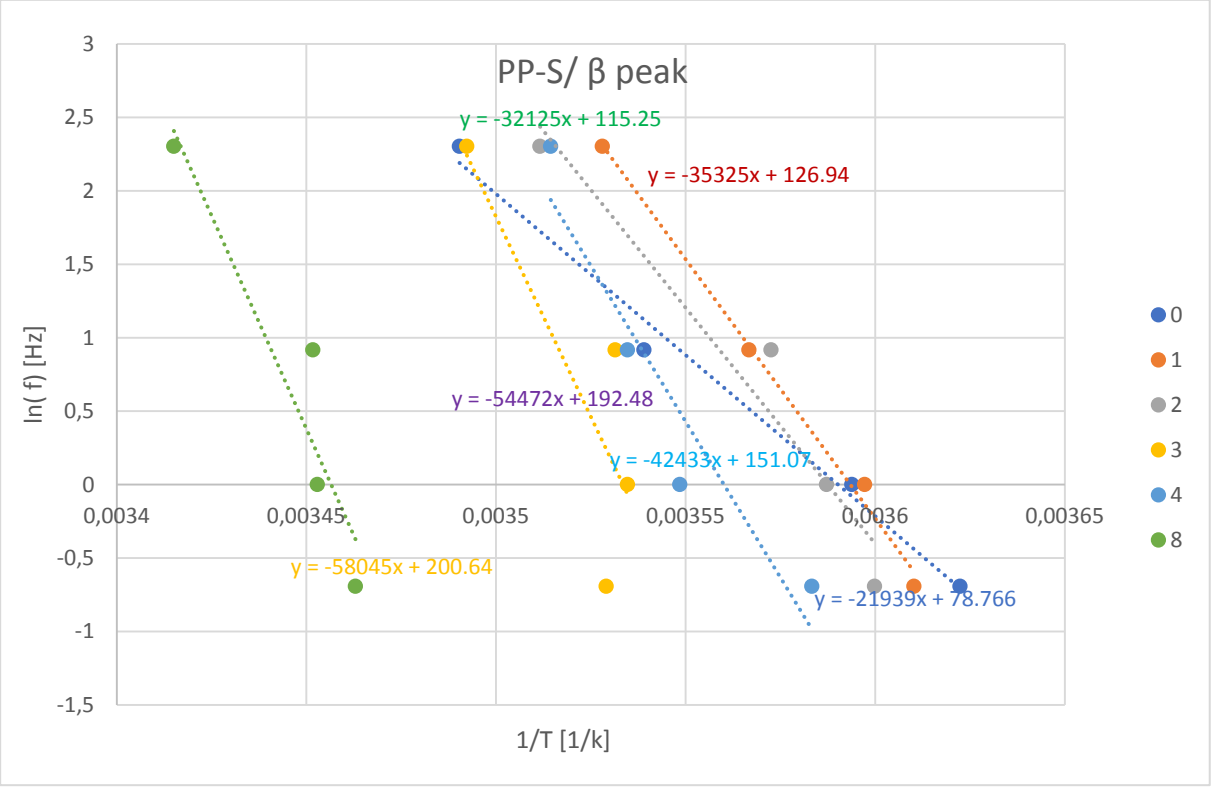

Figure A-2: Arrhenius formula presentation for PP-S/ β transition at different cycle number taken from frequencies 0.5, 1.0, 2.5 and 10 Hz.

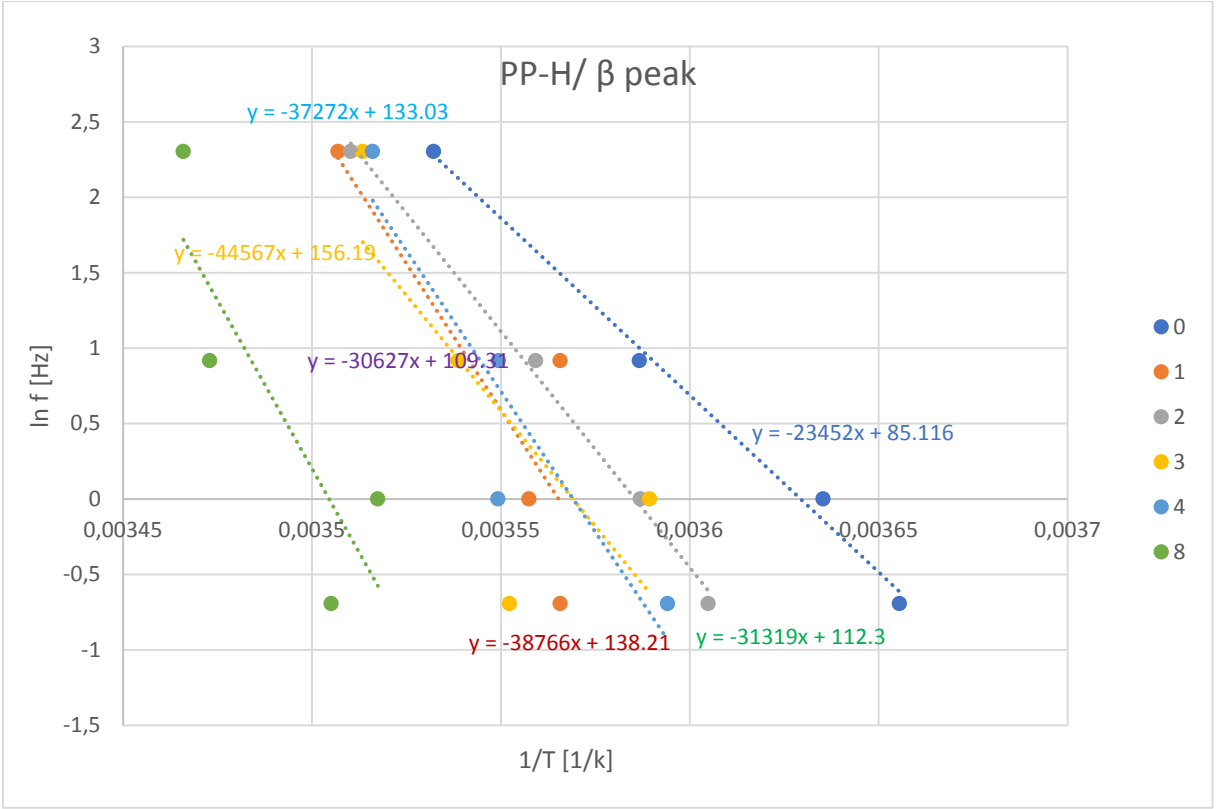

Figure A-3: Arrhenius formula presentation for PP-H/ β transition at different cycle number taken from frequencies 0.5, 1.0, 2.5 and 10 Hz.

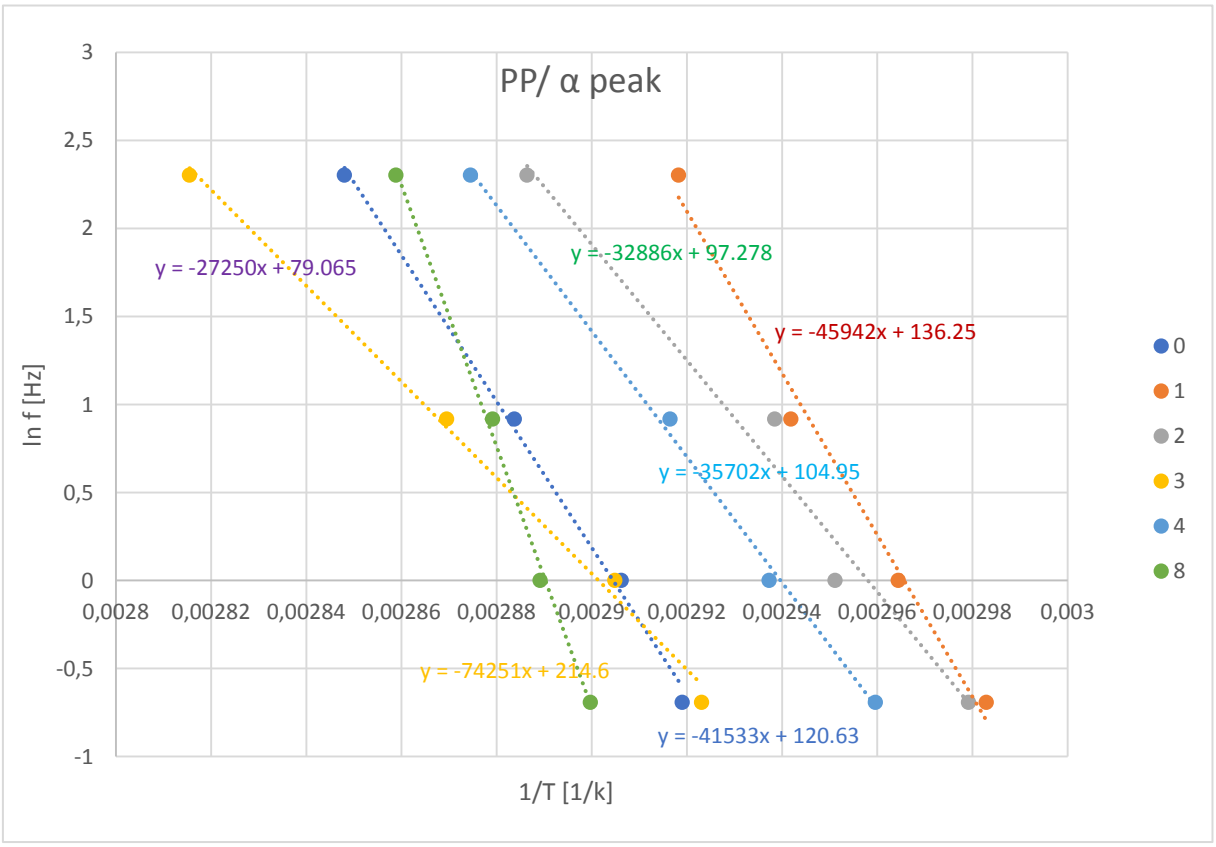

Figure A-4: Arrhenius formula presentation for PP/ α transition at different cycle number taken from frequencies 0.5, 1.0, 2.5 and 10 Hz.

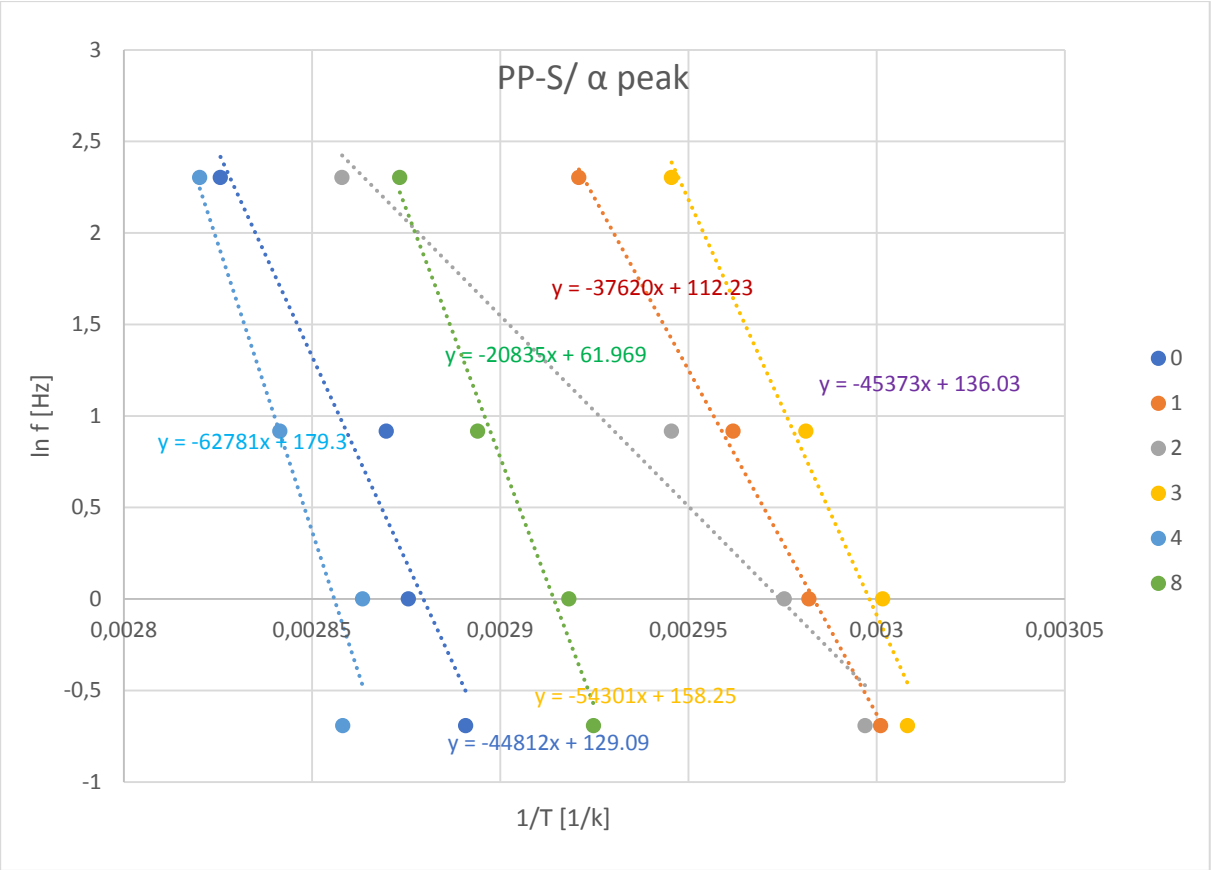

Figure A-5: Arrhenius formula presentation for PP-S/ α transition at different cycle number taken from frequencies 0.5, 1.0, 2.5 and 10 Hz.

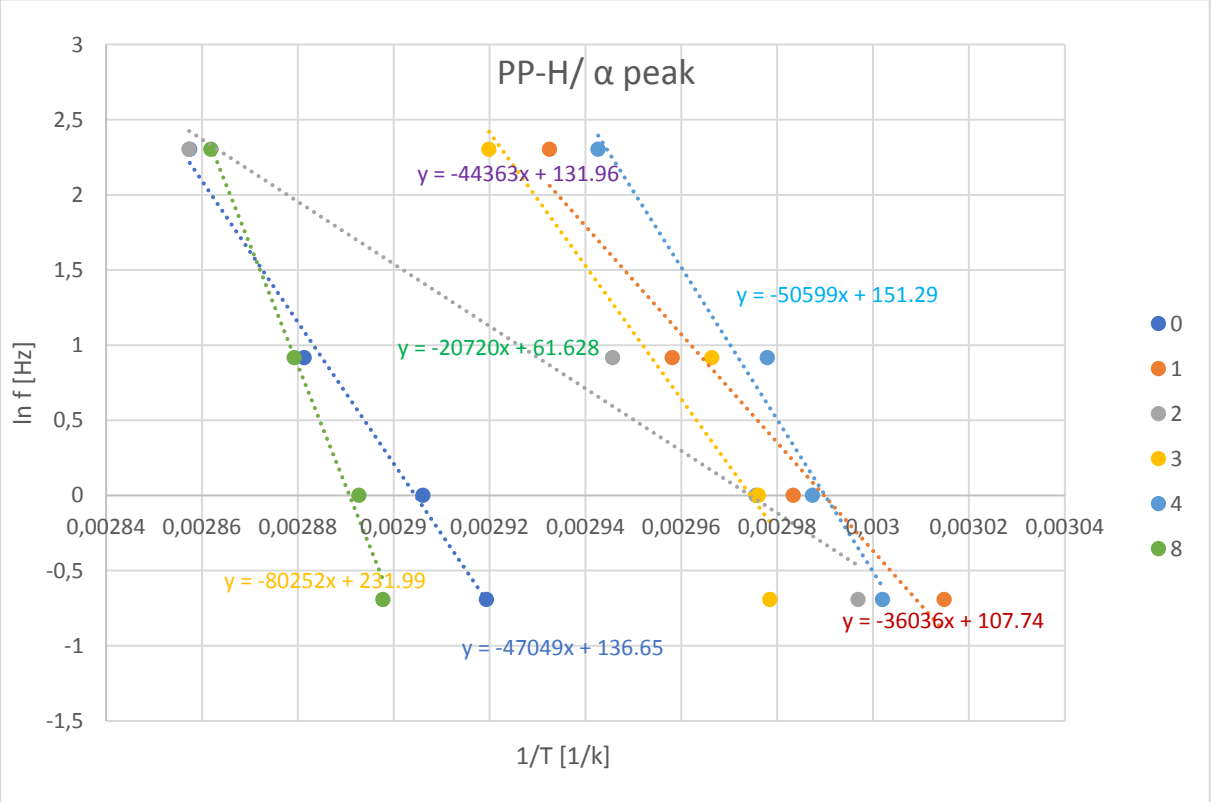

Figure A-6: Arrhenius formula presentation for PP-H/ α transition at different cycle number taken from frequencies 0.5, 1.0, 2.5 and 10 Hz.

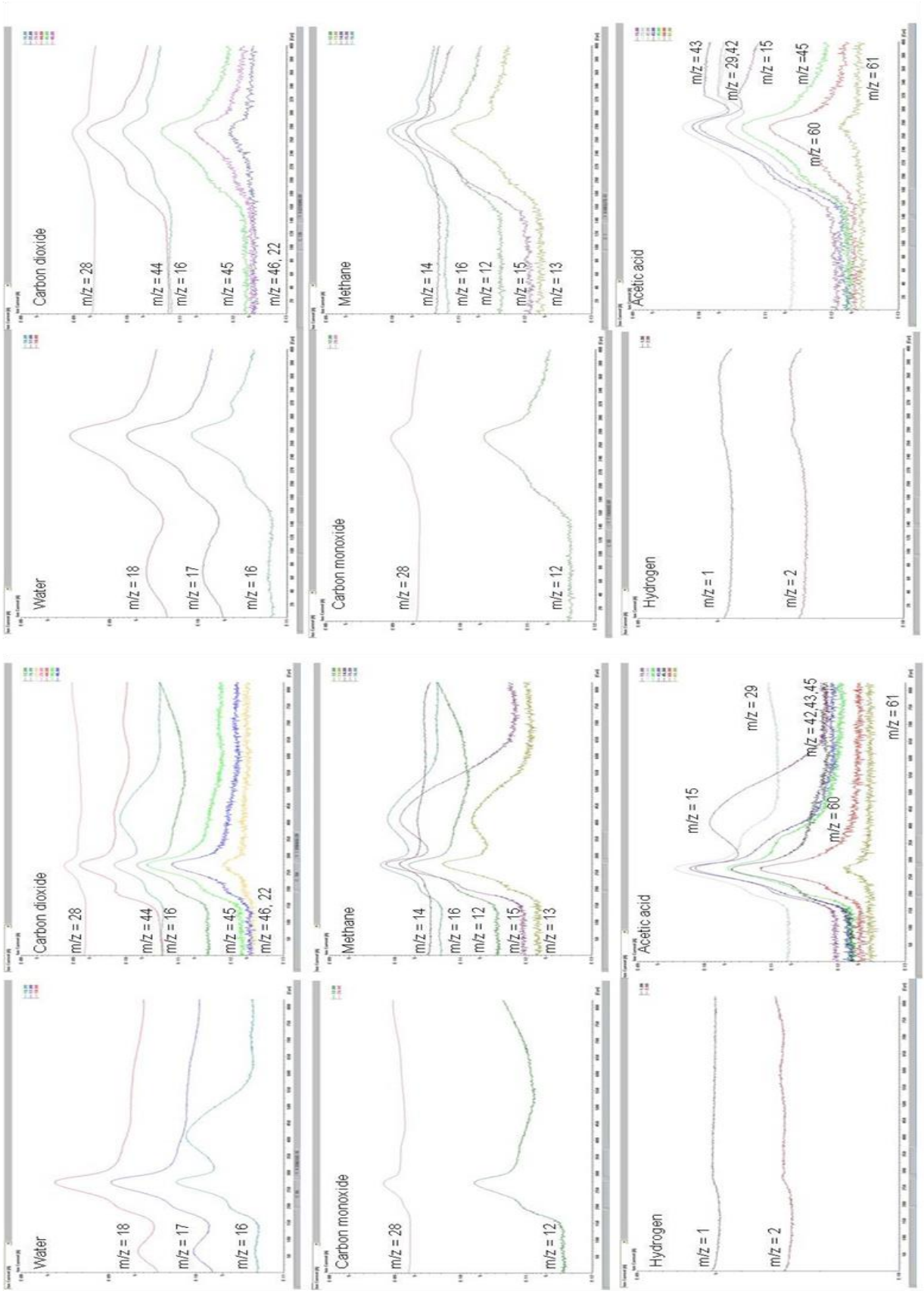

Figure **A**-7: Completed mass spectra of original Hemp fibers (left) and PP-H (right) also in appendix

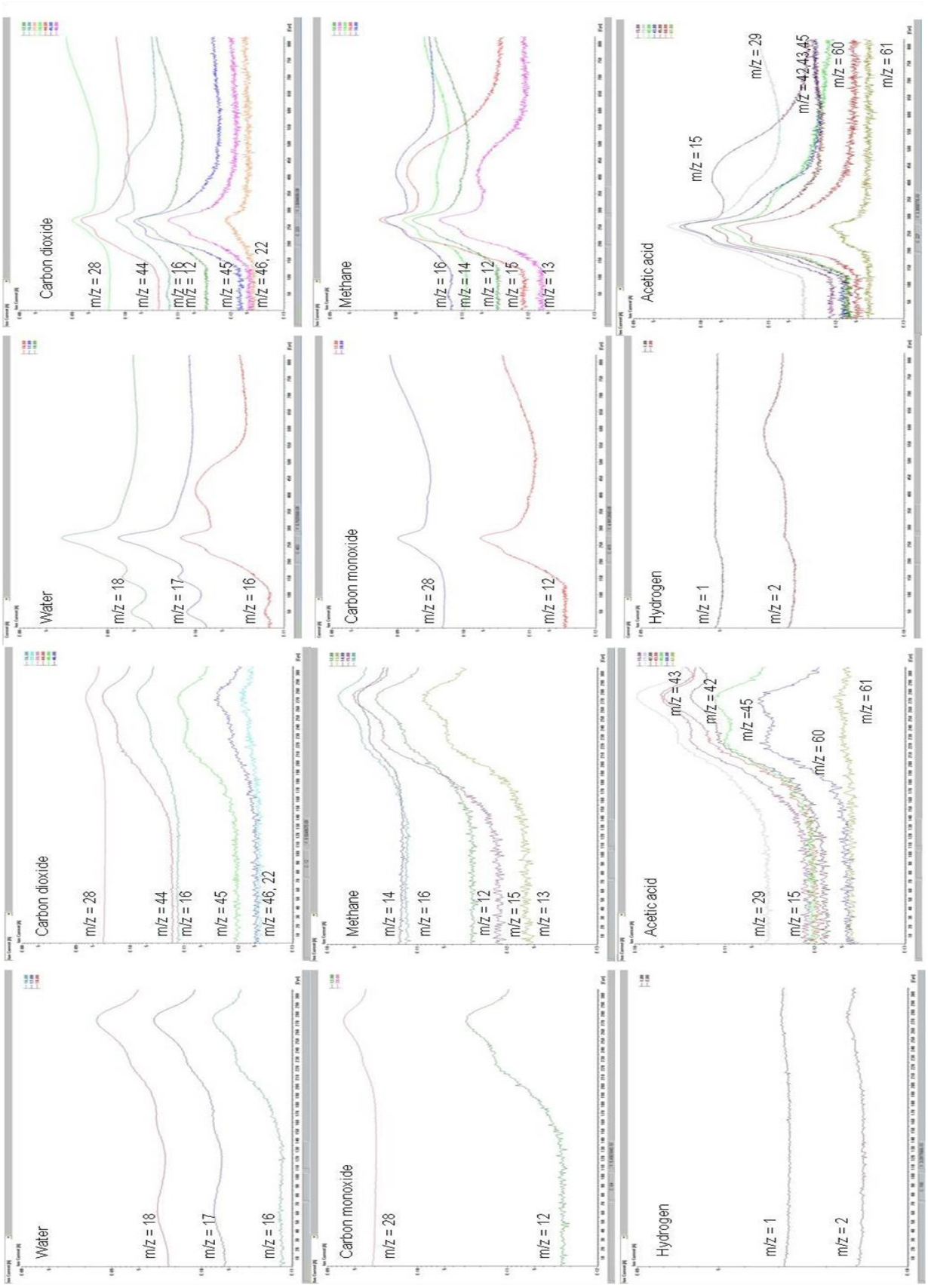

Figure A-8: Completed mass spectra of original Sisal fibers (left) and PP-S (right)

Publications

Co-authored Book Chapter

“Towards the Flow Pattern Simulation of Cellulosic Fiber Thermoplastic Composites during Injection Molding: Material Characterization”, A. El-Sabbagh, A. Ramzy, L. Steuernagel, D. Meiners and G. Ziegmann, Chapter 7 in : “Cellulose and Cellulose Derivatives: Synthesis, Modification, Nanostructure and Applications” edited by Ibrahim Y. Mondal, Nova Science Publishers, Inc., New York, USA, 2015 ISBN: 978-1-63483-553-4

Peer Reviewed Articles

“Developing a New Generation of Sisal Composite Fibres for Use in Industrial Applications” A. Ramzy, D. Beermann, L. Steuernagel, D. Meiners, G. Ziegmann; Composites Part B: Engineering 66, 287-298

“Rheology of Natural Fibers Thermoplastic Compounds: Flow Length and Fiber Distribution” A. Ramzy, A. El-Sabbagh, L. Steuernagel, G. Ziegmann, D. Meiners; Journal of Applied Polymer Science 131 (3)

“Flowability and Fiber Content Homogeneity of Natural Fiber Polypropylene Composites in Injection Molding” A. El-Sabbagh, A. Ramzy, L. Steuernagel, D. Meiners; AIP Conference Proceedings 1779 (1), 060010

„Notes on Mechanical Elements in Processing Natural fibre Thermoplastic Composites: Extrusion” A. El-Sabbagh, A. Ramzy, L. Steuernagel; First International Conference on Resource Efficiency in Interorganizational Networks-ResEff 2013

“Investigation in Impregnation and Draping Methods for Natural Fibre Composites” A Ramzy ; Master Thesis – Clausthal University of Technology, 2010

“Verstärkte Folien mit recycelten, lasergeschnittenen und unidirektional gerichteten Kohlenstofffasern zur Herstellung von Großserienprodukten aus kohlenstofffaserverstärkten Kunststoffen (CFK) (Organofolien II: IGF-Vorhaben 17063 N) “ A. Ramzy, G. Ziegmann, D. Meiners et al. ; Achievements Report for the Period 2013 -2015: Clausthal Center of Materials Technology, TU Clausthal, Shaker Verlag, ISBN: 978-3-8440-4809-4

„Mit höchster Präzision. Ein neues Recyclingverfahren für trockene Kohlenstofffaserabfälle ermöglicht die Herstellung von umformungsfähigen Organofolien“ A.Ramzy et al. ; In ReSource, 1/2014, 27. Jg., S. 32-35, Rhombos-Verlag, Berlin

„Recycling of Natural Fibre Thermoplastic Compounds“, A. Ramzy, A. Elsabbagh, L. Steuernagel, D. Meiners, G. Ziegmann ; 1.Niedersächsisches Symposium

Materialtechnik (NSM) - 13. Februar 2015 - Proceedings, Shaker Verlag GmbH, ISBN: 978-3-8440-3403-5

Conferences

„Recyclingmöglichkeiten von faserverstärkten Kunststoffen“ A. Ramzy, G. Ziegmann, D. Meiners ; Kunststofftrends im Automobil, 4 – 5 September 2013, Wolfsburg – Germany.

„Developing a New Generation of Sisal Composite Fibres for Use in Industrial Applications“ A. Ramzy, D. Beermann, L. Steuernagel, G. Ziegmann, D. Meiners ; 4th International Conference on Innovative Natural Fibre Composites for Industrial Applications, 17 – 18 October, 2013, Rome – Italy

„Recycling of Natural Fibre Thermoplastic Compounds“, A. Ramzy, A. Elsabbagh, L. Steuernagel, D. Meiners, G. Ziegmann ; 1.Niedersächsisches Symposium Materialtechnik (NSM) - 13 February 2015, Clausthal – Germany

Curriculum Vitae

Personal Data

Name: Amna Ramzy

Date/ place of Birth: 05.01.1979 in Cairo-Egypt

E-mail: amna.ramzy@gmail.com

Career

03.2011 – 07.2017

Scientific co-worker at Institute of Polymer Materials and Plastics Engineering – Clausthal University of Technology, Germany

03.2006-02.2007

Customer service in XEROX Egypt

06.2004-02.2006

Service Engineer in XEROX Egypt

05.2002 – 12.2003

Training Coordinator and Technical Projects Assistant - First Egyptian for Consulting Services

Education

2008 – 2011 **Master of Science in Materials Engineering**
Clausthal University of Technology

1997 - 2002 **Bachelor of Science in Mechanical Engineering, Production** Design and production engineering, Ain Shams University, Cairo, Egypt

Awards

10.2011 **Prize for junior scientists –** Association of the Friends of the TU Clausthal ‘’Verein von Freunden der TU Clausthal –to award the exceptional study achievements to graduates of the TU Clausthal for the novelty of the Master Thesis